Title
THERMODYNAMICS OF GEOTHERMAL FLUIDS

Author
Rogers, P.S.Z.

Publication Date
1981-03-01

LBL-12356

Lawrence Berkeley Laboratory

UNIVERSITY OF CALIFORNIA, BERKELEY

EARTH SCIENCES DIVISION

MASTER

THERMODYNAMICS OF GEOTHERMAL FLUIDS

Pamela Sue Zukas Rogers
(Ph.D. thesis)

March 1981

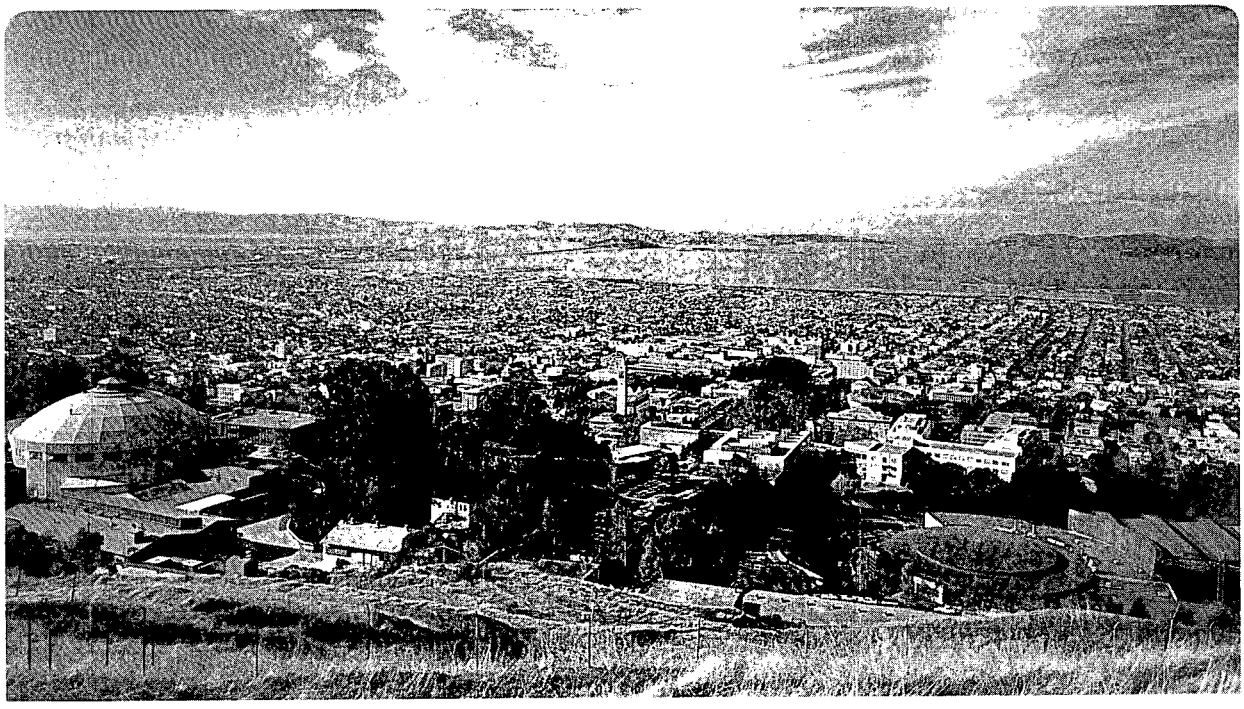

Prepared for the U.S. Department of Energy under Contract W-7405-ENG-48

DISCLAIMER

Thermodynamics of Geothermal Fluids

Pamela Sue Zukas Rogers

Earth Sciences Division
Lawrence Berkeley Laboratory
University of California
Berkeley, CA 94720

This work was supported by the U. S. Department of Energy through Contract W-7405-ENG-48.

MGW

Thermodynamics of Geothermal Fluids

Pamela Sue Zukas Rogers

Abstract

A model to predict the thermodynamic properties of geothermal brines, based on a minimum amount of experimental data on a few key systems, is tested. Sodium chloride is the major electrolyte in most natural brines and geothermal fluids, so that an accurate description of sodium chloride solutions is necessary to develop a model for more complex systems. Volumetric properties of aqueous sodium chloride, taken from the literature, are represented by a parametric equation over the range 0°C to 300°C and 1 bar to 1 kbar. Density measurements at 20 bar needed to complete the volumetric description also are presented. The pressure dependence of activity and thermal properties, derived from the volumetric equation, can be used to complete an equation of state for sodium chloride solutions.

A major part of the effort to build a model for geothermal fluids must be to obtain basic thermodynamic data. A flow calorimeter, used to obtain heat capacity data at high temperatures and pressures, is described. Heat capacity measurements, from 30°C to 200°C and 1 bar to 200 bar, are used to derive values for the activity coefficient and other thermodynamic properties of sodium sulfate solutions as a function of temperature.

Many problems in geothermal energy production and in geochemistry require prediction of the solubility of minerals in a natural brine.

Literature data on the solubility of gypsum in mixed electrolyte solutions have been used to evaluate model parameters for calculating gypsum solubility in seawater and natural brines. Predictions of strontium and barium sulfate solubility in seawater also are given.

K.S.P.

DEDICATION

I wish to dedicate this dissertation to my husband, Scott. Only his continuing support, confidence, and encouragement made it's completion possible. I also thank my parents for the most precious gift they have given me, my education.

ACKNOWLEDGEMENTS

I wish to thank Dr. K. S. Pitzer for his expert and patient guidance in every phase of this project. I would also like to thank Dr. Daniel J. Bradley for his collaboration in obtaining the density data reported in Chapter 2.

This research was supported by the U. S. Department of Energy through Contract W-7405-Eng-48.

TABLE OF CONTENTS

Page

INTRODUCTION 1

Chapter

1 VOLUMETRIC PROPERTIES OF AQUEOUS SODIUM CHLORIDE SOLUTIONS 4

Introduction. 4

Equations 5

1. Review of Pitzer's Equations. 5

2. Derivation of the Volumetric Fitting Equation. 9

Review and Evaluation of Literature Data. 11

Calculations. 16

Discussion. 18

1. Low Temperature and Overall Fit 18

2. Estimation of Uncertainties 20

3. Explanation of Tables 26

Pressure Dependence of Thermodynamic Properties . 35

1. Derivation of Equations 35

2. Estimation of Uncertainties 74

3. Explanation of Tables 75

Conclusion. 77

References. 98

2 MEASUREMENT OF THE DENSITY OF AQUEOUS SODIUM CHLORIDE SOLUTIONS FROM 75°C TO 200°C AT 20 BAR. 101

Introduction. 101

Experimental. 102

1. Description of Apparatus. 102

2. Method. 107

TABLE OF CONTENTS (continued)

Page

3. Derivation of Equations 109

4. Corrections to the Raw Data 110

Results 112

Discussion. 128

Conclusion. 131

References. 134

3 MEASUREMENT OF THE HEAT CAPACITY OF AQUEOUS SODIUM SULFATE SOLUTIONS FROM 30°C TO 200°C. 135

Introduction. 135

Experimental. 136

1. Description of Apparatus. 136

2. Derivation of Equations 145

3. Determination of Power Loss 146

4. Dependence of Heat Capacity on Flow Rate. . 147

5. Error Analysis. 147

Results 151

1. Heat Capacity Measurements. 151

2. Comparison with Literature Data 157

Calculations. 166

1. Review of Equations 166

2. Temperature Dependence of the Heat Capacity 168

3. Prediction of the Enthalpy, Activity, and Osmotic Coefficient 171

4. Comparison with Literature Data 174

Conclusion. 199

References. 200

TABLE OF CONTENTS (continued)

Chapter		Page
4	SOLUBILITY OF CALCIUM, STRONTIUM, AND BARIUM SULFATES IN SALINE WATERS	202
	Introduction.	202
	Literature Review	203
	Equations	205
	Calculations.	208
	Results	211
	Prediction of Gypsum Solubility in Seawater . .	220
	Prediction of Strontium and Barium Sulfate Solubility.	229
	Conclusion.	239
	References.	242

INTRODUCTION

Current interest in geothermal energy and in geopressurized brines has focused attention on the need for a model of aqueous solution properties at high temperatures and pressures. The number of different brines encountered in geothermal applications is large, so that detailed measurements on each of them are impractical. A model that can predict the properties of complex brines, yet is based on a minimum amount of experimental data on a few key systems, is desirable. The primary objective of this research is to develop such a model.

Sodium chloride is the major electrolyte in most natural brines and geothermal fluids. Thus an accurate description of the properties of aqueous sodium chloride solutions is necessary to develop a model for more complex systems. In addition, sodium chloride solutions are the only aqueous solutions that have been extensively studied at high temperatures and pressures. As the first step in providing a model for electrolyte solutions in this region, the volumetric properties of sodium chloride solutions to 300°C and 1 kbar have been incorporated in a parametric fitting equation. This work is presented in Chapter 1. The fitting equation was chosen from a model developed by Pitzer and co-workers[1-5] and tested by them at room temperature. Knowledge of the volumetric properties of a solution yields the pressure dependence of the activity and thermal properties. Pressure dependence information derived from the volumetric fitting equation has been used in this way to complete an equation of state for sodium chloride solutions.[6]

Even the comparatively large body of experimental data on sodium chloride volumetric properties was found to be sketchy at low pressures and high temperatures. Thus a simple apparatus was constructed to

determine the densities of aqueous solutions in this region. A description of the apparatus and results of density measurements at 20 bar are presented in Chapter 2.

Extension of the model to a complex mixture requires some knowledge of the properties of each of the pure electrolytes which make up the solution. However, little experimental data are available for the thermodynamic properties of electrolyte solutions, other than sodium chloride, at high temperatures and pressures. Thus a major part of the effort to build a model for natural brines must be to obtain basic thermodynamic data. Presented in Chapter 3 is the design of a flow microcalorimeter used to obtain heat capacity data at high temperatures and pressures. Aqueous solutions of sodium sulfate have been studied from 35°C to 200°C and 1 bar to 200 bar. The heat capacity measurements have been used to derive values for the activity coefficient of sodium sulfate as a function of temperature.

The usefulness of a model for aqueous solutions at high temperatures and pressures is not limited to geothermal energy systems. Research and engineering design in the fields of desalination, solution mining, solution leaching of mine tailings, and hydrothermal ore deposition, all depend on a knowledge of brine chemistry. Many of these applications require prediction of the solubility of minerals in a natural brine. To determine the effectiveness of Pitzer's model in solubility calculations, recent data on the solubility of gypsum in common and noncommon ion solutions have been used to evaluate the mean activity coefficient of calcium sulfate at high ionic strengths. In Chapter 4, these properties are used to predict the solubility of calcium, barium, and strontium sulfates in seawater and natural brines.

References

1. K. S. Pitzer, J. Phys. Chem. 77, 268 (1973).
2. K. S. Pitzer and G. Mayorga, J. Phys. Chem. 77, 2300 (1973).
3. K. S. Pitzer and G. Mayorga, J. Soln. Chem. 3, 539 (1974).
4. K. S. Pitzer and J. J. Kim, J. Am. Chem. Soc. 96, 5701 (1974).
5. K. S. Pitzer, J. Soln. Chem. 4, 249 (1975).
6. K. S. Pitzer and J. C. Peiper, personal communication.

Chapter 1

VOLUMETRIC PROPERTIES OF AQUEOUS SODIUM CHLORIDE SOLUTIONS

Introduction

Sodium chloride is the major electrolyte in most natural waters and geothermal fluids. Thus, an accurate description of the properties of aqueous sodium chloride solutions is the first step in developing a model to represent these systems at high temperatures and pressures. Literature data for the volumetric properties of NaCl solutions, to concentrations of 5.5 m, from 0°C to 300°C and 1 bar to 1000 bar, have been compiled and critically evaluated. The model equations presented below have been used in conjunction with a least squares fitting routine to obtain a set of parameters capable of reproducing the experimental volumetric data. Derived values for the expansivity and compressibility of the solutions, to concentrations of 4 m, also are presented.

While the volumetric properties of NaCl solutions are of interest in their own right for many research, industrial, and engineering design applications, they are also important because they give the pressure dependence of the free energy, enthalpy, and heat capacity. Equations are given for calculating the pressure dependence of these properties.

The parametric fit of NaCl solution volumetric properties presented here differs from other descriptions found in the literature[1-3] in three important aspects. First, known values of the Debye-Hückel slopes for the apparent molal volume have been included in the fitting equations. Previous descriptions have uniformly ignored the theoretical constraint of a Debye-Hückel term. Secondly, every attempt has been made to reproduce the data to its experimental accuracy and to assure that the

derived values for expansivity and compressibility are reasonable and vary smoothly with temperature, pressure, and molality. Third, the recent volumetric data of Franck and Hilbert[24] at high temperatures have been employed to determine the parametric fit in that region.

Equations

1. Review of Pitzer's Equations

The excess Gibbs free energy, G^{EX}, of a system is the difference between the Gibbs energy of the real system and that of an ideal system. In a solution containing n_1 moles of solvent and n_2 moles of solute,

$$G^{EX} = n_1 \bar{G}_1^{EX} + n_2 \bar{G}_2^{EX} \tag{1}$$

where $\bar{G}_i^{EX}$ is the partial molal excess Gibbs energy of component i. For a completely dissociated, pure electrolyte MX dissolved in n_1 moles of water, the osmotic and activity coefficients are given by

$$\phi - 1 = - \frac{n_1}{\nu m RT} \left(\frac{\partial G^{EX}}{\partial n_1} \right)_{T,P} \tag{2}$$

and

$$\ln \gamma_{\pm} = \frac{1}{\nu RT} \left(\frac{\partial G^{EX}}{\partial n_2} \right)_{T,P} \tag{3}$$

where m is the molality of the solution, ν is the total number of ions in salt MX (ν=2 for NaCl), R is the gas constant, and T is the temperature in Kelvins.

The parametric equation used by Pitzer[4] for the excess Gibbs energy of a binary electrolyte solution is

$$\frac{G^{EX}}{n_1 RT} = -A_\phi \left(\frac{4I}{b}\right) \ln(1+bI^{1/2}) + m^2\, 2\nu_M\nu_X(\beta^{(0)} + \frac{2\beta^{(1)}}{\alpha^2 I}[1-(1+\alpha I^{1/2})e^{-\alpha I^{1/2}}]) + m^3(\nu_M\nu_X)^{3/2}\, C^\phi_{MX}. \tag{4}$$

The corresponding equations for the osmotic and activity coefficients are

$$\phi-1 = -|z_M z_X|\, A_\phi \frac{I^{1/2}}{1+bI^{1/2}} + m\frac{2\nu_M\nu_X}{\nu}\left(\beta^{(0)}_{MX} + \beta^{(1)}_{MX}\, e^{-\alpha I^{1/2}}\right) + m^2 \frac{2(\nu_M\nu_X)^{3/2}}{\nu} C^\phi_{MX} \tag{5}$$

$$\ln\gamma_\pm = -|z_M z_X|\, A_\phi\left(\frac{I^{1/2}}{1+bI^{1/2}} + \frac{2}{b}\ln(1+bI^{1/2})\right) + m\frac{2\nu_M\nu_X}{\nu}\left(2\beta^{(0)}_{MX} + \frac{2\beta^{(1)}_{MX}}{\alpha^2 I}\left(1-(1+\alpha I^{1/2} - \frac{\alpha^2 I}{2})\, e^{-\alpha I^{1/2}}\right)\right) + \frac{3m^2}{2}\left(2\frac{(\nu_M\nu_X)^{3/2}}{\nu} C^\phi_{mx}\right). \tag{6}$$

where the electrolyte MX contains ν_M and ν_X ions of charge z_M and z_X, and $\nu = \nu_M + \nu_X$. I is the ionic strength,

$$I = 1/2 \sum_i m_i z_i^2,$$

and A_ϕ is the Debye-Hückel slope for the osmotic coefficient given by Bradley and Pitzer,[5]

$$A_\phi = 1/3 \left(\frac{2\pi N_0 d_w}{1000}\right)^{1/2} (e^2/DkT)^{3/2}.$$

The leading terms in Equations (5) and (6) are Debye-Hückel terms describing long range electrostatic interactions. The parameters b and α have

fixed values of 1.2 and 2.0 respectively for all 1-1 electrolytes. They are assumed to be temperature and pressure independent in this study. The adjustable parameters $\beta_{MX}^{(0)}$, $\beta_{MX}^{(1)}$, and C_{MX}^{ϕ} account for short-range interactions between ions and for indirect forces arising from the solvent. C_{MX}^{ϕ} depends on triple ion interactions and is important only at high concentrations.

Equations (5), (6), and their temperature derivatives have been used successfully to describe the activity and thermal properties of aqueous sodium chloride solutions. Use of the appropriate pressure derivatives of these equations to describe volumetric properties will make it easy to combine the volumetric results with those for the activity and thermal properties to form a complete equation of state for sodium chloride solutions.

The total volume of the solution, V, is given by the pressure derivative of the total Gibbs energy of the solution,

$$V = \left(\frac{\partial G}{\partial P}\right)_T . \tag{7}$$

The definition of the excess Gibbs energy is

$$G = n_1 \bar{G}_1^{\circ} + n_2 \bar{G}_2^{\circ} + G^{EX} \tag{8}$$

so that the pressure derivative becomes

$$V = n_1 \bar{V}_1^{\circ} + n_2 \bar{V}_2^{\circ} + \left(\frac{\partial G^{EX}}{\partial P}\right)_T . \tag{9}$$

The apparent molal volume is defined as

$$\phi V = \frac{V - n_1 \bar{V}_1^{\circ}}{n_2} , \tag{10}$$

so that from Equation (9),

$$\phi V = \bar{V}_2^{\circ} + \frac{1}{n_2}\left(\frac{\partial G^{EX}}{\partial P}\right)_T . \tag{11}$$

Here $\bar{V}_2^{\circ}$ is the partial molal volume of the solute at infinite dilution. Substitution of Equation (4) into Equation (11) yields the parametric form of the equation for the apparent molal volume,

$$\begin{aligned}\phi V = \bar{V}_2^{\circ} &+ \nu|z_M z_X| \frac{A_v}{2b} \ln(1+bI^{1/2}) \\ &+ \nu RTm\, \beta_v^{(0)} + \frac{2\nu RTm}{\alpha^2 I}\left(1-(1+\alpha I^{1/2})e^{-\alpha I^{1/2}}\right) \beta_v^{(1)} \\ &+ \frac{\nu RTm^2}{2} C_v^{\phi},\end{aligned} \tag{12}$$

with the shorthand equations

$$\begin{aligned}\beta_v^{(0)} &= \frac{2\nu_M\nu_X}{\nu}\left(\frac{\partial \beta_{MX}^{(0)}}{\partial P}\right)_{T,m} \\ \beta_v^{(1)} &= \frac{2\nu_M\nu_X}{\nu}\left(\frac{\partial \beta_{MX}^{(1)}}{\partial P}\right)_{T,m} \\ C_v^{\phi} &= \frac{2(\nu_M\nu_X)^{3/2}}{\nu}\left(\frac{\partial C_{MX}^{\phi}}{\partial P}\right)_{T,m} .\end{aligned} \tag{13}$$

Also,

$$A_v = -4RT\left(\frac{\partial A_{\phi}}{\partial P}\right)_T . \tag{14}$$

Values for A_v over a wide range of temperature and pressure are given by Bradley and Pitzer.[5]

2. Derivation of the Volumetric Fitting Equation

Equation (12) gives the dependence of the apparent molal volume of the solution on $\bar{V}_2^\circ$ and the pressure derivatives of $\beta_{MX}^{(0)}$, $\beta_{MX}^{(1)}$, and C_{MX}^{ϕ}. This form of the equation can be used directly to determine $\bar{V}_2^\circ$, $\beta_v^{(0)}$, $\beta_v^{(1)}$, and C_v^{ϕ} from a least squares fit of experimental data. However, preliminary analysis of the volumetric data over the wide range of temperature considered in this study indicated that this was not the best form of the equation to use at high temperatures. Above 200°C, the value of $\bar{V}_2^\circ$ decreases rapidly with temperature, reaching almost -100 cm^3 mol^{-1} at 300°C, compared to a value of +18 cm^3 mol^{-1} at 25°C. $\bar{V}_2^\circ$ is a measure of the effect of the solute on solvent properties, so that the rapid change in $\bar{V}_2^\circ$ can be related to changes in the properties of pure water and to increased interaction between solute and solvent. One physical explanation for the large negative values of $\bar{V}_2^\circ$ is that addition of salt to pure water at high temperatures results in a "condensation" of water molecules around the solute ions. In effect, as the temperature increases, the ion-dipole interactions between solute ions and water become progressively stronger than the dipole-dipole and hydrogen bonding interactions between water molecules, causing the water molecules to collapse around the solute ions. This explanation is further supported by examination of values for the heat of solution, which become large and negative at high temperatures. Essentially these are a measure of the heat liberated when water in a rather open structure condenses around the added solute ions.

We can use this physical picture to suggest a method of rewriting Equation (12). The purpose here is to avoid trying to fit the temperature dependence of $\bar{V}_2^\circ$ with a parametric equation, since this equation

would necessarily be very complicated.

We begin by assuming that each mole of salt in an electrolyte solution is associated with a certain number, Y, of water molecules. If n_1 is the number of moles of water in the solution, and n_2 is the number of moles of salt, then the number of moles of water associated with solute ions is n_2Y and the number of unassociated water molecules is (n_1-n_2Y). From the definition of the apparent molal volume, the total volume of the solution is

$$V = n_1 \bar{V}_1^{\circ} + n_2 \phi V. \tag{15}$$

Rewriting this equation to explicitly consider the two different classes of water molecules, one obtains

$$V = (n_1-n_2Y) \bar{V}_1^{\circ} + n_2(\phi V + Y\bar{V}_1^{\circ}).$$

The conversion to molality yields

$$V = (1000/M_w - mY) \bar{V}_1^{\circ} + m(\phi V + Y\bar{V}_1^{\circ}), \tag{16}$$

where M_w is the molecular weight of water. We also prefer to consider the apparent molal volume at the particular concentration m_1, where $m_1 = \frac{1000}{YM_w}$, since this property will vary less drastically with temperature than the infinite dilution property. Thus Equation (16) is rewritten as

$$\frac{V}{m} = [\phi V(m_1) + Y\bar{V}_1^{\circ}] + (\frac{1000}{mM_w} - Y) \bar{V}_1^{\circ} + \phi V(m) - \phi V(m_1) \tag{17}$$

Substitution of the parametric equations for ϕV yields

$$v = \left(\frac{m}{1000+mM_2}\right)\left\{\frac{V(m_1)}{m_1} + \left(\frac{1000}{m} - M_w Y\right) v_w \right.$$
$$+ \nu|z_M z_X| \frac{A_v}{2b}\left(\ln(1+bI^{1/2}) - \ln(1+bI_1^{1/2})\right) + \nu RT\, \beta_v^{(0)}\, (m-m_1)$$
$$+ \frac{2\nu RT}{\alpha^2}\beta_v^{(1)}\left(\frac{m}{I}\left(1-(1+\alpha I^{1/2})\, e^{-\alpha I^{1/2}}\right) - \frac{m_1}{I_1}\left(1-(1+\alpha I_1^{1/2})\, e^{-\alpha I_1^{1/2}}\right)\right)$$
$$\left. + \nu/2\ RT\ C_v^{\phi}\ (m^2-m_1^2)\right\}, \tag{18}$$

where v is the specific volume of the solution, v_w is the specific volume of pure water, M_2 is the molecular weight of the solute, I_1 is the ionic strength of the solution at m_1, and $V(m_1)$ is the total volume of the solution containing 1 kg of water, at concentration m_1. The total volume of the solution varies monotonically with temperature, increasing more slowly with temperature the higher the concentration. The value of $Y = 10$ was chosen to yield a concentration, $m_1 = 5.550825$ m, conveniently at the upper concentration limit of the existing data.

Review and Evaluation of Literature Data

The literature sources of volume and density data used in the overall fit of NaCl solution volumetric properties are listed in Table 1, along with estimates of the precision of the data. These data sets have been chosen from a literature search of the references listed in Potter's bibliography[8] and other sources, on the basis of their precision and their coverage of a wide range of temperature, pressure, or molality. Estimates for the precision of the data were taken as stated by the original investigator or as one in the last decimal place of the reported data.

Data reported as a difference in the density or volume of solution versus that of water (Ref. 9-13,16,17) were used in that form. The high

Table 1

Literature Data for NaCl Volumetric Properties

Reference	Temperature Range (°C)	Pressure Range (bar)	Molality Range (molal)	Estimated Precision (ppm)	Standard Deviation of Fit (ppm) I	II
9	0- 55	1.01	.01-1.0	1	25	32
10	50	1.01	.005-1.0	2	18	19
11	5	1.01	.05-3.5	1	53	79
12	25	1.01	.03-3.7	1	10	36
13	1.5-45	1.01	.03-3.0	3	50	54
14	25-85	1-1000	1.-5.7	10	35	60
15	0-50	1-1000	.1-2.0	30	88	90
16	15-45	1.01	.06-5.9	1	20	50
17	0-35	1.01	.01-1.5	1	20	30
18	0-20	1.01	4.-6.0	100	105	127
19	75-200	20.	.1-1.0	50	-	179
20	75-200	20.	.05-4.0	200	-	170
21	200-300	saturation	.2-5.7	1000	-	6675
22,23	100-175	saturation	.1-3.6	100	-	775
24	100-300	100-1000	.02-5.7	1000	-	477
	overall standard deviation of fit				60 ppm	300 ppm*

* Data sets from references 21-23 were omitted from the calculation of the standard deviation.

pressure data of Millero[15] were reported as a difference in density between the solution at the experimental pressure and at one atmosphere, so that actual values of the density at high pressures were calculated using a fit of the one atmosphere literature data as a baseline. The data of Gibson and Loeffler[14] were obtained experimentally as expansivities at one atmosphere and compressibilities at constant temperature. Since the data at 25°C and one atmosphere used as the reference for their measurements agreed to within their experimental error with more recent data, their data were used without correction. The literature data at high temperatures (References 19-24) also were used without correction.

In the high temperature region the major data set is that of Hilbert.[24] This set was chosen over that of Federov[25] since it was judged to be more precise, and it is in considerably better agreement with the low temperature data in the region of overlap. This is illustrated in Figure 1, where the low temperature data of Gibson and Loeffler,[14] and the high temperature data of Hilbert and of Federov are compared. One should also note from Table 1 that there is a large difference between the precision of the data below and above 85°C.

Accurate volumetric properties for pure water are also important, since they enter directly into the fitting Equation (17). A review of the volumetric properties found in the literature[26-33] and in the most widely used steam tables[34-36] showed large discrepancies, especially at pressures near 1 kbar. In addition, Kell and Whalley[29] have made recent corrections to their density data, which are not included in published steam tables. Uematsu _et al._[26] and Kell, McLaurin, and Whalley[30] have published significant, new volumetric data since formulation of the

Figure 1. Comparison of data of Hilbert and Federov. The plotted values are for $(\frac{\partial v}{\partial T})_{P,m} \times 10^5$ ($cm^3\ g^{-1}\ K^{-1}$) at 5.5 molal, calculated from the volumetric data[24,25] as the finite difference over a 50 K interval. Values from Gibson and Loeffler[14] are taken directly from their tables.

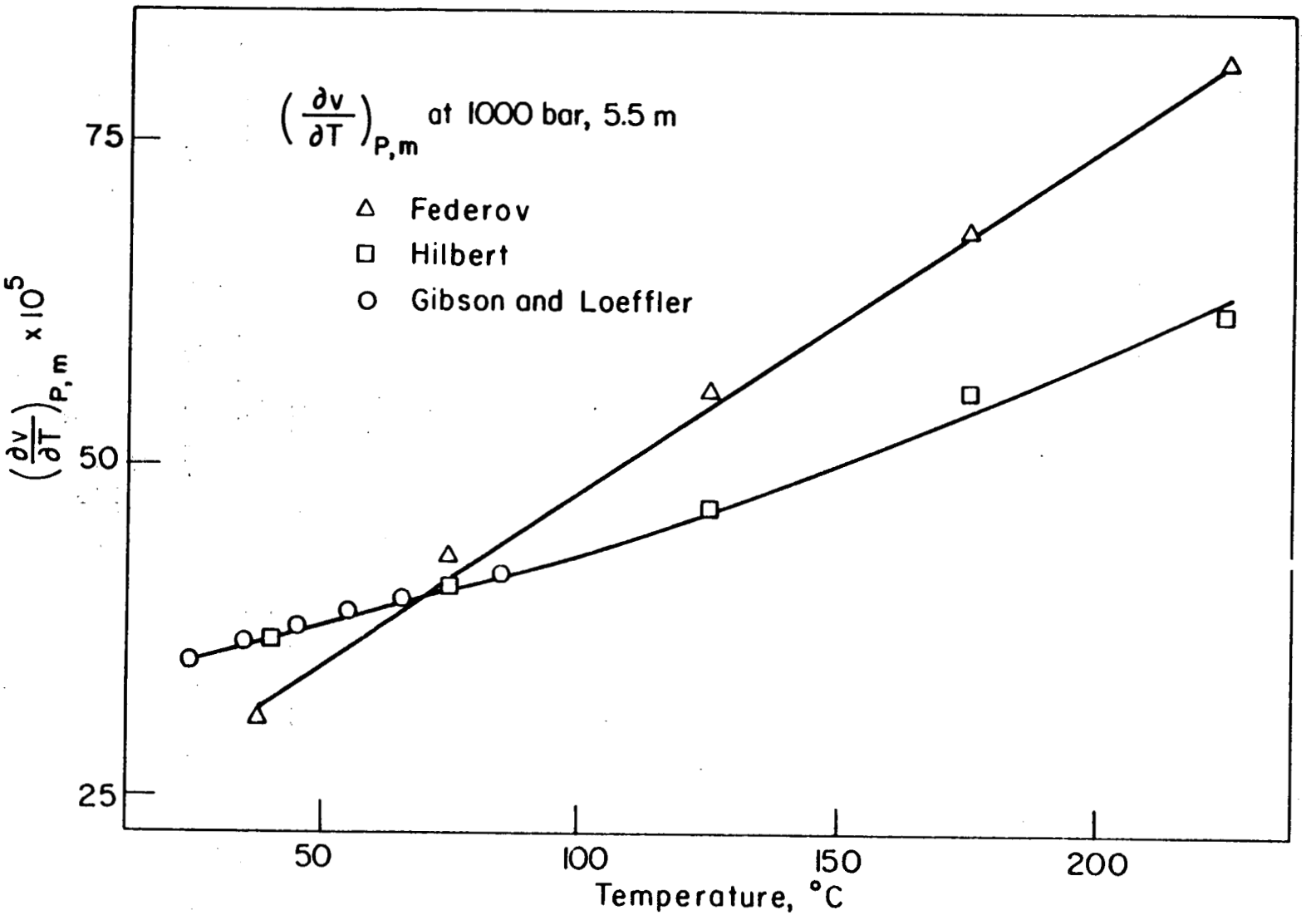
$\left(\frac{\partial v}{\partial T}\right)_{P,m}$ at 1000 bar, 5.5 m
Federov
Hilbert
Gibson and Loeffler
$\left(\frac{\partial v}{\partial T}\right)_{P,m} \times 10^5$
75
50
25
50
100
150
200
Temperature, °C

XBL 812-5192

referenced steam tables. Because of these important changes and additions to the data base, it seemed imperative that a new compilation of the p, v, T properties of water be employed.

Fortunately, Haar, Gallagher, and Kell[37] have completed a new steam table in which they have emphasized reproduction of the volumetric properties of liquid water to within experimental accuracy. Haar has kindly made available to us, prior to publication, a copy of his equations, which have been placed on computer accessible tape for use with the sodium chloride solution fitting routine. It is important that these same values for the volumetric properties of water be used in reproducing the volumetric properties of sodium chloride solutions.

Calculations

The fitting Equation (18) gives the concentration dependence of the volumetric data at a single temperature and pressure. In preliminary isothermal, isobaric calculations, it was found that $\beta_v^{(1)}$ could not be determined from the volumetric data. Therefore

$$\left(\frac{\partial \beta_{MX}^{(1)}}{\partial P}\right)_{T,m}$$

has been set equal to zero throughout this study. The redundancy of $\beta_v^{(1)}$ is not surprising, since $\beta_v^{(1)}$ is important only at low molalities, where the quality of the data is likely to be poorest. Since

$$\left(\frac{\partial \beta_{MX}^{(1)}}{\partial P}\right)_{T,m}$$

cannot be determined, $\beta_{MX}^{(1)}$ will have no pressure dependence, whereas $\beta_{MX}^{(0)}$ and C_{MX}^{ϕ} will depend both on temperature and pressure in the final equation of state.

In order to fit all of the volumetric data listed in Table 1 simultaneously, equations describing the temperature and pressure dependence of $V(m_1)$, $\beta_v^{(0)}$, and C_v^{ϕ} are needed. The optimum forms for these equations are listed below, along with a reduced form of Equation (18) which is specific for NaCl solutions

$$v = \left(\frac{m}{1000+mM_2}\right)\left\{\frac{V(m_1)}{m_1} + \left(\frac{1000}{m} - 10\,M_w\right) v_w + \frac{A_v}{1.2}\left(\ln(1+1.2I^{1/2}) - \ln(1+bI_1^{1/2})\right) + 2RT\,\beta_v^{(0)}\,(m-m_1) + RT\,C_v^{\phi}\,(m^2-m_1^2)\right\} \tag{19}$$

$$V(m_1) = U_1 + U_2T + U_3T^2 + U_4T^3 + (P-P_0)[U_5 + U_6T + U_7T^2] + (P-P_0)^2\,[U_8 + U_9T] \tag{20}$$

$$\beta_v^{(0)} = U_{10} + \frac{U_{11}}{(T-227)} + U_{12}T + U_{13}T^2 + \frac{U_{14}}{(680-T)} + (P-P_0)\left[U_{15} + \frac{U_{16}}{(T-227)} + U_{17}T + U_{18}T^2 + \frac{U_{19}}{(680-T)}\right] + (P-P_0)^2\left[U_{20} + \frac{U_{21}}{(T-227)} + U_{22}T + \frac{U_{23}}{(680-T)}\right] \tag{21}$$

$$C_v^{\phi} = U_{24} + \frac{U_{25}}{(T-227)} + U_{26}T + U_{27}T^2 + \frac{U_{28}}{(680-T)} \tag{22}$$

where

$m_1 = I_1 = 5.550825$ molal

$M_2 = 58.4428$ gm

$M_w = 18.01534$ gm

$R = 83.1440\ cm^3\ bar\ mol^{-1}$

$P_0 = 1.01325$ bar.

Here T is the temperature in Kelvins and P is the pressure in bars. The factors 1/(T-227) and 1/(680-T) are used for convenience as functions which change rapidly in the region of 0°C and 350°C respectively. Expansivities at temperatures below 25°C, derived from the volumetric fit, are fairly sensitive to the value of the low temperature function. For this reason, the value of 227 K was chosen to coincide approximately with the temperature of a thermodynamic singularity for supercooled water reported by Kanno and Angell.[38] Use of the factor 1/(T-227) yields expansivity values that are consistent with those derived directly from the closely spaced volumetric data of Chen, Chen, and Millero[17] at 1 bar. The choice of the high temperature factor has no theoretical significance.

Discussion

1. Low Temperature and Overall Fit

As a result of the large difference in precision of the data sets, a single, overall fit of the high and low temperature data cannot do justice to the quality of the low temperature data. Since we were particularly interested in deriving values for the expansivity of NaCl solutions, the inaccuracy of an overall fit in the low temperature region proved troublesome. For this reason, two different sets of the fitting parameters, U, are presented in Table 2. The first set reproduces the low temperature volumetric data with a high degree of precision, and can be used to obtain values for the volume, expansivity, and compressibility of NaCl solutions to 85°C. The second set reproduces the high temperature data to within the precision level of Hilbert's data and also describes the low temperature data to within an uncertainty of ±150 ppm. It can be used to obtain volumetric properties over the

Table 2

VALUES OF FITTING PARAMETERS

U	SET I LOW TEMPERATURE FIT	SET II OVERALL FIT
1	1.0837195E+03	1.0249125E+03
2	-2.4749323E-01	2.7796679E-01
3	1.2442861E-03	-3.0203919E-04
4	0.	1.4977178E-06
5	-7.7222249E-02	-7.2002329E-02
6	3.2423439E-04	3.1453130E-04
7	-5.7917599E-07	-5.9795994E-07
8	3.3254437E-06	-6.6596010E-06
9	0.	3.0407621E-08
10	-2.1451068E-05	5.3699517E-05
11	2.2324909E-03	2.2020163E-03
12	-6.4950599E-08	-2.6538013E-07
13	2.4503020E-10	8.6255554E-10
14	0.	-2.6829310E-02
15	1.0033371E-07	-1.1173488E-07
16	-1.2784026E-06	-2.6249802E-07
17	-4.6468063E-10	3.4926500E-10
18	5.7054131E-13	-8.3571924E-13
19	0.	3.0669940E-05
20	0.	1.9767979E-11
21	1.3581172E-10	-1.9144105E-10
22	0.	3.1387857E-14
23	0.	-9.6461948E-09
24	-6.8152430E-06	2.2902837E-05
25	-2.5382945E-04	-4.3314252E-04
26	6.2480692E-08	-9.0550901E-08
27	-1.0731284E-10	8.6926600E-11
28	0.	5.1904777E-04

entire temperature range of 0°C to 300°C when this level of precision will suffice. High temperature values for the expansivity and compressibility can be calculated from this overall fit. Values for the volume, compressibility, and expansivity at 50°C calculated from the overall fit parameters agree, within the uncertainty quoted for that fit, with the values calculated from the low temperature parameters. Thus 50°C is the temperature recommended for changing from one set of parameters to the other when properties over a wide range of temperatures are required.

2. Estimation of Uncertainties

The regions of validity and the estimated uncertainties for the volumetric properties calculated from both sets of parameters are summarized in Table 3. In general, the volume of NaCl solutions can be reproduced up to 5.5 m, the compressibility to 5 m, and the expansivity to 4 m. However, below 25°C the molality range on all properties above 1.01 bar is limited to 2 m because of a lack of high concentration data at high pressures.

Estimates of the uncertainty in the expansivity and compressibility between 25°C and 85°C were made by comparing the values derived from the volumetric fit equations and the values tabulated by Gibson and Loeffler.[14] The agreement in values from these two sources at 25°C is shown in Figures 2 and 3. At high temperatures, estimation of the precision of these properties becomes more difficult because of the wide and irregular spacing of Hilbert's measurements. However, assuming that the maximum precision in the fit of the volume is ±1000 ppm over a 50 K temperature interval or a 500 bar pressure interval, the uncertainties in derived values of the expansion and compression are both about ±5%.

Table 3

Estimated Uncertainty in Volumetric Properties

Property	Temperature Range (°C)	Pressure Range (bar)	Concentration Range (molal)	Estimated Confidence Limits: Low Temperature Fit (I)	Estimated Confidence Limits: High Temperature (Fit (II)
Volume	0 - 25	1.01	0 - 5.5	120 ppm	150 ppm
	0 - 25	1 - 1000	0 - 2.0	120 ppm	150 ppm
	25 - 85	1 - 1000	0 - 5.5	70 ppm	150 ppm
	85 - 300	1 - 1000	0 - 5.5	-	700 ppm
Expansivity	0 - 25	1.01	0 - 4.0	1%	(not recommended)
	0 - 25	1 - 1000	0 - 2.0	1%	
	25 - 85	1 - 1000	0 - 4.0	1%	5%
	85 - 300	1 - 1000	0 - 4.0	-	5%
Compressibility	0 - 25	1 - 1000	0 - 2.0	.5%	(not recommended)
	25 - 85	1 - 1000	0 - 5.0	.5%	5%
	85 - 300	1 - 1000	0 - 5.0	-	5%

Figure 2. Comparison of expansivity values for NaCl solutions at 25°C. Solid lines represent values of $\left(\frac{\partial v}{\partial T}\right)_{P,m} \times 10^4$ ($cm^3\ g^{-1}\ K^{-1}$) calculated from the volumetric fit. Points are from the tables of Gibson and Loeffler.[14]

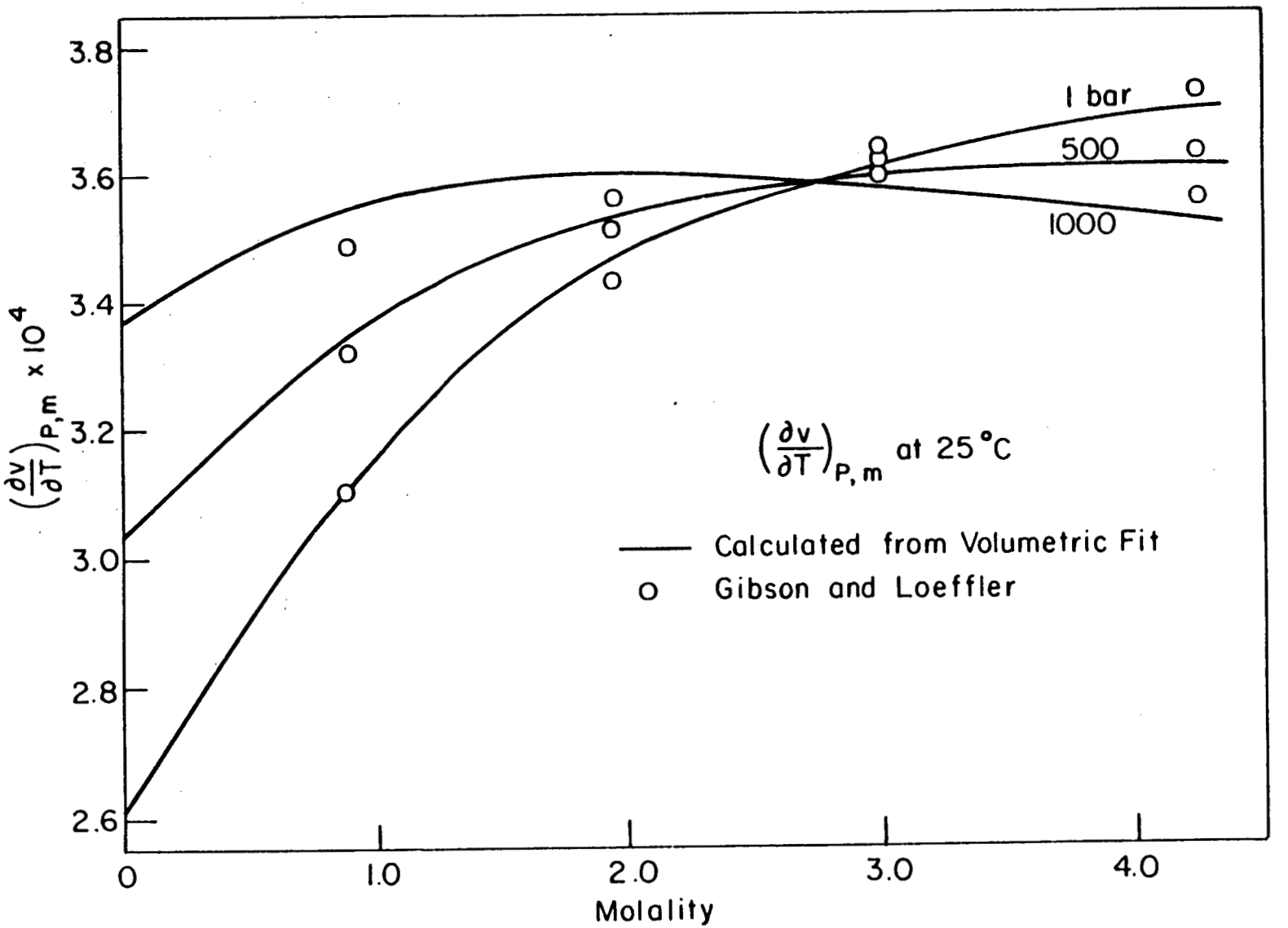
3.8
3.6
3.4
3.2
3.0
2.8
2.6
$\left(\frac{\partial v}{\partial T}\right)_{P,m} \times 10^4$
0
1.0
2.0
3.0
4.0
Molality
1 bar
500
1000
$\left(\frac{\partial v}{\partial T}\right)_{P,m}$ at 25 °C
Calculated from Volumetric Fit
Gibson and Loeffler

XBL 812-5193

Figure 3. Comparison of compressibility values for NaCl solutions at 25°C. Solid lines represent values of $-(\frac{\partial v}{\partial P})_{T,m} \times 10^5$ ($cm^3\ g^{-1}\ bar^{-1}$) calculated from the volumetric fit. Points are from the tables of Gibson and Loeffler.[14]

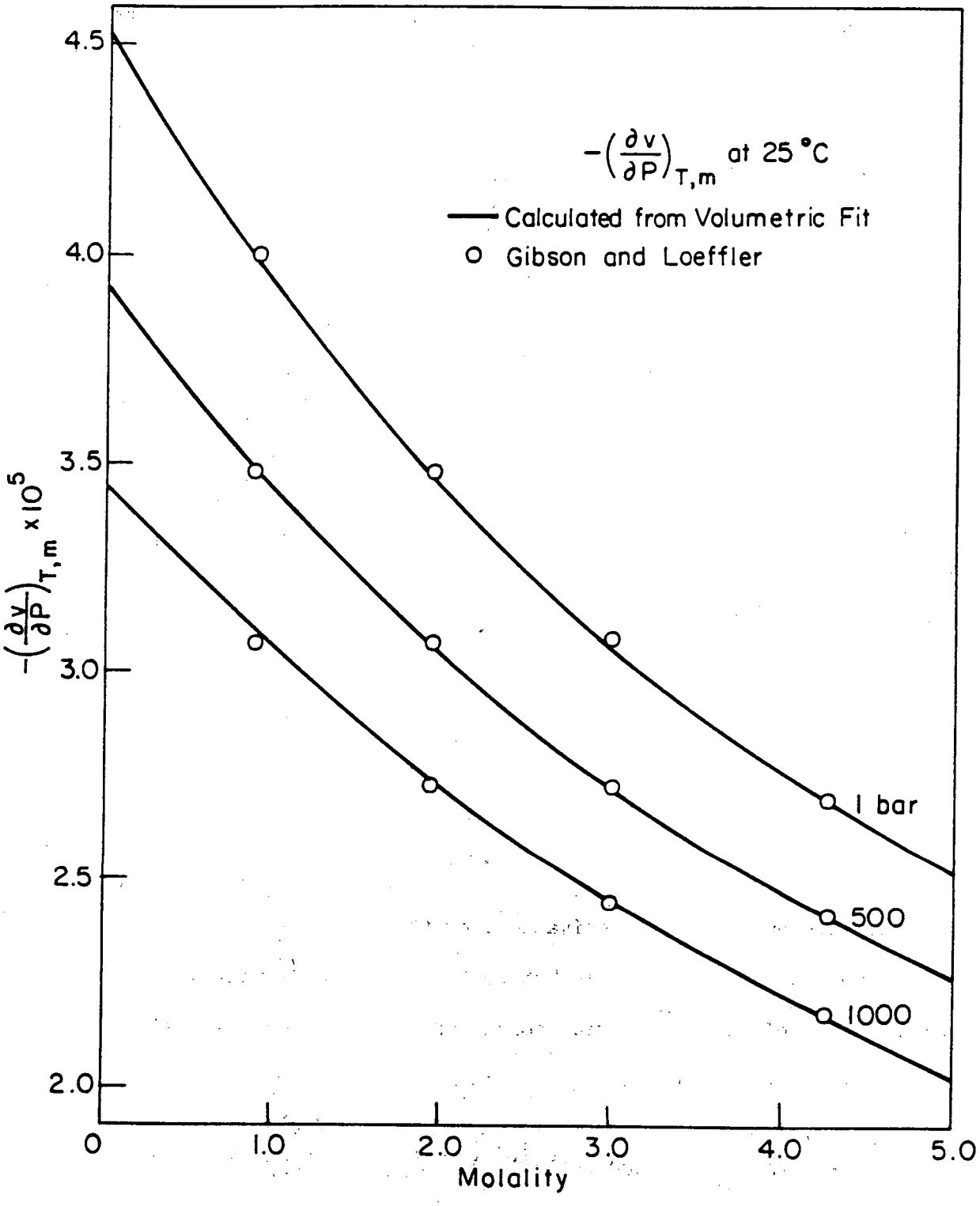
$-\left(\frac{\partial v}{\partial P}\right)_{T,m}$ at 25 °C
Calculated from Volumetric Fit
Gibson and Loeffler
1 bar
500
1000
$-\left(\frac{\partial v}{\partial P}\right)_{T,m} \times 10^5$
4.5
4.0
3.5
3.0
2.5
2.0
0
1.0
2.0
3.0
4.0
5.0
Molality

XBL 812-5189

The compressibilities derived from the volumetric fit differ from those of Rowe and Chou[39] by as much as 10%. The values for the compressibility of pure water used by Rowe and Chou also differ by as much as 3% from those of Haar;[37] however, this difference can not account for the total discrepancy in the compressibilities of sodium chloride solutions.

3. Explanation of Tables

Values of the apparent molal volume at infinite dilution also can be obtained from the fitting parameters and the calculated values of the specific volume. The change in the fitting parameters $\frac{V(m_1)}{m_1}$, $\beta_v^{(0)}$, and C_v^{ϕ} with temperature is shown in Figures 4-6, and the temperature dependence of $\bar{V}_2^{\circ}$ is shown in Figure 7. Values of v_w, $\bar{V}_2^{\circ}$, $\beta_v^{(0)}$, C_v^{ϕ}, and the Debye-Hückel slopes are listed at ten degree intervals in Table 4. These can be used directly in Equation (12) to calculate the apparent molal volumes of sodium chloride solutions. The specific volume of a solution can be obtained through the identity

$$v = \frac{m^{\phi}V+1000v_w}{(1000+mM_2)} . \tag{23}$$

The temperature and pressure derivatives of the parameters and the volume of pure water are given in Tables 5 and 6. The expansivity and compressibility of sodium chloride solutions can be calculated using these values and the following equations:

$$\frac{1}{v}\left(\frac{\partial v}{\partial T}\right)_{P,m} = \frac{1}{v(1000+mM_2)}\left\{1000\left(\frac{\partial v_w}{\partial T}\right)_P + m\left[\left(\frac{\partial \bar{V}_2^{\circ}}{\partial T}\right)_P + \frac{A_x}{b}(1+bI^{1/2}) + 2RTm\left(\frac{\partial \beta_v^{(0)}}{\partial T}\right)_P + RTm^2\left(\frac{\partial C_v^{\phi}}{\partial T}\right)_P\right]\right\} \tag{24}$$

Figure 4. Fitting parameter $\frac{V(m_1)}{m_1}$ as a function of temperature.

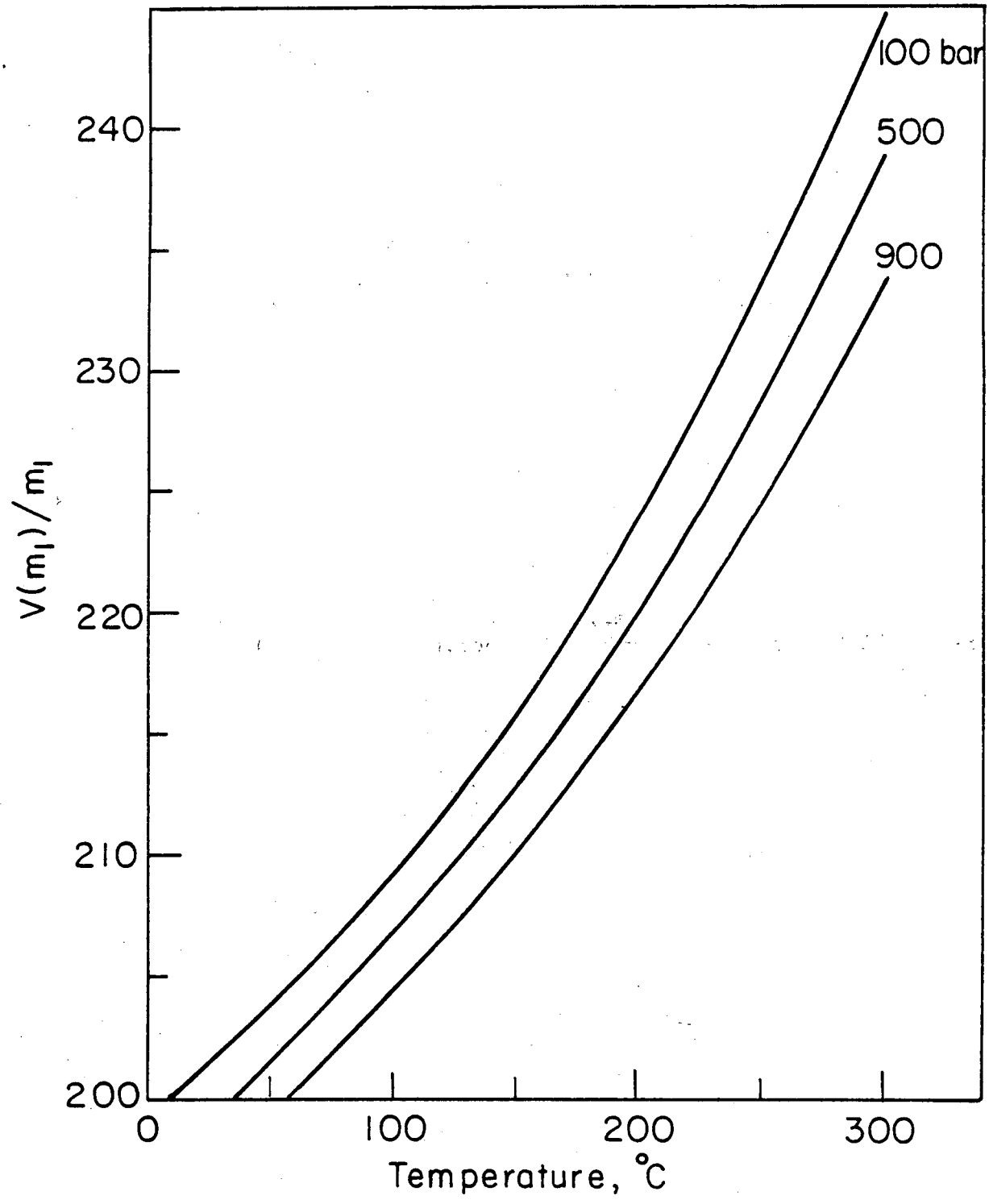
100 bar
500
900
240
230
220
210
200
V(m_l)/m_l
0
100
200
300
Temperature, °C

XBL 812-5186

Figure 5. Fitting parameter $\beta_v^{(0)}$ as a function of temperature.

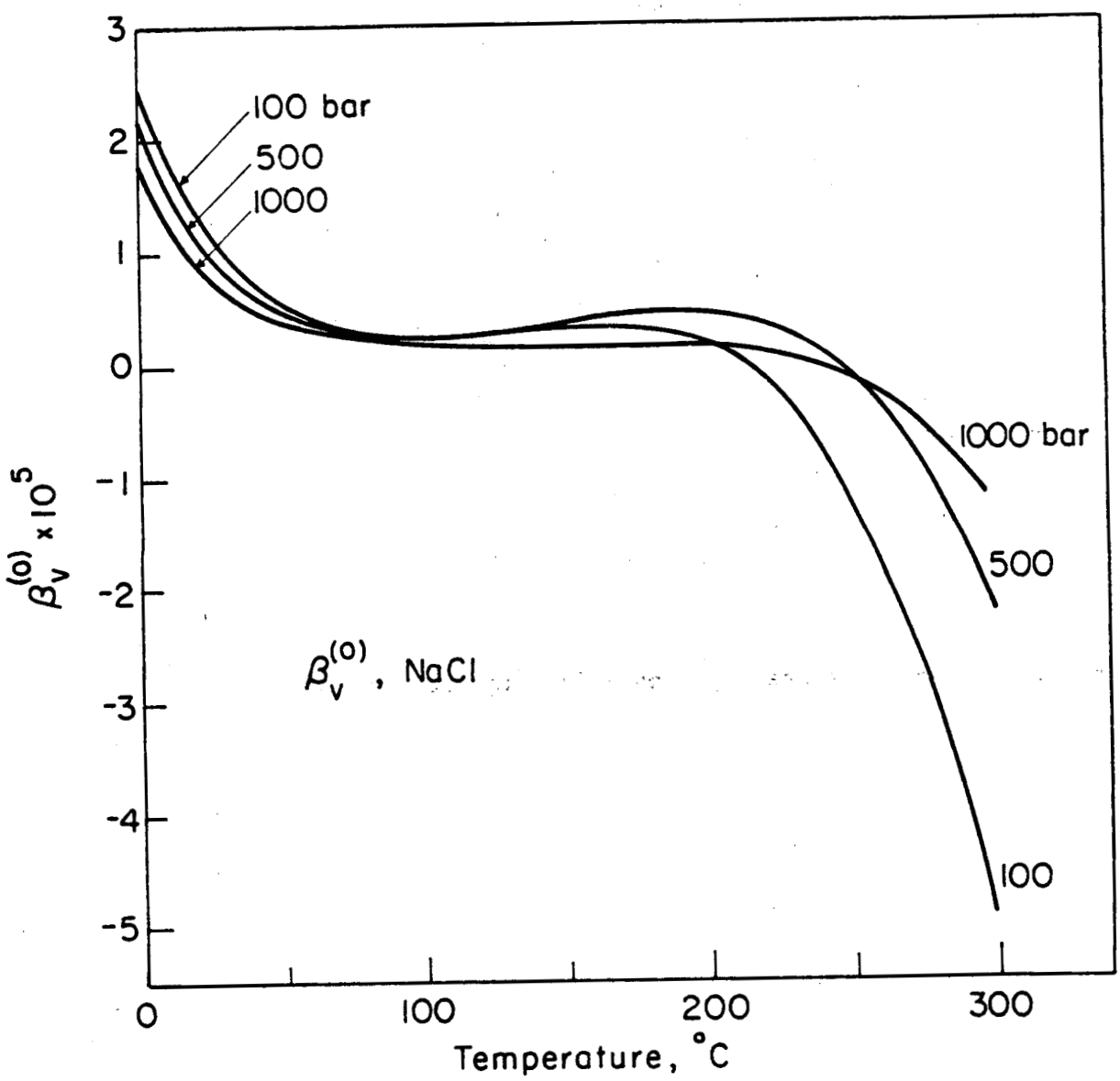
3
2
1
0
-1
-2
-3
-4
-5
$\beta_v^{(o)} \times 10^5$
100 bar
500
1000
1000 bar
500
100
$\beta_v^{(o)}$, NaCl
0
100
200
300
Temperature, °C

XBL 812-5172

Figure 6. Fitting parameter C_v^{ϕ} as a function of temperature.

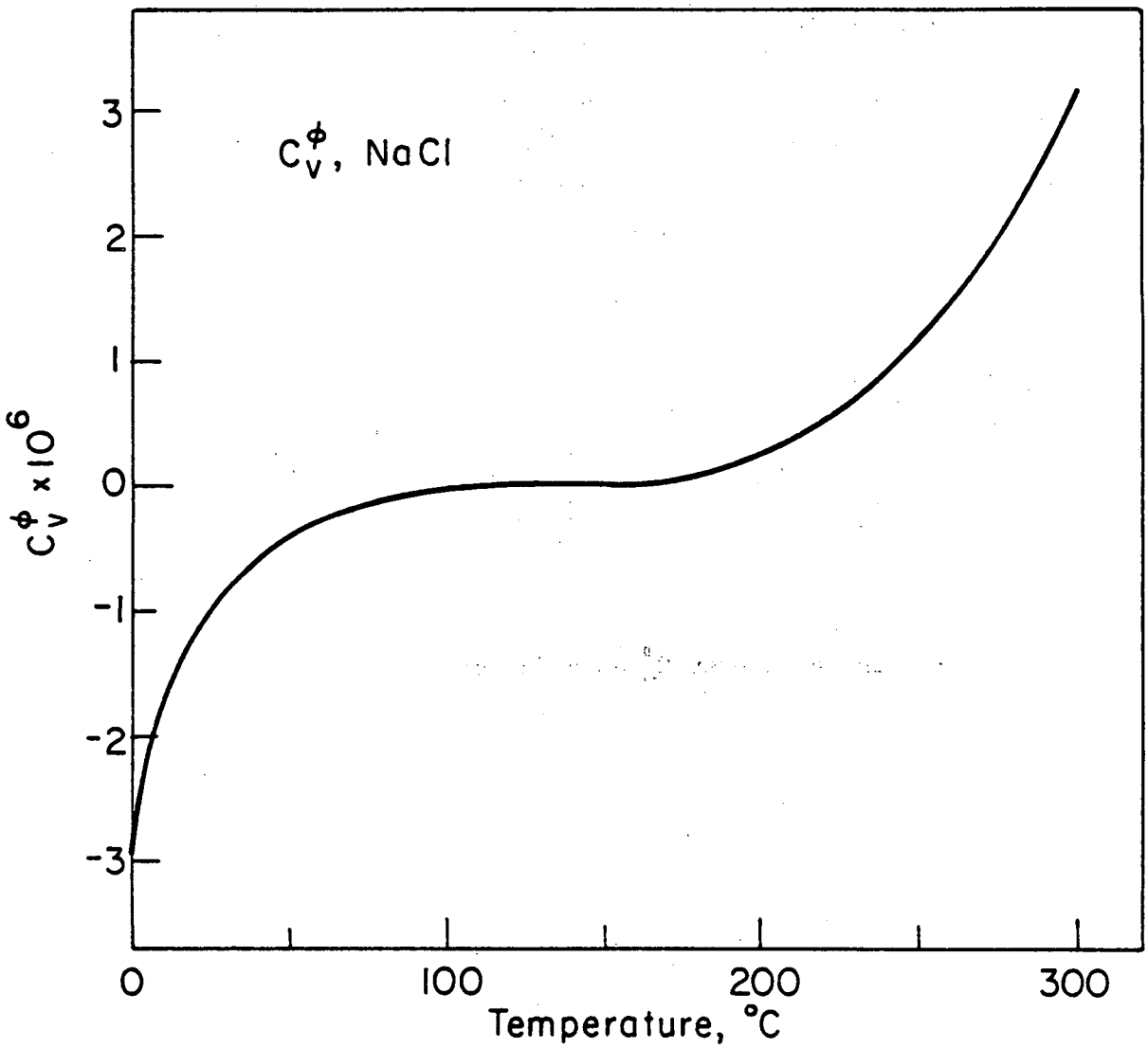
C_V^ϕ, NaCl
$C_V^\phi \times 10^6$
3
2
1
0
-1
-2
-3
0
100
200
300
Temperature, °C

XBL 812-5173

Figure 7. The apparent molal volume at infinite dilution, $\bar{V}_2^{\circ}$, for NaCl solutions as a function of temperature.

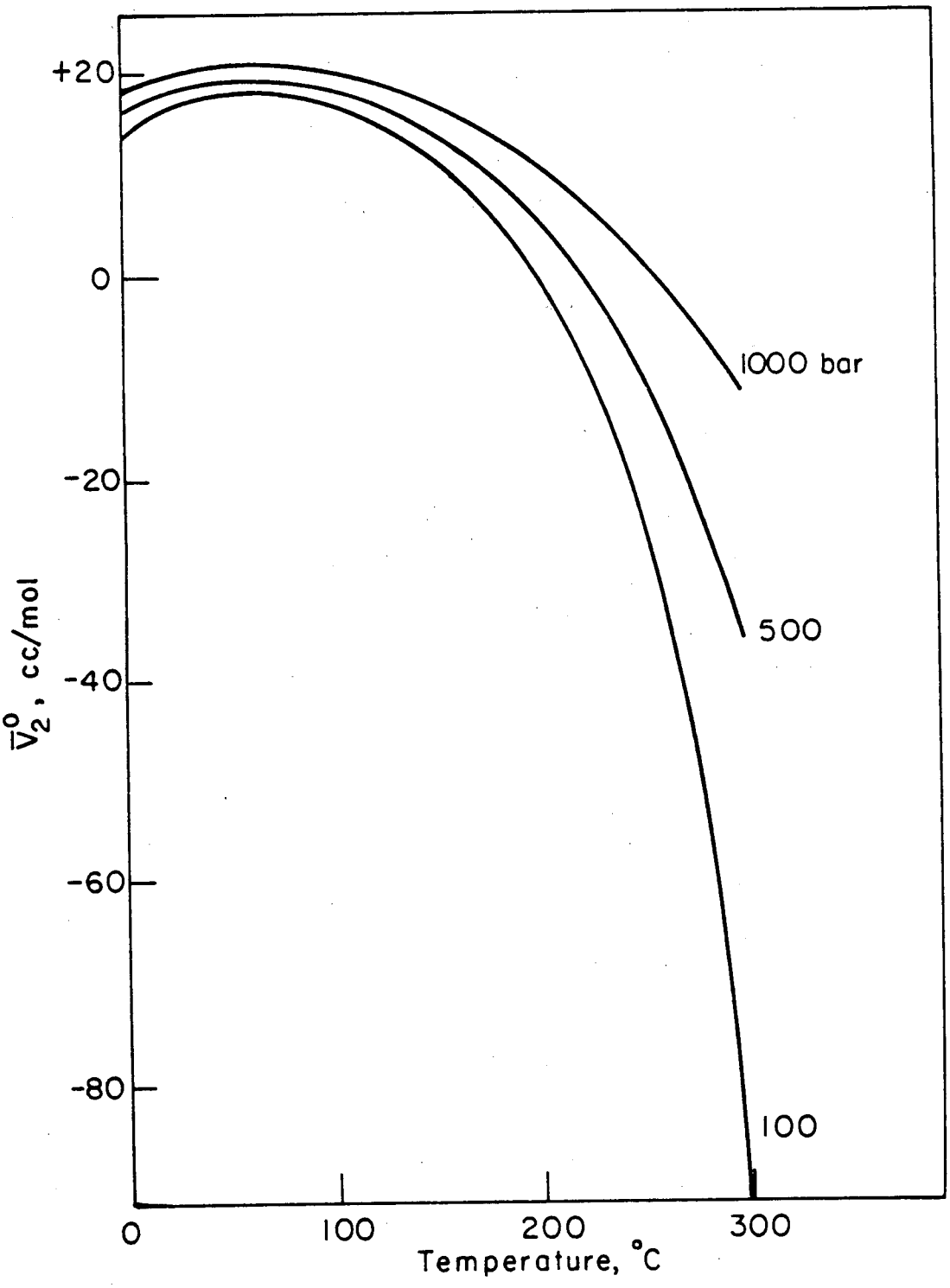
+20
0
-20
-40
-60
-80
$\bar{V}_2^o$, cc/mol
1000 bar
500
100
0
100
200
300
Temperature, °C

XBL 812-5187

$$\frac{1}{v}\left(\frac{\partial v}{\partial P}\right)_{T,m} = \frac{1}{v(1000+mM_2)}\left\{1000\left(\frac{\partial v_w}{\partial P}\right)_T + m\left[\left(\frac{\partial \bar{V}_2^{\circ}}{\partial P}\right)_T + \frac{A_k(1+bI^{1/2})}{b} + 2RTm\left(\frac{\partial \beta_v^{(0)}}{\partial P}\right)_T + RTm^2\left(\frac{\partial C_v^{\phi}}{\partial P}\right)_T\right]\right\}. \tag{25}$$

A_x and A_k are the Debye-Hückel slopes for the expansivity and compressibility of electrolyte solutions and are given in Paper XII.[5] In Tables 4-6, the low temperature fit (Parameter Set I) has been used from 0°C to 50°C. The overall fit (Parameter Set II) has been used above 50°C, accounting the discontinuity in the parameters observed in the tables at 50°C. Even though the parameters are discontinuous at 50°C, calculated values of the specific volume, expansivity, and compressibility at this temperature agree within the uncertainty limits quoted for the overall fit. For convenience, values of the specific volume, expansivity, and compressibility at rounded concentrations are given in Tables 7-9.

Pressure Dependence of Thermodynamic Properties

1. Derivation of Equations

Knowledge of the volumetric properties of the solution also can be used to calculate the pressure dependence of activity and thermal properties. A review of the equations for the enthalpy and heat capacity, as given by Silvester and Pitzer,[6] is presented before the pressure dependent equations are derived.

The relative enthalpy of an electrolyte solution, L, is defined as the difference between the total enthalpy of the solution and the enthalpy of the solution in its standard state,

$$L = H - H^{\circ}. \tag{26}$$

Table 4

Parameters for Calculation of the Apparent Molal Volume

T	P	v_w	D-H Slope	$\bar{V}_2^\circ$	$\beta_v^{(0)}$	C_v^ϕ
°C	bar	$\frac{cm^3}{g}$	$\frac{cm^3}{mol}$	$\frac{cm^3}{mol}$	$\frac{g}{mol\ bar}$	$\frac{g^2}{mol^2\ bar}$
0	1	1.000171	1.504E+00	1.327E+01	2.746E-05	-3.26E-06
10	1	1.000259	1.643E+00	1.506E+01	1.956E-05	-2.25E-06
20	1	1.001771	1.793E+00	1.625E+01	1.431E-05	-1.56E-06
25	1	1.002947	1.875E+00	1.668E+01	1.234E-05	-1.29E-06
30	1	1.004365	1.962E+00	1.702E+01	1.069E-05	-1.07E-06
40	1	1.007851	2.153E+00	1.750E+01	8.152E-06	-7.19E-07
50	1	1.012115	2.372E+00	1.774E+01	6.366E-06	-4.71E-07
50	1	1.012115	2.372E+00	1.782E+01	5.733E-06	-3.32E-07
60	1	1.017087	2.622E+00	1.791E+01	4.415E-06	-2.00E-07
70	1	1.022724	2.909E+00	1.781E+01	3.513E-06	-1.22E-07
80	1	1.028999	3.238E+00	1.754E+01	2.925E-06	-7.97E-08
90	1	1.035897	3.615E+00	1.710E+01	2.577E-06	-6.02E-08
100	1	1.043414	4.050E+00	1.649E+01	2.408E-06	-5.46E-08
110	1	1.051530	4.550E+00	1.571E+01	2.368E-06	-5.59E-08
120	2	1.060271	5.127E+00	1.475E+01	2.412E-06	-5.87E-08
130	3	1.069653	5.795E+00	1.360E+01	2.498E-06	-5.87E-08
140	4	1.079700	6.572E+00	1.226E+01	2.587E-06	-5.23E-08
150	5	1.090444	7.477E+00	1.070E+01	2.637E-06	-3.65E-08
160	6	1.101926	8.536E+00	8.911E+00	2.606E-06	-8.63E-09
170	8	1.114196	9.779E+00	6.863E+00	2.448E-06	3.36E-08
180	10	1.127316	1.125E+01	4.523E+00	2.112E-06	9.24E-08
190	13	1.141359	1.299E+01	1.849E+00	1.542E-06	1.70E-07
200	16	1.156413	1.506E+01	-1.215E+00	6.729E-07	2.69E-07
210	19	1.172584	1.756E+01	-4.742E+00	-5.691E-07	3.91E-07
220	23	1.190001	2.058E+01	-8.826E+00	-2.272E-06	5.38E-07
230	28	1.208817	2.425E+01	-1.360E+01	-4.538E-06	7.15E-07
240	33	1.229223	2.878E+01	-1.923E+01	-7.494E-06	9.24E-07
250	40	1.251452	3.440E+01	-2.596E+01	-1.129E-05	1.17E-06
260	47	1.275795	4.149E+01	-3.414E+01	-1.612E-05	1.45E-06
270	55	1.302623	5.052E+01	-4.426E+01	-2.221E-05	1.79E-06
280	64	1.332417	6.224E+01	-5.704E+01	-2.987E-05	2.18E-06
290	74	1.365815	7.775E+01	-7.360E+01	-3.951E-05	2.63E-06
300	86	1.403691	9.873E+01	-9.508E+01	-5.167E-05	3.17E-06

Table 4

Parameters for Calculation of the Apparent Molal Volume

T	P	v_w	D-H Slope	$\bar{V}_2^\circ$	$\beta_v^{(0)}$	C_v^ϕ
°C	bar	$\frac{cm^3}{g}$	$\frac{cm^3}{mol}$	$\frac{cm^3}{mol}$	$\frac{g}{mol\ bar}$	$\frac{g^2}{mol^2\ bar}$
0	200	.990367	1.462E+00	1.452E+01	2.525E-05	-3.26E-06
10	200	.991052	1.587E+00	1.607E+01	1.801E-05	-2.25E-06
20	200	.992910	1.724E+00	1.711E+01	1.317E-05	-1.56E-06
25	200	.994196	1.799E+00	1.749E+01	1.133E-05	-1.29E-06
30	200	.995690	1.879E+00	1.780E+01	9.792E-06	-1.07E-06
40	200	.999244	2.055E+00	1.824E+01	7.404E-06	-7.19E-07
50	200	1.003486	2.255E+00	1.846E+01	5.717E-06	-4.71E-07
50	200	1.003486	2.255E+00	1.852E+01	5.187E-06	-3.32E-07
60	200	1.008358	2.484E+00	1.858E+01	4.005E-06	-2.00E-07
70	200	1.013825	2.745E+00	1.848E+01	3.224E-06	-1.22E-07
80	200	1.019865	3.043E+00	1.822E+01	2.746E-06	-7.97E-08
90	200	1.026463	3.383E+00	1.780E+01	2.502E-06	-6.02E-09
100	200	1.033614	3.772E+00	1.723E+01	2.434E-06	-5.46E-08
110	200	1.041317	4.217E+00	1.650E+01	2.497E-06	-5.59E-08
120	200	1.049580	4.728E+00	1.561E+01	2.651E-06	-5.87E-08
130	200	1.058416	5.315E+00	1.456E+01	2.859E-06	-5.87E-08
140	200	1.067844	5.991E+00	1.333E+01	3.086E-06	-5.23E-08
150	200	1.077890	6.773E+00	1.192E+01	3.296E-06	-3.65E-08
160	200	1.088587	7.679E+00	1.031E+01	3.453E-06	-8.63E-09
170	200	1.099978	8.734E+00	8.473E+00	3.517E-06	3.36E-08
180	200	1.112113	9.967E+00	6.399E+00	3.444E-06	9.24E-08
190	200	1.125054	1.141E+01	4.052E+00	3.185E-06	1.70E-07
200	200	1.138874	1.312E+01	1.396E+00	2.684E-06	2.69E-07
210	200	1.153664	1.515E+01	-1.618E+00	1.872E-06	3.91E-07
220	200	1.169532	1.758E+01	-5.055E+00	6.700E-07	5.38E-07
230	200	1.186608	2.051E+01	-9.001E+00	-1.019E-06	7.15E-07
240	200	1.205052	2.407E+01	-1.357E+01	-3.314E-06	9.24E-07
250	200	1.225063	2.846E+01	-1.892E+01	-6.363E-06	1.17E-06
260	200	1.246892	3.392E+01	-2.529E+01	-1.036E-05	1.45E-06
270	200	1.270855	4.083E+01	-3.300E+01	-1.553E-05	1.79E-06
280	200	1.297370	4.974E+01	-4.257E+01	-2.221E-05	2.18E-06
290	200	1.326994	6.147E+01	-5.477E+01	-3.082E-05	2.63E-06
300	200	1.360501	7.737E+01	-7.091E+01	-4.195E-05	3.17E-06

Table 4

Parameters for Calculation of the Apparent Molal Volume

T	P	v_w	D-H Slope	$\bar{V}_2^\circ$	$\beta_v^{(0)}$	C_v^ϕ
°C	bar	$\frac{cm^3}{g}$	$\frac{cm^3}{mol}$	$\frac{cm^3}{mol}$	$\frac{g}{mol\ bar}$	$\frac{g^2}{mol^2\ bar}$
0	400	.981139	1.419E+00	1.566E+01	2.325E-05	-3.26E-06
10	400	.982347	1.532E+00	1.698E+01	1.665E-05	-2.25E-06
20	400	.984517	1.657E+00	1.789E+01	1.217E-05	-1.56E-06
25	400	.985902	1.726E+00	1.822E+01	1.047E-05	-1.29E-06
30	400	.987468	1.799E+00	1.850E+01	9.028E-06	-1.07E-06
40	400	.991092	1.961E+00	1.889E+01	6.779E-06	-7.19E-07
50	400	.995322	2.145E+00	1.910E+01	5.177E-06	-4.71E-07
50	400	.995322	2.145E+00	1.914E+01	4.708E-06	-3.32E-07
60	400	1.000115	2.355E+00	1.919E+01	3.642E-06	-2.00E-07
70	400	1.005441	2.593E+00	1.909E+01	2.953E-06	-1.22E-07
80	400	1.011282	2.864E+00	1.884E+01	2.552E-06	-7.97E-08
90	400	1.017626	3.171E+00	1.845E+01	2.371E-06	-6.02E-08
100	400	1.024466	3.520E+00	1.792E+01	2.359E-06	-5.46E-08
110	400	1.031802	3.918E+00	1.725E+01	2.474E-06	-5.59E-08
120	400	1.039636	4.370E+00	1.644E+01	2.681E-06	-5.87E-08
130	400	1.047976	4.886E+00	1.548E+01	2.947E-06	-5.87E-08
140	400	1.056837	5.476E+00	1.437E+01	3.242E-06	-5.23E-08
150	400	1.066235	6.151E+00	1.310E+01	3.538E-06	-3.65E-08
160	400	1.076195	6.927E+00	1.165E+01	3.803E-06	-8.63E-09
170	400	1.086745	7.819E+00	1.002E+01	4.007E-06	3.36E-08
180	400	1.097921	8.848E+00	8.196E+00	4.115E-06	9.24E-08
190	400	1.109765	1.004E+01	6.150E+00	4.087E-06	1.70E-07
200	400	1.122329	1.143E+01	3.863E+00	3.880E-06	2.69E-07
210	400	1.135670	1.305E+01	1.307E+00	3.441E-06	3.91E-07
220	400	1.149859	1.494E+01	-1.555E+00	2.708E-06	5.38E-07
230	400	1.164978	1.718E+01	-4.765E+00	1.608E-06	7.15E-07
240	400	1.181124	1.984E+01	-8.380E+00	4.760E-08	9.24E-07
250	400	1.198411	2.302E+01	-1.247E+01	-2.086E-06	1.17E-06
260	400	1.216977	2.686E+01	-1.714E+01	-4.937E-06	1.45E-06
270	400	1.236985	3.153E+01	-2.251E+01	-8.692E-06	1.79E-06
280	400	1.258636	3.728E+01	-2.876E+01	-1.359E-05	2.18E-06
290	400	1.282174	4.446E+01	-3.613E+01	-1.997E-05	2.63E-06
300	400	1.307904	5.358E+01	-4.501E+01	-2.826E-05	3.17E-06

Table 4

Parameters for Calculation of the Apparent Molal Volume

T	P	v_w	D-H Slope	$\bar{V}_2^\circ$	$\beta_v^{(0)}$	C_v^ϕ
°C	bar	$\frac{cm^3}{g}$	$\frac{cm^3}{mol}$	$\frac{cm^3}{mol}$	$\frac{g}{mol\ bar}$	$\frac{g^2}{mol^2\ bar}$
0	600	.972473	1.379E+00	1.668E+01	2.150E-05	-3.26E-06
10	600	.974133	1.479E+00	1.780E+01	1.548E-05	-2.25E-06
20	600	.976579	1.594E+00	1.858E+01	1.135E-05	-1.56E-06
25	600	.978056	1.657E+00	1.888E+01	9.756E-06	-1.29E-06
30	600	.979687	1.724E+00	1.912E+01	8.406E-06	-1.07E-06
40	600	.983379	1.873E+00	1.947E+01	6.279E-06	-7.19E-07
50	600	.987606	2.043E+00	1.967E+01	4.750E-06	-4.71E-07
50	600	.987606	2.043E+00	1.970E+01	4.300E-06	-3.32E-07
60	600	.992334	2.235E+00	1.974E+01	3.328E-06	-2.00E-07
70	600	.997542	2.453E+00	1.964E+01	2.704E-06	-1.22E-07
80	600	1.003214	2.699E+00	1.941E+01	2.344E-06	-7.97E-08
90	600	1.009341	2.978E+00	1.906E+01	2.186E-06	-6.02E-08
100	600	1.015916	3.293E+00	1.858E+01	2.183E-06	-5.46E-08
110	600	1.022937	3.649E+00	1.798E+01	2.297E-06	-5.59E-08
120	600	1.030405	4.052E+00	1.725E+01	2.496E-06	-5.87E-08
130	600	1.038326	4.509E+00	1.639E+01	2.753E-06	-5.87E-08
140	600	1.046708	5.027E+00	1.540E+01	3.043E-06	-5.23E-08
150	600	1.055564	5.615E+00	1.426E+01	3.341E-06	-3.65E-08
160	600	1.064911	6.284E+00	1.298E+01	3.623E-06	-8.63E-09
170	600	1.074770	7.046E+00	1.155E+01	3.863E-06	3.36E-08
180	600	1.085167	7.917E+00	9.942E+00	4.036E-06	9.24E-08
190	600	1.096132	8.913E+00	8.158E+00	4.110E-06	1.70E-07
200	600	1.107700	1.006E+01	6.180E+00	4.053E-06	2.69E-07
210	600	1.119913	1.137E+01	3.989E+00	3.825E-06	3.91E-07
220	600	1.132819	1.289E+01	1.564E+00	3.379E-06	5.38E-07
230	600	1.146474	1.465E+01	-1.117E+00	2.660E-06	7.15E-07
240	600	1.160941	1.669E+01	-4.085E+00	1.600E-06	9.24E-07
250	600	1.176293	1.908E+01	-7.373E+00	1.148E-07	1.17E-06
260	600	1.192615	2.189E+01	-1.102E+01	-1.904E-06	1.45E-06
270	600	1.210005	2.521E+01	-1.508E+01	-4.592E-06	1.79E-06
280	600	1.228578	2.917E+01	-1.961E+01	-8.131E-06	2.18E-06
290	600	1.248465	3.391E+01	-2.468E+01	-1.276E-05	2.63E-06
300	600	1.269825	3.967E+01	-3.037E+01	-1.881E-05	3.17E-06

Table 4

Parameters for Calculation of the Apparent Molal Volume

T	P	v_w	D-H Slope	$\bar{V}_2^\circ$	$\beta_v^{(0)}$	C_v^ϕ
°C	bar	$\frac{cm^3}{g}$	$\frac{cm^3}{mol}$	$\frac{cm^3}{mol}$	$\frac{g}{mol\ bar}$	$\frac{g^2}{mol^2\ bar}$
0	800	.964329	1.341E+00	1.759E+01	1.997E-05	-3.26E-06
10	800	.966373	1.431E+00	1.853E+01	1.450E-05	-2.25E-06
20	800	.969059	1.535E+00	1.920E+01	1.069E-05	-1.56E-06
25	800	.970616	1.593E+00	1.946E+01	9.198E-06	-1.29E-06
30	800	.972306	1.655E+00	1.967E+01	7.926E-06	-1.07E-06
40	800	.976061	1.792E+00	1.999E+01	5.905E-06	-7.19E-07
50	800	.980288	1.948E+00	2.016E+01	4.436E-06	-4.71E-07
50	800	.980288	1.948E+00	2.020E+01	3.964E-06	-3.32E-07
60	800	.984963	2.125E+00	2.024E+01	3.062E-06	-2.00E-07
70	800	.990070	2.324E+00	2.015E+01	2.474E-06	-1.22E-07
80	800	.995597	2.549E+00	1.995E+01	2.121E-06	-7.97E-08
90	800	1.001536	2.803E+00	1.964E+01	1.946E-06	-6.02E-08
100	800	1.007881	3.088E+00	1.922E+01	1.905E-06	-5.46E-08
110	800	1.014629	3.409E+00	1.870E+01	1.965E-06	-5.59E-08
120	800	1.021781	3.770E+00	1.806E+01	2.098E-06	-5.87E-08
130	800	1.029340	4.176E+00	1.731E+01	2.279E-06	-5.87E-08
140	800	1.037312	4.634E+00	1.645E+01	2.488E-06	-5.23E-08
150	800	1.045706	5.150E+00	1.546E+01	2.705E-06	-3.65E-08
160	800	1.054535	5.732E+00	1.435E+01	2.910E-06	-8.63E-09
170	800	1.063813	6.390E+00	1.311E+01	3.084E-06	3.36E-08
180	800	1.073560	7.134E+00	1.173E+01	3.206E-06	9.24E-08
190	800	1.083798	7.976E+00	1.020E+01	3.254E-06	1.70E-07
200	800	1.094554	8.932E+00	8.510E+00	3.203E-06	2.69E-07
210	800	1.105857	1.002E+01	6.647E+00	3.023E-06	3.91E-07
220	800	1.117742	1.125E+01	4.599E+00	2.682E-06	5.38E-07
230	800	1.130248	1.267E+01	2.351E+00	2.139E-06	7.15E-07
240	800	1.143419	1.428E+01	-1.131E-01	1.345E-06	9.24E-07
250	800	1.157306	1.613E+01	-2.812E+00	2.390E-07	1.17E-06
260	800	1.171965	1.827E+01	-5.763E+00	-1.255E-06	1.45E-06
270	800	1.187460	2.073E+01	-8.986E+00	-3.235E-06	1.79E-06
280	800	1.203864	2.359E+01	-1.250E+01	-5.829E-06	2.18E-06
290	800	1.221257	2.692E+01	-1.632E+01	-9.211E-06	2.63E-06
300	800	1.239733	3.082E+01	-2.044E+01	-1.361E-05	3.17E-06

Table 4

Parameters for Calculation of the Apparent Molal Volume

T	P	v_w	D-H Slope	$\bar{V}_2^\circ$	$\beta_v^{(0)}$	C_v^ϕ
°C	bar	$\frac{cm^3}{g}$	$\frac{cm^3}{mol}$	$\frac{cm^3}{mol}$	$\frac{g}{mol\ bar}$	$\frac{g^2}{mol^2\ bar}$
0	1000	.956683	1.307E+00	1.840E+01	1.869E-05	-3.26E-06
10	1000	.959040	1.386E+00	1.917E+01	1.372E-05	-2.25E-06
20	1000	.961926	1.480E+00	1.974E+01	1.019E-05	-1.56E-06
25	1000	.963552	1.533E+00	1.997E+01	8.792E-06	-1.29E-06
30	1000	.965293	1.590E+00	2.016E+01	7.590E-06	-1.07E-06
40	1000	.969102	1.716E+00	2.044E+01	5.658E-06	-7.19E-07
50	1000	.973330	1.860E+00	2.061E+01	4.235E-06	-4.71E-07
50	1000	.973330	1.860E+00	2.065E+01	3.698E-06	-3.32E-07
60	1000	.977959	2.022E+00	2.069E+01	2.845E-06	-2.00E-07
70	1000	.982978	2.206E+00	2.063E+01	2.265E-06	-1.22E-07
80	1000	.988378	2.412E+00	2.047E+01	1.884E-06	-7.97E-08
90	1000	.994152	2.643E+00	2.021E+01	1.651E-06	-6.02E-08
100	1000	1.000295	2.902E+00	1.987E+01	1.526E-06	-5.46E-08
110	1000	1.006805	3.192E+00	1.943E+01	1.480E-06	-5.59E-08
120	1000	1.013681	3.517E+00	1.890E+01	1.486E-06	-5.87E-08
130	1000	1.020925	3.881E+00	1.827E+01	1.525E-06	-5.87E-08
140	1000	1.028541	4.288E+00	1.755E+01	1.579E-06	-5.23E-08
150	1000	1.036535	4.743E+00	1.674E+01	1.631E-06	-3.65E-08
160	1000	1.044917	5.254E+00	1.581E+01	1.667E-06	-8.63E-09
170	1000	1.053699	5.827E+00	1.478E+01	1.670E-06	3.36E-08
180	1000	1.062894	6.469E+00	1.364E+01	1.627E-06	9.24E-08
190	1000	1.072519	7.190E+00	1.237E+01	1.519E-06	1.70E-07
200	1000	1.082595	7.999E+00	1.097E+01	1.329E-06	2.69E-07
210	1000	1.093143	8.910E+00	9.435E+00	1.036E-06	3.91E-07
220	1000	1.104190	9.935E+00	7.751E+00	6.171E-07	5.38E-07
230	1000	1.115764	1.109E+01	5.910E+00	4.313E-08	7.15E-07
240	1000	1.127898	1.239E+01	3.899E+00	-7.197E-07	9.24E-07
250	1000	1.140627	1.387E+01	1.709E+00	-1.713E-06	1.17E-06
260	1000	1.153991	1.553E+01	-6.714E-01	-2.991E-06	1.45E-06
270	1000	1.168034	1.743E+01	-3.251E+00	-4.620E-06	1.79E-06
280	1000	1.182806	1.957E+01	-6.037E+00	-6.688E-06	2.18E-06
290	1000	1.198361	2.202E+01	-9.027E+00	-9.315E-06	2.63E-06
300	1000	1.214758	2.482E+01	-1.221E+01	-1.266E-05	3.17E-06

Table 5

Parameters for Calculation of the Expansivity[a]

T	P	$\left(\frac{\partial v_w}{\partial T}\right)_P$	D-H Slope	$\left(\frac{\partial \bar{V}_2^\circ}{\partial T}\right)_P$	$\left(\frac{\partial \beta_v^{(0)}}{\partial T}\right)_P$	$\left(\frac{\partial C_v^\phi}{\partial T}\right)_P$
(°C)	(bar)	$\frac{cm^3}{gK}$	$\frac{cm^3}{mol\ K}$	$\frac{cm^3}{mol\ K}$	$\frac{g}{mol\ bar\ K}$	$\frac{g^2}{mol^2\ bar\ K}$
0	1	-8.022E-05	1.37E-02	2.21E-01	-9.79E-07	1.23E-07
10	1	8.747E-05	1.43E-02	1.44E-01	-6.34E-07	8.22E-08
20	1	2.094E-04	1.59E-02	9.57E-02	-4.31E-07	5.76E-08
25	1	2.602E-04	1.68E-02	7.72E-02	-3.60E-07	4.86E-08
30	1	3.064E-04	1.79E-02	6.13E-02	-3.01E-07	4.12E-08
40	1	3.890E-04	2.05E-02	3.49E-02	-2.12E-07	2.95E-08
50	1	4.627E-04	2.34E-02	1.32E-02	-1.48E-07	2.06E-08
50	1	4.627E-04	2.34E-02	1.85E-02	-1.57E-07	1.66E-08
60	1	5.310E-04	2.68E-02	-5.92E-04	-1.09E-07	1.01E-08
70	1	5.959E-04	3.07E-02	-1.85E-02	-7.31E-08	5.79E-09
80	1	6.588E-04	3.52E-02	-3.57E-02	-4.57E-08	2.92E-09
90	1	7.207E-04	4.04E-02	-5.27E-02	-2.49E-08	1.12E-09
100	1	7.826E-04	4.66E-02	-6.98E-02	-9.69E-09	1.13E-10
110	1	8.452E-04	5.37E-02	-8.72E-02	8.51E-10	-2.85E-10
120	2	9.093E-04	6.22E-02	-1.05E-01	7.09E-09	-2.02E-10
130	3	9.758E-04	7.22E-02	-1.25E-01	9.23E-09	2.69E-10
140	4	1.045E-03	8.40E-02	-1.45E-01	7.29E-09	1.07E-09
150	5	1.119E-03	9.82E-02	-1.68E-01	1.11E-09	2.14E-09
160	6	1.198E-03	1.15E-01	-1.93E-01	-9.56E-09	3.46E-09
170	8	1.283E-03	1.36E-01	-2.20E-01	-2.52E-08	5.02E-09
180	10	1.376E-03	1.61E-01	-2.52E-01	-4.63E-08	6.79E-09
190	13	1.479E-03	1.92E-01	-2.89E-01	-7.38E-08	8.77E-09
200	16	1.593E-03	2.31E-01	-3.33E-01	-1.09E-07	1.10E-08
210	19	1.720E-03	2.79E-01	-3.86E-01	-1.52E-07	1.34E-08
220	23	1.865E-03	3.40E-01	-4.51E-01	-2.05E-07	1.62E-08
230	28	2.030E-03	4.19E-01	-5.32E-01	-2.71E-07	1.92E-08
240	33	2.222E-03	5.22E-01	-6.37E-01	-3.52E-07	2.26E-08
250	40	2.447E-03	6.57E-01	-7.73E-01	-4.51E-07	2.64E-08
260	47	2.714E-03	8.40E-01	-9.57E-01	-5.74E-07	3.08E-08
270	55	3.037E-03	1.09E+00	-1.21E+00	-7.26E-07	3.59E-08
280	64	3.436E-03	1.44E+00	-1.57E+00	-9.17E-07	4.19E-08
290	74	3.939E-03	1.95E+00	-2.09E+00	-1.16E-06	4.92E-08
300	86	4.594E-03	2.72E+00	-2.88E+00	-1.47E-06	5.82E-08

Table 5

Parameters for Calculation of the Expansivity[a]

T	P	$\left(\frac{\partial v_w}{\partial T}\right)_P$	D-H Slope	$\left(\frac{\partial \bar{V}_2^\circ}{\partial T}\right)_P$	$\left(\frac{\partial \beta_v^{(0)}}{\partial T}\right)_P$	$\left(\frac{\partial C_v^\phi}{\partial T}\right)_P$
(°C)	(bar)	$\frac{cm^3}{gK}$	$\frac{cm^3}{mol\ K}$	$\frac{cm^3}{mol\ K}$	$\frac{g}{mol\ bar\ K}$	$\frac{g^2}{mol^2\ bar\ K}$
0	200	-2.807E-06	1.21E-02	1.89E-01	-8.93E-07	1.23E-07
10	200	1.326E-04	1.30E-02	1.26E-01	-5.83E-07	8.22E-08
20	200	2.350E-04	1.45E-02	8.47E-02	-4.00E-07	5.76E-08
25	200	2.785E-04	1.55E-02	6.89E-02	-3.35E-07	4.86E-08
30	200	3.185E-04	1.65E-02	5.52E-02	-2.82E-07	4.12E-08
40	200	3.909E-04	1.88E-02	3.22E-02	-2.00E-07	2.95E-08
50	200	4.564E-04	2.14E-02	1.30E-02	-1.40E-07	2.06E-08
50	200	4.564E-04	2.14E-02	1.57E-02	-1.42E-07	1.66E-08
60	200	5.175E-04	2.44E-02	-1.88E-03	-9.63E-08	1.01E-08
70	200	5.756E-04	2.79E-02	-1.83E-02	-6.16E-08	5.79E-09
80	200	6.320E-04	3.18E-02	-3.40E-02	-3.51E-08	2.92E-09
90	200	6.875E-04	3.63E-02	-4.95E-02	-1.48E-08	1.12E-09
100	200	7.426E-04	4.16E-02	-6.50E-02	5.06E-10	1.13E-10
110	200	7.982E-04	4.76E-02	-8.07E-02	1.15E-08	-2.85E-10
120	200	8.547E-04	5.47E-02	-9.70E-02	1.87E-08	-2.02E-10
130	200	9.128E-04	6.29E-02	-1.14E-01	2.23E-08	2.69E-10
140	200	9.732E-04	7.26E-02	-1.32E-01	2.24E-08	1.07E-09
150	200	1.037E-03	8.40E-02	-1.51E-01	1.90E-08	2.14E-09
160	200	1.104E-03	9.76E-02	-1.72E-01	1.17E-08	3.46E-09
170	200	1.175E-03	1.14E-01	-1.95E-01	3.28E-10	5.02E-09
180	200	1.253E-03	1.33E-01	-2.20E-01	-1.57E-08	6.79E-09
190	200	1.337E-03	1.57E-01	-2.49E-01	-3.70E-08	8.77E-09
200	200	1.429E-03	1.86E-01	-2.83E-01	-6.45E-08	1.10E-08
210	200	1.531E-03	2.21E-01	-3.21E-01	-9.92E-08	1.34E-08
220	200	1.645E-03	2.66E-01	-3.67E-01	-1.43E-07	1.62E-08
230	200	1.773E-03	3.22E-01	-4.23E-01	-1.97E-07	1.92E-08
240	200	1.919E-03	3.94E-01	-4.93E-01	-2.64E-07	2.26E-08
250	200	2.087E-03	4.87E-01	-5.81E-01	-3.49E-07	2.64E-08
260	200	2.284E-03	6.11E-01	-6.97E-01	-4.54E-07	3.08E-08
270	200	2.516E-03	7.80E-01	-8.54E-01	-5.87E-07	3.59E-08
280	200	2.796E-03	1.01E+00	-1.07E+00	-7.56E-07	4.19E-08
290	200	3.141E-03	1.35E+00	-1.39E+00	-9.75E-07	4.92E-08
300	200	3.578E-03	1.86E+00	-1.87E+00	-1.26E-06	5.82E-08

Table 5

Parameters for Calculation of the Expansivity[a]

T	P	$\left(\frac{\partial v_w}{\partial T}\right)_P$	D-H Slope	$\left(\frac{\partial \bar{V}_2^\circ}{\partial T}\right)_P$	$\left(\frac{\partial \beta_v^{(0)}}{\partial T}\right)_P$	$\left(\frac{\partial C_v^\phi}{T}\right)_P$
(°C)	(bar)	$\frac{cm^3}{gK}$	$\frac{cm^3}{mol\ K}$	$\frac{cm^3}{mol\ K}$	$\frac{g}{mol\ bar\ K}$	$\frac{g^2}{mol^2\ bar\ K}$
0	400	6.392E-05	1.07E-02	1.60E-01	-8.11E-07	1.23E-07
10	400	1.727E-04	1.18E-02	1.09E-01	-5.36E-07	8.22E-08
20	400	2.583E-04	1.33E-02	7.44E-02	-3.72E-07	5.76E-08
25	400	2.955E-04	1.42E-02	6.11E-02	-3.13E-07	4.86E-08
30	400	3.302E-04	1.52E-02	4.94E-02	-2.65E-07	4.12E-08
40	400	3.936E-04	1.73E-02	2.95E-02	-1.89E-07	2.95E-08
50	400	4.517E-04	1.96E-02	1.26E-02	-1.34E-07	2.06E-08
50	400	4.517E-04	1.96E-02	1.32E-02	-1.29E-07	1.66E-08
60	400	5.063E-04	2.23E-02	-2.74E-03	-8.60E-08	1.01E-08
70	400	5.586E-04	2.54E-02	-1.76E-02	-5.32E-08	5.79E-09
80	400	6.094E-04	2.88E-02	-3.19E-02	-2.82E-08	2.92E-09
90	400	6.593E-04	3.27E-02	-4.59E-02	-8.88E-09	1.12E-09
100	400	7.088E-04	3.72E-02	-5.99E-02	5.80E-09	1.13E-10
110	400	7.584E-04	4.24E-02	-7.40E-02	1.66E-08	-2.85E-10
120	400	8.086E-04	4.83E-02	-8.85E-02	2.41E-08	-2.02E-10
130	400	8.598E-04	5.51E-02	-1.03E-01	2.86E-08	2.69E-10
140	400	9.126E-04	6.30E-02	-1.19E-01	3.00E-08	1.07E-09
150	400	9.675E-04	7.23E-02	-1.36E-01	2.86E-08	2.14E-09
160	400	1.025E-03	8.30E-02	-1.53E-01	2.40E-08	3.46E-09
170	400	1.086E-03	9.57E-02	-1.73E-01	1.62E-08	5.02E-09
180	400	1.150E-03	1.11E-01	-1.93E-01	4.69E-09	6.79E-09
190	400	1.219E-03	1.28E-01	-2.16E-01	-1.09E-08	8.77E-09
200	400	1.294E-03	1.50E-01	-2.42E-01	-3.14E-08	1.10E-08
210	400	1.375E-03	1.75E-01	-2.70E-01	-5.75E-08	1.34E-08
220	400	1.464E-03	2.06E-01	-3.03E-01	-9.03E-08	1.62E-08
230	400	1.561E-03	2.43E-01	-3.40E-01	-1.31E-07	1.92E-08
240	400	1.670E-03	2.90E-01	-3.84E-01	-1.83E-07	2.26E-08
250	400	1.790E-03	3.48E-01	-4.36E-01	-2.47E-07	2.64E-08
260	400	1.926E-03	4.22E-01	-4.99E-01	-3.27E-07	3.08E-08
270	400	2.079E-03	5.16E-01	-5.77E-01	-4.28E-07	3.59E-08
280	400	2.255E-03	6.40E-01	-6.76E-01	-5.57E-07	4.19E-08
290	400	2.458E-03	8.05E-01	-8.05E-01	-7.25E-07	4.92E-08
300	400	2.695E-03	1.03E+00	-9.79E-01	-9.44E-07	5.82E-08

Table 5

Parameters for Calculation of the Expansivity[a]

T	P	$\left(\frac{\partial v_w}{\partial T}\right)_P$	D-H Slope	$\left(\frac{\partial \bar{V}_2^\circ}{\partial T}\right)_P$	$\left(\frac{\partial \beta_v^{(0)}}{\partial T}\right)_P$	$\left(\frac{\partial C_v^\phi}{\partial T}\right)_P$
(°C)	(bar)	$\frac{cm^3}{gK}$	$\frac{cm^3}{mol\ K}$	$\frac{cm^3}{mol\ K}$	$\frac{g}{mol\ bar\ K}$	$\frac{g^2}{mol^2\ bar\ K}$
0	600	1.211E-04	9.52E-03	1.34E-01	-7.34E-07	1.23E-07
10	600	2.079E-04	1.07E-02	9.29E-02	-4.92E-07	8.22E-08
20	600	2.793E-04	1.22E-02	6.50E-02	-3.46E-07	5.76E-08
25	600	3.111E-04	1.31E-02	5.39E-02	-2.93E-07	4.86E-08
30	600	3.410E-04	1.39E-02	4.40E-02	-2.49E-07	4.12E-08
40	600	3.966E-04	1.59E-02	2.69E-02	-1.80E-07	2.95E-08
50	600	4.482E-04	1.80E-02	1.19E-02	-1.28E-07	2.06E-08
50	600	4.482E-04	1.80E-02	1.12E-02	-1.18E-07	1.66E-08
60	600	4.971E-04	2.05E-02	-3.02E-03	-7.82E-08	1.01E-08
70	600	5.442E-04	2.32E-02	-1.63E-02	-4.80E-08	5.79E-09
80	600	5.901E-04	2.62E-02	-2.91E-02	-2.50E-08	2.92E-09
90	600	6.352E-04	2.96E-02	-4.16E-02	-7.34E-09	1.12E-09
100	600	6.798E-04	3.35E-02	-5.41E-02	6.12E-09	1.13E-10
110	600	7.244E-04	3.79E-02	-6.66E-02	1.62E-08	-2.85E-10
120	600	7.693E-04	4.29E-02	-7.94E-02	2.33E-08	-2.02E-10
130	600	8.150E-04	4.86E-02	-9.25E-02	2.77E-08	2.69E-10
140	600	8.617E-04	5.51E-02	-1.06E-01	2.98E-08	1.07E-09
150	600	9.098E-04	6.27E-02	-1.21E-01	2.94E-08	2.14E-09
160	600	9.599E-04	7.13E-02	-1.36E-01	2.66E-08	3.46E-09
170	600	1.012E-03	8.14E-02	-1.52E-01	2.11E-08	5.02E-09
180	600	1.068E-03	9.30E-02	-1.69E-01	1.29E-08	6.79E-09
190	600	1.126E-03	1.07E-01	-1.88E-01	1.47E-09	8.77E-09
200	600	1.188E-03	1.22E-01	-2.08E-01	-1.36E-08	1.10E-08
210	600	1.255E-03	1.41E-01	-2.30E-01	-3.29E-08	1.34E-08
220	600	1.327E-03	1.63E-01	-2.55E-01	-5.72E-08	1.62E-08
230	600	1.405E-03	1.89E-01	-2.82E-01	-8.77E-08	1.92E-08
240	600	1.490E-03	2.21E-01	-3.12E-01	-1.26E-07	2.26E-08
250	600	1.582E-03	2.59E-01	-3.46E-01	-1.73E-07	2.64E-08
260	600	1.684E-03	3.05E-01	-3.85E-01	-2.33E-07	3.08E-08
270	600	1.796E-03	3.61E-01	-4.28E-01	-3.08E-07	3.59E-08
280	600	1.921E-03	4.32E-01	-4.78E-01	-4.04E-07	4.19E-08
290	600	2.060E-03	5.21E-01	-5.37E-01	-5.28E-07	4.92E-08
300	600	2.215E-03	6.35E-01	-6.04E-01	-6.90E-07	5.82E-08

Table 5

Parameters for Calculation of the Expansivity[a]

T	P	$\left(\frac{\partial v_w}{\partial T}\right)_P$	D-H Slope	$\left(\frac{\partial \bar{V}_2^\circ}{\partial T}\right)_P$	$\left(\frac{\partial \beta_v^{(0)}}{\partial T}\right)_P$	$\left(\frac{\partial C_v^\phi}{\partial T}\right)_P$
(°C)	(bar)	$\frac{cm^3}{gK}$	$\frac{cm^3}{mol\ K}$	$\frac{cm^3}{mol\ K}$	$\frac{g}{mol\ bar\ K}$	$\frac{g^2}{mol^2\ bar\ K}$
0	800	1.689E-04	8.34E-03	1.10E-01	-6.63E-07	1.23E-07
10	800	2.381E-04	9.67E-03	7.87E-02	-4.51E-07	8.22E-08
20	800	2.978E-04	1.12E-02	5.65E-02	-3.22E-07	5.76E-08
25	800	3.249E-04	1.20E-02	4.74E-02	-2.75E-07	4.86E-08
30	800	3.508E-04	1.28E-02	3.91E-02	-2.35E-07	4.12E-08
40	800	3.995E-04	1.46E-02	2.44E-02	-1.72E-07	2.95E-08
50	800	4.454E-04	1.66E-02	1.12E-02	-1.24E-07	2.06E-08
50	800	4.454E-04	1.66E-02	9.84E-03	-1.09E-07	1.66E-08
60	800	4.893E-04	1.88E-02	-2.60E-03	-7.29E-08	1.01E-08
70	800	5.319E-04	2.12E-02	-1.43E-02	-4.59E-08	5.79E-09
80	800	5.734E-04	2.39E-02	-2.55E-02	-2.56E-08	2.92E-09
90	800	6.142E-04	2.69E-02	-3.64E-02	-1.02E-08	1.12E-09
100	800	6.547E-04	3.02E-02	-4.73E-02	1.48E-09	1.13E-10
110	800	6.950E-04	3.40E-02	-5.82E-02	1.01E-08	-2.85E-10
120	800	7.355E-04	3.83E-02	-6.92E-02	1.61E-08	-2.02E-10
130	800	7.764E-04	4.31E-02	-8.06E-02	1.99E-08	2.69E-10
140	800	8.181E-04	4.86E-02	-9.23E-02	2.16E-08	1.07E-09
150	800	8.609E-04	5.48E-02	-1.05E-01	2.14E-08	2.14E-09
160	800	9.050E-04	6.18E-02	-1.17E-01	1.93E-08	3.46E-09
170	800	9.509E-04	6.99E-02	-1.31E-01	1.52E-08	5.02E-09
180	800	9.989E-04	7.91E-02	-1.45E-01	8.89E-09	6.79E-09
190	800	1.049E-03	8.96E-02	-1.61E-01	2.66E-10	8.77E-09
200	800	1.102E-03	1.02E-01	-1.77E-01	-1.10E-08	1.10E-08
210	800	1.159E-03	1.16E-01	-1.95E-01	-2.54E-08	1.34E-08
220	800	1.219E-03	1.32E-01	-2.15E-01	-4.35E-08	1.62E-08
230	800	1.283E-03	1.51E-01	-2.35E-01	-6.60E-08	1.92E-08
240	800	1.352E-03	1.73E-01	-2.58E-01	-9.39E-08	2.26E-08
250	800	1.426E-03	1.99E-01	-2.82E-01	-1.29E-07	2.64E-08
260	800	1.507E-03	2.29E-01	-3.08E-01	-1.72E-07	3.08E-08
270	800	1.594E-03	2.65E-01	-3.37E-01	-2.26E-07	3.59E-08
280	800	1.688E-03	3.08E-01	-3.66E-01	-2.95E-07	4.19E-08
290	800	1.792E-03	3.60E-01	-3.97E-01	-3.85E-07	4.92E-08
300	800	1.905E-03	4.23E-01	-4.28E-01	-5.02E-07	5.82E-08

Table 5

Parameters for Calculation of the Expansivity[a]

T	P	$\left(\frac{\partial v_w}{\partial T}\right)_P$	D-H Slope	$\left(\frac{\partial \bar{V}_2^\circ}{\partial T}\right)_P$	$\left(\frac{\partial \beta_v^{(0)}}{\partial T}\right)_P$	$\left(\frac{\partial C_v^\phi}{\partial T}\right)_P$
(°C)	(bar)	$\frac{cm^3}{gK}$	$\frac{cm^3}{mol\ K}$	$\frac{cm^3}{mol\ K}$	$\frac{g}{mol\ bar\ K}$	$\frac{g^2}{mol^2\ bar\ K}$
0	1000	2.072E-04	7.18E-03	8.92E-02	-5.96E-07	1.23E-07
10	1000	2.631E-04	8.66E-03	6.62E-02	-4.14E-07	8.22E-08
20	1000	3.134E-04	1.02E-02	4.89E-02	-3.01E-07	5.76E-08
25	1000	3.368E-04	1.10E-02	4.16E-02	-2.59E-07	4.86E-08
30	1000	3.593E-04	1.18E-02	3.48E-02	-2.23E-07	4.12E-08
40	1000	4.022E-04	1.35E-02	2.22E-02	-1.66E-07	2.95E-08
50	1000	4.431E-04	1.53E-02	1.05E-02	-1.20E-07	2.06E-08
50	1000	4.431E-04	1.53E-02	9.21E-03	-1.02E-07	1.66E-08
60	1000	4.826E-04	1.73E-02	-1.38E-03	-7.02E-08	1.01E-08
70	1000	5.211E-04	1.94E-02	-1.13E-02	-4.70E-08	5.79E-09
80	1000	5.588E-04	2.18E-02	-2.08E-02	-2.99E-08	2.92E-09
90	1000	5.959E-04	2.45E-02	-3.01E-02	-1.73E-08	1.12E-09
100	1000	6.327E-04	2.74E-02	-3.93E-02	-8.14E-09	1.13E-10
110	1000	6.693E-04	3.07E-02	-4.84E-02	-1.66E-09	-2.85E-10
120	1000	7.059E-04	3.43E-02	-5.77E-02	2.58E-09	-2.02E-10
130	1000	7.429E-04	3.84E-02	-6.71E-02	4.92E-09	2.69E-10
140	1000	7.804E-04	4.31E-02	-7.69E-02	5.57E-09	1.07E-09
150	1000	8.187E-04	4.82E-02	-8.70E-02	4.66E-09	2.14E-09
160	1000	8.580E-04	5.40E-02	-9.76E-02	2.22E-09	3.46E-09
170	1000	8.986E-04	6.06E-02	-1.09E-01	-1.73E-09	5.02E-09
180	1000	9.407E-04	6.80E-02	-1.21E-01	-7.29E-09	6.79E-09
190	1000	9.847E-04	7.63E-02	-1.33E-01	-1.46E-08	8.77E-09
200	1000	1.031E-03	8.58E-02	-1.46E-01	-2.38E-08	1.10E-08
210	1000	1.079E-03	9.65E-02	-1.61E-01	-3.52E-08	1.34E-08
220	1000	1.131E-03	1.09E-01	-1.76E-01	-4.91E-08	1.62E-08
230	1000	1.185E-03	1.23E-01	-1.92E-01	-6.62E-08	1.92E-08
240	1000	1.242E-03	1.38E-01	-2.10E-01	-8.70E-08	2.26E-08
250	1000	1.304E-03	1.57E-01	-2.28E-01	-1.13E-07	2.64E-08
260	1000	1.370E-03	1.77E-01	-2.48E-01	-1.44E-07	3.08E-08
270	1000	1.440E-03	2.01E-01	-2.68E-01	-1.83E-07	3.59E-08
280	1000	1.515E-03	2.29E-01	-2.89E-01	-2.32E-07	4.19E-08
290	1000	1.597E-03	2.61E-01	-3.09E-01	-2.95E-07	4.92E-08
300	1000	1.684E-03	2.99E-01	-3.28E-01	-3.78E-07	5.82E-08

Table 6

Parameters for Calculation of the Compressibility

T	P	$\left(\frac{\partial v_w}{\partial P}\right)_T$	D-H Slope	$\left(\frac{\partial \bar{V}_2^\circ}{\partial P}\right)_T$	$\left(\frac{\partial \beta_v^{(0)}}{\partial P}\right)_T$
°C	bar	$\frac{cm^3}{g\ bar}$	$\frac{cm^3}{mol\ bar}$	$\frac{cm^3}{mol\ bar}$	$\frac{g}{mol\ bar^2}$
0	1	-5.101E-05	-2.01E-04	6.63E-03	-1.17E-08
10	1	-4.777E-05	-2.81E-04	5.34E-03	-8.27E-09
20	1	-4.593E-05	-3.51E-04	4.58E-03	-6.18E-09
25	1	-4.535E-05	-3.88E-04	4.34E-03	-5.46E-09
30	1	-4.496E-05	-4.25E-04	4.15E-03	-4.89E-09
40	1	-4.462E-05	-5.08E-04	3.93E-03	-4.07E-09
50	1	-4.477E-05	-6.04E-04	3.87E-03	-3.54E-09
50	1	-4.477E-05	-6.04E-04	3.70E-03	-2.92E-09
60	1	-4.533E-05	-7.18E-04	3.59E-03	-2.18E-09
70	1	-4.627E-05	-8.55E-04	3.56E-03	-1.50E-09
80	1	-4.757E-05	-1.02E-03	3.60E-03	-8.65E-10
90	1	-4.921E-05	-1.22E-03	3.71E-03	-2.44E-10
100	1	-5.122E-05	-1.47E-03	3.91E-03	3.82E-10
110	1	-5.361E-05	-1.77E-03	4.19E-03	1.03E-09
120	2	-5.641E-05	-2.14E-03	4.58E-03	1.74E-09
130	3	-5.966E-05	-2.60E-03	5.08E-03	2.52E-09
140	4	-6.343E-05	-3.17E-03	5.73E-03	3.41E-09
150	5	-6.777E-05	-3.88E-03	6.54E-03	4.44E-09
160	6	-7.279E-05	-4.78E-03	7.58E-03	5.66E-09
170	8	-7.860E-05	-5.93E-03	8.89E-03	7.09E-09
180	10	-8.535E-05	-7.38E-03	1.06E-02	8.79E-09
190	13	-9.320E-05	-9.25E-03	1.27E-02	1.08E-08
200	16	-1.024E-04	-1.17E-02	1.55E-02	1.33E-08
210	19	-1.133E-04	-1.49E-02	1.91E-02	1.62E-08
220	23	-1.262E-04	-1.91E-02	2.39E-02	1.97E-08
230	28	-1.418E-04	-2.47E-02	3.04E-02	2.38E-08
240	33	-1.607E-04	-3.23E-02	3.92E-02	2.89E-08
250	40	-1.839E-04	-4.27E-02	5.13E-02	3.49E-08
260	47	-2.130E-04	-5.72E-02	6.84E-02	4.22E-08
270	55	-2.499E-04	-7.78E-02	9.27E-02	5.10E-08
280	64	-2.980E-04	-1.08E-01	1.28E-01	6.17E-08
290	74	-3.622E-04	-1.52E-01	1.81E-01	7.49E-08
300	86	-4.507E-04	-2.18E-01	2.61E-01	9.12E-08

Table 6

Parameters for Calculation of the Compressibility

T	P	$\left(\frac{\partial v_w}{\partial P}\right)_T$	D-H Slope	$\left(\frac{\partial \bar{V}_2^\circ}{\partial P}\right)_T$	$\left(\frac{\partial \beta_v^{(0)}}{\partial P}\right)_T$
°C	bar	$\frac{cm^3}{g\ bar}$	$\frac{cm^3}{mol\ bar}$	$\frac{cm^3}{mol\ bar}$	$\frac{g}{mol\ bar^2}$
0	200	-4.764E-05	-2.15E-04	5.98E-03	-1.06E-08
10	200	-4.484E-05	-2.81E-04	4.8[illegible]E-03	-7.30E-09
20	200	-4.320E-05	-3.42E-04	4.10E-03	-5.37E-09
25	200	-4.267E-05	-3.75E-04	3.87E-03	-4.70E-09
30	200	-4.230E-05	-4.08E-04	3.69E-03	-4.18E-09
40	200	-4.195E-05	-4.82E-04	3.48E-03	-3.44E-09
50	200	-4.204E-05	-5.69E-04	3.40E-03	-2.98E-09
50	200	-4.204E-05	-5.69E-04	3.29E-03	-2.57E-09
60	200	-4.248E-05	-6.71E-04	3.20E-03	-1.94E-09
70	200	-4.325E-05	-7.92E-04	3.18E-03	-1.40E-09
80	200	-4.433E-05	-9.37E-04	3.24E-03	-9.35E-10
90	200	-4.571E-05	-1.11E-03	3.37E-03	-5.16E-10
100	200	-4.740E-05	-1.33E-03	3.57E-03	-1.22E-10
110	200	-4.939E-05	-1.58E-03	3.86E-03	2.69E-10
120	200	-5.173E-05	-1.90E-03	4.23E-03	6.81E-10
130	200	-5.443E-05	-2.28E-03	4.70E-03	1.14E-09
140	200	-5.754E-05	-2.76E-03	5.29E-03	1.67E-09
150	200	-6.110E-05	-3.35E-03	6.01E-03	2.30E-09
160	200	-6.517E-05	-4.08E-03	6.90E-03	3.08E-09
170	200	-6.984E-05	-4.99E-03	7.98E-03	4.04E-09
180	200	-7.520E-05	-6.14E-03	9.32E-03	5.23E-09
190	200	-8.137E-05	-7.59E-03	1.10E-02	6.71E-09
200	200	-8.851E-05	-9.46E-03	1.31E-02	8.54E-09
210	200	-9.681E-05	-1.19E-02	1.57E-02	1.08E-08
220	200	-1.065E-04	-1.50E-02	1.91E-02	1.36E-08
230	200	-1.180E-04	-1.91E-02	2.36E-02	1.71E-08
240	200	-1.317E-04	-2.46E-02	2.95E-02	2.13E-08
250	200	-1.482E-04	-3.21E-02	3.76E-02	2.66E-08
260	200	-1.684E-04	-4.24E-02	4.88E-02	3.31E-08
270	200	-1.935E-04	-5.69E-02	6.46E-02	4.11E-08
280	200	-2.253E-04	-7.79E-02	8.78E-02	5.10E-08
290	200	-2.665E-04	-1.09E-01	1.23E-01	6.34E-08
300	200	-3.217E-04	-1.57E-01	1.77E-01	7.91E-08

Table 6

Parameters for Calculation of the Compressibility

T	P	$\left(\frac{\partial v_w}{\partial P}\right)_T$	D-H Slope	$\left(\frac{\partial \bar{V}_2^\circ}{\partial P}\right)_T$	$\left(\frac{\partial \beta_v^{(0)}}{P}\right)_T$
°C	bar	$\frac{cm^3}{g\ bar}$	$\frac{cm^3}{mol\ bar}$	$\frac{cm^3}{mol\ bar}$	$\frac{g}{mol\ bar^2}$
0	400	-4.469E-05	-2.11E-04	5.39E-03	-9.38E-09
10	400	-4.226E-05	-2.70E-04	4.31E-03	-6.34E-09
20	400	-4.079E-05	-3.26E-04	3.67E-03	-4.54E-09
25	400	-4.031E-05	-3.55E-04	3.45E-03	-3.94E-09
30	400	-3.997E-05	-3.86E-04	3.29E-03	-3.47E-09
40	400	-3.962E-05	-4.53E-04	3.08E-03	-2.81E-09
50	400	-3.965E-05	-5.31E-04	3.01E-03	-2.42E-09
50	400	-3.965E-05	-5.31E-04	2.94E-03	-2.22E-09
60	400	-4.001E-05	-6.22E-04	2.87E-03	-1.69E-09
70	400	-4.065E-05	-7.30E-04	2.88E-03	-1.30E-09
80	400	-4.157E-05	-8.58E-04	2.97E-03	-1.01E-09
90	400	-4.274E-05	-1.01E-03	3.12E-03	-7.89E-10
100	400	-4.417E-05	-1.20E-03	3.36E-03	-6.28E-10
110	400	-4.586E-05	-1.42E-03	3.67E-03	-5.02E-10
120	400	-4.784E-05	-1.68E-03	4.06E-03	-3.88E-10
130	400	-5.011E-05	-2.01E-03	4.54E-03	-2.65E-10
140	400	-5.270E-05	-2.40E-03	5.12E-03	-1.08E-10
150	400	-5.565E-05	-2.88E-03	5.81E-03	1.11E-10
160	400	-5.899E-05	-3.47E-03	6.64E-03	4.24E-10
170	400	-6.278E-05	-4.19E-03	7.61E-03	8.66E-10
180	400	-6.708E-05	-5.09E-03	8.77E-03	1.48E-09
190	400	-7.195E-05	-6.20E-03	1.01E-02	2.31E-09
200	400	-7.750E-05	-7.60E-03	1.18E-02	3.42E-09
210	400	-8.383E-05	-9.35E-03	1.38E-02	4.88E-09
220	400	-9.108E-05	-1.16E-02	1.62E-02	6.77E-09
230	400	-9.944E-05	-1.44E-02	1.93E-02	9.20E-09
240	400	-1.091E-04	-1.81E-02	2.31E-02	1.23E-08
250	400	-1.204E-04	-2.29E-02	2.80E-02	1.62E-08
260	400	-1.336E-04	-2.93E-02	3.44E-02	2.11E-08
270	400	-1.493E-04	-3.78E-02	4.29E-02	2.74E-08
280	400	-1.681E-04	-4.94E-02	5.44E-02	3.52E-08
290	400	-1.907E-04	-6.56E-02	7.05E-02	4.52E-08
300	400	-2.185E-04	-8.86E-02	9.35E-02	5.78E-08

Table 6

Parameters for Calculation of the Compressibility

T	P	$\left(\frac{\partial v_w}{\partial P}\right)_T$	D-H Slope	$\left(\frac{\partial \bar{V}_2^\circ}{\partial P}\right)_T$	$\left(\frac{\partial \beta_v^{(0)}}{\partial P}\right)_T$
°C	bar	$\frac{cm^3}{g\ bar}$	$\frac{cm^3}{mol\ bar}$	$\frac{cm^3}{mol\ bar}$	$\frac{g}{mol\ bar^2}$
0	600	-4.200E-05	-1.97E-04	4.83E-03	-8.20E-09
10	600	-3.991E-05	-2.53E-04	3.86E-03	-5.37E-09
20	600	-3.862E-05	-3.06E-04	3.27E-03	-3.72E-09
25	600	-3.819E-05	-3.33E-04	3.07E-03	-3.17E-09
30	600	-3.787E-05	-3.62E-04	2.92E-03	-2.75E-09
40	600	-3.755E-05	-4.23E-04	2.73E-03	-2.18E-09
50	600	-3.755E-05	-4.94E-04	2.66E-03	-1.85E-09
50	600	-3.755E-05	-4.94E-04	2.65E-03	-1.86E-09
60	600	-3.784E-05	-5.76E-04	2.61E-03	-1.45E-09
70	600	-3.838E-05	-6.72E-04	2.65E-03	-1.20E-09
80	600	-3.916E-05	-7.85E-04	2.77E-03	-1.08E-09
90	600	-4.017E-05	-9.19E-04	2.97E-03	-1.06E-09
100	600	-4.140E-05	-1.08E-03	3.24E-03	-1.13E-09
110	600	-4.286E-05	-1.27E-03	3.59E-03	-1.27E-09
120	600	-4.456E-05	-1.50E-03	4.03E-03	-1.46E-09
130	600	-4.650E-05	-1.77E-03	4.55E-03	-1.67E-09
140	600	-4.871E-05	-2.10E-03	5.17E-03	-1.88E-09
150	600	-5.120E-05	-2.49E-03	5.88E-03	-2.08E-09
160	600	-5.401E-05	-2.97E-03	6.71E-03	-2.23E-09
170	600	-5.716E-05	-3.55E-03	7.67E-03	-2.31E-09
180	600	-6.070E-05	-4.26E-03	8.77E-03	-2.27E-09
190	600	-6.468E-05	-5.12E-03	1.00E-02	-2.08E-09
200	600	-6.915E-05	-6.18E-03	1.15E-02	-1.69E-09
210	600	-7.418E-05	-7.49E-03	1.32E-02	-1.04E-09
220	600	-7.986E-05	-9.12E-03	1.52E-02	-6.61E-11
230	600	-8.628E-05	-1.11E-02	1.75E-02	1.33E-09
240	600	-9.358E-05	-1.37E-02	2.03E-02	3.24E-09
250	600	-1.019E-04	-1.69E-02	2.36E-02	5.81E-09
260	600	-1.114E-04	-2.10E-02	2.77E-02	9.21E-09
270	600	-1.224E-04	-2.63E-02	3.28E-02	1.36E-08
280	600	-1.351E-04	-3.32E-02	3.91E-02	1.94E-08
290	600	-1.498E-04	-4.22E-02	4.73E-02	2.69E-08
300	600	-1.671E-04	-5.43E-02	5.80E-02	3.66E-08

Table 6

Parameters for Calculation of the Compressibility

T	P	$\left(\frac{\partial v_w}{\partial P}\right)_T$	D-H Slope	$\left(\frac{\partial \bar{V}_2^\circ}{\partial P}\right)_T$	$\left(\frac{\partial \beta_v^{(0)}}{\partial P}\right)_T$
°C	bar	$\frac{cm^3}{g\ bar}$	$\frac{cm^3}{mol\ bar}$	$\frac{cm^3}{mol\ bar}$	$\frac{g}{mol\ bar^2}$
0	800	-3.946E-05	-1.80E-04	4.30E-03	-7.02E-09
10	800	-3.772E-05	-2.34E-04	3.43E-03	-4.40E-09
20	800	-3.661E-05	-2.85E-04	2.90E-03	-2.90E-09
25	800	-3.624E-05	-3.10E-04	2.72E-03	-2.41E-09
30	800	-3.596E-05	-3.37E-04	2.59E-03	-2.04E-09
40	800	-3.567E-05	-3.94E-04	2.42E-03	-1.55E-09
50	800	-3.566E-05	-4.58E-04	2.35E-03	-1.29E-09
50	800	-3.566E-05	-4.58E-04	2.39E-03	-1.50E-09
60	800	-3.591E-05	-5.32E-04	2.38E-03	-1.21E-09
70	800	-3.637E-05	-6.17E-04	2.47E-03	-1.10E-09
80	800	-3.705E-05	-7.18E-04	2.63E-03	-1.15E-09
90	800	-3.793E-05	-8.36E-04	2.88E-03	-1.34E-09
100	800	-3.900E-05	-9.75E-04	3.21E-03	-1.64E-09
110	800	-4.028E-05	-1.14E-03	3.62E-03	-2.04E-09
120	800	-4.175E-05	-1.33E-03	4.11E-03	-2.53E-09
130	800	-4.343E-05	-1.57E-03	4.70E-03	-3.07E-09
140	800	-4.534E-05	-1.84E-03	5.37E-03	-3.66E-09
150	800	-4.748E-05	-2.17E-03	6.15E-03	-4.27E-09
160	800	-4.988E-05	-2.56E-03	7.04E-03	-4.89E-09
170	800	-5.255E-05	-3.03E-03	8.05E-03	-5.48E-09
180	800	-5.554E-05	-3.60E-03	9.18E-03	-6.02E-09
190	800	-5.886E-05	-4.28E-03	1.05E-02	-6.48E-09
200	800	-6.256E-05	-5.10E-03	1.19E-02	-6.81E-09
210	800	-6.668E-05	-6.10E-03	1.35E-02	-6.97E-09
220	800	-7.128E-05	-7.31E-03	1.53E-02	-6.91E-09
230	800	-7.642E-05	-8.79E-03	1.74E-02	-6.54E-09
240	800	-8.217E-05	-1.06E-02	1.97E-02	-5.80E-09
250	800	-8.863E-05	-1.28E-02	2.24E-02	-4.57E-09
260	800	-9.590E-05	-1.56E-02	2.54E-02	-2.72E-09
270	800	-1.041E-04	-1.91E-02	2.90E-02	-6.86E-11
280	800	-1.134E-04	-2.34E-02	3.31E-02	3.61E-09
290	800	-1.240E-04	-2.89E-02	3.79E-02	8.62E-09
300	800	-1.360E-04	-3.59E-02	4.37E-02	1.54E-08

Table 6

Parameters for Calculation of the Compressibility

T	P	$\left(\frac{\partial v_w}{\partial P}\right)_T$	D-H Slope	$\left(\frac{\partial \bar{V}_2^\circ}{\partial P}\right)_T$	$\left(\frac{\partial \beta_v^{(0)}}{\partial P}\right)_T$
°C	bar	$\frac{cm^3}{g\ bar}$	$\frac{cm^3}{mol\ bar}$	$\frac{cm^3}{mol\ bar}$	$\frac{g}{mol\ bar^2}$
0	1000	-3.701E-05	-1.63E-04	3.78E-03	-5.85E-09
10	1000	-3.563E-05	-2.15E-04	3.02E-03	-3.43E-09
20	1000	-3.473E-05	-2.64E-04	2.56E-03	-2.08E-09
25	1000	-3.442E-05	-2.88E-04	2.40E-03	-1.65E-09
30	1000	-3.419E-05	-3.13E-04	2.28E-03	-1.33E-09
40	1000	-3.394E-05	-3.65E-04	2.14E-03	-9.22E-10
50	1000	-3.394E-05	-4.24E-04	2.07E-03	-7.22E-10
50	1000	-3.394E-05	-4.24E-04	2.16E-03	-1.15E-09
60	1000	-3.416E-05	-4.91E-04	2.20E-03	-9.62E-10
70	1000	-3.457E-05	-5.68E-04	2.33E-03	-9.95E-10
80	1000	-3.517E-05	-6.57E-04	2.54E-03	-1.22E-09
90	1000	-3.594E-05	-7.62E-04	2.84E-03	-1.61E-09
100	1000	-3.689E-05	-8.84E-04	3.23E-03	-2.15E-09
110	1000	-3.801E-05	-1.03E-03	3.71E-03	-2.81E-09
120	1000	-3.931E-05	-1.19E-03	4.28E-03	-3.59E-09
130	1000	-4.078E-05	-1.39E-03	4.95E-03	-4.47E-09
140	1000	-4.245E-05	-1.63E-03	5.71E-03	-5.44E-09
150	1000	-4.431E-05	-1.90E-03	6.59E-03	-6.47E-09
160	1000	-4.639E-05	-2.23E-03	7.57E-03	-7.55E-09
170	1000	-4.870E-05	-2.61E-03	8.67E-03	-8.66E-09
180	1000	-5.125E-05	-3.07E-03	9.90E-03	-9.77E-09
190	1000	-5.408E-05	-3.61E-03	1.13E-02	-1.09E-08
200	1000	-5.721E-05	-4.26E-03	1.28E-02	-1.19E-08
210	1000	-6.066E-05	-5.03E-03	1.45E-02	-1.29E-08
220	1000	-6.448E-05	-5.95E-03	1.63E-02	-1.37E-08
230	1000	-6.871E-05	-7.06E-03	1.83E-02	-1.44E-08
240	1000	-7.340E-05	-8.39E-03	2.06E-02	-1.48E-08
250	1000	-7.859E-05	-1.00E-02	2.31E-02	-1.50E-08
260	1000	-8.437E-05	-1.19E-02	2.58E-02	-1.46E-08
270	1000	-9.080E-05	-1.43E-02	2.88E-02	-1.38E-08
280	1000	-9.797E-05	-1.72E-02	3.22E-02	-1.22E-08
290	1000	-1.060E-04	-2.07E-02	3.58E-02	-9.65E-09
300	1000	-1.150E-04	-2.51E-02	3.98E-02	-5.85E-09

Table 7

Specific Volumes of Aqueous Sodium Chloride Solutions ($cm^3\ g^{-1}$)

TEMP (°C)	PRESS (BAR)	MOLALITY .1000	.2500	.5000	.7500	1.0000	2.0000	3.0000	4.0000	5.0000
0	1	.995732	.989259	.978889	.968991	.959525	.925426	.896292	.870996	.848646
10	1	.995998	.989781	.979804	.970256	.961101	.927905	.899262	.874201	.851958
20	1	.997620	.991564	.981833	.972505	.963544	.930909	.902565	.877643	.855469
25	1	.998834	.992832	.983185	.973932	.965038	.932590	.904339	.879457	.857301
30	1	1.000279	.994319	.984735	.975539	.966694	.934382	.906194	.881334	.859185
40	1	1.003796	.997883	.988374	.979243	.970455	.938287	.910145	.885276	.863108
50	1	1.008064	1.002161	.992668	.983551	.974772	.942603	.914411	.889473	.867241
50	1	1.0081	1.0022	.9927	.9836	.9748	.9427	.9145	.8895	.8673
60	1	1.0130	1.0071	.9976	.9885	.9797	.9474	.9191	.8940	.8716
70	1	1.0186	1.0127	1.0031	.9939	.9851	.9526	.9240	.8987	.8762
80	1	1.0249	1.0188	1.0092	.9999	.9909	.9581	.9293	.9037	.8809
90	1	1.0317	1.0256	1.0157	1.0063	.9972	.9640	.9348	.9089	.8858
100	1	1.0391	1.0329	1.0228	1.0133	1.0040	.9703	.9406	.9144	.8910
110	1	1.0471	1.0407	1.0305	1.0207	1.0113	.9769	.9468	.9201	.8964
120	2	1.0557	1.0491	1.0386	1.0286	1.0190	.9839	.9532	.9261	.9020
130	3	1.0649	1.0582	1.0474	1.0371	1.0272	.9912	.9599	.9323	.9078
140	4	1.0748	1.0678	1.0567	1.0461	1.0359	.9990	.9670	.9388	.9139
150	5	1.0854	1.0781	1.0666	1.0556	1.0452	1.0072	.9744	.9456	.9202
160	6	1.0966	1.0891	1.0771	1.0658	1.0550	1.0159	.9821	.9527	.9267
170	8	1.1087	1.1008	1.0884	1.0766	1.0654	1.0250	.9903	.9601	.9335
180	10	1.1215	1.1133	1.1003	1.0881	1.0765	1.0347	.9989	.9678	.9406
190	13	1.1353	1.1266	1.1131	1.1004	1.0883	1.0449	1.0079	.9759	.9479
200	16	1.1500	1.1409	1.1268	1.1134	1.1008	1.0558	1.0175	.9844	.9556
210	19	1.1658	1.1562	1.1413	1.1274	1.1142	1.0673	1.0276	.9933	.9635
220	23	1.1828	1.1727	1.1570	1.1424	1.1286	1.0796	1.0382	1.0027	.9718
230	28	1.2011	1.1904	1.1738	1.1584	1.1440	1.0927	1.0496	1.0125	.9804
240	33	1.2209	1.2095	1.1920	1.1757	1.1605	1.1068	1.0616	1.0229	.9893
250	40	1.2425	1.2303	1.2116	1.1944	1.1783	1.1218	1.0744	1.0338	.9986
260	47	1.2661	1.2529	1.2330	1.2146	1.1976	1.1379	1.0881	1.0454	1.0082
270	55	1.2920	1.2777	1.2562	1.2366	1.2184	1.1552	1.1027	1.0575	1.0182
280	64	1.3206	1.3050	1.2817	1.2606	1.2411	1.1739	1.1182	1.0704	1.0286
290	74	1.3526	1.3353	1.3097	1.2868	1.2657	1.1938	1.1347	1.0839	1.0394
300	86	1.3886	1.3691	1.3407	1.3155	1.2926	1.2151	1.1520	1.0979	1.0504

Table 7

Specific Volumes of Aqueous Sodium Chloride Solutions ($cm^3\ g^{-1}$)

TEMP (°C)	PRESS (BAR)	MOLALITY .1000	.2500	.5000	.7500	1.0000	2.0000	3.0000	4.0000	5.0000
0	200	.986107	.979894	.969937	.960426	.951324	.918469			
10	200	.986943	.980946	.971317	.962097	.953251	.921123			
20	200	.988895	.983034	.973613	.964577	.955893	.924219			
25	200	.990212	.984397	.975047	.966075	.957446	.925922	.898408	.874105	.852393
30	200	.991729	.985950	.976653	.967728	.959139	.927724	.900255	.875964	.854257
40	200	.995310	.989570	.980336	.971464	.962921	.931614	.904167	.879856	.858128
50	200	.999554	.993820	.984597	.975734	.967196	.935872	.908366	.883982	.862192
50	200	.9996	.9938	.9846	.9758	.9672	.9359	.9084	.8840	.8622
60	200	1.0044	.9987	.9894	.9805	.9720	.9405	.9129	.8884	.8664
70	200	1.0098	1.0041	.9947	.9858	.9772	.9455	.9177	.8929	.8708
80	200	1.0158	1.0100	1.0006	.9915	.9828	.9508	.9227	.8977	.8754
90	200	1.0224	1.0164	1.0068	.9977	.9888	.9565	.9280	.9027	.8802
100	200	1.0294	1.0233	1.0136	1.0043	.9953	.9624	.9335	.9080	.8852
110	200	1.0370	1.0308	1.0209	1.0113	1.0022	.9687	.9394	.9134	.8903
120	200	1.0452	1.0388	1.0286	1.0188	1.0095	.9753	.9455	.9191	.8957
130	200	1.0539	1.0473	1.0368	1.0268	1.0172	.9823	.9518	.9250	.9013
140	200	1.0631	1.0563	1.0455	1.0353	1.0254	.9896	.9585	.9312	.9071
150	200	1.0730	1.0660	1.0548	1.0442	1.0341	.9973	.9655	.9376	.9131
160	200	1.0835	1.0762	1.0647	1.0537	1.0432	1.0054	.9728	.9443	.9194
170	200	1.0947	1.0871	1.0751	1.0637	1.0529	1.0139	.9804	.9513	.9259
180	200	1.1066	1.0987	1.0862	1.0744	1.0632	1.0229	.9885	.9586	.9326
190	200	1.1192	1.1110	1.0980	1.0857	1.0741	1.0324	.9969	.9663	.9397
200	200	1.1327	1.1241	1.1105	1.0978	1.0857	1.0425	1.0058	.9743	.9470
210	200	1.1472	1.1381	1.1239	1.1106	1.0980	1.0531	1.0152	.9827	.9547
220	200	1.1627	1.1531	1.1383	1.1243	1.1112	1.0645	1.0251	.9915	.9626
230	200	1.1794	1.1693	1.1536	1.1390	1.1253	1.0766	1.0357	1.0008	.9709
240	200	1.1973	1.1867	1.1702	1.1548	1.1404	1.0896	1.0470	1.0107	.9796
250	200	1.2168	1.2055	1.1880	1.1719	1.1567	1.1035	1.0590	1.0211	.9887
260	200	1.2380	1.2259	1.2074	1.1904	1.1744	1.1185	1.0719	1.0322	.9981
270	200	1.2613	1.2483	1.2286	1.2105	1.1936	1.1348	1.0858	1.0441	1.0081
280	200	1.2869	1.2729	1.2517	1.2325	1.2146	1.1524	1.1008	1.0567	1.0185
290	200	1.3154	1.3001	1.2773	1.2566	1.2375	1.1716	1.1170	1.0702	1.0295
300	200	1.3476	1.3307	1.3057	1.2833	1.2628	1.1925	1.1345	1.0846	1.0410

Table 7

Specific Volumes of Aqueous Sodium Chloride Solutions ($cm^3\ g^{-1}$)

TEMP (°C)	PRESS (BAR)	MOLALITY .1000	.2500	.5000	.7500	1.0000	2.0000	3.0000	4.0000	5.0000
0	400	.977044	.971070	.961490	.952335	.943568	.911854			
10	400	.978376	.972581	.963271	.954353	.945792	.914647			
20	400	.980625	.974942	.965806	.957038	.948608	.917820			
25	400	.982037	.976394	.967316	.958601	.950215	.919544	.892715	.868956	.847668
30	400	.983622	.978008	.968974	.960297	.951944	.921355	.894554	.870797	.849512
40	400	.987267	.981686	.972702	.964068	.955750	.925234	.898430	.874641	.853332
50	400	.991498	.985919	.976942	.968310	.959992	.929443	.902569	.878700	.857327
50	400	.9915	.9859	.9770	.9683	.9600	.9295	.9026	.8787	.8574
60	400	.9963	.9907	.9817	.9730	.9647	.9340	.9070	.8829	.8615
70	400	1.0016	.9959	.9869	.9781	.9697	.9388	.9116	.8874	.8658
80	400	1.0074	1.0016	.9925	.9837	.9752	.9439	.9165	.8920	.8702
90	400	1.0136	1.0078	.9985	.9896	.9810	.9494	.9216	.8969	.8748
100	400	1.0204	1.0145	1.0050	.9959	.9872	.9551	.9269	.9019	.8796
110	400	1.0276	1.0216	1.0119	1.0026	.9937	.9611	.9325	.9071	.8846
120	400	1.0353	1.0291	1.0192	1.0098	1.0006	.9674	.9383	.9126	.8897
130	400	1.0436	1.0372	1.0270	1.0173	1.0080	.9740	.9443	.9182	.8951
140	400	1.0523	1.0457	1.0352	1.0252	1.0157	.9809	.9506	.9241	.9006
150	400	1.0615	1.0547	1.0439	1.0336	1.0238	.9881	.9572	.9202	.9064
160	400	1.0713	1.0643	1.0531	1.0425	1.0323	.9957	.9641	.9365	.9123
170	400	1.0816	1.0743	1.0628	1.0518	1.0413	1.0036	.9712	.9431	.9185
180	400	1.0926	1.0850	1.0730	1.0617	1.0508	1.0119	.9787	.9499	.9249
190	400	1.1042	1.0963	1.0838	1.0720	1.0608	1.0207	.9865	.9571	.9315
200	400	1.1165	1.1082	1.0953	1.0830	1.0714	1.0299	.9947	.9645	.9384
210	400	1.1296	1.1209	1.1074	1.0946	1.0826	1.0396	1.0033	.9723	.9456
220	400	1.1434	1.1344	1.1202	1.1070	1.0944	1.0498	1.0123	.9804	.9531
230	400	1.1582	1.1487	1.1339	1.1201	1.1070	1.0607	1.0218	.9889	.9608
240	400	1.1740	1.1640	1.1485	1.1340	1.1203	1.0722	1.0319	.9979	.9689
250	400	1.1908	1.1803	1.1640	1.1489	1.1346	1.0845	1.0426	1.0073	.9773
260	400	1.2089	1.1978	1.1807	1.1648	1.1499	1.0976	1.0541	1.0173	.9861
270	400	1.2284	1.2166	1.1986	1.1819	1.1663	1.1117	1.0663	1.0279	.9953
280	400	1.2494	1.2369	1.2179	1.2004	1.1840	1.1269	1.0794	1.0392	1.0050
290	400	1.2723	1.2590	1.2388	1.2204	1.2032	1.1433	1.0935	1.0512	1.0151
300	400	1.2972	1.2830	1.2616	1.2421	1.2240	1.1612	1.1089	1.0642	1.0257

Table 7

Specific Volumes of Aqueous Sodium Chloride Solutions ($cm^3\ g^{-1}$)

TEMP (°C)	PRESS (BAR)	MOLALITY .1000	.2500	.5000	.7500	1.0000	2.0000	3.0000	4.0000	5.0000
0	600	.968527	.962771	.953537	.944706	.936244	.905577			
10	600	.970289	.964678	.955661	.947019	.938718	.908479			
20	600	.972800	.967282	.958405	.949884	.941687	.911717			
25	600	.974299	.968812	.959983	.951504	.943341	.913457	.887267	.864024	.843145
30	600	.975946	.970483	.961690	.953240	.945103	.915277	.889098	.865848	.844970
40	600	.979655	.974217	.965462	.957045	.948933	.919146	.892942	.869647	.848740
50	600	.983879	.978442	.969688	.961268	.953151	.923312	.897026	.873642	.852668
50	600	.9839	.9784	.9697	.9613	.9532	.9233	.8970	.8736	.8527
60	600	.9886	.9831	.9743	.9659	.9577	.9278	.9013	.8778	.8567
70	600	.9938	.9883	.9794	.9709	.9627	.9325	.9058	.8821	.8609
80	600	.9994	.9938	.9849	.9763	.9680	.9375	.9106	.8867	.8653
90	600	1.0055	.9998	.9907	.9820	.9736	.9427	.9155	.8913	.8697
100	600	1.0119	1.0062	.9970	.9881	.9795	.9482	.9207	.8962	.8744
110	600	1.0189	1.0130	1.0036	.9945	.9858	.9540	.9260	.9013	.8792
120	600	1.0262	1.0202	1.0106	1.0013	.9925	.9600	.9316	.9065	.8841
130	600	1.0340	1.0279	1.0180	1.0085	.9994	.9663	.9374	.9119	.8893
140	600	1.0423	1.0359	1.0258	1.0161	1.0068	.9729	.9434	.9175	.8946
150	600	1.0510	1.0444	1.0340	1.0240	1.0145	.9798	.9497	.9233	.9001
160	600	1.0602	1.0534	1.0426	1.0323	1.0225	.9869	.9562	.9294	.9058
170	600	1.0699	1.0628	1.0517	1.0411	1.0310	.9944	.9630	.9356	.9117
180	600	1.0801	1.0728	1.0612	1.0503	1.0398	1.0022	.9700	.9421	.9177
190	600	1.0908	1.0832	1.0713	1.0599	1.0492	1.0104	.9773	.9488	.9241
200	600	1.1021	1.0943	1.0818	1.0701	1.0589	1.0189	.9850	.9558	.9306
210	600	1.1141	1.1059	1.0930	1.0808	1.0692	1.0279	.9929	.9630	.9374
220	600	1.1267	1.1182	1.1047	1.0920	1.0800	1.0373	1.0013	.9706	.9444
230	600	1.1401	1.1311	1.1171	1.1039	1.0914	1.0472	1.0100	.9785	.9517
240	600	1.1542	1.1448	1.1302	1.1165	1.1035	1.0576	1.0192	.9867	.9592
250	600	1.1692	1.1594	1.1441	1.1298	1.1163	1.0686	1.0289	.9954	.9671
260	600	1.1852	1.1748	1.1588	1.1439	1.1298	1.0803	1.0391	1.0044	.9753
270	600	1.2021	1.1913	1.1745	1.1589	1.1443	1.0928	1.0500	1.0140	.9838
280	600	1.2203	1.2088	1.1913	1.1750	1.1597	1.1061	1.0616	1.0241	.9927
290	600	1.2397	1.2276	1.2092	1.1922	1.1763	1.1204	1.0740	1.0349	1.0020
300	600	1.2605	1.2478	1.2285	1.2107	1.1941	1.1359	1.0875	1.0465	1.0118

Table 7

Specific Volumes of Aqueous Sodium Chloride Solutions ($cm^3\ g^{-1}$)

TEMP (°C)	PRESS (BAR)	MOLALITY .1000	.2500	.5000	.7500	1.0000	2.0000	3.0000	4.0000	5.0000
0	800	.960519	.954961	.946041	.937506	.929323	.899616			
10	800	.962645	.957201	.948451	.940061	.932000	.902598			
20	800	.965383	.960014	.951375	.943079	.935097	.905884			
25	800	.966958	.961614	.953013	.944750	.936793	.907639	.882050	.859300	.838822
30	800	.968661	.963336	.954762	.946522	.938584	.909464	.883872	.861107	.840628
40	800	.972428	.967122	.958577	.950358	.942436	.913324	.887686	.864862	.844349
50	800	.976651	.971342	.962792	.954567	.946634	.917453	.891718	.868797	.848212
50	800	.9767	.9713	.9628	.9546	.9466	.9175	.8917	.8688	.8482
60	800	.9813	.9760	.9674	.9591	.9512	.9218	.8959	.8729	.8522
70	800	.9864	.9810	.9724	.9640	.9560	.9265	.9004	.8771	.8563
80	800	.9919	.9864	.9777	.9693	.9612	.9313	.9050	.8816	.8606
90	800	.9977	.9922	.9834	.9749	.9666	.9365	.9098	.8861	.8649
100	800	1.0040	.9984	.9894	.9808	.9724	.9418	.9149	.8909	.8695
110	800	1.0107	1.0050	.9958	.9870	.9785	.9474	.9201	.8958	.8741
120	800	1.0177	1.0119	1.0025	.9935	.9849	.9532	.9255	.9009	.8789
130	800	1.0252	1.0192	1.0096	1.0004	.9916	.9593	.9311	.9061	.8839
140	800	1.0330	1.0269	1.0170	1.0076	.9986	.9657	.9369	.9115	.8890
150	800	1.0413	1.0350	1.0249	1.0152	1.0060	.9723	.9429	.9171	.8943
160	800	1.0500	1.0435	1.0330	1.0231	1.0136	.9791	.9492	.9229	.8997
170	800	1.0591	1.0524	1.0416	1.0314	1.0216	.9862	.9556	.9289	.9054
180	800	1.0687	1.0617	1.0506	1.0401	1.0300	.9937	.9623	.9351	.9112
190	800	1.0787	1.0715	1.0600	1.0492	1.0388	1.0014	.9693	.9415	.9172
200	800	1.0893	1.0818	1.0699	1.0587	1.0479	1.0094	.9765	.9481	.9234
210	800	1.1004	1.0926	1.0802	1.0686	1.0575	1.0178	.9840	.9550	.9298
220	800	1.1120	1.1039	1.0911	1.0790	1.0676	1.0266	.9919	.9621	.9365
230	800	1.1243	1.1158	1.1025	1.0900	1.0781	1.0358	1.0000	.9695	.9434
240	800	1.1371	1.1283	1.1145	1.1015	1.0892	1.0454	1.0085	.9772	.9505
250	800	1.1507	1.1415	1.1271	1.1136	1.1008	1.0555	1.0174	.9852	.9579
260	800	1.1651	1.1554	1.1404	1.1264	1.1131	1.0661	1.0267	.9935	.9655
270	800	1.1802	1.1701	1.1545	1.1399	1.1261	1.0773	1.0366	1.0023	.9735
280	800	1.1962	1.1857	1.1694	1.1541	1.1398	1.0892	1.0470	1.0115	.9817
290	800	1.2132	1.2022	1.1852	1.1693	1.1544	1.1019	1.0580	1.0212	.9904
300	800	1.2313	1.2197	1.2020	1.1855	1.1700	1.1155	1.0699	1.0315	.9994

Table 7

Specific Volumes of Aqueous Sodium Chloride Solutions ($cm^3\ g^{-1}$)

TEMP (°C)	PRESS (BAR)	MOLALITY .1000	.2500	.5000	.7500	1.0000	2.0000	3.0000	4.0000	5.0000
0	1000	.952997	.947618	.938982	.930716	.922786	.893956			
10	1000	.955416	.950125	.941619	.933460	.925617	.896986			
20	1000	.958344	.953112	.944690	.936602	.928817	.900307			
25	1000	.959984	.954771	.946379	.938314	.930547	.902071	.877050	.854776	.834697
30	1000	.961734	.956536	.948165	.940116	.932362	.903900	.878863	.856567	.836484
40	1000	.965552	.960367	.952015	.943979	.936232	.907750	.882646	.860279	.840156
50	1000	.969775	.964584	.956222	.948174	.940412	.911844	.886630	.864156	.843954
50	1000	.9698	.9646	.9562	.9482	.9404	.9119	.8866	.8641	.8439
60	1000	.9744	.9692	.9608	.9527	.9449	.9162	.8908	.8682	.8479
70	1000	.9794	.9741	.9657	.9575	.9497	.9208	.8952	.8724	.8520
80	1000	.9847	.9794	.9709	.9627	.9547	.9255	.8997	.8768	.8561
90	1000	.9905	.9851	.9764	.9681	.9601	.9306	.9045	.8813	.8604
100	1000	.9965	.9911	.9823	.9739	.9657	.9358	.9094	.8859	.8648
110	1000	1.0030	.9974	.9885	.9799	.9716	.9413	.9145	.8907	.8694
120	1000	1.0098	1.0041	.9950	.9862	.9778	.9470	.9198	.8957	.8741
130	1000	1.0169	1.0111	1.0018	.9929	.9843	.9529	.9253	.9008	.8789
140	1000	1.0244	1.0185	1.0090	.9999	.9911	.9591	.9310	.9061	.8838
150	1000	1.0323	1.0262	1.0164	1.0071	.9982	.9655	.9368	.9115	.8889
160	1000	1.0406	1.0343	1.0243	1.0147	1.0055	.9721	.9429	.9171	.8942
170	1000	1.0492	1.0427	1.0324	1.0226	1.0132	.9790	.9492	.9229	.8996
180	1000	1.0582	1.0516	1.0410	1.0309	1.0212	.9861	.9556	.9289	.9052
190	1000	1.0677	1.0608	1.0499	1.0395	1.0296	.9935	.9623	.9350	.9110
200	1000	1.0776	1.0705	1.0592	1.0485	1.0383	1.0012	.9693	.9414	.9169
210	1000	1.0880	1.0806	1.0689	1.0579	1.0473	1.0092	.9765	.9480	.9230
220	1000	1.0988	1.0912	1.0791	1.0677	1.0568	1.0176	.9839	.9548	.9294
230	1000	1.1102	1.1022	1.0897	1.0779	1.0667	1.0262	.9916	.9618	.9359
240	1000	1.1221	1.1138	1.1008	1.0886	1.0770	1.0353	.9997	.9691	.9427
250	1000	1.1345	1.1260	1.1125	1.0998	1.0878	1.0447	1.0080	.9766	.9496
260	1000	1.1476	1.1387	1.1247	1.1116	1.0991	1.0545	1.0167	.9844	.9568
270	1000	1.1614	1.1521	1.1375	1.1239	1.1110	1.0649	1.0258	.9926	.9643
280	1000	1.1758	1.1661	1.1510	1.1369	1.1235	1.0757	1.0354	1.0011	.9720
290	1000	1.1911	1.1810	1.1652	1.1505	1.1366	1.0871	1.0454	1.0099	.9801
300	1000	1.2071	1.1966	1.1802	1.1650	1.1506	1.0993	1.0560	1.0192	.9884

Table 8

Expansivities of Sodium Chloride Solutions: $\frac{1}{v}\left(\frac{\partial v}{\partial T}\right)_{P,m} \times 10^3$ K

TEMP (°C)	PRESS (BAR)	MOLALITY .100	.250	.500	.750	1.000	2.000	3.000	4.000
0	1	-.058	-.026	.024	.069	.110	.237	.313	.355
10	1	.102	.123	.156	.186	.213	.297	.349	.380
20	1	.218	.232	.254	.274	.292	.349	.384	.406
25	1	.267	.278	.296	.312	.327	.373	.401	.420
30	1	.311	.320	.334	.347	.359	.395	.418	.433
40	1	.389	.394	.402	.410	.417	.438	.451	.460
50	1	.458	.460	.464	.467	.470	.479	.484	.486
50	1	.46	.46	.47	.47	.47	.49	.49	.49
60	1	.52	.52	.52	.52	.52	.52	.52	.52
70	1	.58	.58	.58	.57	.57	.56	.55	.54
80	1	.64	.63	.63	.62	.61	.60	.58	.56
90	1	.69	.68	.67	.67	.66	.63	.61	.59
100	1	.74	.73	.72	.71	.70	.66	.64	.61
110	1	.80	.78	.77	.75	.74	.70	.66	.64
120	2	.85	.84	.82	.80	.78	.73	.69	.66
130	3	.90	.89	.86	.85	.83	.77	.72	.69
140	4	.96	.94	.91	.89	.87	.80	.75	.71
150	5	1.01	.99	.97	.94	.92	.84	.78	.74
160	6	1.07	1.05	1.02	.99	.97	.88	.82	.77
170	8	1.13	1.11	1.08	1.05	1.02	.93	.86	.80
180	10	1.20	1.18	1.14	1.11	1.08	.98	.90	.83
190	13	1.27	1.25	1.21	1.17	1.14	1.03	.94	.86
200	16	1.35	1.32	1.28	1.24	1.20	1.08	.99	.90
210	19	1.44	1.41	1.36	1.32	1.28	1.15	1.04	.94
220	23	1.54	1.50	1.45	1.40	1.36	1.21	1.09	.99
230	28	1.65	1.60	1.54	1.49	1.45	1.29	1.15	1.03
240	33	1.77	1.72	1.65	1.60	1.55	1.37	1.22	1.09
250	40	1.91	1.85	1.78	1.71	1.66	1.46	1.30	1.14
260	47	2.07	2.01	1.92	1.85	1.78	1.56	1.38	1.20
270	55	2.27	2.19	2.08	2.00	1.92	1.67	1.46	1.26
280	64	2.50	2.40	2.27	2.17	2.08	1.79	1.55	1.33
290	74	2.78	2.66	2.50	2.36	2.25	1.91	1.64	1.39
300	86	3.13	2.97	2.76	2.59	2.45	2.02	1.71	1.44

Table 8

Expansivities of Sodium Chloride Solutions: $\frac{1}{v}\left(\frac{\partial v}{\partial T}\right)_{P,m} \times 10^3$ K

TEMP (°C)	PRESS (BAR)	MOLALITY .100	.250	.500	.750	1.000	2.000	3.000	4.000
0	200	.016	.044	.086	.125	.159	.264		
10	200	.146	.165	.193	.219	.242	.313		
20	200	.245	.257	.276	.294	.309	.358		
25	200	.287	.297	.312	.326	.339	.379	.403	.419
30	200	.325	.333	.346	.357	.367	.399	.418	.431
40	200	.394	.399	.406	.413	.419	.438	.449	.456
50	200	.456	.458	.461	.464	.466	.474	.478	.480
50	200	.46	.46	.46	.47	.47	.48	.48	.48
60	200	.51	.51	.51	.51	.51	.51	.51	.50
70	200	.57	.56	.56	.56	.55	.54	.53	.53
80	200	.62	.61	.60	.60	.59	.58	.56	.55
90	200	.66	.66	.65	.64	.63	.61	.58	.57
100	200	.71	.70	.69	.68	.67	.64	.61	.59
110	200	.76	.75	.73	.72	.71	.67	.63	.61
120	200	.81	.79	.78	.76	.74	.70	.66	.63
130	200	.85	.84	.82	.80	.78	.73	.68	.65
140	200	.90	.88	.86	.84	.82	.76	.71	.68
150	200	.95	.93	.91	.88	.86	.79	.74	.70
160	200	1.00	.98	.95	.93	.90	.83	.77	.72
170	200	1.05	1.03	1.00	.97	.95	.86	.80	.75
180	200	1.11	1.09	1.05	1.02	.99	.90	.83	.78
190	200	1.17	1.14	1.11	1.08	1.05	.95	.87	.81
200	200	1.23	1.21	1.17	1.13	1.10	.99	.91	.84
210	200	1.30	1.27	1.23	1.19	1.16	1.04	.95	.88
220	200	1.38	1.35	1.30	1.26	1.23	1.10	1.00	.91
230	200	1.47	1.43	1.38	1.34	1.30	1.16	1.05	.96
240	200	1.56	1.52	1.47	1.42	1.38	1.23	1.11	1.00
250	200	1.67	1.63	1.57	1.51	1.47	1.31	1.18	1.05
260	200	1.79	1.74	1.67	1.62	1.57	1.40	1.25	1.11
270	200	1.93	1.88	1.80	1.74	1.68	1.49	1.33	1.17
280	200	2.10	2.03	1.94	1.87	1.80	1.60	1.42	1.24
290	200	2.30	2.21	2.11	2.02	1.94	1.71	1.51	1.31
300	200	2.54	2.43	2.30	2.19	2.10	1.82	1.60	1.37

Table 8

Expansivities of Sodium Chloride Solutions: $\frac{1}{v}\left(\frac{\partial v}{\partial T}\right)_{P,m} \times 10^3$ K

TEMP (°C)	PRESS (BAR)	MOLALITY .100	.250	.500	.750	1.000	2.000	3.000	4.000
0	400	.081	.105	.140	.172	.201	.285		
10	400	.187	.202	.227	.248	.268	.326		
20	400	.270	.280	.297	.312	.325	.366		
25	400	.306	.314	.328	.340	.351	.384	.404	.418
30	400	.339	.346	.357	.367	.376	.403	.419	.429
40	400	.400	.404	.410	.416	.422	.437	.446	.452
50	400	.455	.456	.459	.462	.464	.470	.473	.474
50	400	.45	.46	.46	.46	.46	.47	.47	.47
60	400	.51	.50	.50	.50	.50	.50	.50	.49
70	400	.55	.55	.55	.54	.54	.53	.52	.51
80	400	.60	.59	.59	.58	.58	.56	.54	.53
90	400	.64	.64	.63	.62	.61	.59	.57	.55
100	400	.69	.68	.67	.65	.65	.61	.59	.57
110	400	.73	.72	.70	.69	.68	.64	.61	.59
120	400	.77	.76	.74	.73	.71	.67	.63	.61
130	400	.81	.80	.78	.76	.75	.69	.65	.63
140	400	.85	.84	.82	.80	.78	.72	.68	.65
150	400	.90	.88	.86	.83	.81	.75	.70	.67
160	400	.94	.92	.90	.87	.85	.78	.73	.69
170	400	.98	.97	.94	.91	.89	.81	.75	.71
180	400	1.03	1.01	.98	.95	.93	.84	.78	.74
190	400	1.08	1.06	1.03	1.00	.97	.88	.81	.76
200	400	1.13	1.11	1.07	1.04	1.01	.92	.84	.79
210	400	1.19	1.16	1.13	1.09	1.06	.96	.88	.82
220	400	1.25	1.22	1.18	1.15	1.11	1.00	.92	.85
230	400	1.32	1.29	1.24	1.21	1.17	1.05	.96	.88
240	400	1.39	1.36	1.31	1.27	1.23	1.11	1.01	.92
250	400	1.47	1.43	1.38	1.34	1.30	1.17	1.06	.96
260	400	1.55	1.51	1.46	1.42	1.38	1.24	1.12	1.01
270	400	1.65	1.61	1.55	1.50	1.46	1.31	1.19	1.06
280	400	1.75	1.71	1.65	1.60	1.55	1.40	1.26	1.12
290	400	1.87	1.82	1.76	1.71	1.66	1.50	1.35	1.19
300	400	2.01	1.96	1.88	1.83	1.78	1.61	1.45	1.27

Table 8

Expansivities of Sodium Chloride Solutions: $\frac{1}{v}\left(\frac{\partial v}{\partial T}\right)_{P,m} \times 10^3$ K

TEMP (°C)	PRESS (BAR)	MOLALITY .100	.250	.500	.750	1.000	2.000	3.000	4.000
0	600	.138	.157	.187	.213	.236	.302		
10	600	.223	.236	.256	.275	.291	.338		
20	600	.292	.301	.316	.328	.340	.373		
25	600	.323	.331	.342	.353	.362	.390	.406	.416
30	600	.352	.358	.368	.376	.384	.406	.419	.427
40	600	.406	.409	.415	.420	.424	.437	.444	.448
50	600	.455	.456	.458	.460	.462	.467	.468	.468
50	600	.45	.46	.46	.46	.46	.47	.47	.47
60	600	.50	.50	.50	.50	.50	.49	.49	.48
70	600	.54	.54	.54	.53	.53	.52	.51	.50
80	600	.58	.58	.57	.57	.56	.55	.53	.52
90	600	.62	.62	.61	.60	.59	.57	.55	.54
100	600	.66	.66	.64	.63	.63	.59	.57	.55
110	600	.70	.69	.68	.67	.66	.62	.59	.57
120	600	.74	.73	.71	.70	.69	.64	.61	.59
130	600	.78	.76	.75	.73	.72	.67	.63	.60
140	600	.81	.80	.78	.76	.75	.69	.65	.62
150	600	.85	.84	.81	.79	.78	.72	.67	.64
160	600	.89	.87	.85	.83	.81	.74	.69	.66
170	600	.93	.91	.88	.86	.84	.77	.72	.68
180	600	.97	.95	.92	.90	.87	.80	.74	.70
190	600	1.01	.99	.96	.93	.91	.83	.76	.72
200	600	1.06	1.03	1.00	.97	.95	.86	.79	.74
210	600	1.10	1.08	1.05	1.01	.99	.89	.82	.77
220	600	1.15	1.13	1.09	1.06	1.03	.93	.85	.80
230	600	1.20	1.18	1.14	1.11	1.07	.97	.89	.82
240	600	1.26	1.23	1.19	1.16	1.12	1.01	.92	.85
250	600	1.32	1.29	1.25	1.21	1.18	1.06	.97	.89
260	600	1.39	1.36	1.31	1.27	1.24	1.12	1.01	.93
270	600	1.46	1.43	1.38	1.34	1.30	1.18	1.07	.97
280	600	1.53	1.50	1.45	1.41	1.38	1.25	1.13	1.02
290	600	1.62	1.58	1.54	1.50	1.46	1.33	1.20	1.08
300	600	1.71	1.68	1.63	1.59	1.55	1.42	1.29	1.15

Table 8

Expansivities of Sodium Chloride Solutions: $\frac{1}{v}\left(\frac{\partial v}{\partial T}\right)_{P,m} \times 10^3$ K

TEMP (°C)	PRESS (BAR)	MOLALITY .100	.250	.500	.750	1.000	2.000	3.000	4.000
0	800	.186	.202	.226	.246	.265	.315		
10	800	.254	.265	.282	.297	.310	.347		
20	800	.313	.320	.332	.343	.353	.379		
25	800	.339	.346	.356	.365	.372	.395	.407	.415
30	800	.364	.370	.378	.385	.391	.409	.419	.425
40	800	.411	.414	.419	.424	.427	.438	.442	.445
50	800	.455	.456	.458	.460	.461	.464	.464	.463
50	800	.45	.46	.46	.46	.46	.46	.46	.46
60	800	.50	.50	.49	.49	.49	.49	.48	.48
70	800	.54	.53	.53	.53	.52	.51	.50	.50
80	800	.57	.57	.56	.56	.55	.54	.52	.51
90	800	.61	.60	.60	.59	.58	.56	.54	.53
100	800	.64	.64	.63	.62	.61	.58	.56	.54
110	800	.68	.67	.66	.65	.64	.60	.58	.56
120	800	.71	.70	.69	.68	.66	.63	.60	.57
130	800	.75	.74	.72	.70	.69	.65	.61	.59
140	800	.78	.77	.75	.73	.72	.67	.63	.60
150	800	.81	.80	.78	.76	.75	.69	.65	.62
160	800	.85	.83	.81	.79	.77	.71	.67	.64
170	800	.88	.87	.84	.82	.80	.74	.69	.65
180	800	.92	.90	.88	.85	.83	.76	.71	.67
190	800	.95	.94	.91	.88	.86	.79	.73	.69
200	800	.99	.97	.94	.92	.89	.81	.75	.71
210	800	1.03	1.01	.98	.95	.93	.84	.78	.73
220	800	1.07	1.05	1.02	.99	.96	.87	.80	.75
230	800	1.12	1.09	1.06	1.03	1.00	.91	.83	.78
240	800	1.16	1.14	1.10	1.07	1.04	.94	.86	.80
250	800	1.21	1.19	1.15	1.12	1.09	.98	.90	.83
260	800	1.26	1.24	1.20	1.16	1.13	1.02	.93	.86
270	800	1.32	1.29	1.25	1.22	1.18	1.07	.98	.89
280	800	1.38	1.35	1.31	1.27	1.24	1.13	1.02	.93
290	800	1.44	1.41	1.37	1.34	1.31	1.19	1.08	.98
300	800	1.51	1.48	1.44	1.41	1.38	1.26	1.15	1.03

Table 8

Expansivities of Sodium Chloride Solutions: $\frac{1}{v}\left(\frac{\partial v}{\partial T}\right)_{P,m} \times 10^3$ K

TEMP (°C)	PRESS (BAR)	MOLALITY .100	.250	.500	.750	1.000	2.000	3.000	4.000
0	1000	.225	.238	.257	.273	.286	.322		
10	1000	.281	.290	.304	.316	.326	.354		
20	1000	.330	.337	.347	.356	.363	.384		
25	1000	.353	.359	.367	.375	.381	.398	.407	.414
30	1000	.375	.380	.387	.393	.398	.412	.419	.423
40	1000	.417	.419	.423	.427	.430	.438	.440	.441
50	1000	.456	.457	.458	.459	.461	.462	.460	.458
50	1000	.46	.46	.46	.46	.46	.46	.46	.46
60	1000	.49	.49	.49	.49	.49	.49	.48	.48
70	1000	.53	.53	.52	.52	.52	.51	.50	.49
80	1000	.56	.56	.55	.55	.55	.53	.52	.51
90	1000	.60	.59	.58	.58	.57	.55	.53	.52
100	1000	.63	.62	.61	.61	.60	.57	.55	.53
110	1000	.66	.65	.64	.63	.62	.59	.57	.55
120	1000	.69	.68	.67	.66	.65	.61	.59	.56
130	1000	.72	.71	.70	.69	.67	.63	.60	.58
140	1000	.75	.74	.73	.71	.70	.65	.62	.59
150	1000	.78	.77	.75	.74	.72	.67	.64	.61
160	1000	.81	.80	.78	.76	.75	.70	.65	.62
170	1000	.84	.83	.81	.79	.77	.72	.67	.64
180	1000	.87	.86	.84	.82	.80	.74	.69	.65
190	1000	.91	.89	.87	.85	.83	.76	.71	.67
200	1000	.94	.92	.90	.88	.85	.78	.73	.69
210	1000	.97	.96	.93	.91	.88	.81	.75	.70
220	1000	1.01	.99	.96	.94	.91	.83	.77	.72
230	1000	1.05	1.03	1.00	.97	.95	.86	.79	.74
240	1000	1.09	1.06	1.03	1.01	.98	.89	.82	.76
250	1000	1.13	1.10	1.07	1.04	1.02	.92	.85	.79
260	1000	1.17	1.15	1.11	1.08	1.05	.96	.87	.81
270	1000	1.21	1.19	1.16	1.12	1.10	.99	.91	.84
280	1000	1.26	1.24	1.20	1.17	1.14	1.03	.94	.87
290	1000	1.31	1.29	1.25	1.22	1.19	1.08	.98	.90
300	1000	1.37	1.34	1.31	1.28	1.25	1.14	1.03	.94

Table 9

Compressibilities of Sodium Chloride Solutions: $\frac{1}{v}\left(\frac{\partial v}{\partial P}\right)_{T,m} \times 10^4$ bar

TEMP (°C)	PRESS (BAR)	MOLALITY .100	.250	.500	.750	1.000	2.000	3.000	4.000	5.000
0	1	.503	.492	.475	.459	.443	.389	.346	.315	.294
10	1	.472	.463	.449	.436	.423	.377	.341	.313	.294
20	1	.453	.446	.433	.422	.411	.371	.338	.313	.294
25	1	.447	.440	.428	.417	.407	.369	.337	.313	.294
30	1	.443	.436	.425	.414	.404	.367	.337	.313	.294
40	1	.438	.432	.421	.411	.401	.367	.338	.315	.296
50	1	.438	.431	.421	.411	.402	.369	.340	.317	.299
50	1	.44	.43	.42	.41	.40	.37	.34	.32	.30
60	1	.44	.44	.43	.42	.41	.38	.35	.32	.30
70	1	.45	.44	.43	.42	.42	.38	.36	.33	.31
80	1	.46	.45	.44	.43	.43	.39	.37	.34	.32
90	1	.47	.47	.46	.45	.44	.41	.38	.35	.33
100	1	.49	.48	.47	.46	.45	.42	.39	.37	.34
110	1	.51	.50	.49	.48	.47	.44	.41	.38	.35
120	2	.53	.52	.51	.50	.49	.46	.43	.39	.36
130	3	.55	.55	.54	.53	.52	.48	.44	.41	.38
140	4	.58	.57	.56	.55	.54	.50	.47	.43	.39
150	5	.62	.61	.60	.58	.57	.53	.49	.45	.41
160	6	.65	.65	.63	.62	.61	.56	.52	.47	.42
170	8	.70	.69	.67	.66	.65	.60	.55	.50	.44
180	10	.75	.74	.72	.71	.69	.64	.58	.52	.46
190	13	.81	.80	.78	.76	.74	.68	.62	.55	.48
200	16	.87	.86	.84	.82	.80	.73	.66	.59	.50
210	19	.95	.94	.91	.89	.87	.79	.71	.63	.53
220	23	1.05	1.03	1.00	.97	.95	.86	.77	.67	.56
230	28	1.15	1.13	1.10	1.07	1.04	.93	.83	.71	.58
240	33	1.28	1.25	1.21	1.18	1.14	1.02	.89	.76	.61
250	40	1.44	1.40	1.35	1.30	1.26	1.11	.97	.82	.64
260	47	1.63	1.58	1.52	1.46	1.41	1.23	1.06	.88	.68
270	55	1.87	1.81	1.72	1.65	1.58	1.35	1.15	.94	.71
280	64	2.17	2.09	1.97	1.87	1.79	1.50	1.25	1.01	.75
290	74	2.56	2.45	2.29	2.16	2.04	1.67	1.37	1.08	.79
300	86	3.08	2.92	2.71	2.53	2.37	1.87	1.49	1.15	.82

Table 9

Compressibilities of Sodium Chloride Solutions: $\frac{1}{v}\left(\frac{\partial v}{\partial P}\right)_{T,m} \times 10^4$ bar

TEMP (°C)	PRESS (BAR)	MOLALITY .100	.250	.500	.750	1.000	2.000	3.000	4.000	5.000
0	200	.474	.465	.449	.434	.420	.370			
10	200	.447	.439	.426	.414	.402	.360			
20	200	.430	.423	.412	.401	.391	.355			
25	200	.425	.418	.407	.397	.388	.353	.324	.301	.283
30	200	.420	.414	.404	.394	.385	.352	.324	.301	.284
40	200	.416	.410	.400	.391	.382	.351	.325	.303	.286
50	200	.415	.409	.400	.391	.383	.352	.327	.305	.288
50	200	.41	.41	.40	.39	.38	.35	.33	.31	.29
60	200	.42	.41	.40	.40	.39	.36	.33	.31	.29
70	200	.42	.42	.41	.40	.39	.36	.34	.32	.30
80	200	.43	.43	.42	.41	.40	.37	.35	.33	.31
90	200	.44	.44	.43	.42	.41	.38	.36	.33	.31
100	200	.45	.45	.44	.43	.42	.40	.37	.34	.32
110	200	.47	.46	.46	.45	.44	.41	.38	.36	.33
120	200	.49	.48	.47	.46	.46	.42	.40	.37	.34
130	200	.51	.50	.49	.48	.48	.44	.41	.38	.36
140	200	.53	.53	.52	.51	.50	.46	.43	.40	.37
150	200	.56	.55	.54	.53	.52	.48	.45	.42	.38
160	200	.59	.58	.57	.56	.55	.51	.47	.43	.40
170	200	.63	.62	.61	.59	.58	.54	.50	.46	.41
180	200	.67	.66	.64	.63	.62	.57	.52	.48	.43
190	200	.71	.70	.69	.67	.66	.61	.56	.50	.45
200	200	.77	.76	.74	.72	.70	.65	.59	.53	.47
210	200	.83	.81	.79	.77	.76	.69	.63	.56	.49
220	200	.90	.88	.86	.84	.82	.75	.67	.60	.52
230	200	.98	.96	.93	.91	.89	.80	.72	.64	.54
240	200	1.07	1.05	1.02	.99	.97	.87	.78	.68	.57
250	200	1.19	1.16	1.12	1.09	1.06	.95	.84	.73	.60
260	200	1.32	1.29	1.24	1.20	1.16	1.03	.91	.78	.63
270	200	1.49	1.44	1.38	1.33	1.29	1.13	.99	.84	.67
280	200	1.69	1.63	1.55	1.49	1.43	1.24	1.07	.90	.70
290	200	1.94	1.87	1.76	1.68	1.60	1.36	1.16	.96	.73
300	200	2.27	2.17	2.02	1.90	1.80	1.48	1.24	1.01	.77

Table 9

Compressibilities of Sodium Chloride Solutions: $\frac{1}{v}\left(\frac{\partial v}{\partial P}\right)_{T,m} \times 10^4$ bar

TEMP (°C)	PRESS (BAR)	MOLALITY .100	.250	.500	.750	1.000	2.000	3.000	4.000	5.000
0	400	.449	.440	.426	.412	.399	.353			
10	400	.425	.418	.406	.395	.384	.345			
20	400	.410	.404	.393	.383	.374	.340			
25	400	.405	.399	.389	.380	.371	.339	.312	.290	.273
30	400	.401	.395	.386	.377	.368	.337	.312	.290	.273
40	400	.396	.391	.382	.374	.366	.337	.312	.292	.275
50	400	.395	.390	.381	.373	.365	.338	.314	.294	.278
50	400	.39	.39	.38	.37	.37	.34	.31	.29	.28
60	400	.40	.39	.38	.38	.37	.34	.32	.30	.28
70	400	.40	.40	.39	.38	.37	.35	.32	.30	.29
80	400	.41	.40	.39	.39	.38	.35	.33	.31	.29
90	400	.42	.41	.40	.40	.39	.36	.34	.32	.30
100	400	.43	.42	.41	.41	.40	.37	.35	.33	.31
110	400	.44	.43	.43	.42	.41	.38	.36	.33	.32
120	400	.46	.45	.44	.43	.42	.39	.37	.35	.32
130	400	.47	.47	.46	.45	.44	.41	.38	.36	.34
140	400	.49	.49	.48	.47	.46	.42	.40	.37	.35
150	400	.52	.51	.50	.49	.48	.44	.41	.38	.36
160	400	.54	.53	.52	.51	.50	.46	.43	.40	.37
170	400	.57	.56	.55	.54	.52	.48	.45	.42	.39
180	400	.60	.59	.58	.57	.55	.51	.47	.44	.40
190	400	.64	.63	.61	.60	.59	.54	.49	.46	.42
200	400	.68	.67	.65	.64	.62	.57	.52	.48	.44
210	400	.73	.71	.70	.68	.66	.60	.55	.50	.46
220	400	.78	.77	.74	.72	.71	.64	.59	.53	.48
230	400	.84	.82	.80	.78	.76	.69	.63	.56	.50
240	400	.91	.89	.86	.84	.82	.74	.67	.60	.52
250	400	.99	.96	.93	.91	.88	.80	.72	.64	.55
260	400	1.08	1.05	1.02	.99	.96	.86	.77	.68	.58
270	400	1.18	1.15	1.11	1.07	1.04	.94	.83	.73	.61
280	400	1.30	1.27	1.22	1.18	1.14	1.02	.90	.78	.64
290	400	1.45	1.40	1.34	1.29	1.25	1.11	.98	.84	.68
300	400	1.62	1.56	1.49	1.42	1.37	1.20	1.05	.90	.71

Table 9

Compressibilities of Sodium Chloride Solutions: $\frac{1}{v}\left(\frac{\partial v}{\partial P}\right)_{T,m} \times 10^4$ bar

TEMP (°C)	PRESS (BAR)	MOLALITY .100	.250	.500	.750	1.000	2.000	3.000	4.000	5.000
0	600	.426	.418	.405	.392	.380	.338			
10	600	.405	.398	.387	.377	.367	.331			
20	600	.391	.386	.376	.367	.358	.327			
25	600	.387	.381	.372	.364	.355	.326	.300	.279	.262
30	600	.383	.378	.369	.361	.353	.325	.300	.280	.263
40	600	.378	.373	.365	.358	.350	.324	.301	.281	.265
50	600	.377	.372	.364	.357	.350	.324	.302	.283	.267
50	600	.38	.37	.36	.36	.35	.32	.30	.28	.27
60	600	.38	.37	.37	.36	.35	.33	.31	.29	.27
70	600	.38	.38	.37	.36	.36	.33	.31	.29	.27
80	600	.39	.38	.37	.37	.36	.34	.31	.30	.28
90	600	.39	.39	.38	.37	.37	.34	.32	.30	.28
100	600	.40	.40	.39	.38	.38	.35	.33	.31	.29
110	600	.42	.41	.40	.39	.39	.36	.33	.31	.30
120	600	.43	.42	.41	.40	.40	.37	.34	.32	.31
130	600	.44	.44	.43	.42	.41	.38	.35	.33	.31
140	600	.46	.45	.44	.43	.42	.39	.36	.34	.32
150	600	.48	.47	.46	.45	.44	.40	.38	.35	.34
160	600	.50	.49	.48	.47	.46	.42	.39	.37	.35
170	600	.52	.52	.50	.49	.48	.44	.40	.38	.36
180	600	.55	.54	.53	.51	.50	.45	.42	.39	.37
190	600	.58	.57	.55	.54	.52	.48	.44	.41	.39
200	600	.61	.60	.58	.57	.55	.50	.46	.43	.40
210	600	.65	.64	.62	.60	.58	.53	.48	.45	.42
220	600	.69	.68	.66	.64	.62	.56	.51	.47	.44
230	600	.74	.72	.70	.68	.66	.59	.54	.50	.46
240	600	.79	.77	.75	.72	.70	.63	.57	.52	.48
250	600	.85	.83	.80	.78	.75	.67	.61	.56	.50
260	600	.92	.89	.86	.83	.81	.72	.65	.59	.53
270	600	.99	.97	.93	.90	.87	.78	.70	.63	.56
280	600	1.08	1.05	1.01	.97	.94	.85	.76	.68	.58
290	600	1.17	1.14	1.10	1.06	1.03	.92	.82	.73	.62
300	600	1.28	1.25	1.20	1.15	1.12	1.00	.90	.78	.65

Table 9

Compressibilities of Sodium Chloride Solutions: $\frac{1}{v}\left(\frac{\partial v}{\partial P}\right)_{T,m} \times 10^4$ bar

TEMP (°C)	PRESS (BAR)	MOLALITY .100	.250	.500	.750	1.000	2.000	3.000	4.000	5.000
0	800	.404	.397	.384	.373	.362	.323			
10	800	.386	.380	.370	.360	.351	.318			
20	800	.374	.369	.360	.352	.344	.315			
25	800	.370	.365	.357	.349	.341	.313	.289	.269	.252
30	800	.367	.362	.354	.346	.339	.313	.289	.269	.252
40	800	.362	.358	.350	.343	.337	.312	.290	.271	.254
50	800	.361	.356	.349	.343	.336	.312	.291	.273	.257
50	800	.36	.36	.35	.34	.34	.31	.29	.27	.26
60	800	.36	.36	.35	.34	.34	.31	.29	.27	.26
70	800	.36	.36	.35	.35	.34	.32	.30	.28	.26
80	800	.37	.36	.36	.35	.34	.32	.30	.28	.27
90	800	.38	.37	.36	.36	.35	.32	.30	.28	.27
100	800	.38	.38	.37	.36	.36	.33	.31	.29	.27
110	800	.39	.39	.38	.37	.36	.34	.31	.29	.28
120	800	.40	.40	.39	.38	.37	.34	.32	.30	.29
130	800	.42	.41	.40	.39	.38	.35	.33	.31	.29
140	800	.43	.42	.41	.40	.39	.36	.33	.31	.30
150	800	.45	.44	.43	.42	.40	.37	.34	.32	.31
160	800	.47	.46	.44	.43	.42	.38	.35	.33	.32
170	800	.49	.48	.46	.45	.43	.39	.36	.34	.33
180	800	.51	.50	.48	.47	.45	.40	.37	.35	.34
190	800	.53	.52	.50	.49	.47	.42	.39	.37	.36
200	800	.56	.55	.53	.51	.49	.44	.40	.38	.37
210	800	.59	.58	.55	.53	.52	.46	.42	.39	.38
220	800	.63	.61	.58	.56	.54	.48	.44	.41	.40
230	800	.66	.64	.62	.59	.57	.50	.46	.43	.42
240	800	.70	.68	.66	.63	.61	.53	.48	.45	.44
250	800	.75	.73	.70	.67	.64	.57	.51	.48	.46
260	800	.80	.78	.74	.71	.69	.60	.54	.50	.48
270	800	.86	.83	.80	.76	.74	.65	.58	.53	.50
280	800	.92	.89	.85	.82	.79	.70	.62	.57	.53
290	800	.99	.96	.92	.88	.85	.75	.68	.61	.55
300	800	1.07	1.04	.99	.96	.92	.82	.74	.66	.59

Table 9

Compressibilities of Sodium Chloride Solutions: $\frac{1}{v}\left(\frac{\partial v}{\partial P}\right)_{T,m} \times 10^4$ bar

TEMP (°C)	PRESS (BAR)	MOLALITY .100	.250	.500	.750	1.000	2.000	3.000	4.000	5.000
0	1000	.382	.375	.365	.354	.344	.308			
10	1000	.368	.362	.353	.344	.336	.305			
20	1000	.358	.353	.345	.337	.330	.303			
25	1000	.354	.349	.342	.335	.328	.302	.279	.259	.241
30	1000	.351	.347	.340	.333	.326	.301	.279	.259	.242
40	1000	.347	.343	.337	.330	.324	.301	.280	.261	.244
50	1000	.346	.342	.336	.329	.323	.301	.281	.263	.246
50	1000	.35	.34	.34	.33	.32	.30	.28	.26	.25
60	1000	.35	.34	.34	.33	.32	.30	.28	.26	.25
70	1000	.35	.34	.34	.33	.33	.30	.28	.26	.25
80	1000	.35	.35	.34	.33	.33	.30	.28	.27	.25
90	1000	.36	.35	.35	.34	.33	.31	.29	.27	.25
100	1000	.37	.36	.35	.34	.34	.31	.29	.27	.26
110	1000	.37	.37	.36	.35	.34	.31	.29	.27	.26
120	1000	.38	.38	.37	.36	.35	.32	.30	.28	.27
130	1000	.39	.39	.38	.37	.36	.32	.30	.28	.27
140	1000	.41	.40	.39	.37	.36	.33	.30	.29	.28
150	1000	.42	.41	.40	.39	.37	.33	.31	.29	.29
160	1000	.44	.43	.41	.40	.38	.34	.31	.30	.30
170	1000	.45	.44	.43	.41	.40	.35	.32	.31	.31
180	1000	.47	.46	.44	.42	.41	.36	.33	.31	.31
190	1000	.49	.48	.46	.44	.42	.37	.34	.32	.33
200	1000	.52	.50	.48	.46	.44	.38	.34	.33	.34
210	1000	.54	.53	.50	.48	.46	.39	.36	.34	.35
220	1000	.57	.55	.52	.50	.48	.41	.37	.35	.36
230	1000	.60	.58	.55	.52	.50	.42	.38	.37	.38
240	1000	.63	.61	.58	.55	.52	.44	.40	.38	.39
250	1000	.67	.65	.61	.58	.55	.46	.41	.40	.41
260	1000	.71	.69	.65	.61	.58	.49	.44	.42	.43
270	1000	.76	.73	.69	.65	.62	.52	.46	.44	.44
280	1000	.81	.77	.73	.69	.66	.55	.49	.46	.47
290	1000	.86	.83	.78	.74	.70	.59	.53	.49	.49
300	1000	.92	.89	.84	.79	.76	.64	.57	.53	.52

The relative enthalpy is related to the excess Gibbs energy of the solution by the equation

$$L = G^{EX} - T\left(\frac{\partial G^{EX}}{\partial T}\right)_{P,m} = -T^2\left(\frac{\partial G^{EX}/T}{\partial T}\right)_{P,m} \tag{27}$$

The apparent molal enthalpy is defined as

$$\phi L = \frac{L}{n_2} . \tag{28}$$

The parametric form of the equation for the apparent molal enthalpy is,[6]

$$\begin{aligned}\phi L = {} & \nu|z_m z_x| \frac{A_H}{2b} \ln(1+bI^{1/2}) \\ & - \nu RT^2 m \left(\frac{2\nu_m \nu_x}{\nu}\right)\left(\frac{\partial \beta^{(0)}_{MX}}{\partial T}\right)_{P,m} \\ & - \frac{2\nu RT^2 m}{\alpha^2 I}\left(1-(1+\alpha I^{1/2})e^{-\alpha I^{1/2}}\right)\left(\frac{2\nu_m \nu_x}{\nu}\right)\left(\frac{\partial \beta^{(1)}_{MX}}{\partial T}\right)_{P,m} \\ & - \frac{\nu}{2} RT^2 m^2 \left(\frac{2(\nu_m \nu_x)^{3/2}}{\nu}\right)\left(\frac{\partial C^{\phi}_{MX}}{\partial T}\right)_{P,m} ,\end{aligned} \tag{29}$$

where A_H is the Debye-Hückel enthalpy slope given in paper VII.[5]

The experimental determination of the enthalpy of an electrolyte solution is made through heat of dilution or heat of solution measurements. The molar heat of dilution $\Delta\bar{H}_D$ is the heat change per mole measured when a solution at concentration m_1 is diluted to concentration m_2, and it is related to the apparent molal enthalpies at m_2 and m_1 by

$$\Delta\bar{H}_D = \phi L(m_2) - \phi L(m_1). \tag{30}$$

The molar heat of solution, $\Delta\bar{H}_s$, is the heat change measured when one mole of salt is dissolved in enough water to form a solution of

concentration m. It is related to the apparent molal enthalpy by

$$\Delta\bar{H}_s = \Delta\bar{H}_s^{\circ} + \phi L, \tag{31}$$

where $\Delta\bar{H}_s^{\circ}$ is the heat of solution at infinite dilution. The apparent molal heat capacity is defined as the difference between the heat capacity of the solution and the heat capacity of pure water contained in the solution, per mole of salt,

$$\phi C_p = \frac{C_p - n_1\bar{C}_{p_1}^{\circ}}{n_2} . \tag{32}$$

The apparent molal heat capacity is related to the apparent molal enthalpy by

$$\phi C_p = \bar{C}_{p_2}^{\circ} + \left(\frac{\partial \phi L}{\partial T}\right)_{P,m} \tag{33}$$

where $\bar{C}_{p_2}^{\circ}$ is the partial molal heat capacity of the solute at infinite dilution. Combining Equation (33) and the temperature derivative of Equation (29) yields

$$\begin{aligned}\phi C_p = {} & \bar{C}_{p_2}^{\circ} + \nu|z_m z_x| \frac{A_J}{2b} \ln(1+bI^{1/2}) \\ & - \nu RT^2 m\left(\frac{2\nu_m\nu_x}{\nu}\right)\left[\left(\frac{\partial^2\beta_{MX}^{(0)}}{\partial T^2}\right)_{P,m} + \frac{2}{T}\left(\frac{\partial\beta_{MX}^{(0)}}{\partial T}\right)_{P,m}\right] \\ & - \frac{2\nu RT^2 m}{\alpha^2 I}\left(1-(1+\alpha I^{1/2})e^{-\alpha I^{1/2}}\right)\left(\frac{2\nu_m\nu_x}{\nu}\right)\left[\left(\frac{\partial^2\beta_{MX}^{(1)}}{\partial T^2}\right)_{P,m} + \frac{2}{T}\left(\frac{\partial\beta_{MX}^{(1)}}{\partial T}\right)_{P,m}\right] \\ & - \frac{\nu}{2} RT^2 m^2\left(\frac{2(\nu_m\nu_x)^{3/2}}{\nu}\right)\left[\left(\frac{\partial^2 C_{MX}^{\phi}}{\partial T^2}\right)_{P,m} + \frac{2}{T}\left(\frac{\partial C_{MX}^{\phi}}{\partial T}\right)_{P,m}\right],\end{aligned} \tag{34}$$

where A_J is the Debye-Hückel slope for the heat capacity given in paper XII.[5]

Finally, the pressure dependence of the activity and thermal properties can be found by taking the derivatives of Equations (5), (6), (29), and (34) with respect to pressure. Equations are given below for the change in these properties in going from an initial pressure P_1 to a final pressure P_2.

$$\phi(P_2) - \phi(P_1) = -|z_m z_x| (A_\phi(P_2) - A_\phi(P_1) \frac{I^{1/2}}{1+bI^{1/2}} + \int_{P_1}^{P_2} \{m\beta_v^{(0)} + m\beta_v^{(1)} e^{-\alpha I^{1/2}} + m^2 C_v^\phi\} dP \tag{35}$$

$$\ln\gamma_\pm(P_2) - \ln\gamma_\pm(P_1) = -|z_m z_x| (A_\phi(P_2)-A_\phi(P_1))\left(\frac{I^{1/2}}{1+I^{1/2}} + \frac{2}{b} \ln(1+bI^{1/2})\right) + \int_{P_1}^{P_2} \left\{2m\beta_v^{(0)} + \frac{2m\beta_v^{(1)}}{\alpha^2 I} (1-(1+\alpha I^{1/2} - \frac{\alpha^2 I}{2})e^{-\alpha I^{1/2}}) + \frac{3}{2} m^2 C_v^\phi\right\} dP \tag{36}$$

$$\phi L(P_2) - \phi L(P_1) = \nu|z_m z_x| \frac{1}{2b} (A_H(P_2)-A_H(P_1)) \ln(1+bI^{1/2}) - \int_{P_1}^{P_2} \left\{\nu RT^2 m\left(\frac{\partial\beta_v^{(0)}}{\partial T}\right)_{P,m} + \frac{2\nu RT^2 m}{\alpha^2 I}\left(\frac{\beta_v^{(1)}}{\partial T}\right)_{P,m} (1-(1+\alpha I^{1/2})e^{-\alpha I^{1/2}}) + \frac{\nu RT^2 m^2}{2}\left(\frac{\partial C_v^\phi}{\partial T}\right)_{P,m}\right\} dP \tag{37}$$

$$\phi C_p(P_2) - \phi C_p(P_1) = \nu|z_m z_x| \frac{1}{2b} (A_J(P_2)-A_J(P_1)) \ln(1+bI^{1/2}) - \int_{P_1}^{P_2} \left\{\nu RT^2 m\left[\left(\frac{\partial^2\beta_v^{(0)}}{\partial T^2}\right)_{P,m} + \frac{2}{T}\left(\frac{\partial\beta_v^{(0)}}{\partial T}\right)_{P,m}\right]\right. \tag{38}$$

continued

$$+ \frac{2\nu RT^2 m}{\alpha^2 I}\left[\left(\frac{\partial^2 \beta_v^{(1)}}{\partial T^2}\right)_{P,m} + \frac{2}{T}\left(\frac{\partial \beta_v^{(1)}}{\partial T}\right)_{P,m}\right](1-(1+\alpha I^{1/2})e^{-\alpha I^{1/2}})$$

$$+ \frac{\nu RT^2 m^2}{2}\left[\left(\frac{\partial^2 C_v^{\phi}}{\partial T^2}\right)_{P,m} + \frac{2}{T}\left(\frac{\partial C_v^{\phi}}{\partial T}\right)_{P,m}\right] + T\left(\frac{\partial^2 \bar{V}_2^{\circ}}{\partial T^2}\right)_P \Bigg\} dP. \tag{38}$$

To determine the pressure dependence of heat of solution data, the change in $\Delta\bar{H}_s^{\circ}$ with pressure is also needed. The heat of solution at infinite dilution is related to the partial molal enthalpy of the solute at infinite dilution, $\bar{H}_2^{\circ}$, and the molal enthalpy of the solid salt, $\bar{H}(s)$, by the equation

$$\Delta\bar{H}_s^{\circ} = \bar{H}_2^{\circ} - \bar{H}(s). \tag{39}$$

The change with pressure is

$$\left(\frac{\partial \Delta\bar{H}_s^{\circ}}{\partial P}\right)_T = \bar{V}_2^{\circ} - T\left(\frac{\partial \bar{V}_2^{\circ}}{\partial T}\right)_P - \left\{\bar{V}(s) + T\left(\frac{\partial \bar{V}(s)}{\partial T}\right)_P\right\}, \tag{40}$$

where $\bar{V}_2^{\circ}$ is the partial molal volume of the solute at infinite dilution and $\bar{V}(s)$ is the molal volume of the pure salt in the solid phase. Since the temperature and pressure dependences of the volume of the solid are small, the integral of the term in brackets can be approximated as

$$\int_{P_1}^{P_2} \left\{\bar{V}(s) + T\left(\frac{\partial \bar{V}(s)}{\partial T}\right)_P\right\} dP \approx \bar{V}(s)_{298K}\,(P_2 - P_1).$$

This approximation is accurate to .04J mol^{-1} bar^{-1}, so it is sufficient in comparison to the larger uncertainty in the pressure dependence of $\bar{H}_2^{\circ}$.

The pressure dependence of $\Delta\bar{H}_s^{\circ}$ now reduces to,

$$\Delta\bar{H}_s^\circ(P_2) - \Delta\bar{H}_s^\circ(P_1) = \int_{P_1}^{P_2} \left\{ \bar{V}_2^\circ - T\left(\frac{\partial \bar{V}_2^\circ}{\partial T}\right)_P \right\} dP - \bar{V}(s)(P_2 - P_1), \qquad (41)$$

with $\bar{V}(s) = 26.994\ cm^3\ mol^{-1}$ at 25°C.[40]

2. Estimation of Uncertainties

The error accumulated in a pressure correction is difficult to determine because of the multiple operations needed to obtain the final value. The pressure dependence of an osmotic or activity coefficient is known most accurately, since only terms describing the specific volume of the NaCl solution as a function of pressure are required for the calculation. An estimated error of 10% in the pressure correction results in an uncertainty of ±.009 in the osmotic coefficient at 300°C and 1000 bar. For comparison, the experimental uncertainty in the measured osmotic coefficient at saturation pressure is ±.005.

The uncertainty in a pressure correction for enthalpy and heat capacity data will be larger, since these corrections require information on the first and second temperature derivatives of the volume of the NaCl solution. The minimum uncertainty in a pressure correction can be estimated by comparing values obtained from the low temperature fit and the overall fit in the region of overlap. Minimum uncertainties are $\pm 20\ J\ mol^{-1}$ for the apparent molal enthalpy and $\pm 2\ J\ K^{-1}\ mol^{-1}$ for the apparent molal heat capacity. At high temperatures, recent enthalpy and heat capacity data reported at elevated pressures can be used to assess the uncertainty in the pressure corrections. Busey[41] lists enthalpy of dilution data at 66 to 105 bar and 400 bar. Comparison of the low pressure data corrected up to 177 bar and the high pressure data adjusted down to 177 bar shows that the corrected values are in agreement

approximately within the scatter of the measured enthalpies. The heat capacity data of Tanner and Lamb[42] at 1 bar and of Likke and Bromley[43] at saturation pressures can be corrected to 177 bar for comparison with the data of Smith-Magowan and Wood.[44] Again, the differences between the high pressure data and the data adjusted to 177 bar are comparable to the observed scatter in the measured heat capacities. An estimated error of 20% for the pressure correction gives an uncertainty in the correction to 200 bar of the same magnitude as the experimental uncertainty in the measured enthalpies and heat capacities. Thus this value has been chosen as the estimated uncertainty in the pressure corrections for these quantities. The percent uncertainty should remain fairly constant for corrections over larger pressure intervals, so that the absolute error in a pressure adjustment from saturation pressure to 1000 bar will be four or five times as large as the uncertainty in a correction from saturation pressure to 200 bar. Table 10 lists the estimated percent uncertainties in the pressure adjustments, along with the range of experimental uncertainties for existing activity, enthalpy, and heat capacity data.

3. Explanation of Tables

The pressure dependences of the osmotic and activity coefficients, the heat of solution, and the apparent molal enthalpy and heat capacity are given in Tables 11-15. Values are listed as the change in a thermodynamic property due to a pressure change from the saturation pressure of pure water to 200, 400, 600, or 1000 bar. Thus the table values can be added directly to experimental data along the saturation curve to obtain the corresponding high pressure values. Of course, other pressure adjustments, for example, from 200 bar to 400 bar, can be obtained by

Table 10

Pressure Dependence of Thermodynamic Properties

Property	Uncertainty Estimates: Pressure Dependence	Correction to 200 bar		Experimental Data[c]
ϕ	10%	.002	(300°C)	.005
$\ln\gamma_{\pm}$	10%	.002	(50°C)	.002
$\Delta\bar{H}_D$	20%[a]	20 J mol^{-1}	(25°C)	4 J/mol
		30 J mol^{-1}	(100°C)	20 J/mol[d]
		250 J mol^{-1}	(200°C)	65 J/mol[d]
		1,500 J mol^{-1}	(300°C)	1,000 J/mol[d]
$\Delta\bar{H}_s$	20%[a]	20 J mol^{-1}	(25°C)	16 J/mol
		60 J mol^{-1}	(100°C)	100 J/mol
		400 J mol^{-1}	(200°C)	160 J/mol
ϕC_p	20%[b]	2 J K^{-1} mol^{-1}	(25°C)	1 J K^{-1} mol^{-1}
		4 J K^{-1} mol^{-1}	(200°C)	4 J K^{-1} mol^{-1}
		50 J K^{-1} mol^{-1}	(300°C)	

[a] Uncertainty is 20% or 20 J mol^{-1}, whichever is greater.

[b] Uncertainty is 20% or 2 J K^{-1} mol^{-1}, whichever is greater.

[c] Values from Table III of Reference 45, unless otherwise noted.

[d] Values from a least squares fit of data from Reference 41.

taking the difference of two table values.

Above 25°C, pressure corrections calculated from the low temperature fit and the overall fit are in good agreement compared to the 10% or 20% estimated uncertainty. Thus for simplicity, all values listed in Tables 11-15 were calculated using only the overall fit (Parameter Set II).

Conclusion

Accurate calculation of the volumetric properties of sodium chloride solutions over a wide range of concentration, temperature, and pressure is possible with the equations presented above. Recent improvements in the data base, including the high temperature data of Hilbert and high concentration data at 20 bar, have been used. Special attention has been paid to the behavior of the expansivity and compressibility values derived from the volumetric fit. Because the temperature and pressure dependences of the volumetric fit have been carefully controlled, calculation of the pressure dependence of activity, enthalpy, and heat capacity data is possible. The change in these properties due to a pressure change from saturation pressure to 200 bar generally can be calculated with an uncertainty comparable to the experimental uncertainty in direct measurements of these quantities. This important property of the volumetric fit will allow it to be combined with a temperature dependent tabulation of activity data to form a complete equation of state for sodium chloride solutions.

Table 11

Pressure Dependence of the Activity Coefficient: $\ln\gamma_{\pm}(P_2) - \ln\gamma_{\pm}(P_1)$

TEMP (°C)	P1 (BAR)	P2 (BAR)	MOLALITY .100	.250	.500	.750	1.000	2.000	3.000	4.000
0	1	200	.004	.006	.010	.013	.015	.024		
10	1	200	.003	.006	.008	.011	.013	.020		
20	1	200	.003	.005	.008	.010	.011	.017		
25	1	200	.003	.005	.007	.009	.011	.016	.020	.023
30	1	200	.003	.005	.007	.009	.010	.015	.019	.021
40	1	200	.003	.005	.007	.009	.010	.014	.017	.020
50	1	200	.003	.005	.007	.008	.010	.013	.016	.018
60	1	200	.004	.005	.007	.009	.010	.013	.016	.018
70	1	200	.004	.006	.008	.009	.010	.013	.016	.018
80	1	200	.004	.006	.008	.009	.011	.014	.016	.018
90	1	200	.005	.007	.009	.010	.011	.015	.017	.019
100	1	200	.005	.007	.009	.011	.012	.016	.018	.020
110	1	200	.005	.008	.010	.012	.013	.017	.019	.022
120	2	200	.006	.008	.011	.013	.014	.018	.021	.023
130	3	200	.006	.009	.012	.014	.015	.020	.023	.025
140	4	200	.007	.010	.013	.015	.017	.022	.025	.028
150	5	200	.008	.011	.014	.017	.019	.024	.027	.030
160	6	200	.008	.012	.016	.018	.020	.026	.030	.033
170	8	200	.009	.013	.018	.020	.022	.029	.033	.036
180	10	200	.010	.015	.019	.022	.025	.031	.036	.040
190	13	200	.011	.016	.021	.025	.027	.034	.039	.043
200	16	200	.013	.018	.024	.027	.030	.037	.043	.047
210	19	200	.014	.020	.026	.030	.033	.041	.047	.051
220	23	200	.016	.022	.029	.033	.036	.045	.050	.055
230	28	200	.017	.025	.032	.036	.040	.049	.055	.060
240	33	200	.019	.028	.035	.040	.044	.053	.059	.064
250	40	200	.022	.031	.039	.045	.048	.058	.064	.069
260	47	200	.024	.035	.044	.049	.054	.064	.070	.074
270	55	200	.027	.039	.049	.055	.059	.070	.076	.080
280	64	200	.031	.043	.054	.061	.066	.077	.083	.087
290	74	200	.035	.049	.061	.068	.074	.085	.091	.095
300	86	200	.039	.055	.068	.077	.083	.095	.101	.104

Table 11

Pressure Dependence of the Activity Coefficient: $\ln\gamma_{\pm}(P_2) - \ln\gamma_{\pm}(P_1)$

TEMP (°C)	P1 (BAR)	P2 (BAR)	MOLALITY .100	.250	.500	.750	1.000	2.000	3.000	4.000
0	1	400	.007	.012	.019	.024	.030	.047		
10	1	400	.007	.011	.016	.021	.025	.038		
20	1	400	.006	.010	.015	.019	.022	.033		
25	1	400	.006	.010	.014	.018	.021	.031	.038	.043
30	1	400	.006	.010	.014	.017	.020	.029	.036	.041
40	1	400	.007	.010	.014	.017	.019	.027	.033	.038
50	1	400	.007	.010	.014	.017	.019	.026	.031	.035
60	1	400	.007	.011	.014	.017	.019	.025	.030	.034
70	1	400	.008	.011	.015	.017	.019	.026	.030	.034
80	1	400	.008	.012	.016	.018	.020	.027	.031	.035
90	1	400	.009	.013	.017	.020	.022	.028	.033	.037
100	1	400	.009	.014	.018	.021	.023	.030	.035	.039
110	1	400	.010	.015	.020	.023	.025	.033	.038	.042
120	2	400	.011	.016	.021	.025	.028	.035	.041	.046
130	3	400	.012	.018	.023	.027	.030	.039	.045	.050
140	4	400	.013	.020	.026	.030	.033	.042	.049	.055
150	5	400	.015	.022	.028	.033	.036	.046	.054	.060
160	6	400	.016	.024	.031	.036	.040	.051	.059	.066
170	8	400	.018	.026	.034	.040	.044	.056	.065	.072
180	10	400	.020	.029	.038	.044	.048	.062	.071	.079
190	13	400	.022	.032	.042	.048	.053	.068	.078	.087
200	16	400	.025	.036	.046	.053	.059	.074	.085	.095
210	19	400	.028	.040	.051	.059	.065	.082	.094	.103
220	23	400	.031	.044	.057	.065	.072	.090	.102	.113
230	28	400	.035	.050	.064	.073	.080	.099	.112	.123
240	33	400	.039	.056	.071	.081	.089	.109	.122	.133
250	40	400	.044	.063	.080	.091	.099	.121	.134	.145
260	47	400	.050	.071	.090	.102	.111	.134	.148	.159
270	55	400	.057	.081	.102	.116	.125	.149	.163	.174
280	64	400	.066	.093	.117	.132	.142	.168	.182	.192
290	74	400	.076	.107	.135	.151	.163	.190	.204	.214
300	86	400	.089	.125	.157	.176	.189	.218	.232	.241

Table 11

Pressure Dependence of the Activity Coefficient: $\ln\gamma_{\pm}(P_2) - \ln\gamma_{\pm}(P_1)$

TEMP (°C)	P1 (BAR)	P2 (BAR)	MOLALITY .100	.250	.500	.750	1.000	2.000	3.000	4.000
0	1	600	.010	.018	.027	.036	.043	.067		
10	1	600	.010	.016	.024	.030	.036	.055		
20	1	600	.009	.015	.022	.027	.032	.047		
25	1	600	.009	.015	.021	.026	.030	.044	.055	.063
30	1	600	.009	.015	.021	.025	.029	.042	.052	.059
40	1	600	.010	.015	.020	.024	.028	.039	.048	.054
50	1	600	.010	.015	.020	.024	.027	.037	.045	.051
60	1	600	.010	.015	.021	.024	.028	.037	.044	.050
70	1	600	.011	.016	.022	.025	.028	.038	.044	.050
80	1	600	.012	.017	.023	.027	.030	.039	.046	.051
90	1	600	.013	.019	.024	.028	.032	.041	.048	.054
100	1	600	.014	.020	.026	.031	.034	.044	.051	.057
110	1	600	.015	.022	.028	.033	.037	.047	.055	.061
120	2	600	.016	.024	.031	.036	.040	.051	.060	.066
130	3	600	.018	.026	.034	.039	.044	.056	.065	.073
140	4	600	.019	.028	.037	.043	.048	.061	.071	.079
150	5	600	.021	.031	.040	.047	.052	.067	.078	.087
160	6	600	.024	.034	.045	.052	.058	.074	.086	.096
170	8	600	.026	.038	.049	.057	.063	.081	.094	.105
180	10	600	.029	.042	.054	.063	.070	.089	.103	.115
190	13	600	.032	.046	.060	.069	.077	.098	.113	.126
200	16	600	.035	.051	.066	.076	.085	.108	.124	.138
210	19	600	.039	.057	.073	.085	.093	.118	.136	.151
220	23	600	.044	.063	.081	.094	.103	.130	.149	.165
230	28	600	.049	.071	.091	.104	.115	.143	.163	.179
240	33	600	.055	.079	.101	.116	.127	.157	.178	.196
250	40	600	.063	.089	.114	.130	.142	.174	.195	.213
260	47	600	.071	.101	.128	.146	.159	.192	.214	.233
270	55	600	.081	.115	.145	.164	.179	.214	.237	.254
280	64	600	.093	.131	.165	.187	.202	.240	.262	.280
290	74	600	.107	.151	.190	.214	.231	.271	.293	.310
300	86	600	.125	.176	.220	.247	.266	.308	.330	.346

Table 11

Pressure Dependence of the Activity Coefficient: $\ln\gamma_{\pm}(P_2) - \ln\gamma_{\pm}(P_1)$

TEMP (°C)	P1 (BAR)	P2 (BAR)	MOLALITY .100	.250	.500	.750	1.000	2.000	3.000	4.000
0	1	1000	.016	.028	.043	.056	.067	.104		
10	1	1000	.015	.025	.038	.048	.057	.086		
20	1	1000	.015	.024	.035	.043	.051	.075		
25	1	1000	.015	.023	.033	.041	.048	.069	.085	.096
30	1	1000	.015	.023	.033	.040	.046	.066	.081	.091
40	1	1000	.015	.023	.032	.038	.044	.061	.074	.084
50	1	1000	.016	.024	.032	.038	.043	.059	.070	.080
60	1	1000	.017	.025	.033	.039	.043	.058	.069	.078
70	1	1000	.018	.026	.034	.040	.045	.059	.069	.078
80	1	1000	.019	.027	.036	.042	.047	.061	.071	.080
90	1	1000	.020	.029	.038	.045	.050	.064	.075	.084
100	1	1000	.022	.031	.041	.048	.053	.068	.080	.089
110	1	1000	.023	.034	.044	.051	.057	.074	.085	.095
120	2	1000	.025	.037	.048	.056	.062	.080	.092	.103
130	3	1000	.027	.040	.052	.061	.067	.087	.101	.112
140	4	1000	.030	.044	.057	.066	.074	.095	.110	.122
150	5	1000	.033	.048	.062	.072	.080	.103	.120	.134
160	6	1000	.036	.052	.068	.079	.088	.113	.132	.147
170	8	1000	.039	.057	.075	.087	.096	.124	.144	.161
180	10	1000	.043	.063	.082	.095	.106	.136	.158	.176
190	13	1000	.048	.069	.090	.105	.116	.149	.172	.193
200	16	1000	.053	.077	.099	.115	.128	.163	.188	.210
210	19	1000	.059	.085	.110	.127	.140	.178	.206	.230
220	23	1000	.065	.094	.121	.140	.154	.195	.225	.250
230	28	1000	.073	.104	.134	.155	.170	.214	.245	.272
240	33	1000	.081	.116	.149	.171	.188	.235	.268	.296
250	40	1000	.091	.130	.166	.190	.209	.258	.292	.322
260	47	1000	.103	.146	.186	.212	.232	.284	.320	.350
270	55	1000	.116	.165	.209	.237	.259	.313	.350	.382
280	64	1000	.132	.187	.236	.267	.290	.348	.385	.417
290	74	1000	.151	.213	.268	.303	.328	.388	.425	.456
300	86	1000	.175	.245	.307	.346	.373	.436	.473	.503

Table 12

Pressure Dependence of the Osmotic Coefficient: $\phi(P_2) - \phi(P_1)$

TEMP (°C)	P1 (BAR)	P2 (BAR)	MOLALITY .100	.250	.500	.750	1.000	2.000	3.000	4.000
0	1	200	.001	.002	.004	.005	.006	.010		
10	1	200	.001	.002	.003	.004	.005	.007		
20	1	200	.001	.002	.003	.003	.004	.006		
25	1	200	.001	.002	.002	.003	.004	.006	.007	.008
30	1	200	.001	.002	.002	.003	.003	.005	.006	.007
40	1	200	.001	.002	.002	.003	.003	.005	.006	.006
50	1	200	.001	.002	.002	.003	.003	.004	.005	.006
60	1	200	.001	.002	.002	.003	.003	.004	.005	.005
70	1	200	.001	.002	.002	.003	.003	.004	.005	.005
80	1	200	.001	.002	.002	.003	.003	.004	.005	.005
90	1	200	.001	.002	.002	.003	.003	.004	.005	.005
100	1	200	.001	.002	.003	.003	.003	.004	.005	.005
110	1	200	.002	.002	.003	.003	.004	.005	.005	.006
120	2	200	.002	.002	.003	.004	.004	.005	.006	.006
130	3	200	.002	.003	.003	.004	.004	.005	.006	.007
140	4	200	.002	.003	.004	.004	.005	.006	.007	.007
150	5	200	.002	.003	.004	.005	.005	.006	.007	.008
160	6	200	.003	.004	.004	.005	.006	.007	.008	.009
170	8	200	.003	.004	.005	.006	.006	.008	.009	.010
180	10	200	.003	.004	.005	.006	.007	.008	.009	.010
190	13	200	.003	.005	.006	.007	.007	.009	.010	.011
200	16	200	.004	.005	.006	.007	.008	.009	.011	.012
210	19	200	.004	.006	.007	.008	.009	.010	.011	.012
220	23	200	.005	.006	.008	.009	.009	.011	.012	.013
230	28	200	.005	.007	.009	.009	.010	.012	.013	.014
240	33	200	.006	.008	.009	.010	.011	.012	.013	.014
250	40	200	.006	.009	.010	.011	.012	.013	.014	.014
260	47	200	.007	.010	.011	.012	.013	.014	.014	.015
270	55	200	.008	.011	.013	.014	.014	.015	.015	.015
280	64	200	.009	.012	.014	.015	.015	.016	.015	.015
290	74	200	.010	.013	.016	.017	.017	.017	.016	.015
300	86	200	.011	.015	.017	.018	.019	.018	.017	.015

Table 12

Pressure Dependence of the Osmotic Coefficient: $\phi(P_2) - \phi(P_1)$

TEMP (°C)	P1 (BAR)	P2 (BAR)	MOLALITY .100	.250	.500	.750	1.000	2.000	3.000	4.000
0	1	400	.002	.004	.007	.010	.012	.018		
10	1	400	.002	.004	.006	.008	.009	.014		
20	1	400	.002	.003	.005	.007	.008	.012		
25	1	400	.002	.003	.005	.006	.007	.011	.013	.015
30	1	400	.002	.003	.005	.006	.007	.010	.012	.014
40	1	400	.002	.003	.004	.005	.006	.009	.011	.012
50	1	400	.002	.003	.004	.005	.006	.008	.010	.011
60	1	400	.002	.003	.004	.005	.006	.008	.009	.010
70	1	400	.002	.003	.004	.005	.006	.007	.009	.010
80	1	400	.002	.004	.004	.005	.006	.007	.009	.010
90	1	400	.003	.004	.005	.005	.006	.008	.009	.010
100	1	400	.003	.004	.005	.006	.006	.008	.010	.011
110	1	400	.003	.004	.006	.006	.007	.009	.010	.011
120	2	400	.003	.005	.006	.007	.008	.010	.011	.012
130	3	400	.004	.005	.007	.008	.008	.010	.012	.013
140	4	400	.004	.006	.007	.008	.009	.011	.013	.015
150	5	400	.004	.006	.008	.009	.010	.012	.014	.016
160	6	400	.005	.007	.009	.010	.011	.014	.016	.018
170	8	400	.005	.008	.010	.011	.012	.015	.017	.019
180	10	400	.006	.008	.011	.012	.013	.016	.019	.021
190	13	400	.007	.009	.012	.013	.014	.018	.020	.023
200	16	400	.007	.010	.013	.014	.016	.019	.022	.024
210	19	400	.008	.011	.014	.016	.017	.021	.024	.026
220	23	400	.009	.013	.016	.017	.019	.022	.025	.028
230	28	400	.010	.014	.017	.019	.021	.024	.027	.029
240	33	400	.012	.016	.019	.021	.022	.026	.028	.031
250	40	400	.013	.018	.021	.023	.025	.028	.030	.032
260	47	400	.015	.020	.024	.026	.027	.030	.031	.033
270	55	400	.017	.023	.027	.029	.030	.032	.033	.034
280	64	400	.019	.026	.030	.032	.034	.035	.035	.035
290	74	400	.022	.030	.035	.037	.038	.038	.037	.036
300	86	400	.026	.034	.040	.042	.043	.042	.040	.037

Table 12

Pressure Dependence of the Osmotic Coefficient: $\phi(P_2) - \phi(P_1)$

TEMP (°C)	P1 (BAR)	P2 (BAR)	MOLALITY .100	.250	.500	.750	1.000	2.000	3.000	4.000
0	1	600	.004	.006	.010	.014	.017	.026		
10	1	600	.003	.006	.009	.011	.014	.021		
20	1	600	.003	.005	.008	.010	.011	.017		
25	1	600	.003	.005	.007	.009	.010	.016	.019	.021
30	1	600	.003	.005	.007	.008	.010	.014	.018	.020
40	1	600	.003	.005	.006	.008	.009	.013	.015	.017
50	1	600	.003	.005	.006	.007	.008	.012	.014	.016
60	1	600	.003	.005	.006	.007	.008	.011	.013	.015
70	1	600	.003	.005	.006	.007	.008	.011	.013	.014
80	1	600	.004	.005	.007	.008	.008	.011	.013	.014
90	1	600	.004	.005	.007	.008	.009	.011	.013	.015
100	1	600	.004	.006	.007	.009	.009	.012	.014	.016
110	1	600	.005	.006	.008	.009	.010	.013	.015	.017
120	2	600	.005	.007	.009	.010	.011	.014	.016	.018
130	3	600	.005	.008	.010	.011	.012	.015	.018	.020
140	4	600	.006	.008	.010	.012	.013	.017	.019	.022
150	5	600	.006	.009	.011	.013	.014	.018	.021	.024
160	6	600	.007	.010	.013	.014	.016	.020	.023	.026
170	8	600	.008	.011	.014	.016	.017	.022	.025	.028
180	10	600	.009	.012	.015	.017	.019	.024	.028	.031
190	13	600	.010	.013	.017	.019	.021	.026	.030	.034
200	16	600	.011	.015	.018	.021	.023	.028	.033	.037
210	19	600	.012	.016	.020	.023	.025	.031	.035	.039
220	23	600	.013	.018	.022	.025	.027	.033	.038	.042
230	28	600	.015	.020	.025	.028	.030	.036	.040	.045
240	33	600	.017	.022	.027	.030	.033	.038	.043	.047
250	40	600	.019	.025	.030	.034	.036	.041	.045	.049
260	47	600	.021	.028	.034	.037	.039	.044	.048	.051
270	55	600	.024	.032	.038	.041	.043	.047	.050	.053
280	64	600	.027	.036	.043	.046	.048	.051	.053	.055
290	74	600	.032	.042	.049	.052	.054	.056	.055	.056
300	86	600	.037	.048	.056	.060	.061	.061	.059	.057

Table 12

Pressure Dependence of the Osmotic Coefficient: $\phi(P_2) - \phi(P_1)$

TEMP (°C)	P1 (BAR)	P2 (BAR)	MOLALITY .100	.250	.500	.750	1.000	2.000	3.000	4.000
0	1	1000	.006	.010	.016	.022	.026	.040		
10	1	1000	.005	.009	.014	.018	.021	.032		
20	1	1000	.005	.008	.012	.015	.018	.026		
25	1	1000	.005	.008	.011	.014	.016	.024	.029	.031
30	1	1000	.005	.007	.011	.013	.015	.022	.027	.029
40	1	1000	.005	.007	.010	.012	.014	.020	.024	.027
50	1	1000	.005	.007	.010	.012	.013	.018	.022	.024
60	1	1000	.005	.007	.010	.011	.013	.017	.020	.023
70	1	1000	.005	.008	.010	.011	.013	.017	.020	.022
80	1	1000	.006	.008	.010	.012	.013	.017	.020	.022
90	1	1000	.006	.009	.011	.012	.014	.018	.021	.023
100	1	1000	.007	.009	.012	.013	.015	.019	.022	.024
110	1	1000	.007	.010	.013	.014	.016	.020	.023	.026
120	2	1000	.008	.011	.014	.016	.017	.022	.025	.028
130	3	1000	.008	.012	.015	.017	.019	.023	.027	.030
140	4	1000	.009	.013	.016	.018	.020	.026	.030	.033
150	5	1000	.010	.014	.018	.020	.022	.028	.032	.036
160	6	1000	.011	.015	.019	.022	.024	.031	.036	.040
170	8	1000	.012	.017	.021	.024	.026	.033	.039	.044
180	10	1000	.013	.018	.023	.026	.029	.036	.042	.048
190	13	1000	.014	.020	.025	.029	.032	.040	.046	.052
200	16	1000	.016	.022	.028	.031	.034	.043	.050	.057
210	19	1000	.018	.024	.030	.034	.038	.047	.054	.061
220	23	1000	.020	.027	.033	.038	.041	.050	.058	.066
230	28	1000	.022	.030	.037	.041	.045	.054	.062	.070
240	33	1000	.024	.033	.041	.045	.049	.058	.066	.075
250	40	1000	.027	.037	.045	.050	.053	.062	.070	.079
260	47	1000	.031	.041	.050	.055	.058	.067	.074	.083
270	55	1000	.034	.046	.055	.060	.064	.072	.078	.086
280	64	1000	.039	.052	.062	.067	.070	.077	.082	.089
290	74	1000	.045	.059	.070	.075	.078	.082	.086	.091
300	86	1000	.051	.068	.079	.084	.087	.089	.090	.093

Table 13

Pressure Dependence of the Heat of Solution: $\frac{\Delta\bar{H}_s}{RT}(P_2) - \frac{\Delta\bar{H}_s}{RT}(P_1)$

TEMP (°C)	P1 (BAR)	P2 (BAR)	$\frac{\bar{H}_2^\circ}{RT}$	MOLALITY .001	.005	.010	.020	.030	.040	.050	.100
25	1	200	-4.2E-02	-2.6E-01	-2.6E-01	-2.6E-01	-2.6E-01	-2.6E-01	-2.6E-01	-2.6E-01	-2.6E-01
30	1	200	-8.6E-03	-2.2E-01	-2.2E-01	-2.2E-01	-2.2E-01	-2.2E-01	-2.2E-01	-2.2E-01	-2.2E-01
40	1	200	4.7E-02	-1.6E-01	-1.6E-01	-1.6E-01	-1.6E-01	-1.6E-01	-1.6E-01	-1.6E-01	-1.6E-01
50	1	200	9.4E-02	-1.0E-01	-1.1E-01	-1.1E-01	-1.1E-01	-1.1E-01	-1.1E-01	-1.1E-01	-1.1E-01
60	1	200	1.3E-01	-5.9E-02	-6.0E-02	-6.1E-02	-6.3E-02	-6.4E-02	-6.4E-02	-6.5E-02	-6.7E-02
70	1	200	1.7E-01	-1.7E-02	-1.9E-02	-2.0E-02	-2.2E-02	-2.3E-02	-2.4E-02	-2.5E-02	-2.8E-02
80	1	200	2.0E-01	2.2E-02	2.0E-02	1.9E-02	1.6E-02	1.5E-02	1.4E-02	1.3E-02	8.9E-03
90	1	200	2.4E-01	6.0E-02	5.7E-02	5.5E-02	5.3E-02	5.1E-02	4.9E-02	4.8E-02	4.4E-02
100	1	200	2.7E-01	9.6E-02	9.3E-02	9.1E-02	8.8E-02	8.6E-02	8.4E-02	8.3E-02	7.7E-02
110	1	200	3.0E-01	1.3E-01	1.3E-01	1.3E-01	1.2E-01	1.2E-01	1.2E-01	1.2E-01	1.1E-01
120	2	200	3.3E-01	1.7E-01	1.6E-01	1.6E-01	1.6E-01	1.5E-01	1.5E-01	1.5E-01	1.4E-01
130	3	200	3.7E-01	2.0E-01	2.0E-01	2.0E-01	1.9E-01	1.9E-01	1.9E-01	1.8E-01	1.7E-01
140	4	200	4.0E-01	2.4E-01	2.4E-01	2.3E-01	2.3E-01	2.2E-01	2.2E-01	2.2E-01	2.1E-01
150	5	200	4.4E-01	2.8E-01	2.8E-01	2.7E-01	2.7E-01	2.6E-01	2.6E-01	2.5E-01	2.4E-01
160	6	200	4.8E-01	3.3E-01	3.2E-01	3.1E-01	3.1E-01	3.0E-01	3.0E-01	2.9E-01	2.8E-01
170	8	200	5.2E-01	3.7E-01	3.6E-01	3.6E-01	3.5E-01	3.4E-01	3.4E-01	3.3E-01	3.2E-01
180	10	200	5.7E-01	4.2E-01	4.1E-01	4.1E-01	4.0E-01	3.9E-01	3.8E-01	3.8E-01	3.6E-01
190	13	200	6.2E-01	4.8E-01	4.7E-01	4.6E-01	4.5E-01	4.4E-01	4.3E-01	4.2E-01	4.0E-01
200	16	200	6.8E-01	5.4E-01	5.3E-01	5.2E-01	5.0E-01	4.9E-01	4.9E-01	4.8E-01	4.5E-01
210	19	200	7.5E-01	6.2E-01	6.0E-01	5.9E-01	5.7E-01	5.6E-01	5.5E-01	5.4E-01	5.1E-01
220	23	200	8.3E-01	7.0E-01	6.8E-01	6.7E-01	6.5E-01	6.3E-01	6.2E-01	6.1E-01	5.7E-01
230	28	200	9.4E-01	8.0E-01	7.8E-01	7.6E-01	7.4E-01	7.2E-01	7.1E-01	6.9E-01	6.5E-01
240	33	200	1.1E+00	9.3E-01	9.0E-01	8.8E-01	8.5E-01	8.3E-01	8.1E-01	8.0E-01	7.4E-01
250	40	200	1.2E+00	1.1E+00	1.0E+00	1.0E+00	9.8E-01	9.6E-01	9.4E-01	9.2E-01	8.6E-01
260	47	200	1.4E+00	1.3E+00	1.2E+00	1.2E+00	1.2E+00	1.1E+00	1.1E+00	1.1E+00	1.0E+00
270	55	200	1.7E+00	1.5E+00	1.5E+00	1.4E+00	1.4E+00	1.3E+00	1.3E+00	1.3E+00	1.2E+00
280	64	200	2.0E+00	1.8E+00	1.8E+00	1.7E+00	1.7E+00	1.6E+00	1.6E+00	1.5E+00	1.4E+00
290	74	200	2.4E+00	2.3E+00	2.2E+00	2.1E+00	2.0E+00	2.0E+00	1.9E+00	1.9E+00	1.7E+00
300	86	200	3.0E+00	2.9E+00	2.8E+00	2.7E+00	2.6E+00	2.5E+00	2.4E+00	2.4E+00	2.2E+00

Table 13

Pressure Dependence of the Heat of Solution: $\frac{\Delta\bar{H}_s}{RT}(P_2) - \frac{\Delta\bar{H}_s}{RT}(P_1)$

TEMP (°C)	P1 (BAR)	P2 (BAR)	$\frac{\bar{H}_2^\circ}{RT}$	MOLALITY .001	.005	.010	.020	.030	.040	.050	.100
25	1	400	-5.8E-02	-4.9E-01	-4.9E-01	-4.9E-01	-4.9E-01	-4.9E-01	-4.9E-01	-4.9E-01	-4.9E-01
30	1	400	5.1E-03	-4.2E-01	-4.2E-01	-4.2E-01	-4.2E-01	-4.2E-01	-4.2E-01	-4.2E-01	-4.2E-01
40	1	400	1.1E-01	-3.0E-01	-3.0E-01	-3.0E-01	-3.0E-01	-3.0E-01	-3.1E-01	-3.1E-01	-3.1E-01
50	1	400	2.0E-01	-2.0E-01	-2.0E-01	-2.0E-01	-2.0E-01	-2.1E-01	-2.1E-01	-2.1E-01	-2.1E-01
60	1	400	2.8E-01	-1.1E-01	-1.1E-01	-1.2E-01	-1.2E-01	-1.2E-01	-1.2E-01	-1.2E-01	-1.3E-01
70	1	400	3.5E-01	-3.0E-02	-3.3E-02	-3.6E-02	-3.9E-02	-4.2E-02	-4.3E-02	-4.5E-02	-5.1E-02
80	1	400	4.1E-01	4.5E-02	4.1E-02	3.8E-02	3.4E-02	3.1E-02	2.9E-02	2.7E-02	1.9E-02
90	1	400	4.7E-01	1.2E-01	1.1E-01	1.1E-01	1.0E-01	1.0E-01	9.7E-02	9.5E-02	8.6E-02
100	1	400	5.3E-01	1.9E-01	1.8E-01	1.8E-01	1.7E-01	1.7E-01	1.6E-01	1.6E-01	1.5E-01
110	1	400	5.9E-01	2.5E-01	2.5E-01	2.4E-01	2.4E-01	2.3E-01	2.3E-01	2.2E-01	2.1E-01
120	2	400	6.5E-01	3.2E-01	3.2E-01	3.1E-01	3.0E-01	3.0E-01	2.9E-01	2.9E-01	2.7E-01
130	3	400	7.2E-01	3.9E-01	3.8E-01	3.8E-01	3.7E-01	3.6E-01	3.6E-01	3.5E-01	3.4E-01
140	4	400	7.8E-01	4.7E-01	4.6E-01	4.5E-01	4.4E-01	4.3E-01	4.3E-01	4.2E-01	4.0E-01
150	5	400	8.5E-01	5.4E-01	5.3E-01	5.2E-01	5.1E-01	5.0E-01	4.9E-01	4.9E-01	4.7E-01
160	6	400	9.3E-01	6.2E-01	6.1E-01	6.0E-01	5.9E-01	5.8E-01	5.7E-01	5.6E-01	5.3E-01
170	8	400	1.0E+00	7.1E-01	7.0E-01	6.8E-01	6.7E-01	6.6E-01	6.5E-01	6.4E-01	6.1E-01
180	10	400	1.1E+00	8.1E-01	7.9E-01	7.8E-01	7.6E-01	7.4E-01	7.3E-01	7.2E-01	6.9E-01
190	13	400	1.2E+00	9.2E-01	8.9E-01	8.8E-01	8.6E-01	8.4E-01	8.3E-01	8.1E-01	7.7E-01
200	16	400	1.3E+00	1.0E+00	1.0E+00	9.9E-01	9.7E-01	9.5E-01	9.3E-01	9.2E-01	8.7E-01
210	19	400	1.5E+00	1.2E+00	1.1E+00	1.1E+00	1.1E+00	1.1E+00	1.1E+00	1.0E+00	9.8E-01
220	23	400	1.6E+00	1.3E+00	1.3E+00	1.3E+00	1.2E+00	1.2E+00	1.2E+00	1.2E+00	1.1E+00
230	28	400	1.8E+00	1.5E+00	1.5E+00	1.5E+00	1.4E+00	1.4E+00	1.4E+00	1.3E+00	1.2E+00
240	33	400	2.1E+00	1.8E+00	1.7E+00	1.7E+00	1.6E+00	1.6E+00	1.6E+00	1.5E+00	1.4E+00
250	40	400	2.3E+00	2.1E+00	2.0E+00	2.0E+00	1.9E+00	1.8E+00	1.8E+00	1.8E+00	1.6E+00
260	47	400	2.7E+00	2.4E+00	2.4E+00	2.3E+00	2.2E+00	2.2E+00	2.1E+00	2.1E+00	1.9E+00
270	55	400	3.2E+00	2.9E+00	2.8E+00	2.7E+00	2.6E+00	2.6E+00	2.5E+00	2.5E+00	2.3E+00
280	64	400	3.9E+00	3.6E+00	3.4E+00	3.3E+00	3.2E+00	3.1E+00	3.0E+00	3.0E+00	2.7E+00
290	74	400	4.8E+00	4.4E+00	4.3E+00	4.2E+00	4.0E+00	3.9E+00	3.8E+00	3.7E+00	3.4E+00
300	86	400	6.0E+00	5.7E+00	5.5E+00	5.3E+00	5.1E+00	4.9E+00	4.8E+00	4.7E+00	4.3E+00

Table 13

Pressure Dependence of the Heat of Solution: $\frac{\Delta\bar{H}_s}{RT}(P_2) - \frac{\Delta\bar{H}_s}{RT}(P_1)$

TEMP (C)	P1 (BAR)	P2 (BAR)	$\frac{\bar{H}_2^\circ}{RT}$	MOLALITY .001	.005	.010	.020	.030	.040	.050	.100
25	1	600	-5.0E-02	-7.0E-01	-7.0E-01	-7.0E-01	-7.0E-01	-7.0E-01	-7.0E-01	-7.0E-01	-7.0E-01
30	1	600	4.0E-02	-6.0E-01	-6.0E-01	-6.0E-01	-6.0E-01	-6.0E-01	-6.0E-01	-6.0E-01	-6.0E-01
40	1	600	1.9E-01	-4.3E-01	-4.3E-01	-4.3E-01	-4.3E-01	-4.3E-01	-4.4E-01	-4.4E-01	-4.4E-01
50	1	600	3.1E-01	-2.8E-01	-2.9E-01	-2.9E-01	-2.9E-01	-2.9E-01	-2.9E-01	-3.0E-01	-3.0E-01
60	1	600	4.2E-01	-1.6E-01	-1.6E-01	-1.6E-01	-1.7E-01	-1.7E-01	-1.7E-01	-1.7E-01	-1.8E-^1
70	1	600	5.2E-01	-4.1E-02	-4.6E-02	-4.9E-02	-5.4E-02	-5.7E-02	-6.0E-02	-6.3E-02	-7.1E-02
80	1	600	6.1E-01	6.6E-02	6.0E-02	5.6E-02	5.0E-02	4.6E-02	4.3E-02	4.0E-02	3.0E-02
90	1	600	7.0E-01	1.7E-01	1.6E-01	1.6E-01	1.5E-01	1.4E-01	1.4E-01	1.4E-01	1.2E-01
100	1	600	7.9E-01	2.7E-01	2.6E-01	2.5E-01	2.5E-01	2.4E-01	2.4E-01	2.3E-01	2.2E-01
110	1	600	8.7E-01	3.6E-01	3.6E-01	3.5E-01	3.4E-01	3.3E-01	3.3E-01	3.2E-01	3.1E-01
120	2	600	9.6E-01	4.6E-01	4.5E-01	4.4E-01	4.3E-01	4.3E-01	4.2E-01	4.1E-01	3.9E-01
130	3	600	1.0E+00	5.6E-01	5.5E-01	5.4E-01	5.3E-01	5.2E-01	5.1E-01	5.1E-01	4.8E-01
140	4	600	1.1E+00	6.7E-01	6.5E-01	6.4E-01	6.3E-01	6.2E-01	6.1E-01	6.0E-01	5.7E-01
150	5	600	1.2E+00	7.7E-01	7.6E-01	7.5E-01	7.3E-01	7.2E-01	7.1E-01	7.0E-01	6.7E-01
160	6	600	1.3E+00	8.9E-01	8.7E-01	8.5E-01	8.4E-01	8.2E-01	8.1E-01	8.0E-01	7.6E-01
170	8	600	1.5E+00	1.0E+00	9.9E-01	9.7E-01	9.5E-01	9.3E-01	9.2E-01	9.1E-01	8.7E-01
180	10	600	1.6E+00	1.1E+00	1.1E+00	1.1E+00	1.1E+00	1.1E+00	1.0E+00	1.0E+00	9.8E-01
190	13	600	1.7E+00	1.3E+00	1.3E+00	1.2E+00	1.2E+00	1.2E+00	1.2E+00	1.2E+00	1.1E+00
200	16	600	1.9E+00	1.5E+00	1.4E+00	1.4E+00	1.4E+00	1.3E+00	1.3E+00	1.3E+00	1.2E+00
210	19	600	2.1E+00	1.7E+00	1.6E+00	1.6E+00	1.5E+00	1.5E+00	1.5E+00	1.5E+00	1.4E+00
220	23	600	2.3E+00	1.9E+00	1.8E+00	1.8E+00	1.7E+00	1.7E+00	1.7E+00	1.6E+00	1.5E+00
230	28	600	2.5E+00	2.1E+00	2.1E+00	2.0E+00	2.0E+00	1.9E+00	1.9E+00	1.8E+00	1.7E+00
240	33	600	2.9E+00	2.4E+00	2.4E+00	2.3E+00	2.2E+00	2.2E+00	2.1E+00	2.1E+00	2.0E+00
250	40	600	3.2E+00	2.8E+00	2.7E+00	2.7E+00	2.6E+00	2.5E+00	2.5E+00	2.4E+00	2.2E+00
260	47	600	3.7E+00	3.3E+00	3.2E+00	3.1E+00	3.0E+00	2.9E+00	2.8E+00	2.8E+00	2.6E+00
270	55	600	4.3E+00	3.9E+00	3.7E+00	3.7E+00	3.5E+00	3.4E+00	3.3E+00	3.3E+00	3.0E+00
280	64	600	5.1E+00	4.7E+00	4.5E+00	4.4E+00	4.2E+00	4.1E+00	4.0E+00	3.9E+00	3.6E+00
290	74	600	6.2E+00	5.7E+00	5.5E+00	5.4E+00	5.1E+00	5.0E+00	4.9E+00	4.8E+00	4.4E+00
300	86	600	7.7E+00	7.2E+00	6.9E+00	6.7E+00	6.4E+00	6.2E+00	6.1E+00	5.9E+00	5.4E+00

Table 13

Pressure Dependence of the Heat of Solution: $\frac{\Delta\bar{H}_s}{RT}(P_2) - \frac{\Delta\bar{H}_s}{RT}(P_1)$

TEMP (°C)	P1 (BAR)	P2 (BAR)	$\frac{\bar{H}_2^\circ}{RT}$	MOLALITY .001	.005	.010	.020	.030	.040	.050	.100
25	1	1000	3.4E-02	-1.0E+00	-1.0E+00	-1.0E+00	-1.0E+00	-1.0E+00	-1.0E+00	-1.0E+00	-1.0E+00
30	1	1000	1.6E-01	-8.9E-01	-9.0E-01	-9.0E-01	-9.0E-01	-9.0E-01	-9.0E-01	-9.0E-01	-9.0E-01
40	1	1000	3.8E-01	-6.4E-01	-6.5E-01	-6.5E-01	-6.5E-01	-6.5E-01	-6.6E-01	-6.6E-01	-6.6E-01
50	1	1000	5.7E-01	-4.3E-01	-4.3E-01	-4.4E-01	-4.4E-01	-4.4E-01	-4.5E-01	-4.5E-01	-4.5E-01
60	1	1000	7.3E-01	-2.4E-01	-2.4E-01	-2.5E-01	-2.5E-01	-2.6E-01	-2.6E-01	-2.6E-01	-2.7E-01
70	1	1000	8.7E-01	-6.5E-02	-7.3E-02	-7.8E-02	-8.5E-02	-9.0E-02	-9.4E-02	-9.8E-02	-1.1E-01
80	1	1000	1.0E+00	9.5E-02	8.6E-02	8.0E-02	7.2E-02	6.5E-02	6.0E-02	5.6E-02	4.0E-02
90	1	1000	1.1E+00	2.5E-01	2.4E-01	2.3E-01	2.2E-01	2.1E-01	2.1E-01	2.0E-01	1.8E-01
100	1	1000	1.3E+00	4.0E-01	3.8E-01	3.8E-01	3.6E-01	3.5E-01	3.5E-01	3.4E-01	3.2E-01
110	1	1000	1.4E+00	5.4E-01	5.3E-01	5.2E-01	5.0E-01	4.9E-01	4.9E-01	4.8E-01	4.5E-01
120	2	1000	1.5E+00	6.9E-01	6.7E-01	6.6E-01	6.4E-01	6.3E-01	6.2E-01	6.1E-01	5.8E-01
130	3	1000	1.6E+00	8.3E-01	8.2E-01	8.0E-01	7.8E-01	7.7E-01	7.6E-01	7.5E-01	7.2E-01
140	4	1000	1.8E+00	9.9E-01	9.6E-01	9.5E-01	9.3E-01	9.1E-01	9.0E-01	8.9E-01	8.5E-01
150	5	1000	1.9E+00	1.1E+00	1.1E+00	1.1E+00	1.1E+00	1.1E+00	1.0E+00	1.0E+00	9.8E-01
160	6	1000	2.1E+00	1.3E+00	1.3E+00	1.3E+00	1.2E+00	1.2E+00	1.2E+00	1.2E+00	1.1E+00
170	8	1000	2.2E+00	1.5E+00	1.5E+00	1.4E+00	1.4E+00	1.4E+00	1.4E+00	1.3E+00	1.3E+00
180	10	1000	2.4E+00	1.7E+00	1.6E+00	1.6E+00	1.6E+00	1.5E+00	1.5E+00	1.5E+00	1.4E+00
190	13	1000	2.6E+00	1.9E+00	1.8E+00	1.8E+00	1.8E+00	1.7E+00	1.7E+00	1.7E+00	1.6E+00
200	16	1000	2.8E+00	2.1E+00	2.1E+00	2.0E+00	2.0E+00	1.9E+00	1.9E+00	1.9E+00	1.8E+00
210	19	1000	3.1E+00	2.4E+00	2.3E+00	2.3E+00	2.2E+00	2.2E+00	2.1E+00	2.1E+00	2.0E+00
220	23	1000	3.4E+00	2.7E+00	2.6E+00	2.6E+00	2.5E+00	2.4E+00	2.4E+00	2.4E+00	2.2E+00
230	28	1000	3.7E+00	3.0E+00	2.9E+00	2.9E+00	2.8E+00	2.7E+00	2.7E+00	2.6E+00	2.5E+00
240	33	1000	4.1E+00	3.4E+00	3.3E+00	3.2E+00	3.1E+00	3.1E+00	3.0E+00	3.0E+00	2.8E+00
250	40	1000	4.6E+00	3.9E+00	3.8E+00	3.7E+00	3.6E+00	3.5E+00	3.4E+00	3.3E+00	3.1E+00
260	47	1000	5.2E+00	4.5E+00	4.3E+00	4.2E+00	4.1E+00	4.0E+00	3.9E+00	3.8E+00	3.5E+00
270	55	1000	5.9E+00	5.2E+00	5.0E+00	4.9E+00	4.7E+00	4.6E+00	4.5E+00	4.4E+00	4.1E+00
280	64	1000	6.8E+00	6.1E+00	5.9E+00	5.7E+00	5.5E+00	5.3E+00	5.2E+00	5.1E+00	4.7E+00
290	74	1000	8.0E+00	7.3E+00	7.0E+00	6.8E+00	6.5E+00	6.3E+00	6.2E+00	6.0E+00	5.6E+00
300	86	1000	9.7E+00	8.9E+00	8.5E+00	8.3E+00	7.9E+00	7.7E+00	7.5E+00	7.3E+00	6.7E+00

Table 14

Pressure Dependence of the Apparent Molal Enthalpy: $\frac{\phi_L}{RT}(P_2) - \frac{\phi_L}{RT}(P_1)$

TEMP (°C)	P1 (BAR)	P2 (BAR)	MOLALITY .100	.250	.500	.750	1.000	2.000	3.000	4.000
25	1	200	-2.2E-03	1.1E-03	8.3E-03	1.6E-02	2.4E-02	5.3E-02	7.8E-02	9.8E-02
30	1	200	-3.4E-03	-1.3E-03	4.2E-03	1.0E-02	1.7E-02	4.1E-02	6.3E-02	8.0E-02
40	1	200	-5.6E-03	-5.6E-03	-2.9E-03	6.4E-04	4.6E-03	2.1E-02	3.6E-02	4.8E-02
50	1	200	-7.9E-03	-9.5E-03	-9.3E-03	-7.8E-03	-5.8E-03	4.0E-03	1.4E-02	2.3E-02
60	1	200	-1.0E-02	-1.3E-02	-1.5E-02	-1.6E-02	-1.5E-02	-1.1E-02	-5.4E-03	-9.0E-05
70	1	200	-1.3E-02	-1.7E-02	-2.1E-02	-2.3E-02	-2.4E-02	-2.5E-02	-2.3E-02	-2.1E-02
80	1	200	-1.5E-02	-2.2E-02	-2.7E-02	-3.1E-02	-3.3E-02	-3.8E-02	-4.0E-02	-4.1E-02
90	1	200	-1.8E-02	-2.6E-02	-3.4E-02	-3.9E-02	-4.2E-02	-5.1E-02	-5.7E-02	-6.0E-02
100	1	200	-2.1E-02	-3.1E-02	-4.1E-02	-4.7E-02	-5.2E-02	-6.5E-02	-7.3E-02	-7.9E-02
110	1	200	-2.5E-02	-3.7E-02	-4.8E-02	-5.6E-02	-6.2E-02	-7.9E-02	-9.0E-02	-9.9E-02
120	2	200	-2.9E-02	-4.3E-02	-5.7E-02	-6.6E-02	-7.4E-02	-9.4E-02	-1.1E-01	-1.2E-01
130	3	200	-3.4E-02	-5.0E-02	-6.6E-02	-7.8E-02	-8.6E-02	-1.1E-01	-1.3E-01	-1.4E-01
140	4	200	-4.0E-02	-5.9E-02	-7.7E-02	-9.0E-02	-1.0E-01	-1.3E-01	-1.5E-01	-1.6E-01
150	5	200	-4.7E-02	-6.9E-02	-9.0E-02	-1.0E-01	-1.2E-01	-1.5E-01	-1.7E-01	-1.9E-01
160	6	200	-5.5E-02	-8.0E-02	-1.0E-01	-1.2E-01	-1.3E-01	-1.7E-01	-1.9E-01	-2.1E-01
170	8	200	-6.4E-02	-9.3E-02	-1.2E-01	-1.4E-01	-1.6E-01	-2.0E-01	-2.2E-01	-2.4E-01
180	10	200	-7.5E-02	-1.1E-01	-1.4E-01	-1.6E-01	-1.8E-01	-2.2E-01	-2.5E-01	-2.8E-01
190	13	200	-8.8E-02	-1.3E-01	-1.7E-01	-1.9E-01	-2.1E-01	-2.6E-01	-2.9E-01	-3.1E-01
200	16	200	-1.0E-01	-1.5E-01	-1.9E-01	-2.2E-01	-2.4E-01	-3.0E-01	-3.3E-01	-3.6E-01
210	19	200	-1.2E-01	-1.8E-01	-2.3E-01	-2.6E-01	-2.9E-01	-3.5E-01	-3.8E-01	-4.1E-01
220	23	200	-1.5E-01	-2.1E-01	-2.7E-01	-3.1E-01	-3.4E-01	-4.1E-01	-4.5E-01	-4.7E-01
230	28	200	-1.8E-01	-2.5E-01	-3.2E-01	-3.7E-01	-4.0E-01	-4.8E-01	-5.2E-01	-5.5E-01
240	33	200	-2.1E-01	-3.0E-01	-3.9E-01	-4.4E-01	-4.8E-01	-5.7E-01	-6.2E-01	-6.4E-01
250	40	200	-2.6E-01	-3.7E-01	-4.7E-01	-5.3E-01	-5.8E-01	-6.8E-01	-7.4E-01	-7.6E-01
260	47	200	-3.1E-01	-4.5E-01	-5.7E-01	-6.5E-01	-7.0E-01	-8.3E-01	-8.9E-01	-9.2E-01
270	55	200	-3.8E-01	-5.5E-01	-7.0E-01	-8.0E-01	-8.6E-01	-1.0E+00	-1.1E+00	-1.1E+00
280	64	200	-4.8E-01	-6.8E-01	-8.7E-01	-9.9E-01	-1.1E+00	-1.3E+00	-1.4E+00	-1.4E+00
290	74	200	-6.0E-01	-8.6E-01	-1.1E+00	-1.2E+00	-1.4E+00	-1.6E+00	-1.7E+00	-1.8E+00
300	86	200	-7.6E-01	-1.1E+00	-1.4E+00	-1.6E+00	-1.7E+00	-2.1E+00	-2.2E+00	-2.3E+00

Table 14

Pressure Dependence of the Apparent Molal Enthalpy: $\frac{\phi_L}{RT}(P_2) - \frac{\phi_L}{RT}(P_1)$

TEMP (°C)	P1 (BAR)	P2 (BAR)	MOLALITY .100	.250	.500	.750	1.000	2.000	3.000	4.000
25	1	400	-3.9E-03	-2.5E-03	1.7E-02	3.2E-02	4.7E-02	1.0E-01	1.5E-01	1.9E-01
30	1	400	-6.3E-03	-2.1E-03	8.6E-03	2.1E-02	3.3E-02	8.0E-02	1.2E-01	1.5E-01
40	1	400	-1.1E-02	-1.0E-02	-5.4E-03	1.6E-03	9.2E-03	4.0E-02	6.9E-02	9.2E-02
50	1	400	-1.5E-02	-1.8E-02	-1.8E-02	-1.5E-02	-1.1E-02	7.5E-03	2.6E-02	4.2E-02
60	1	400	-1.9E-02	-2.6E-02	-2.9E-02	-3.0E-02	-2.9E-02	-2.1E-02	-1.1E-02	-1.9E-03
70	1	400	-2.4E-02	-3.3E-02	-4.1E-02	-4.4E-02	-4.7E-02	-4.8E-02	-4.6E-02	-4.2E-02
80	1	400	-2.9E-02	-4.1E-02	-5.2E-02	-5.9E-02	-6.4E-02	-7.4E-02	-7.8E-02	-8.0E-02
90	1	400	-3.4E-02	-5.0E-02	-6.4E-02	-7.4E-02	-8.1E-02	-9.9E-02	-1.1E-01	-1.2E-01
100	1	400	-4.1E-02	-5.9E-02	-7.7E-02	-9.0E-02	-9.9E-02	-1.3E-01	-1.4E-01	-1.5E-01
110	1	400	-4.8E-02	-7.0E-02	-9.2E-02	-1.1E-01	-1.2E-01	-1.5E-01	-1.7E-01	-1.9E-01
120	2	400	-5.5E-02	-8.2E-02	-1.1E-01	-1.3E-01	-1.4E-01	-1.8E-01	-2.1E-01	-2.3E-01
130	3	400	-6.5E-02	-9.5E-02	-1.3E-01	-1.5E-01	-1.6E-01	-2.1E-01	-2.4E-01	-2.7E-01
140	4	400	-7.5E-02	-1.1E-01	-1.5E-01	-1.7E-01	-1.9E-01	-2.4E-01	-2.8E-01	-3.1E-01
150	5	400	-8.8E-02	-1.3E-01	-1.7E-01	-2.0E-01	-2.2E-01	-2.8E-01	-3.3E-01	-3.6E-01
160	6	400	-1.0E-01	-1.5E-01	-2.0E-01	-2.3E-01	-2.5E-01	-3.2E-01	-3.7E-01	-4.1E-01
170	8	400	-1.2E-01	-1.7E-01	-2.3E-01	-2.6E-01	-2.9E-01	-3.7E-01	-4.2E-01	-4.7E-01
180	10	400	-1.4E-01	-2.0E-01	-2.7E-01	-3.1E-01	-3.4E-01	-4.3E-01	-4.8E-01	-5.3E-01
190	13	400	-1.6E-01	-2.4E-01	-3.1E-01	-3.6E-01	-3.9E-01	-4.9E-01	-5.5E-01	-6.0E-01
200	16	400	-1.9E-01	-2.8E-01	-3.6E-01	-4.2E-01	-4.6E-01	-5.7E-01	-6.3E-01	-6.8E-01
210	19	400	-2.3E-01	-3.3E-01	-4.3E-01	-4.9E-01	-5.4E-01	-6.6E-01	-7.3E-01	-7.8E-01
220	23	400	-2.7E-01	-4.0E-01	-5.1E-01	-5.8E-01	-6.4E-01	-7.7E-01	-8.5E-01	-9.0E-01
230	28	400	-3.3E-01	-4.7E-01	-6.1E-01	-6.9E-01	-7.5E-01	-9.0E-01	-9.9E-01	-1.0E+00
240	33	400	-4.0E-01	-5.7E-01	-7.3E-01	-8.3E-01	-9.0E-01	-1.1E+00	-1.2E+00	-1.2E+00
250	40	400	-4.8E-01	-6.9E-01	-8.8E-01	-1.0E+00	-1.1E+00	-1.3E+00	-1.4E+00	-1.5E+00
260	47	400	-5.9E-01	-8.5E-01	-1.1E+00	-1.2E+00	-1.3E+00	-1.6E+00	-1.7E+00	-1.8E+00
270	55	400	-7.4E-01	-1.1E+00	-1.3E+00	-1.5E+00	-1.7E+00	-1.9E+00	-2.1E+00	-2.2E+00
280	64	400	-9.3E-01	-1.3E+00	-1.7E+00	-1.9E+00	-2.1E+00	-2.4E+00	-2.6E+00	-2.7E+00
290	74	400	-1.2E+00	-1.7E+00	-2.2E+00	-2.5E+00	-2.7E+00	-3.1E+00	-3.3E+00	-3.4E+00
300	86	400	-1.6E+00	-2.2E+00	-2.8E+00	-3.2E+00	-3.5E+00	-4.1E+00	-4.4E+00	-4.5E+00

Table 14

Pressure Dependence of the Apparent Molal Enthalpy: $\frac{\phi_L}{RT}(P_2) - \frac{\phi_L}{RT}(P_1)$

TEMP (°C)	P1 (BAR)	P2 (BAR)	MOLALITY .100	.250	.500	.750	1.000	2.000	3.000	4.000
25	1	600	-5.4E-03	4.2E-03	2.5E-02	4.7E-02	6.9E-02	1.5E-01	2.2E-01	2.7E-01
30	1	600	-8.8E-03	-2.6E-03	1.3E-02	3.0E-02	4.8E-02	1.2E-01	1.7E-01	2.2E-01
40	1	600	-1.5E-02	-1.5E-02	-7.3E-03	2.7E-03	1.4E-02	5.8E-02	9.8E-02	1.3E-01
50	1	600	-2.1E-02	-2.6E-02	-2.5E-02	-2.1E-02	-1.6E-02	1.1E-02	3.6E-02	5.8E-02
60	1	600	-2.8E-02	-3.7E-02	-4.2E-02	-4.3E-02	-4.2E-02	-3.1E-02	-1.7E-02	-4.6E-03
70	1	600	-3.4E-02	-4.7E-02	-5.8E-02	-6.4E-02	-6.7E-02	-6.9E-02	-6.6E-02	-6.2E-02
80	1	600	-4.1E-02	-5.9E-02	-7.5E-02	-8.4E-02	-9.1E-02	-1.1E-01	-1.1E-01	-1.2E-01
90	1	600	-4.9E-02	-7.1E-02	-9.2E-02	-1.1E-01	-1.2E-01	-1.4E-01	-1.6E-01	-1.7E-01
100	1	600	-5.8E-02	-8.4E-02	-1.1E-01	-1.3E-01	-1.4E-01	-1.8E-01	-2.0E-01	-2.2E-01
110	1	600	-6.7E-02	-9.9E-02	-1.3E-01	-1.5E-01	-1.7E-01	-2.2E-01	-2.5E-01	-2.8E-01
120	2	600	-7.8E-02	-1.2E-01	-1.5E-01	-1.8E-01	-2.0E-01	-2.6E-01	-3.0E-01	-3.3E-01
130	3	600	-9.1E-02	-1.3E-01	-1.8E-01	-2.1E-01	-2.3E-01	-3.0E-01	-3.5E-01	-3.9E-01
140	4	600	-1.1E-01	-1.6E-01	-2.1E-01	-2.4E-01	-2.7E-01	-3.5E-01	-4.0E-01	-4.5E-01
150	5	600	-1.2E-01	-1.8E-01	-2.4E-01	-2.8E-01	-3.1E-01	-4.0E-01	-4.6E-01	-5.1E-01
160	6	600	-1.4E-01	-2.1E-01	-2.7E-01	-3.2E-01	-3.6E-01	-4.6E-01	-5.3E-01	-5.9E-01
170	8	600	-1.7E-01	-2.4E-01	-3.2E-01	-3.7E-01	-4.1E-01	-5.2E-01	-6.0E-01	-6.6E-01
180	10	600	-1.9E-01	-2.8E-01	-3.7E-01	-4.3E-01	-4.7E-01	-6.0E-01	-6.8E-01	-7.5E-01
190	13	600	-2.3E-01	-3.3E-01	-4.3E-01	-5.0E-01	-5.5E-01	-6.8E-01	-7.8E-01	-8.5E-01
200	16	600	-2.7E-01	-3.9E-01	-5.0E-01	-5.8E-01	-6.3E-01	-7.9E-01	-8.8E-01	-9.6E-01
210	19	600	-3.1E-01	-4.5E-01	-5.9E-01	-6.7E-01	-7.4E-01	-9.1E-01	-1.0E+00	-1.1E+00
220	23	600	-3.7E-01	-5.4E-01	-6.9E-01	-7.9E-01	-8.7E-01	-1.1E+00	-1.2E+00	-1.2E+00
230	28	600	-4.4E-01	-6.4E-01	-8.2E-01	-9.4E-01	-1.0E+00	-1.2E+00	-1.4E+00	-1.4E+00
240	33	600	-5.3E-01	-7.7E-01	-9.8E-01	-1.1E+00	-1.2E+00	-1.5E+00	-1.6E+00	-1.7E+00
250	40	600	-6.5E-01	-9.3E-01	-1.2E+00	-1.3E+00	-1.5E+00	-1.7E+00	-1.9E+00	-2.0E+00
260	47	600	-7.9E-01	-1.1E+00	-1.4E+00	-1.6E+00	-1.8E+00	-2.1E+00	-2.2E+00	-2.3E+00
270	55	600	-9.8E-01	-1.4E+00	-1.8E+00	-2.0E+00	-2.2E+00	-2.6E+00	-2.7E+00	-2.8E+00
280	64	600	-1.2E+00	-1.7E+00	-2.2E+00	-2.5E+00	-2.7E+00	-3.2E+00	-3.4E+00	-3.5E+00
290	74	600	-1.6E+00	-2.2E+00	-2.8E+00	-3.2E+00	-3.5E+00	-4.0E+00	-4.3E+00	-4.4E+00
300	86	600	-2.0E+00	-2.9E+00	-3.7E+00	-4.1E+00	-4.5E+00	-5.2E+00	-5.6E+00	-5.7E+00

Table 14

Pressure Dependence of the Apparent Molal Enthalpy: $\frac{\phi_L}{RT}(P_2) - \frac{\phi_L}{RT}(P_1)$

TEMP (°C)	P1 (BAR)	P2 (BAR)	MOLALITY .100	.250	.500	.750	1.000	2.000	3.000	4.000
25	1	1000	-7.4E-03	7.8E-03	4.0E-02	7.4E-02	1.1E-01	2.3E-01	3.3E-01	4.1E-01
30	1	1000	-1.3E-02	-2.8E-03	2.2E-02	4.8E-02	7.6E-02	1.8E-01	2.6E-01	3.3E-01
40	1	1000	-2.3E-02	-2.2E-02	-1.0E-02	5.3E-03	2.2E-02	9.0E-02	1.5E-01	1.9E-01
50	1	1000	-3.2E-02	-3.9E-02	-3.8E-02	-3.1E-02	-2.3E-02	1.7E-02	5.4E-02	8.6E-02
60	1	1000	-4.2E-02	-5.5E-02	-6.3E-02	-6.4E-02	-6.3E-02	-4.7E-02	-2.7E-02	-8.9E-03
70	1	1000	-5.1E-02	-7.1E-02	-8.7E-02	-9.6E-02	-1.0E-01	-1.0E-01	-1.0E-01	-9.5E-02
80	1	1000	-6.2E-02	-8.8E-02	-1.1E-01	-1.3E-01	-1.4E-01	-1.6E-01	-1.7E-01	-1.8E-01
90	1	1000	-7.3E-02	-1.1E-01	-1.4E-01	-1.6E-01	-1.7E-01	-2.1E-01	-2.4E-01	-2.5E-01
100	1	1000	-8.6E-02	-1.3E-01	-1.6E-01	-1.9E-01	-2.1E-01	-2.7E-01	-3.0E-01	-3.3E-01
110	1	1000	-1.0E-01	-1.5E-01	-1.9E-01	-2.3E-01	-2.5E-01	-3.2E-01	-3.7E-01	-4.1E-01
120	2	1000	-1.2E-01	-1.7E-01	-2.3E-01	-2.6E-01	-2.9E-01	-3.8E-01	-4.4E-01	-4.9E-01
130	3	1000	-1.3E-01	-2.0E-01	-2.6E-01	-3.1E-01	-3.4E-01	-4.4E-01	-5.2E-01	-5.7E-01
140	4	1000	-1.5E-01	-2.3E-01	-3.0E-01	-3.5E-01	-3.9E-01	-5.1E-01	-5.9E-01	-6.6E-01
150	5	1000	-1.8E-01	-2.6E-01	-3.5E-01	-4.1E-01	-4.5E-01	-5.8E-01	-6.8F-01	-7.6E-01
160	6	1000	-2.1E-01	-3.0E-01	-4.0E-01	-4.6E-01	-5.2E-01	-6.7E-01	-7.7E-01	-8.6E-01
170	8	1000	-2.4E-01	-3.5E-01	-4.6E-01	-5.3E-01	-5.9E-01	-7.6E-01	-8.7E-01	-9.7E-01
180	10	1000	-2.8E-01	-4.0E-01	-5.3E-01	-6.1E-01	-6.8E-01	-8.6E-01	-9.9E-01	-1.1E+00
190	13	1000	-3.2E-01	-4.7E-01	-6.1E-01	-7.0E-01	-7.8E-01	-9.8E-01	-1.1E+00	-1.2E+00
200	16	1000	-3.7E-01	-5.4E-01	-7.0E-01	-8.1E-01	-9.0E-01	-1.1E+00	-1.3E+00	-1.4E+00
210	19	1000	-4.4E-01	-6.3E-01	-8.2E-01	-9.4E-01	-1.0E+00	-1.3E+00	-1.4E+00	-1.6E+00
220	23	1000	-5.1E-01	-7.4E-01	-9.6E-01	-1.1E+00	-1.2E+00	-1.5E+00	-1.6E+00	-1.8E+00
230	28	1000	-6.1E-01	-8.7E-01	-1.1E+00	-1.3E+00	-1.4E+00	-1.7E+00	-1.9E+00	-2.0E+00
240	33	1000	-7.2E-01	-1.0E+00	-1.3E+00	-1.5E+00	-1.6E+00	-2.0E+00	-2.2E+00	-2.3E+00
250	40	1000	-8.6E-01	-1.2E+00	-1.6E+00	-1.8E+00	-2.0E+00	-2.3E+00	-2.5E+00	-2.7E+00
260	47	1000	-1.0E+00	-1.5E+00	-1.9E+00	-2.2E+00	-2.3E+00	-2.8E+00	-3.0E+00	-3.1E+00
270	55	1000	-1.3E+00	-1.8E+00	-2.3E+00	-2.6E+00	-2.8E+00	-3.3E+00	-3.5E+00	-3.7E+00
280	64	1000	-1.6E+00	-2.2E+00	-2.8E+00	-3.2E+00	-3.5E+00	-4.0E+00	-4.3E+00	-4.4E+00
290	74	1000	-2.0E+00	-2.8E+00	-3.5E+00	-4.0E+00	-4.3E+00	-5.0E+00	-5.3E+00	-5.4E+00
300	86	1000	-2.5E+00	-3.5E+00	-4.5E+00	-5.1E+00	-5.5E+00	-6.3E+00	-6.7E+00	-6.8E+00

Table 15

Pressure Dependence of the Apparent Molal Heat Capacity: $\frac{\phi C_p}{R}(P_2) - \frac{\phi C_p}{R}(P_1)$

TEMP (°C)	P1 (BAR)	P2 (BAR)	$\frac{\bar{C}^{\circ}_{p_2}}{R}$	MOLALITY .100	.250	.500	.750	1.000	2.000	3.000	4.000
25	1	200	2.1E+00	2.0E+00	1.9E+00	1.8E+00	1.7E+00	1.6E+00	1.4E+00	1.1E+00	9.9E-01
30	1	200	1.9E+00	1.8E+00	1.7E+00	1.7E+00	1.6E+00	1.5E+00	1.2E+00	1.0E+00	9.1E-01
40	1	200	1.6E+00	1.6E+00	1.5E+00	1.4E+00	1.3E+00	1.3E+00	1.1E+00	9.1E-01	8.0E-01
50	1	200	1.5E+00	1.4E+00	1.3E+00	1.3E+00	1.2E+00	1.2E+00	9.8E-01	8.4E-01	7.3E-01
60	1	200	1.4E+00	1.3E+00	1.3E+00	1.2E+00	1.1E+00	1.1E+00	9.2E-01	7.9E-01	6.9E-01
70	1	200	1.4E+00	1.3E+00	1.2E+00	1.1E+00	1.1E+00	1.0E+00	8.9E-01	7.6E-01	6.6E-01
80	1	200	1.4E+00	1.3E+00	1.2E+00	1.1E+00	1.1E+00	1.0E+00	8.7E-01	7.5E-01	6.5E-01
90	1	200	1.4E+00	1.3E+00	1.2E+00	1.1E+00	1.1E+00	1.0E+00	8.7E-01	7.5E-01	6.5E-01
100	1	200	1.5E+00	1.3E+00	1.2E+00	1.1E+00	1.1E+00	1.0E+00	8.8E-01	7.6E-01	6.6E-01
110	1	200	1.5E+00	1.4E+00	1.3E+00	1.2E+00	1.1E+00	1.1E+00	9.0E-01	7.8E-01	6.7E-01
120	2	200	1.6E+00	1.4E+00	1.3E+00	1.2E+00	1.2E+00	1.1E+00	9.3E-01	8.0E-01	7.0E-01
130	3	200	1.8E+00	1.5E+00	1.4E+00	1.3E+00	1.2E+00	1.1E+00	9.7E-01	8.4E-01	7.4E-01
140	4	200	1.9E+00	1.6E+00	1.5E+00	1.4E+00	1.3E+00	1.2E+00	1.0E+00	8.9E-01	7.9E-01
150	5	200	2.2E+00	1.8E+00	1.6E+00	1.5E+00	1.4E+00	1.3E+00	1.1E+00	9.5E-01	8.5E-01
160	6	200	2.4E+00	2.0E+00	1.8E+00	1.6E+00	1.5E+00	1.4E+00	1.2E+00	1.0E+00	9.3E-01
170	8	200	2.8E+00	2.2E+00	2.0E+00	1.8E+00	1.6E+00	1.5E+00	1.3E+00	1.1E+00	1.0E+00
180	10	200	3.2E+00	2.5E+00	2.2E+00	2.0E+00	1.8E+00	1.7E+00	1.4E+00	1.2E+00	1.1E+00
190	13	200	3.7E+00	2.9E+00	2.5E+00	2.2E+00	2.0E+00	1.9E+00	1.5E+00	1.4E+00	1.3E+00
200	16	200	4.4E+00	3.4E+00	2.9E+00	2.5E+00	2.3E+00	2.1E+00	1.7E+00	1.5E+00	1.5E+00
210	19	200	5.3E+00	4.0E+00	3.4E+00	3.0E+00	2.6E+00	2.4E+00	2.0E+00	1.8E+00	1.7E+00
220	23	200	6.5E+00	4.8E+00	4.1E+00	3.5E+00	3.1E+00	2.9E+00	2.3E+00	2.0E+00	1.9E+00
230	28	200	8.0E+00	6.0E+00	5.1E+00	4.3E+00	3.8E+00	3.4E+00	2.7E+00	2.4E+00	2.3E+00
240	33	200	1.0E+01	7.5E+00	6.4E+00	5.3E+00	4.7E+00	4.2E+00	3.3E+00	2.9E+00	2.7E+00
250	40	200	1.3E+01	9.7E+00	8.2E+00	6.8E+00	6.0E+00	5.4E+00	4.0E+00	3.5E+00	3.3E+00
260	47	200	1.7E+01	1.3E+01	1.1E+01	8.9E+00	7.8E+00	6.9E+00	5.1E+00	4.4E+00	4.0E+00
270	55	200	2.3E+01	1.7E+01	1.4E+01	1.2E+01	1.0E+01	9.3E+00	6.7E+00	5.6E+00	5.0E+00
280	64	200	3.2E+01	2.4E+01	2.0E+01	1.6E+01	1.4E+01	1.3E+01	9.1E+00	7.3E+00	6.3E+00
290	74	200	4.5E+01	3.3E+01	2.8E+01	2.3E+01	2.0E+01	1.8E+01	1.3E+01	9.9E+00	8.3E+00
300	86	200	6.6E+01	4.9E+01	4.1E+01	3.4E+01	3.0E+01	2.6E+01	1.8E+01	1.4E+01	1.1E+01

Table 15

Pressure Dependence of the Apparent Molal Heat Capacity: $\frac{\phi_{C_p}}{R}(P_2) - \frac{\phi_{C_p}}{R}(P_1)$

TEMP (°C)	P1 (BAR)	P2 (BAR)	$\frac{\bar{C}^{\circ}_{p_2}}{R}$	MOLALITY .100	.250	.500	.750	1.000	2.000	3.000	4.000
25	1	400	4.0E+00	3.8E+00	3.7E+00	3.5E+00	3.3E+00	3.1E+00	2.5E+00	2.1E+00	1.8E+00
30	1	400	3.6E+00	3.4E+00	3.3E+00	3.1E+00	3.0E+00	2.8E+00	2.3E+00	2.0E+00	1.7E+00
40	1	400	3.1E+00	3.0E+00	2.9E+00	2.7E+00	2.6E+00	2.4E+00	2.0E+00	1.7E+00	1.5E+00
50	1	400	2.8E+00	2.7E+00	2.6E+00	2.4E+00	2.3E+00	2.2E+00	1.9E+00	1.6E+00	1.4E+00
60	1	400	2.7E+00	2.5E+00	2.4E+00	2.3E+00	2.2E+00	2.1E+00	1.8E+00	1.5E+00	1.3E+00
70	1	400	2.6E+00	2.4E+00	2.3E+00	2.2E+00	2.1E+00	2.0E+00	1.7E+00	1.5E+00	1.3E+00
80	1	400	2.6E+00	2.4E+00	2.3E+00	2.2E+00	2.1E+00	2.0E+00	1.7E+00	1.4E+00	1.2E+00
90	1	400	2.7E+00	2.4E+00	2.3E+00	2.2E+00	2.1E+00	2.0E+00	1.7E+00	1.4E+00	1.2E+00
100	1	400	2.8E+00	2.5E+00	2.4E+00	2.2E+00	2.1E+00	2.0E+00	1.7E+00	1.4E+00	1.2E+00
110	1	400	2.9E+00	2.6E+00	2.4E+00	2.3E+00	2.1E+00	2.0E+00	1.7E+00	1.5E+00	1.3E+00
120	2	400	3.1E+00	2.7E+00	2.5E+00	2.3E+00	2.2E+00	2.1E+00	1.8E+00	1.5E+00	1.3E+00
130	3	400	3.4E+00	2.9E+00	2.7E+00	2.5E+00	2.3E+00	2.2E+00	1.8E+00	1.6E+00	1.4E+00
140	4	400	3.7E+00	3.1E+00	2.9E+00	2.6E+00	2.4E+00	2.3E+00	1.9E+00	1.7E+00	1.5E+00
150	5	400	4.0E+00	3.4E+00	3.1E+00	2.8E+00	2.6E+00	2.4E+00	2.1E+00	1.8E+00	1.6E+00
160	6	400	4.5E+00	3.7E+00	3.3E+00	3.0E+00	2.8E+00	2.6E+00	2.2E+00	1.9E+00	1.7E+00
170	8	400	5.1E+00	4.1E+00	3.7E+00	3.3E+00	3.0E+00	2.8E+00	2.4E+00	2.1E+00	1.9E+00
180	10	400	5.8E+00	4.6E+00	4.1E+00	3.6E+00	3.3E+00	3.1E+00	2.6E+00	2.3E+00	2.1E+00
190	13	400	6.7E+00	5.3E+00	4.6E+00	4.0E+00	3.7E+00	3.4E+00	2.8E+00	2.5E+00	2.3E+00
200	16	400	7.9E+00	6.1E+00	5.3E+00	4.6E+00	4.1E+00	3.8E+00	3.1E+00	2.8E+00	2.7E+00
210	19	400	9.4E+00	7.1E+00	6.2E+00	5.3E+00	4.7E+00	4.4E+00	3.5E+00	3.2E+00	3.0E+00
220	23	400	1.1E+01	8.5E+00	7.3E+00	6.2E+00	5.5E+00	5.1E+00	4.1E+00	3.7E+00	3.5E+00
230	28	400	1.4E+01	1.0E+01	8.8E+00	7.4E+00	6.6E+00	6.0E+00	4.7E+00	4.2E+00	4.1E+00
240	33	400	1.8E+01	1.3E+01	1.1E+01	9.1E+00	8.0E+00	7.2E+00	5.6E+00	5.0E+00	4.8E+00
250	40	400	2.3E+01	1.7E+01	1.4E+01	1.1E+01	1.0E+01	9.0E+00	6.8E+00	6.0E+00	5.7E+00
260	47	400	3.0E+01	2.2E+01	1.8E+01	1.5E+01	1.3E+01	1.1E+01	8.5E+00	7.4E+00	6.9E+00
270	55	400	4.0E+01	2.9E+01	2.4E+01	2.0E+01	1.7E+01	1.5E+01	1.1E+01	9.3E+00	8.6E+00
280	64	400	5.5E+01	4.0E+01	3.3E+01	2.7E+01	2.3E+01	2.1E+01	1.5E+01	1.2E+01	1.1E+01
290	74	400	7.9E+01	5.7E+01	4.7E+01	3.9E+01	3.3E+01	2.9E+01	2.0E+01	1.6E+01	1.4E+01
300	86	400	1.2E+02	8.4E+01	7.0E+01	5.7E+01	4.9E+01	4.3E+01	2.9E+01	2.3E+01	1.9E+01

Table 15

Pressure Dependence of the Apparent Molal Heat Capacity: $\frac{\phi C_p}{R}(P_2) - \frac{\phi C_p}{R}(P_1)$

TEMP (°C)	P1 (BAR)	P2 (BAR)	$\frac{\bar{C}^{\circ}_{p_2}}{R}$	MOLALITY .100	.250	.500	.750	1.000	2.000	3.000	4.000
25	1	600	5.6E+00	5.4E+00	5.2E+00	4.9E+00	4.6E+00	4.4E+00	3.6E+00	3.0E+00	2.6E+00
30	1	600	5.1E+00	4.9E+00	4.7E+00	4.5E+00	4.2E+00	4.0E+00	3.3E+00	2.7E+00	2.4E+00
40	1	600	4.4E+00	4.2E+00	4.1E+00	3.8E+00	3.6E+00	3.5E+00	2.9E+00	2.4E+00	2.1E+00
50	1	600	4.1E+00	3.8E+00	3.7E+00	3.5E+00	3.3E+00	3.2E+00	2.6E+00	2.2E+00	2.0E+00
60	1	600	3.9E+00	3.6E+00	3.5E+00	3.3E+00	3.1E+00	3.0E+00	2.5E+00	2.1E+00	1.9E+00
70	1	600	3.8E+00	3.5E+00	3.3E+00	3.2E+00	3.0E+00	2.9E+00	2.4E+00	2.1E+00	1.8E+00
80	1	600	3.8E+00	3.5E+00	3.3E+00	3.1E+00	3.0E+00	2.8E+00	2.4E+00	2.0E+00	1.8E+00
90	1	600	3.8E+00	3.5E+00	3.3E+00	3.1E+00	2.9E+00	2.8E+00	2.4E+00	2.0E+00	1.8E+00
100	1	600	4.0E+00	3.6E+00	3.4E+00	3.2E+00	3.0E+00	2.8E+00	2.4E+00	2.1E+00	1.8E+00
110	1	600	4.2E+00	3.7E+00	3.5E+00	3.2E+00	3.1E+00	2.9E+00	2.5E+00	2.1E+00	1.8E+00
120	2	600	4.4E+00	3.9E+00	3.6E+00	3.3E+00	3.2E+00	3.0E+00	2.5E+00	2.2E+00	1.9E+00
130	3	600	4.8E+00	4.1E+00	3.8E+00	3.5E+00	3.3E+00	3.1E+00	2.6E+00	2.3E+00	2.0E+00
140	4	600	5.2E+00	4.4E+00	4.0E+00	3.7E+00	3.5E+00	3.3E+00	2.8E+00	2.4E+00	2.1E+00
150	5	600	5.7E+00	4.7E+00	4.3E+00	3.9E+00	3.7E+00	3.5E+00	2.9E+00	2.5E+00	2.2E+00
160	6	600	6.3E+00	5.2E+00	4.7E+00	4.2E+00	3.9E+00	3.7E+00	3.1E+00	2.7E+00	2.4E+00
170	8	600	7.0E+00	5.7E+00	5.1E+00	4.6E+00	4.2E+00	4.0E+00	3.3E+00	2.9E+00	2.6E+00
180	10	600	8.0E+00	6.4E+00	5.7E+00	5.0E+00	4.6E+00	4.3E+00	3.6E+00	3.2E+00	2.9E+00
190	13	600	9.1E+00	7.2E+00	6.3E+00	5.6E+00	5.1E+00	4.7E+00	3.9E+00	3.5E+00	3.2E+00
200	16	600	1.1E+01	8.2E+00	7.2E+00	6.2E+00	5.6E+00	5.2E+00	4.3E+00	3.9E+00	3.6E+00
210	19	600	1.3E+01	9.5E+00	8.2E+00	7.1E+00	6.4E+00	5.9E+00	4.8E+00	4.3E+00	4.1E+00
220	23	600	1.5E+01	1.1E+01	9.6E+00	8.2E+00	7.3E+00	6.7E+00	5.4E+00	4.9E+00	4.6E+00
230	28	600	1.8E+01	1.3E+01	1.1E+01	9.6E+00	8.5E+00	7.8E+00	6.2E+00	5.6E+00	5.3E+00
240	33	600	2.3E+01	1.6E+01	1.4E+01	1.2E+01	1.0E+01	9.2E+00	7.2E+00	6.4E+00	6.2E+00
250	40	600	2.8E+01	2.1E+01	1.7E+01	1.4E+01	1.2E+01	1.1E+01	8.5E+00	7.6E+00	7.3E+00
260	47	600	3.7E+01	2.6E+01	2.2E+01	1.8E+01	1.5E+01	1.4E+01	1.0E+01	9.1E+00	8.7E+00
270	55	600	4.9E+01	3.5E+01	2.9E+01	2.3E+01	2.0E+01	1.8E+01	1.3E+01	1.1E+01	1.1E+01
280	64	600	6.6E+01	4.7E+01	3.9E+01	3.1E+01	2.7E+01	2.4E+01	1.7E+01	1.4E+01	1.3E+01
290	74	600	9.2E+01	6.5E+01	5.4E+01	4.4E+01	3.7E+01	3.2E+01	2.2E+01	1.8E+01	1.7E+01
300	86	600	1.3E+02	9.5E+01	7.8E+01	6.3E+01	5.4E+01	4.7E+01	3.2E+01	2.5E+01	2.2E+01

Table 15

Pressure Dependence of the Apparent Molal Heat Capacity: $\frac{\phi_{C_p}}{R}(P_2) - \frac{\phi_{C_p}}{R}(P_1)$

TEMP (°C)	P1 (BAR)	P2 (BAR)	$\frac{\bar{C}^{\circ}_{p_2}}{R}$	MOLALITY .100	.250	.500	.750	1.000	2.000	3.000	4.000
25	1	1000	8.3E+00	8.0E+00	7.6E+00	7.2E+00	6.8E+00	6.4E+00	5.1E+00	4.2E+00	3.6E+00
30	1	1000	7.6E+00	7.3E+00	7.0E+00	6.5E+00	6.2E+00	5.8E+00	4.7E+00	3.9E+00	3.4E+00
40	1	1000	6.6E+00	6.3E+00	6.0E+00	5.7E+00	5.4E+00	5.1E+00	4.2E+00	3.5E+00	3.1E+00
50	1	1000	6.1E+00	5.7E+00	5.5E+00	5.2E+00	4.9E+00	4.7E+00	3.9E+00	3.3E+00	2.9E+00
60	1	1000	5.8E+00	5.4E+00	5.2E+00	4.9E+00	4.6E+00	4.4E+00	3.7E+00	3.2E+00	2.8E+00
70	1	1000	5.7E+00	5.3E+00	5.0E+00	4.7E+00	4.5E+00	4.3E+00	3.6E+00	3.1E+00	2.7E+00
80	1	1000	5.6E+00	5.2E+00	4.9E+00	4.7E+00	4.4E+00	4.2E+00	3.6E+00	3.1E+00	2.7E+00
90	1	1000	5.7E+00	5.2E+00	5.0E+00	4.7E+00	4.4E+00	4.2E+00	3.6E+00	3.1E+00	2.7E+00
100	1	1000	5.9E+00	5.3E+00	5.0E+00	4.7E+00	4.5E+00	4.3E+00	3.6E+00	3.1E+00	2.7E+00
110	1	1000	6.2E+00	5.5E+00	5.2E+00	4.8E+00	4.6E+00	4.3E+00	3.7E+00	3.2E+00	2.7E+00
120	2	1000	6.5E+00	5.8E+00	5.4E+00	5.0E+00	4.7E+00	4.5E+00	3.8E+00	3.3E+00	2.8E+00
130	3	1000	7.0E+00	6.1E+00	5.6E+00	5.2E+00	4.9E+00	4.6E+00	3.9E+00	3.4E+00	2.9E+00
140	4	1000	7.5E+00	6.5E+00	6.0E+00	5.5E+00	5.1E+00	4.9E+00	4.1E+00	3.5E+00	3.1E+00
150	5	1000	8.2E+00	6.9E+00	6.4E+00	5.8E+00	5.4E+00	5.1E+00	4.3E+00	3.7E+00	3.3E+00
160	6	1000	9.0E+00	7.5E+00	6.8E+00	6.2E+00	5.8E+00	5.4E+00	4.6E+00	4.0E+00	3.5E+00
170	8	1000	1.0E+01	8.2E+00	7.4E+00	6.7E+00	6.2E+00	5.8E+00	4.9E+00	4.3E+00	3.8E+00
180	10	1000	1.1E+01	9.1E+00	8.1E+00	7.2E+00	6.7E+00	6.2E+00	5.2E+00	4.6E+00	4.1E+00
190	13	1000	1.3E+01	1.0E+01	9.0E+00	7.9E+00	7.3E+00	6.8E+00	5.6E+00	5.0E+00	4.5E+00
200	16	1000	1.5E+01	1.1E+01	1.0E+01	8.7E+00	8.0E+00	7.4E+00	6.1E+00	5.5E+00	5.0E+00
210	19	1000	1.7E+01	1.3E+01	1.1E+01	9.8E+00	8.8E+00	8.2E+00	6.7E+00	6.0E+00	5.6E+00
220	23	1000	2.0E+01	1.5E+01	1.3E+01	1.1E+01	9.9E+00	9.1E+00	7.4E+00	6.7E+00	6.3E+00
230	28	1000	2.4E+01	1.7E+01	1.5E+01	1.3E+01	1.1E+01	1.0E+01	8.3E+00	7.5E+00	7.2E+00
240	33	1000	2.8E+01	2.1E+01	1.8E+01	1.5E+01	1.3E+01	1.2E+01	9.4E+00	8.5E+00	8.2E+00
250	40	1000	3.5E+01	2.5E+01	2.1E+01	1.7E+01	1.5E+01	1.4E+01	1.1E+01	9.7E+00	9.5E+00
260	47	1000	4.4E+01	3.1E+01	2.6E+01	2.1E+01	1.8E+01	1.6E+01	1.3E+01	1.1E+01	1.1E+01
270	55	1000	5.7E+01	4.0E+01	3.3E+01	2.7E+01	2.3E+01	2.0E+01	1.5E+01	1.3E+01	1.3E+01
280	64	1000	7.5E+01	5.2E+01	4.3E+01	3.4E+01	2.9E+01	2.6E+01	1.9E+01	1.6E+01	1.6E+01
290	74	1000	1.0E+02	7.1E+01	5.8E+01	4.6E+01	3.9E+01	3.4E+01	2.4E+01	2.0E+01	1.9E+01
300	86	1000	1.4E+02	1.0E+02	8.1E+01	6.4E+01	5.4E+01	4.7E+01	3.2E+01	2.6E+01	2.4E+01

References

1. J. L. Haas, Jr., Am. J. Sci. 269, 489 (1970).

2. R. W. Potter, III and D. L. Brown, U. S. G. S. Bulletin 1421-C (1977).

3. H. Ozbek, S. L. Phillips, and J. A. Fair (1978). To be published.

4. K. S. Pitzer, J. Phys. Chem. 77, 268 (1973).

5. D. J. Bradley and K. S. Pitzer, J. Phys. Chem. 83, 1599 (1979).

6. L. F. Silvester and K. S. Pitzer, J. Phys. Chem. 81, 1822 (1977).

7. "Handbook of Physical Constants", F. Birch, Ed., Geological Society of America (1942).

8. R. W. Potter, III, D. R. Shaw, and J. L. Haas, Jr., U. S. G. S. Bulletin 1417 (1975).

9. F. J. Millero, J. Phys. Chem. 74, 356 (1970).

10. F. J. Millero, E. V. Hoff, and L. Kahn, J. Soln. Chem. 4, 309 (1972).

11. F. Vaslow, J. Phys. Chem. 73, 3745 (1969).

12. F. Vaslow, J. Phys. Chem. 70, 2286 (1966) and ORNL Report TM-1438 (1965).

13. G. Perron, J. Fortier, and J. E. Desnoyers, J. Chem. Thermo. 7, 1177 (1975).

14. R. E. Gibson and O. H. Loeffler, Annals. NY. Acad. Sci., 51, 727 (1949).

15. C. T. Chen, R. T. Emmet, and F. J. Millero, J. Chem. Eng. Data, 22, 201 (1977).

16. G. Dessauges, N. Miljevic, and W. A. Van Hook, J. Phys. Chem. 84, 2587 (1980).

17. C-T. A. Chen, J. H. Chen, and F. J. Millero, J. Chem. Eng. Data, 25, 307 (1980).

18. "International Critical Tables", McGraw-Hill, New York (1928) Vol 3.

19. A. J. Ellis, J. Chem. Soc. A, 1579 (1966).

20. This Dissertation, Chapter 2.

21. I. Kh. Khaibullin and N. M. Borisov, Teplofiz. Vysokikh Temperatur, 4, 518 (1966).

22. B. M. Fabuss, A. Korosi, and A. K. M. Shamsul Hug, J. Chem. Eng. Data, 11, 325 (1966).

23. A. Korosi and B. M. Fabuss, J. Chem. Eng. Data, 13, 548 (1968).

24. R. Hilbert, Ph.D. Dissertation, University of Karlsruhe, Karlsruhe, West Germany (1979).

25. V. I. Zarembo and M. K. Federov, Zhurnal Prikladnai Khimii, 48, 1949 (1975).

26. I. Tanishita, K. Watanabe, J. Kijima, H. Ishii, K. Oguchi, and M. Uematsu, J. Chem. Thermo, 8, 1 (1976).

27. R. A. Fine and F. J. Millero, J. Chem. Phys. 59, 5529 (1973).

28. A. A. Yayanos, J. Chem. Phys. 64, 429 (1976).

29. G. S. Kell and E. Whalley, J. Chem. Phys. 62, 3496 (1975).

30. G. S. Kell, G. E. McLaurin, and E. Whalley, Proc. R. Soc. Lond. A., 360, 389 (1978).

31. G. S. Kell, J. Chem. Eng. Data, 15, 119 (1970).

32. W. D. Wilson, J. Acoust. Soc. Am. 31, 1067 (1959).

33. V. A. Del Grosso and C. W. Mader, J. Acoust. Soc. Am. 52, 1442 (1972).

34. J. H. Keenan, F. G. Keyes, P. G. Hill, and J. G. Moore, "Steam Tables", John Wiley and Sons, Inc., New York (1969 and 1978).

35. J. Juza, Cesk. Akad. Ued. Rada. Tech. Ved., 1, 76 (1966). E. Schmidt, "Properties of Water and Steam in SI Units", p. 174, Springer-Verlag, Berlin (1969).

36. National Engineering Laboratory, "Steam Tables 1964", H.M.S.O. Edinburgh (1964).

37. L. Haar, J. Gallagher, and G. S. Kell, Contributions to the 9th International Conference on the Properties of Steam, Munich (1979).

38. H. Kanno and C. A. Angell, J. Chem. Phys., 70, 4008 (1979).

39. H. M. Rowe, Jr., and J. C. S. Chou, J. Chem. Eng. Data, 15, 61 (1970).

40. "Handbook of Chemistry and Physics", 45th ed., R. C. Weast, Ed., The Chemical Rubber Co., Cleveland, OH (1965).

41. R. H. Busey, personal communication.

42. J. E. Tanner and F. W. Lamb, J. Soln. Chem. 7, 303 (1978).

43. S. Likke and L. A. Bromley, J. Chem. Eng. Data, 18, 189 (1977).

44. D. Smith-Magowan and R. H. Wood, submitted to J. Chem. Thermo.

45. L. F. Silvester and K. S. Pitzer, Lawrence Berkeley Laboratory Report # 4456 (1976).

Chapter 2

MEASUREMENT OF THE DENSITY OF AQUEOUS SODIUM CHLORIDE SOLUTIONS FROM 75°C TO 200°C AT 20 BAR

Introduction

Few precise determinations of the volumetric properties of electrolyte solutions are available above 100°C. Sodium chloride solutions have been most extensively studied, but even in this case reliable volumetric data near the saturation pressure are scarce. Density data for sodium chloride solutions at 20 bar, which were necessary to complete the description of volumetric properties contained in Chapter 1, are presented in this chapter.

Additional density data at low pressures were required for two reasons. First, we were especially interested in determining the pressure dependence of high temperature activity, enthalpy, and heat capacity data, most of which are taken at saturation pressure. Since the volumetric properties of aqueous solutions vary most rapidly near the saturation pressure, precise data in this region are important in calculations of pressure dependence.

Secondly, the three available sets of density data for sodium chloride solutions at high temperatures and low pressures were either incomplete or inconsistent. The saturation pressure data of Khaibullin and Borisov[1] differ from other data by as much as 1%. The data of Fabuss, Korosi, and Hug[2] are uncertain because of the unknown effect of air contained in their dilatometer. Only the data of Ellis[3] are sufficiently precise for calculations of the pressure dependence of thermal properties. Unfortunately, Ellis' data cover only the low concentration region. Thus additional density data at high concentrations were needed.

Experimental

1. Description of Apparatus

Densities of sodium chloride solutions from 75° to 200°C, at a constant pressure of 20 bars, were determined using a high pressure dilatometer. The dilatometer is similar to that used by Ellis,[3] in which changes in the volume of a solution are measured as a function of temperature. The apparatus is illustrated in Figure 1.

A pressure vessel, constructed of corrosion resistant Haynes[R] Alloy No. 625, contains approximately 9 cm^3 of salt solution. The pressure vessel is connected to a mercury reservoir by .062 inch outside diameter, .007 inch inside diameter, stainless steel capillary tubing. The mercury reservoir, which is made of a coil of .125 inch outside diameter stainless steel tubing, is in turn connected to a glass capillary column. The entire system is pressurized with a high pressure nitrogen gas cylinder.

To avoid possible hysteresis in the volume of the sample cell when the system is pressurized and depressurized, a double bomb system is used. It is illustrated in Figure 2. The sample cell is welded to a thick top cap, so that it is permanently sealed except for the inlet and outlet ports. A thick outer bomb surrounds the sample bomb and is sealed using an annealed copper gasket. The inner and outer vessels are connected on the gas side of the apparatus, so that both can be slowly pressurized at the same time. Thus there is never a pressure difference between the inner and outer vessels.

The high pressure glass to metal seals, used to connect the glass capillary to the stainless steel tubing system, also are of interest. They are constructed of standard swagelock fittings (1/8 inch tubing to

Figure 1. Schematic diagram of the high pressure dilatometer.

High Pressure Dilatometer

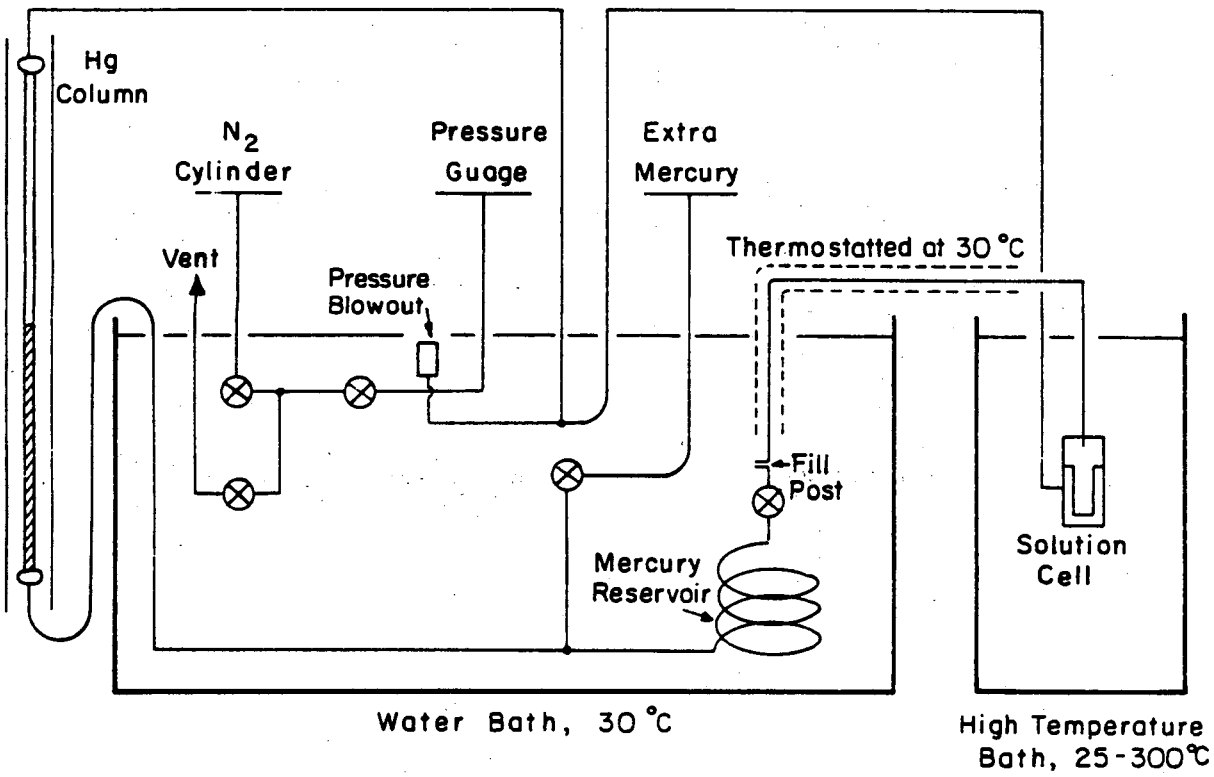

XBL812-5163

Figure 2. Schematic diagram of the high pressure solution cell.

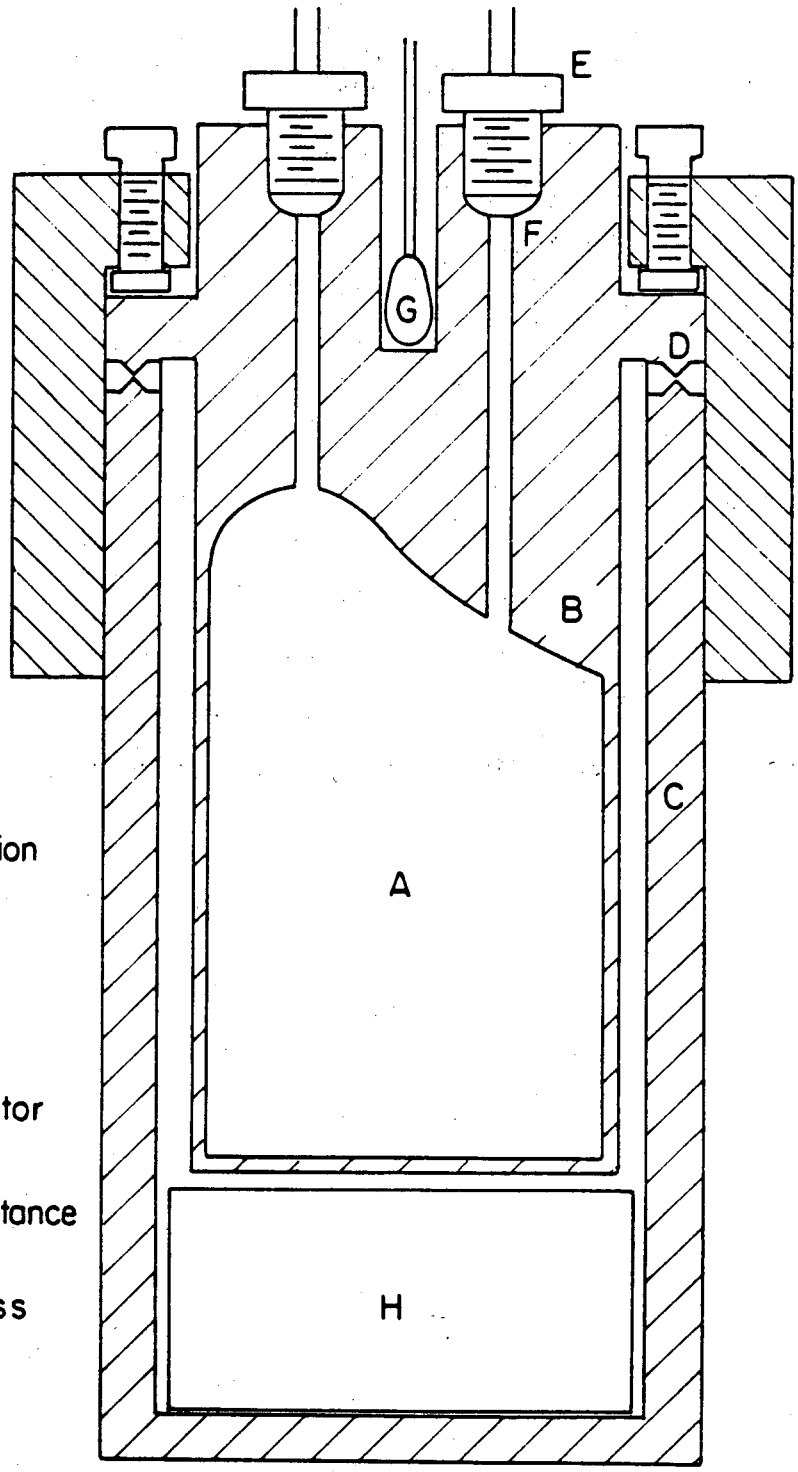

A Aqueous solution
B Inner vessel
C Outer vessel
D Copper seal
E Swage type tubing connector
F Cone
G Platinum resistance thermometer
H Thermal mass

XBL 812-5164

1/4 inch MNPT) which have been drilled out to provide a loose fit for the glass tubing. The glass is simply glued into the fittings with epoxy (G. C. Electronics). Precision bore glass tubing, 1.6 mm internal diameter, is carefully annealed before use. The combination of glass tubing and epoxy seal can contain 1 kbar pressure. For safety, the glass tubing is always surrounded by a plexiglass pressure shield.

Temperature control is achieved using two separate systems. The mercury reservoir and most of the capillary connecting tube are thermostated at 30°C with a well stirred water bath and circulation pump. The temperature of the water bath fluctuates by less than .01 K. The sample cell is surrounded by a large aluminum block and is placed in a high temperature fluidized bath. Temperature control of the fluidized bath is good only to a few tenths of a degree, so the aluminum block serves as a heat sink to reduce temperature fluctuations. With the aluminum block, the temperature of the sample cell is stable to ±.01 K over a period of 30 minutes.

2. Method

The solution density was determined by measuring the change in the volume of the solution as the temperature was raised. To begin a measurement, solution of known molality was prepared with freshly degassed water which had been distilled and passed through a Millipore Q filter system (final resistivity was greater than 18 megaohm). Baker reagent grade NaCℓ was used without further purification. The salt was dried overnight at 200°C and cooled under vacuum before being weighed.

The procedure used to fill the sample cell without introducing any air bubbles was somewhat complicated. The cell was filled and emptied by syringe a minimum of five times to eliminate contamination by any old

solution still in the cell. As the final slug of solution was placed in the sample cell, a fine needle was used to stir the solution in the inlet hole and dislodge any air bubbles trapped in the narrow opening. A syringe containing 10 mℓ of the solution was then attached to the inlet fitting and the solution was forced through the sample cell and the connecting tube, then out an opening at the mercury solution interface. A Swagelock cap used to close this opening was tightened while pressure was applied by the syringe. The syringe was removed and the inlet fitting was topped off with a few drops of solution. As the inlet cap was tightened, solution was forced out through the cracks, displacing any remaining air. Finally the apparatus was pressurized. Any air bubbles in the system could be detected immediately by a large displacement in the level of the mercury column.

The sample cell was then placed in the fluidized bath and the solution was allowed to come to equilibrium at room temperature. The pressure of the system and the level of the mercury column were monitored overnight to check for leakage. The temperature of the sample was increased in 25 K increments, and the height of the mercury column was measured to ±.01 mm at each step using a Wilde cathatometer. The temperature of the sample cell was determined to ±.005 K using a 25 Ω, calibrated platinum resistance thermometer and G-2 Mueller bridge. A bourdon tube pressure gauge (Ashcroft Digiguge Model 7781), calibrated with a Ruska Deadweight Tester, was used to determine the pressure of the system to ±.1 bar. The temperature of the water bath and the room temperature were measured with mercury-in-glass thermometers.

3. Derivation of Equations

The change in the height of the mercury column can be related to the density of the solution as follows. Let T be the experimental temperature, T_R the reference temperature, and T_B the water bath temperature, in degrees Celcius. The density of the solution at the experimental temperature, ρ_T, is equal to the mass of solution in the cell divided by the volume of the cell,

$$\rho_T = \frac{g_T}{V_T} . \tag{1}$$

The mass of solution in the sample cell at temperature T is equal to the mass in the cell at the reference temperature T_R, less the amount that has expanded from the cell. The mass of solution expanded is equal to

$$\Delta h A \rho_{T_B} , \tag{2}$$

where Δh is the total change in the height of the mercury column between temperatures T_R and T, A is the cross-sectional area of the mercury column, and ρ_{T_B} is the density of the solution at the temperature of the water bath. Thus the density of the solution is given by

$$\rho_T = \frac{1}{V_T} [\rho_{T_R} V_{T_R} - \Delta h A \rho_{T_B}] . \tag{3}$$

Assume that the temperature dependence of the volume of the sample cell is

$$V_T = V_B e^{\alpha T} , \tag{4}$$

where V_B is the volume of the cell at 0°C and α is the unknown expansivity of the cell. Substituting Equation (4) into Equation (3) one obtains

$$\rho_T = \rho_{T_R} e^{-\alpha (T-T_R)} - \left(\frac{A}{V_B}\right) \Delta h \rho_{T_B} e^{-\alpha T} .$$

Expansion of the exponential yields

$$\rho_T = \rho_{T_R}[1-\alpha(T-T_R)] - \left(\frac{A}{V_B}\right)\Delta h\rho_{T_B}[1-\alpha T]$$

or

$$\rho_T = \rho_{T_R} - \left(\frac{A}{V_B}\right)\Delta h\rho_{T_B} + \alpha\rho_{T_R}(T_R-T) + \alpha\left(\frac{A}{V_B}\right)T\Delta h\rho_{T_B}. \qquad (5)$$

This is the final equation relating the density of the solution to the observed change in the height of the mercury column.

Equation (5) contains two unknowns, the expansivity of the sample cell (α) and the ratio of the cross sectional area of the column to the volume of the cell at 0°C, $\left(\frac{A}{V_B}\right)$. These are determined in a calibration run using pure water. The values of Δh observed with pure water and the known values of the density of water are used in a nonlinear least squares regression to determine $\left(\frac{A}{V_B}\right)$ and α. Calculation of solution densities from Equation (5) requires knowledge of the solution densities at the reference and water bath temperatures and the experimental pressure.

4. Corrections to the Raw Data

In any experiment a certain number of experimental variables can not be held exactly constant. Therefore small corrections to the raw data are necessary to bring all the data points to the same baseline. In experiments using the high pressure dilatometer, the change in height of the mercury column is observed as a function of sample temperature, and this should be the only experimental variable. Thus small corrections have been made to the observed column height to account for variations in water bath temperature, room temperature, hydrostatic head, and system pressure. To evaluate the effect of each of these variables,

it is helpful to note that a change of .01 mm in the column height corresponds to a change of 2×10^{-6} g/cm^3 in the derived density of the solution.

The change in the mercury column height due to temperature drift in the water bath was measured experimentally, at 20 bar system pressure, as .0093 mm height per .01°C shift in bath temperature. The change in height due to a change in room temperature from 23°C was estimated as

$$\Delta h = h(1.5 \times 10^{-4})(t-23°C)$$

where h is the total height of the mercury column and t is the room temperature in degrees Celcius. The factor 1.5×10^{-4} is derived from the difference in expansion of glass and mercury. The maximum shift in room temperature was 3 K, and the maximum column height was 800 mm, so this correction was always less than .36 mm.

As the mercury rises in the column, it exerts an increasing hydrostatic pressure on the salt solution. By measuring the height of the column above the sample cell, the pressure increase, ΔP, due to hydrostatic head was found to be $\Delta P = .28 + \frac{h}{750.06}$ bar. The applied pressure also is not quite constant since gas must be bled off as the temperature of the sample is raised. Relating these changes in system pressure to changes in the mercury column height complicates analysis of the density data. The change in column height due to a pressure change of about 2 bar was measured directly at 23°C, with pure water in the sample cell, as .22 mm per bar. This value for the compressibility of the system was used to correct both calibration and solution data at the reference temperature. Because the correction was made in this way, each experimental density determination was at a slightly different pressure. The

change in system pressure during one run was about one bar, so even uncorrected data would be in error by less than 50 ppm.

One further correction for the variable mass of solution in the connecting tube was found to be negligible up to 200°C. The unthermostated length of the capillary connecting tube is 40 cm, but half of this length is in the fluidized bath. Thus a sharp gradient from the experimental temperature to the water bath temperature occurs in about 20 cm of the tubing, which has a volume of .005 cm^3. Correction of Equation (2) for the difference in the mass of solution in this portion of the tube at temperatures T and T_R, $m_T - m_{T_R}$, yields the following form of Equation (5):

$$\rho_T = \rho_{T_R} - \left(\frac{A}{V_B}\right) \Delta h \rho_{T_B} + \frac{m_T - m_{T_R}}{A} + \alpha \rho_{T_R} (T_R - T) + \alpha \left(\frac{A}{V_B}\right) \Delta h \rho_{T_B} + \frac{m_T - m_{T_R}}{A} \qquad (6)$$

The difference in $\frac{m_T - m_{T_R}}{V_B}$ for pure water and a 4.4 m solution is found to be only 6×10^{-6} g/cm^3 at T = 200°C. Thus a correction for the mass of solution in the connecting tube is not necessary.

Results

The experimental values for the height of the mercury column were first corrected for changes in water bath temperature, room temperature, hydrostatic head, and applied pressure. The series of values for column height as a function of temperature for each separate solution or calibration run were fit to an equation of the form

$$h = a + bv_w + cv_w T + dT + eT^2$$

using a standard, linear least squares regression. Here v_w is the volume of pure water at temperature T. By examining the regression, any

Table 1

CALIBRATION RUN WITH PURE WATER

TEMP. (°C)	PRESS. (BAR)	DENSITY (GM/CC)	COLUMN HEIGHT (CM)	DENSITY AT REFERENCE TEMP. OF 52.00 C	DENSITY AT WATER BATH TEMP. OF 30.00 C
51.70	19.7	.98806	15.762	.98793	.99648
64.35	19.7	.98173	18.290	.98793	.99649
86.90	19.8	.96826	23.751	.98793	.99649
97.98	20.0	.96072	26.824	.98794	.99650
108.89	19.9	.95273	30.112	.98794	.99649
125.79	20.0	.93932	35.631	.98794	.99650
142.74	20.0	.92461	41.729	.98794	.99650
159.84	20.1	.90849	48.445	.98794	.99650
176.46	20.2	.89153	55.544	.98795	.99651
176.52	20.2	.89146	55.580	.98795	.99651
176.48	20.2	.89151	55.559	.98795	.99651
199.61	20.4	.86558	66.481	.98796	.99651
199.68	20.4	.86549	66.516	.98796	.99651

PREDICTED REFERENCE COLUMN HEIGHT IS 15.815 CM.

Table 1

CALIBRATION RUN WITH PURE WATER

TEMP. (°C)	PRESS. (BAR)	DENSITY (GM/CC)	COLUMN HEIGHT (CM)	DENSITY AT REFERENCE TEMP. OF 25.00 C	DENSITY AT WATER BATH TEMP. OF 30.00 C
20.91	19.6	.99888	13.909	.99790	.99648
20.94	19.6	.99888	13.911	.99790	.99648
76.11	19.8	.97503	23.299	.99791	.99649
76.04	19.8	.97507	23.288	.99791	.99649
150.54	20.1	.91742	47.027	.99792	.99650
150.58	20.1	.91739	47.043	.99792	.99650
176.53	20.2	.89146	57.882	.99793	.99651
176.53	20.2	.89147	57.881	.99793	.99651
176.55	20.2	.89144	57.895	.99793	.99651
176.58	20.2	.89141	57.897	.99793	.99651
200.09	20.3	.86500	69.018	.99793	.99651
200.16	20.3	.86492	69.052	.99793	.99651
200.24	20.3	.86483	69.090	.99793	.99651
200.15	20.3	.86493	69.049	.99793	.99651
200.18	20.3	.86490	69.063	.99793	.99651

PREDICTED REFERENCE COLUMN HEIGHT IS 14.268 CM.

Table 1

CALIBRATION RUN WITH PURE WATER

TEMP. (°C)	PRESS. (BAR)	DENSITY (GM/CC)	COLUMN HEIGHT (CM)	DENSITY AT REFERENCE TEMP. OF 52.00 C	DENSITY AT WATER BATH TEMP. OF 30.00 C
50.07	19.5	.98880	11.899	.98792	.99648
75.67	19.9	.97531	17.332	.98794	.99649
100.19	19.5	.95912	23.924	.98792	.99647
125.72	19.8	.93937	32.019	.98793	.99649
150.67	20.0	.91729	41.173	.98794	.99650
175.40	20.1	.89265	51.451	.98795	.99650
200.61	20.4	.86439	63.355	.98796	.99652

PREDICTED REFERENCE COLUMN HEIGHT IS 12.251 CM.

Table 1

CALIBRATION RUN WITH PURE WATER

TEMP. (°C)	PRESS. (BAR)	DENSITY (GM/CC)	COLUMN HEIGHT (CM)	DENSITY AT REFERENCE TEMP. OF 25.00 C	DENSITY AT WATER BATH TEMP. OF 30.00 C
22.59	19.6	.99850	12.602	.99790	.99648
49.98	19.6	.98885	16.300	.99790	.99648
75.41	19.8	.97545	21.695	.99791	.99649
99.52	19.9	.95962	28.148	.99791	.99649
125.88	20.0	.93924	36.532	.99791	.99650
150.16	20.1	.91778	45.431	.99792	.99650
177.39	20.2	.89055	56.802	.99793	.99651
200.66	20.4	.86433	67.849	.99793	.99652

PREDICTED REFERENCE COLUMN HEIGHT IS 12.818 CM.

Table 1

CALIBRATION RUN WITH PURE WATER

TEMP. (°C)	PRESS. (BAR)	DENSITY (GM/CC)	COLUMN HEIGHT (CM)	DENSITY AT REFERENCE TEMP. OF 25.00 C	DENSITY AT WATER BATH TEMP. OF 30.00 C
22.73	19.7	.99847	12.620	.99790	.99649
50.30	19.6	.98871	16.361	.99790	.99648
50.46	19.6	.98863	16.390	.99790	.99648
75.34	19.8	.97550	21.670	.99791	.99649
100.49	19.9	.95892	28.426	.99791	.99649
125.90	20.0	.93923	36.537	.99791	.99650
150.34	20.2	.91762	45.501	.99792	.99651
175.99	20.2	.89204	56.206	.99793	.99651
199.99	20.4	.86512	67.523	.99793	.99652
200.04	20.4	.86506	67.541	.99793	.99652

PREDICTED REFERENCE COLUMN HEIGHT IS 12.823 CM.

Table 1

CALIBRATION RUN WITH PURE WATER

TEMP. (°C)	PRESS. (BAR)	DENSITY (GM/CC)	COLUMN HEIGHT (CM)	DENSITY AT REFERENCE TEMP. OF 52.00 C	DENSITY AT WATER BATH TEMP. OF 30.00 C
51.07	19.4	.98835	11.810	.98792	.99647
75.71	19.6	.97527	17.047	.98793	.99648
99.97	20.0	.95931	23.572	.98794	.99650
125.63	19.9	.93945	31.754	.98794	.99649
150.24	20.0	.91770	40.785	.98794	.99650
175.26	20.2	.89280	51.191	.98795	.99651
199.99	20.2	.86512	62.833	.98795	.99651

PREDICTED REFERENCE COLUMN HEIGHT IS 11.978 CM.

Table 2

NACL SOLUTION DENSITIES NACL MOLALITY = .0530

TEMP. (°C)	PRESS. (BAR)	DENSITY (GM/CC)	COLUMN HEIGHT (CM)	DENSITY AT REFERENCE TEMP. OF 25.00 C	DENSITY AT WATER BATH TEMP. OF 30.00 C
23.15	19.7	1.00055	13.326	1.00008	.99865
23.16	19.7	1.00055	13.326	1.00008	.99865
50.57	19.6	.99073	17.099	1.00008	.99864
76.38	19.8	.97703	22.584	1.00009	.99865
100.52	19.9	.96107	29.076	1.00010	.99866
126.06	19.9	.94129	37.201	1.00009	.99866
151.76	20.0	.91857	46.612	1.00010	.99866
177.52	20.2	.89284	57.346	1.00011	.99867
201.07	20.5	.86639	68.446	1.00012	.99868
201.13	20.5	.86632	68.475	1.00012	.99868

PREDICTED REFERENCE COLUMN HEIGHT IS 13.497 CM.

CALIBRATION CONSTANTS ARE (A/VB) = .233259E-02/CM

ALPHA = .380903E-04/ C

Table 2

NACL SOLUTION DENSITIES NACL MOLALITY = .2719

TEMP. (°C)	PRESS. (BAR)	DENSITY (GM/CC)	COLUMN HEIGHT (CM)	DENSITY AT REFERENCE TEMP. OF 30.00 C	DENSITY AT WATER BATH TEMP. OF 30.00 C
29.45	19.6	1.00757	13.441	1.00740	1.00740
50.40	19.7	.99944	16.567	1.00740	1.00740
75.43	19.8	.98609	21.859	1.00741	1.00741
100.43	19.9	.96964	28.485	1.00741	1.00741
126.57	20.0	.94961	36.638	1.00742	1.00742
150.70	20.0	.92855	45.279	1.00742	1.00742
175.75	20.1	.90418	55.339	1.00742	1.00742
201.03	20.5	.87653	66.828	1.00744	1.00744

PREDICTED REFERENCE COLUMN HEIGHT IS 13.504 CM.

CALIBRATION CONSTANTS ARE (A/VB) = .233259E-02/CM

ALPHA = .380903E-04/ C

Table 2

NACL SOLUTION DENSITIES NACL MOLALITY = .5571

TEMP. (°C)	PRESS. (BAR)	DENSITY (GM/CC)	COLUMN HEIGHT (CM)	DENSITY AT REFERENCE TEMP. OF 25.00 C	DENSITY AT WATER BATH TEMP. OF 30.00 C
22.71	19.6	1.02082	11.006	1.02014	1.01852
50.53	19.7	1.01010	15.074	1.02015	1.01852
75.34	19.7	.99676	20.300	1.02015	1.01852
100.29	19.8	.98049	26.777	1.02015	1.01853
126.83	19.9	.96049	34.819	1.02016	1.01853
151.26	20.0	.93953	43.313	1.02016	1.01853
125.64	19.9	.96124	34.519	1.02016	1.01853
150.04	20.0	.94046	42.935	1.02016	1.01853
176.06	20.2	.91567	53.049	1.02017	1.01854
199.27	20.4	.89105	63.147	1.02018	1.01855
199.45	20.4	.89086	63.224	1.02018	1.01855

PREDICTED REFERENCE COLUMN HEIGHT IS 11.254 CM.

CALIBRATION CONSTANTS ARE (A/VB) = .233259E-02/CM

ALPHA = .380903E-04/ C

Table 2

NACL SOLUTION DENSITIES NACL MOLALITY = .9775

TEMP. (°C)	PRESS. (BAR)	DENSITY (GM/CC)	COLUMN HEIGHT (CM)	DENSITY AT REFERENCE TEMP. OF 30.00 C	DENSITY AT WATER BATH TEMP. OF 30.00 C
29.42	19.7	1.03464	13.225	1.03442	1.03442
50.28	19.8	1.02570	16.596	1.03443	1.03443
75.24	19.8	1.01219	21.805	1.03442	1.03442
100.50	19.9	.99579	28.223	1.03443	1.03443
126.00	19.9	.97687	35.699	1.03443	1.03443
150.67	20.1	.95634	43.874	1.03444	1.03444
176.64	20.3	.93226	53.530	1.03444	1.03444
201.36	20.5	.90701	63.709	1.03445	1.03445

PREDICTED REFERENCE COLUMN HEIGHT IS 13.304 CM.

CALIBRATION CONSTANTS ARE (A/VB) = .233259E-02/CM

ALPHA = .380903E-04/ C

Table 2

NACL SOLUTION DENSITIES NACL MOLALITY = 1.0360

TEMP. (°C)	PRESS. (BAR)	DENSITY (GM/CC)	COLUMN HEIGHT (CM)	DENSITY AT REFERENCE TEMP. OF 25.00 C	DENSITY AT WATER BATH TEMP. OF 30.00 C
24.84	19.6	1.03843	11.971	1.03837	1.03659
50.45	19.6	1.02776	15.970	1.03837	1.03658
75.84	19.7	1.01392	21.303	1.03838	1.03659
100.32	19.8	.99802	27.511	1.03838	1.03659
125.71	19.9	.97915	34.954	1.03839	1.03660
125.65	19.9	.97918	34.938	1.03839	1.03660
125.74	20.0	.97914	34.957	1.03839	1.03660
151.00	20.1	.95807	43.328	1.03839	1.03661
176.69	20.2	.93428	52.843	1.03840	1.03661
200.47	20.3	.90992	62.644	1.03840	1.03662
200.49	20.3	.90990	62.651	1.03840	1.03662
200.37	20.3	.91001	62.607	1.03840	1.03662
200.37	20.3	.91002	62.604	1.03840	1.03662

PREDICTED REFERENCE COLUMN HEIGHT IS 11.991 CM.

CALIBRATION CONSTANTS ARE (A/VB) = .233259E-02/CM

ALPHA = .380903E-04/ C

Table 2

NACL SOLUTION DENSITIES NACL MOLALITY = 3.0610

TEMP. (°C)	PRESS. (BAR)	DENSITY (GM/CC)	COLUMN HEIGHT (CM)	DENSITY AT REFERENCE TEMP. OF 50.00 C	DENSITY AT WATER BATH TEMP. OF 30.00 C
51.63	19.6	1.09537	15.913	1.09623	1.10620
75.99	19.7	1.08144	20.933	1.09624	1.10620
101.20	19.8	1.06525	26.827	1.09624	1.10620
126.51	19.9	1.04729	33.422	1.09624	1.10620
150.79	20.0	1.02849	40.373	1.09625	1.10621
176.90	20.1	1.00655	48.535	1.09625	1.10621
176.86	20.1	1.00659	48.520	1.09625	1.10621
199.73	20.3	.98583	56.285	1.09626	1.10622
199.84	20.3	.98569	56.339	1.09626	1.10622

PREDICTED REFERENCE COLUMN HEIGHT IS 15.603 CM.

CALIBRATION CONSTANTS ARE (A/VB) = .233259E-02/CM

ALPHA = .380903E-04/ C

Table 2

NACL SOLUTION DENSITIES NACL MOLALITY = 3.2428

TEMP. (°C)	PRESS. (BAR)	DENSITY (GM/CC)	COLUMN HEIGHT (CM)	DENSITY AT REFERENCE TEMP. OF 30.00 C	DENSITY AT WATER BATH TEMP. OF 30.00 C
29.16	19.6	1.11237	17.309	1.11198	1.11198
49.86	19.8	1.10204	20.963	1.11198	1.11198
75.29	19.8	1.08748	26.177	1.11198	1.11198
99.97	19.9	1.07160	31.929	1.11199	1.11199
125.79	20.1	1.05326	38.626	1.11199	1.11199
150.36	20.1	1.03415	45.651	1.11199	1.11199
175.65	20.2	1.01294	53.498	1.11200	1.11200
200.45	20.2	.99038	61.887	1.11200	1.11200

PREDICTED REFERENCE COLUMN HEIGHT IS 17.445 CM.

CALIBRATION CONSTANTS ARE (A/VB) = .233259E-02/CM

ALPHA = .380903E-04/ C

Table 2

NACL SOLUTION DENSITIES NACL MOLALITY = 4.3933

TEMP. (°C)	PRESS. (BAR)	DENSITY (GM/CC)	COLUMN HEIGHT (CM)	DENSITY AT REFERENCE TEMP. OF 30.00 C	DENSITY AT WATER BATH TEMP. OF 30.00 C
29.09	19.7	1.14750	14.690	1.14702	1.14702
50.37	19.7	1.13618	18.579	1.14702	1.14702
76.02	19.7	1.12134	23.728	1.14702	1.14702
75.94	19.7	1.12139	23.711	1.14702	1.14702
100.19	20.0	1.10582	29.165	1.14703	1.14703
126.44	20.0	1.08755	35.611	1.14703	1.14703
126.38	20.0	1.08757	35.602	1.14703	1.14703
150.59	20.0	1.06941	42.052	1.14703	1.14703
175.87	20.1	1.04908	49.314	1.14704	1.14704
200.43	20.3	1.02791	56.916	1.14704	1.14704

PREDICTED REFERENCE COLUMN HEIGHT IS 14.853 CM.

CALIBRATION CONSTANTS ARE (A/VB) = .233259E-02/CM

ALPHA = .380903E-04/ C

points deviating by more than three times the standard deviation of fit could be discarded. The regression also was used to determine the column height at the desired reference temperature.

The data in this form are presented in Tables 1 and 2. The calibration data are listed in Table 1, along with values for the density of pure water given by Haar, Gallagher and Kell.[4] Table 2 lists the solution data and the assumed values of the density of the solution at the reference and water bath temperatures. The latter values were determined from the low temperature fit described in Chapter 1. These two tables provide all the information necessary to calculate solution densities from the experimental observations. The information is recorded here so that anyone desiring to recalculate the solution densities (with improved values for the density of water, for example) can do so with ease.

From this point, calculations involving calibration data and solution data were performed separately. All calibration data and the known values for the density of pure water were used in a non-linear least squares regression to determine the two unknowns in Equation (5). The values for the unknowns and the regression statistics are given in Table 3. The value obtained for the expansivity of the sample bomb (38×10^{-6} K^{-1}) is in good agreement with the expansivity of similar Hastelloy^R alloys[7] (36×10^{-6} K^{-1}).

Table 3

Least Squares Values of $\frac{A}{V_B}$ and α

$$A/V_B = .233259 \times 10^{-2}/\text{cm} \pm .10 \times 10^{-5}/\text{cm}$$

$$\alpha = .380903 \times 10^{-4}\ K^{-1} \pm .37 \times 10^{-6}\ K^{-1}$$

Overall standard deviation of fit for all calibration data is 40 ppm in the density values for pure water.

The solution data, the calculated values for solution densities at the reference and water bath temperatures, and the values of $\left(\frac{A}{V_B}\right)$ and α were then combined to calculate the high temperature solution densities. Since these densities were at odd temperatures and pressures, they were further smoothed to yield densities at rounded temperatures and 20 bar. First the densities were corrected to 20 bar using the compressibility data of Rowe and Chou.[5] Even considering the difference in compressibilities calculated from the Rowe and Chou data and from the volumetric fit (Chapter 1), the maximum error in this correction is 2×10^{-6} g/cm^3.

The constant pressure data were then fit at constant molality to an equation of the form

$$\rho_T = a + b\rho_w + c(T-25) + d(T-25)^2 + e\rho_w(T-25)$$

where T is the temperature in degrees Celcius and ρ_w is the density of water at T and 20.3 bar.

Densities at rounded temperatures calculated from the regression equation are listed in Table 4. The maximum error introduced in correcting the data to rounded temperatures is 2×10^{-5} g/cm^3.

Discussion

The expected precision of the density data can be estimated by calculating the effect of the uncertainty in the calibration constants. Assuming this uncertainty is twice the standard deviation listed in Table 3, the precision in the solution densities can be no better than $\pm 8 \times 10^{-5}$ g/cm^3 at 100°C and $\pm 2.5 \times 10^{-4}$ g/cm^3 at 200°C.

The actual precision in the density data can be estimated by examining the data as a function of molality at constant temperature and

Table 4

Least Squares Fit of NaCl Density Data

	T = 75°C		T = 100°C		T = 125°C	
molality	density (g/cm^3)	Δ^a	density (g/cm^3)	Δ^a	density (g/cm^3)	Δ^a
.0530	.97782	0	.96141	0	.94216	1
.2719	.98633	-7	.96995	-2	.95085	5
.5571	.99695	1	.98068	0	.96184	2
.9775	1.01230	0	.99615	-7	.97764	-13
1.0360	1.01439	-1	.99821	-5	.97970	-6
3.0610	1.08202	-1	1.06604	-5	1.04839	-12
3.2428	1.08764	1	1.07156	7	1.05382	15
4.3933	1.12190	0	1.10594	-1	1.08859	-2
.1[b]	.97961	7	.96314	17	.94397	15
.2	.98348	7	.96708	12	.94801	9
.5	.99489	-2	.97853	5	.95970	2
1.0	1.01316	1	.99691	3	.97832	8
Standard Deviation		4		8		10

Table 4 (continued)

	T = 150°C		T = 175°C		T = 200°C	
molality	density (g/cm^3)	Δ^a	density (g/cm^3)	Δ^a	density (g/cm^3)	Δ^a
.0530	.92021	0	.89549	0	.86767	7
.2719	.92920	-15	.90494	7	.87774	24
.5571	.94055	5	.91676	6	.89024	28
.9975	.95689	0	.93388	-40	.90847	-47
1.0360	.95894	-27	.93592	-16	.91042	0
3.0610	1.02912	-18	1.00820	-27	.98556	-40
3.2428	1.03446	27	1.01348	39	.99081	50
4.3933	1.06986	-4	1.04976	-6	1.02831	-6
.1[b]	.92197	29	.89730	39	.86995	7
.2	.92607	33	.90160	44	.87449	24
.5	.93813	24	.91428	27	.88800	3
1.0	.95747	7	.93438	8	.90898	6
Standard Deviation		23		31		33

[a] $\Delta = [\rho(\text{calculated}) - \rho(\text{experimental})] \times 10^5$ g/cm^3.

[b] Data of Ellis.[3]

pressure. The results of a least squares regression of the rounded density data as a function of molality only, using Equation (12) of Chapter 1, are listed in Table 4. The data of Ellis are included in the regression in order to compare the two sets of density values. Examination of the magnitudes of the residuals listed in Table 4 shows that they increase systematically with temperature. This trend is illustrated in Figure 3, where the residuals at a few molalities are plotted against temperature.

An increase in the uncertainties with temperature is the trend predicted above, but the scatter in the data at 200°C is twice as large as predicted. The most probable source of this error is the presence of air that dissolved in the salt solution during filling of the sample cell. The maximum effect of dissolved air can be estimated by assuming that the solubility of air in the solution is the same as that in pure water (.017 cm^3 air/cm^3 H_2O at 1 atm and 25°C) and that the solubility at 200°C and 20 bar is negligible. In this case .01 cm^3 of air would be present in the sample cell at 200°C and 20 bar, resulting in a systematic density error of about 3×10^{-4} g/cm^3. On this basis, a conservative value for the uncertainty in the data at 200°C would be ±400 ppm, in closer agreement with the observed variation in the data. Within these limits, the present data are in agreement with those of Ellis.[3]

Conclusions

The densities of sodium chloride solutions at 20 bar, from .05 m to 4.5 m and 75°C to 200°C, have been measured using a high pressure dilatometer. The precision of the data decreases from $\pm 2 \times 10^{-4}$ g/cm^3 at 100°C to $\pm 5 \times 10^{-4}$ g/cm^3 at 200°C. This uncertainty is an order of

Figure 3. Density residuals as a function of temperature. Plotted values represent the difference of experimental densities and smoothed values obtained from a least squares regression of the density data as a function of molality only.

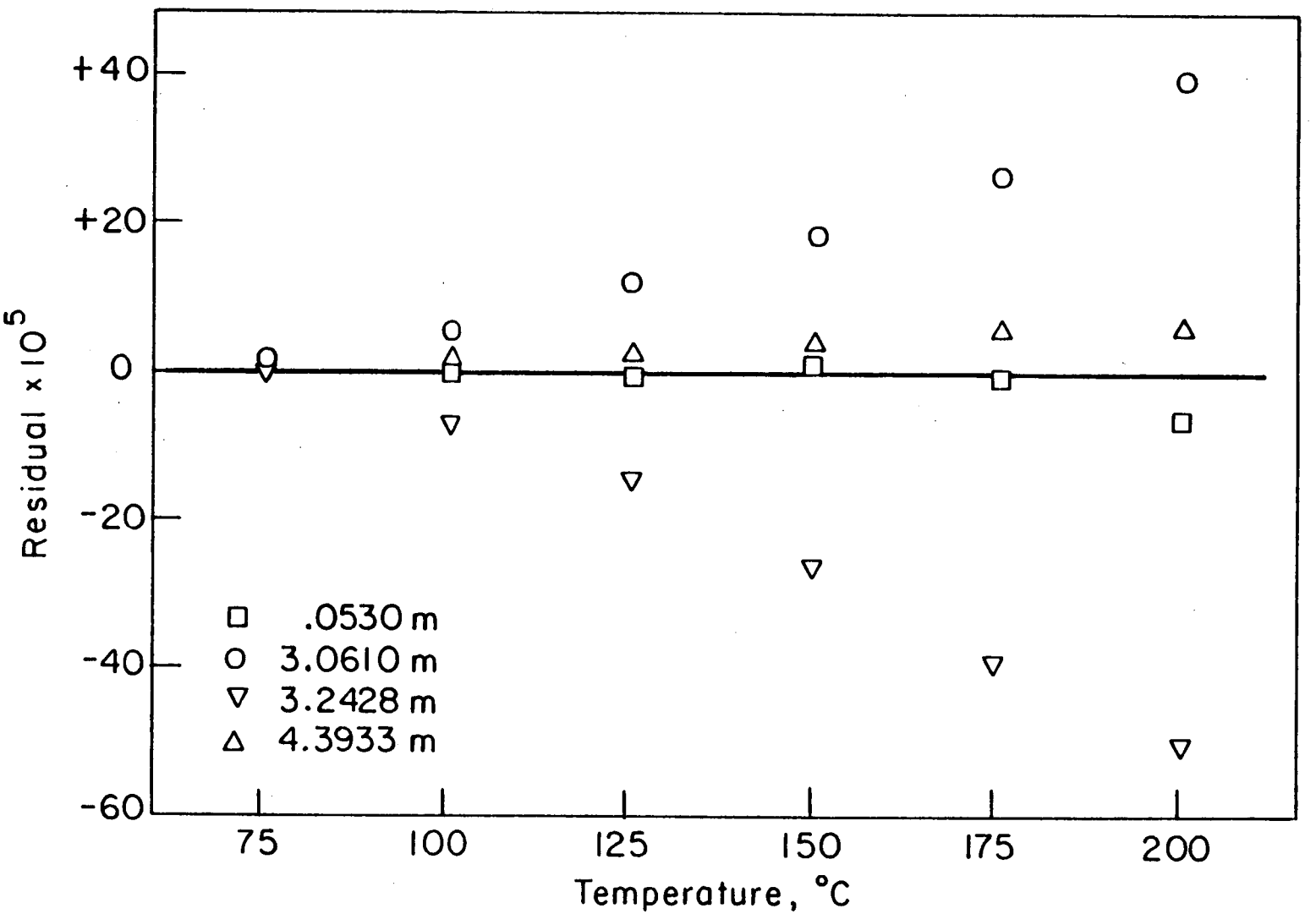
+40
+20
0
-20
-40
-60
Residual x 10^5
75
100
125
150
175
200
Temperature, °C
.0530 m
3.0610 m
3.2428 m
4.3933 m

XBL 812-5169

magnitude larger than that quoted by Ellis,[3] but it is a factor of four better than that given by Hilbert.[6] The data greatly extend the concentration range covered by Ellis,[3] and thus fill an important void in the sodium chloride data base.

References

1. I. Kh. Khaibullin and W. M. Borisov, Teplofiz. Vysokikh Temperatur, 4, 518 (1966).

2. B. M. Fabuss, A. Korosi, and A. K. M. Shamsul Hug, J. Chem. Eng. Data, 11, 325 (1966).

3. A. J. Ellis, J. Chem. Soc. A, 1579 (1966).

4. L. Haar, J. Gallagher, and G. S. Kell, Contributions to the 9th International Conference on the Properties of Steam, Munich (1979).

5. A. M. Rowe, Jr. and J. C. S. Chou, J. Chem. Eng. Data, 15, 61 (1970).

6. R. Hilbert, Doctoral Dissertation, University of Karlsruhe, Karlsruhe, West Germany (1979).

7. "Hastelloy C-276", Stellite Division, Cabot Corporation, Kokomo, Indiana, 1973.

Chapter 3

MEASUREMENT OF THE HEAT CAPACITY OF AQUEOUS SODIUM SULFATE SOLUTIONS FROM 30°C to 200°C

Introduction

A major part of the effort to build a model for natural brines must be to obtain basic thermodynamic data for electrolyte solutions over a wide range of temperature and pressure. Heat capacity measurements are ideal for this purpose, since the data can be integrated to yield enthalpy and activity information. The purpose of this chapter is to show that the method of flow calorimetry, developed by Picker, Leduc, Philip, and Desnoyers[1] for use at room temperature, can be adapted for use at high temperatures and pressures.

Flow calorimetry has many features which make it ideal for use at high temperature. Since the experimental fluid flows through the calorimeter, it is possible to keep the calorimeter temperature constant while changing samples. Fluid flowing through the calorimeter can also be kept at constant pressure, allowing measurements along isobars rather than along the saturated vapor pressure curve. The capability to extend measurements to high pressures is limited only by the fluid pump and the back pressure regulation system. The fast response and high sensitivity which make flow calorimetry powerful at room temperature also are advantageous at high temperatures.

To show that flow microcalorimetry can be used at high temperatures, a prototype calorimeter has been constructed and tested from 30°C to 200°C and 1 bar to 200 bar.

Aqueous solutions of sodium sulfate were chosen as the experimental fluid because sodium sulfate is a major component of natural brines. Solutions containing chloride ions were avoided because of the possibility of chloride ion stress-corrosion cracking in the stainless steel tubing used to construct the prototype calorimeter.

The heat capacity measurements obtained with the high temperature calorimeter are five times more precise than those in the literature.[2] In addition, osmotic coefficients obtained by integrating the heat capacity data are in good agreement with existing data.

Experimental

1. Description of Apparatus

The high temperature, flow calorimeter is an adaptation of the design originally used by Picker, et al.[1] The calorimeter, illustrated in Figure 1, is constructed of small, thin walled tubing (.059 inch outside diameter by .009 in wall stainless steel for the prototype). Solution flows through the tubing and past a heater where it is heated ~3 K. The heater is made of 1 m of "Thermocoax"[R] insulated nichrome heating wire (Amperes Electronics) which has a resistance of 50 Ωm^{-1} and is wound around the tubing to form a helix about 5 cm long. The heated solution then flows through a 2 cm long spiral in the tubing, which surrounds a temperature sensor. Both the inconel clad heating wire and the thin walled, stainless steel thermometer well are silver solded to the tubing for good thermal contact. The temperature sensor is a four lead, 1000 Ω platinum resistance thermometer (Rosemount #146MA) which is cemented into the well with high temperature ceramic cement. A second, identical loop serves as the reference side of the calorimeter.

Figure 1. High Temperature Flow Calorimeter.

A. Stainless steel jacket

B. Copper cylinder

C. Vacuum

D. Heater

E. Temperature sensor

F. Supporting tube containing electrical leads and vacuum connection

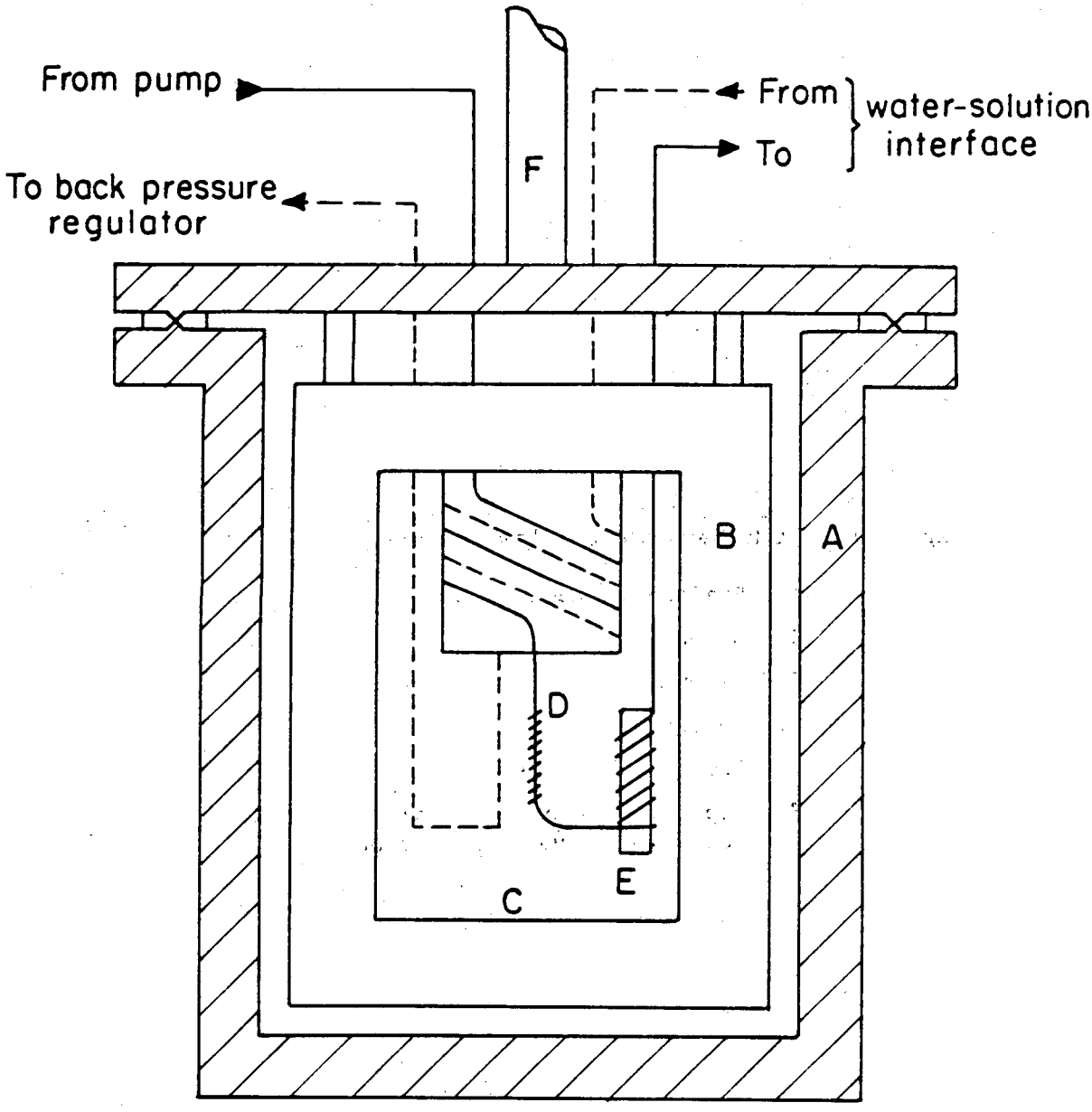
From pump
To back pressure regulator
F
From
To
water-solution interface
B
A
D
E
C

XBL 812-5165

The calorimeter is supported on and surrounded by a large copper cylinder, which serves both as thermal mass and adiabatic shield. The copper cylinder is contained in a stainless steel vacuum jacket. The pressure inside the calorimeter is held below 20 μ with a vacuum pump and monitored with a thermocouple gauge.

The whole assembly is heated in a fluidized bath, which is controlled with an iron-constantan thermocouple sensor and Electromax III controller (Leeds and Northrup) to about ± .1 K. The large thermal mass of the copper cylinder provides temperature stability of better than .01 K during the course of a measurement. Because both sides of the calorimeter are equally affected by temperature fluctuations, the temperature difference between reference and working sides is stable to .0005 K. This temperature difference is measured directly using a calibrated, G-2 Mueller bridge with a microvolt amplifier (Leeds and Northrup) and recorder serving as the galvanometer. The temperature of the copper cylinder is measured using a calibrated, 25 Ω platinum resistance thermometer (Burns Engineering) and the Mueller bridge. The cylinder temperature is monitored during a run using a Wheatstone bridge (Leeds and Northrup), a second microvolt amplifier, and a recorder.

The flow system for the calorimeter is shown in Figure 2. Freshly degassed water is drawn from the reservoir, through a cooling loop, and into a reciprocating, double piston pump (Altex Model 100). This pump was chosen because it has an electronic feedback system which monitors the flow rate and adjusts the piston speed to level out flow rate pulses. The water is pumped through 2 m of thermostating tubing in the fluidized bath, through 45 cm of tubing in thermal contact with the copper cylinder, and then through the reference side of the calorimeter. The water then

Figure 2. Flow system for the high temperature calorimeter.

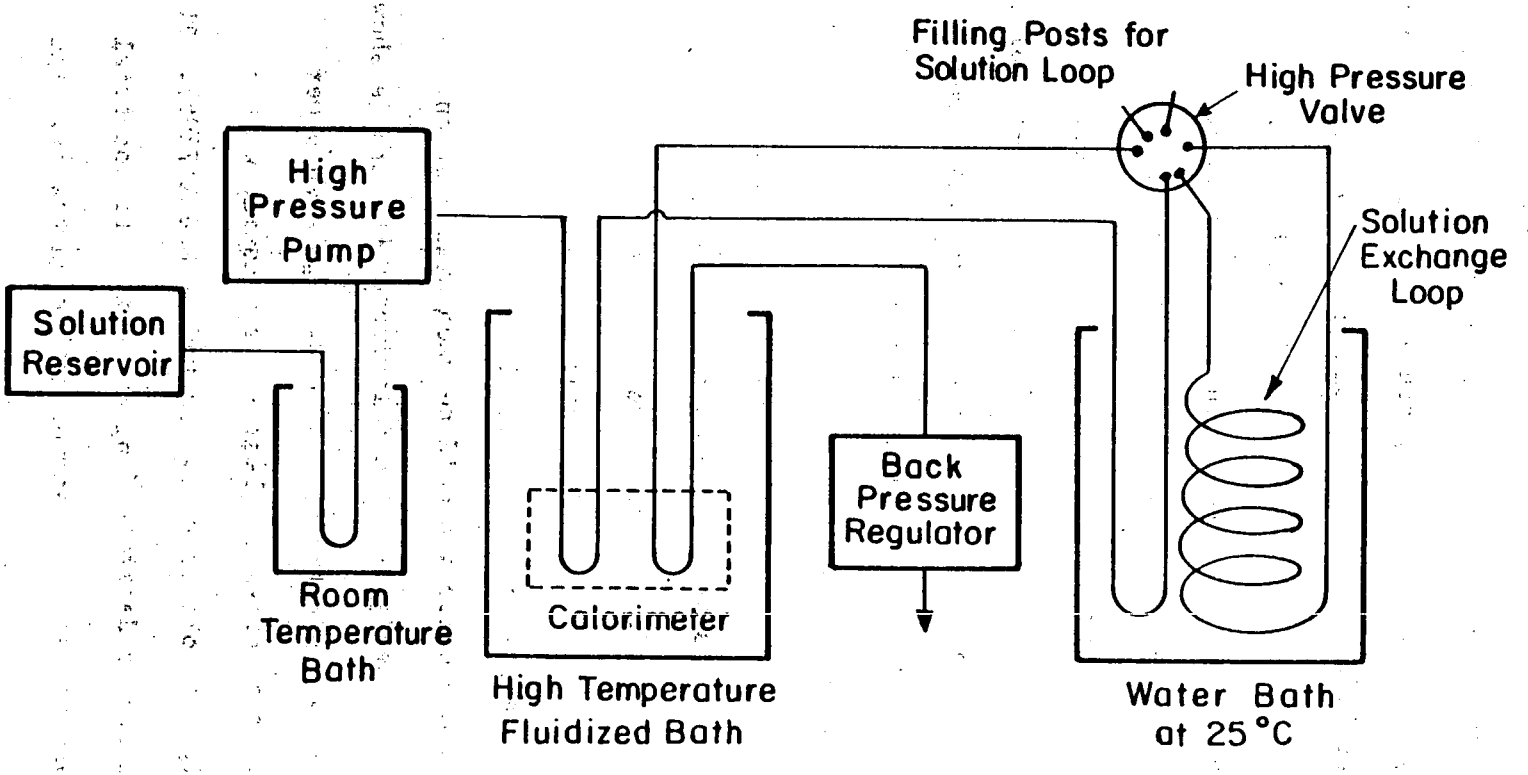
Filling Posts for
Solution Loop
High Pressure
Valve
High
Pressure
Pump
Solution
Reservoir
Solution
Exchange
Loop
Back
Pressure
Regulator
Room
Temperature
Bath
Calorimeter
High Temperature
Fluidized Bath
Water Bath
at 25 °C

XBL 812-5162

exits the fluidized bath and passes through 2 m of tubing thermostated at 25°C. At this point a high pressure solution injection valve (Altex Model 905) is used to direct the water either through the working side of the calorimeter or into a coil of tubing containing 15 ml of sample solution thermostated at 25°C. The water displaces an equal volume of sample, which is then fed through the working side of the calorimeter. Finally, the water or solution leaves the high pressure flow system through a back pressure regulator (Grove Model S-91xw). The system pressure is monitored to ± 1 bar with a pressure transducer calibrated against a Bourdon tube pressure gauge (Ashcroft Digigauge Model 7781).

The solutions used in this study were prepared from Baker reagent grade anhydrous sodium sulfate, which was dried overnight at 180°C and cooled in a vacuum desiccator. All solutions were prepared by weight, and all weights were corrected for air buoyancy. At room temperature (22°C) sodium sulfate solutions are saturated at 1.56 molal. Since supersaturated solutions of sodium sulfate are relatively stable, a few attempts were made to load the solution coil with samples at high concentrations. These attempts were not entirely successful, and the few data points reported above 1.5 m should be used with caution.

The electronic circuit design for the calorimeter heaters is shown in Figure 3. The heaters are powered by a 5 volt, regulated power supply, and the voltage drop across the heaters is measured with a calibrated, 5½ place digital voltmeter (System Donner Model 7205). The current through the heaters is determined by measuring the potential drop across 30 Ω standard resistors in series with each heater. The power to one heater can be reduced by increasing the series resistance of the circuit with a decade resistance box (Leeds and Northrup). All

Figure 3. Circuit diagram for calorimeter heaters.

Circuit Diagram for Calorimeter Heaters

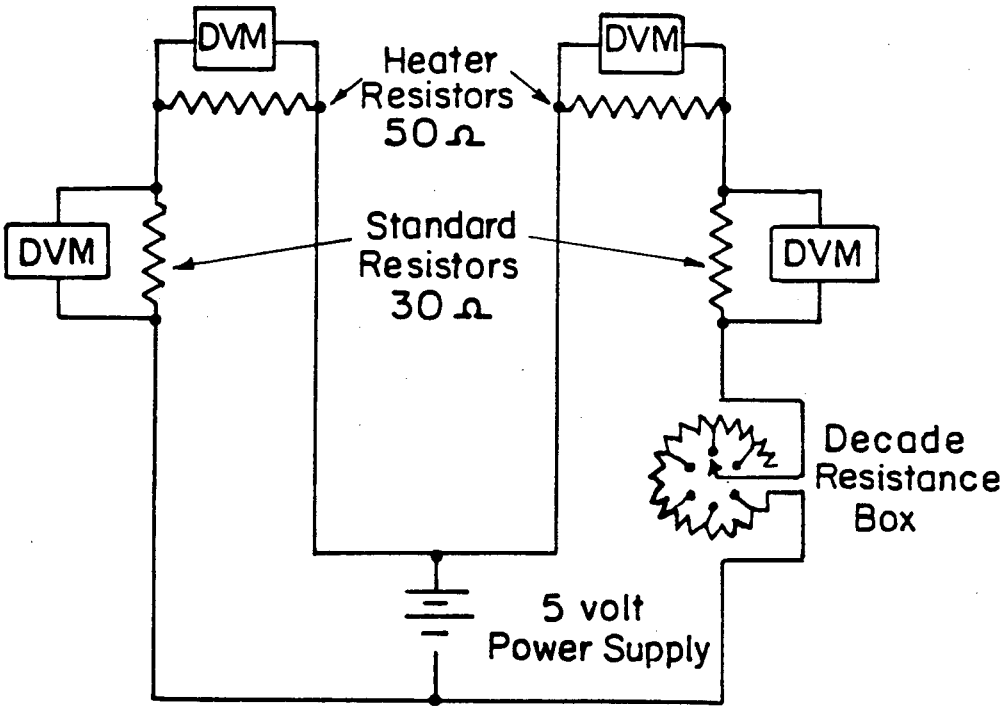

XBL 812-5161

heater leads from the calorimeter to its supporting block are 30 gauge gold wire. The heater power leads are silver soldered to the heater wire, and the potential leads are connected halfway between the heater and the calorimeter support.

2. Derivation of Equations

When water is flowing through both sides of the calorimeter, the power in the heaters can be adjusted to equalize the temperature rise in both sides. The temperature rise in the working side is given by

$$T = \frac{P_w - L}{f_w \, c_{p_w}} \tag{1}$$

where p_w is the total power dissipated by the heater, L is the power loss, f_w is the mass flow rate of the water, and c_{p_w} is the specific heat capacity of pure water. When a sample solution is flowing through the working side, the heater power can again be adjusted so that the temperature rise of the solution matches the unchanged temperature rise of water in the reference side. In this case

$$T = \frac{P_s - L}{f_s \, c_{p_s}} \tag{2}$$

where the power input, flow rate, and heat capacity are those of the sample solution. The power loss in the working side of the calorimeter is assumed to depend only on the temperature rise. Then the ratio of the heat capacity of the solution to that of pure water is given directly by

$$\frac{c_{p_s}}{c_{p_w}} = \left(\frac{f_w}{f_s}\right)\left(\frac{P_s - L}{P_w - L}\right) . \tag{3}$$

This formula can be further reduced by noting that the water displaces an equal volume of solution at 25°C, if we assume that the volume effects of the small amount of mixing at the water/solution interface are negligible. In this case,

$$\frac{f_w}{\rho_w} = \frac{f_s}{\rho_s} \tag{4}$$

where ρ_s and ρ_w are the densities of the solution and water at 25°C. The final equation for the heat capacity ratio is

$$\frac{c_{p_s}}{c_{p_w}} = \left(\frac{P_s - L}{P_w - L}\right)\left(\frac{\rho_w}{\rho_s}\right)_{25°C} \tag{5}$$

where the density ratio is taken at 25°C and the system pressure.

3. Determination of Power Loss

To determine the heat capacity ratio given in Equation (5), it is necessary to measure both the total power input to the calorimeter heater and the amount of that power lost through conduction, convection, and radiation. The use of a calibrated, platinum resistance thermometer as the temperature sensor is an advantage in this regard, since the temperature rise in the working side of the calorimeter, due to a given amount of power in the heater, can be measured directly. In practice, the temperature rise is measured with water flowing through the working side of the calorimeter, and the mass flow rate of water is determined by weighing the water discharged from the calorimeter in a given time interval. Application of Equation (1) yields the value of the power loss.

Determination of the power loss was repeated between every two or three heat capacity measurements. The average power loss for a 3 K temperature rise, as a function of the calorimeter temperature, is shown in Figure 4. The power loss increases rapidly with calorimeter temperature, showing the importance of its accurate determination.

4. Dependence of Heat Capacity on Flow Rate

In testing the operation of the calorimeter at high temperatures, it is important to show that the heat capacity determination does not depend on flow rate. For this reason, a series of preliminary measurements on 2.0 m NaCl solutions, at varying flow rates, were taken at 77°C. The results, given in Table 1, show that the experimental ratio, $\frac{P_s - L}{P_w - L}$, does not change when the flow rate is varied by $\pm$ 25%.

Table 1

Dependence of Heat Capacity on Flow Rate
(2.0026 m NaCl, 76.76°C, 1 bar)

Flow Rate (g/min)	$\frac{P_s - L}{P_w - L}$
.547	.9575
.742	.9574
.952	.9575

5. Error Analysis

The precision of a heat capacity determination depends on the precision in the measurement of the total power, the power loss on the working side of the calorimeter, and the temperature difference between the reference and working sides. The uncertainty in the measurement of the total power with the digital voltmeter is negligible. Uncertainty

Figure 4. Power loss from calorimeter heater.

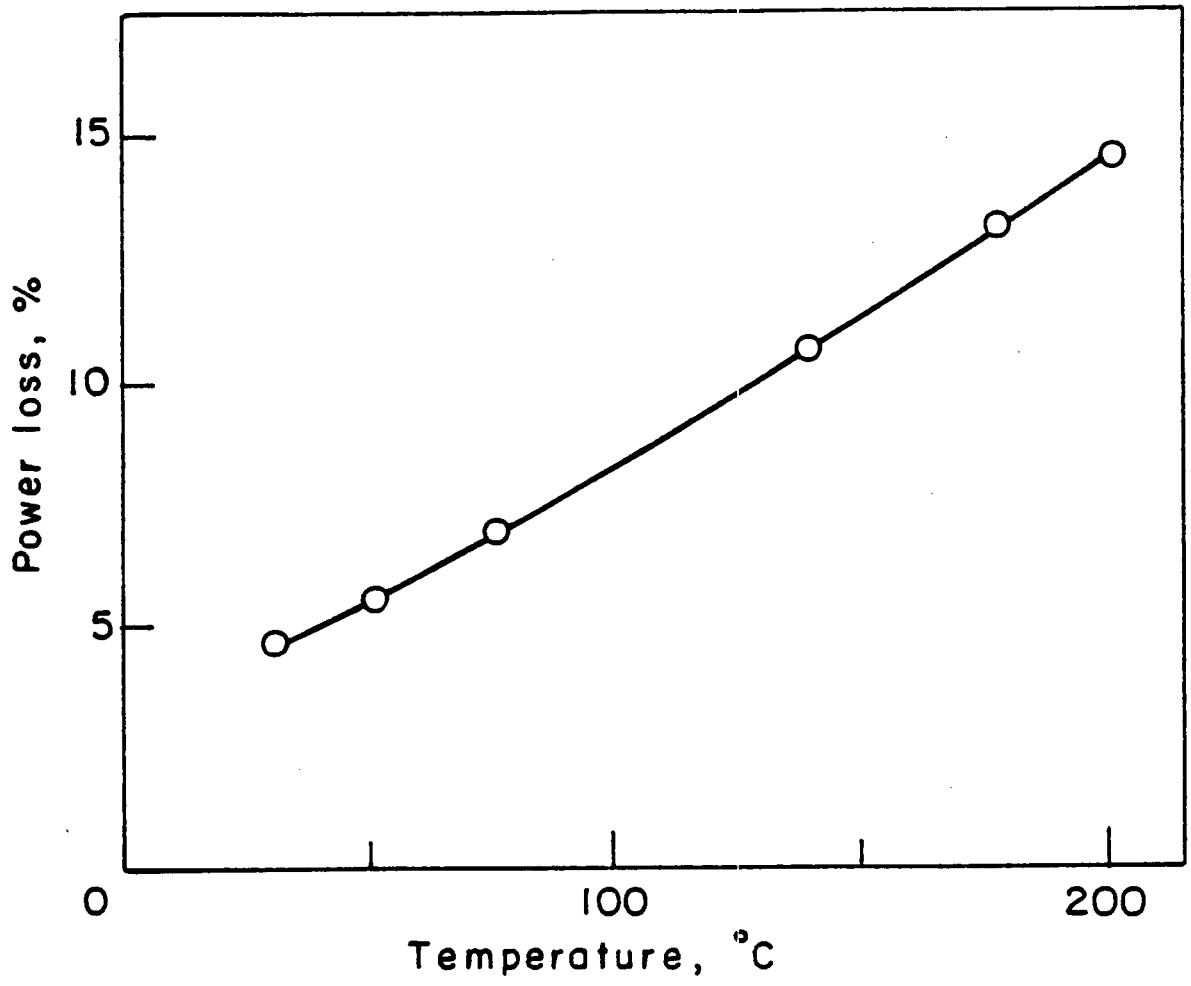

XBL 812-5170

in the power loss, resulting from uncertainties of $\pm$ .01 K in the temperature rise and of $\pm$ .001 g/min in the flow rate, can be estimated from Equation (1). Assuming an average total power of .185 J, temperature rise of 3 K, flow rate of .8 g min^{-1}, and heat capacity of 4.25 g^{-1} K^{-1}, the power loss is

$$L = P - (T \pm .01)\left(\frac{f_w + .001}{60}\right) c_{p_w} = .017 \pm .001 \text{ J}.$$

Because the experimental ratio is never smaller than .97, the uncertainty of $\pm$ .001 J in the power loss results in a maximum uncertainty of $\pm$ .00015 J in the experimental ratio,

$$\frac{P_s - L}{P_w - L}.$$

The temperatures of the two sides of the calorimeter are matched to within $\pm$ .001 K. From Equations (1) and (2), the resulting uncertainty in the experimental ratio is

$$\frac{P_s - L}{P_w - L} \pm .001 \frac{f_s\, c_{p_s}}{P_w - L} \approx \frac{P_s - L}{P_w - L} \pm .00035.$$

The total uncertainty in the experimental ratio is $\pm$ .0005, and this is roughly equivalent to $\pm$ .002 J g^{-1} K^{-1} in the value of the specific heat capacity.

Possible sources of systematic error include error in the determination of the temperature of the calorimeter and of the thermostating bath for the solution exchange column, error in the voltage readings from the digital voltmeter, and error in determining the molalities of the solutions. These possible systematic errors have been minimized by

frequent calibration of all thermometers, the Mueller Bridge, the digital voltmeter, and the balance used to prepare the solutions.

Results

1. Heat Capacity Measurements

The results of heat capacity measurements of sodium sulfate solutions from 30°C to 200°C are given in Table 2. The direct experimental ratio,

$$\frac{P_s - L}{P_w - L} = \left(\frac{c_{p_s}}{c_{p_w}}\right)\left(\frac{\rho_s}{\rho_w}\right),$$

is listed in the second column so that the heat capacity of the solution can be recomputed to reflect any future changes in the accepted values of the heat capacity of water or the densities of sodium sulfate solutions. The values listed for the heat capacity of water below 95°C were taken from Stimson,[3] while those above 95°C were taken from the steam tables of Haar, Gallagher, and Kell.[4]

Density data for sodium sulfate solutions at 25°C, given in the literature,[5-7] were fit as a function of molality, m, using an equation specific for the 2-1 charge type of sodium sulfate,

$$\begin{aligned}\phi V = \bar{V}_2^{\circ} &+ \frac{3A_v}{1.2}\ln(1+1.2\ I^{\frac{1}{2}}) + 4RTm\ \beta_v^{(0)} \\ &+ \frac{2RTm}{I}\left(1-(1+2I^{\frac{1}{2}})\ e^{-2I^{\frac{1}{2}}}\right)\beta_v^{(1)} + \sqrt{2}\ RTm^2\ C_v^{\phi},\end{aligned} \tag{6}$$

where ϕV is the apparent molal volume, I is the ionic strength, R is the gas constant, T is the temperature in kelvins, A_v is the Debye Hückel slope, and $\bar{V}_2^{\circ}$ is the apparent molal volume at infinite dilution. The

Table 2

Na_2SO_4 Heat Capacity Data

T = 304.62 K (31.47°C)

molality	$\left(\frac{c_{p_s}}{c_{p_w}}\right)_T$	$\left(\frac{\rho_s}{\rho_w}\right)_{25°C}$	$\rho_s(25°C)(g/cm^3)$	$c_{p_s}(Jg^{-1}K^{-1})$	$\phi C_p(Jmol^{-1}K^{-1})$
	P = 1.01 bar		P = 1.01 bar	P = 1.01 bar	P = 1.01 bar
0	1.0000		.997047	4.1780	-
.0528	.9978		1.0038	4.1408	-116.
.0528	.9977		1.0038	4.1403	-126.
.0995	.9960		1.0097	4.1092	-108.
.2491	.9917		1.0279	4.0188	- 68.3
.4986	.9884		1.0572	3.8946	- 15.2
.7486	.9878		1.0853	3.7913	22.0
.9995	.9891		1.1125	3.7036	51.4
1.9407	.9939		1.2060	3.4329	103.7

T = 324.00 K (50.85°C)

molality	$\left(\frac{c_{p_s}}{c_{p_w}}\right)_T$	$\left(\frac{\rho_s}{\rho_w}\right)_{25°C}$	$\rho_s(25°C)(g/cm^3)$	$c_{p_s}(Jg^{-1}K^{-1})$	$\phi C_p(Jmol^{-1}K^{-1})$
	P = 1.01 bar		P = 1.01 bar	P = 1.01 bar	P = 1.01 bar
0	1.0000		.997047	4.1807	-
.0500	.9980		1.0034	4.1457	-111.
.1092	.9966		1.0109	4.1095	- 68.3
.2832	.9935		1.0320	4.0128	- 22.9
.2832	.9937		1.0320	4.0137	- 19.6
.4995	.9911		1.0573	3.9073	7.6
.4995	.9916		1.0573	3.9093	11.9
.7487	.9910		1.0854	3.8058	39.8
1.0089	.9921		1.1135	3.7139	64.8
1.4430	.9967		1.1581	3.5873	98.3
2.0394	1.0064		1.2152	3.4522	133.1

Table 2 (continued)

T = 349.18 K (76.03°C)

molality	$\left(\frac{c_{p_s}}{c_{p_w}}\right)_T \left(\frac{\rho_s}{\rho_w}\right)_{25°C}$	$\rho_s(25°C)(g/cm^3)$	$c_{p_s}(Jg^{-1}K^{-1})$	$\phi C_p(Jmol^{-1}K^{-1})$
	P = 1.01 bar	P = 1.01 bar	P = 1.01 bar	P = 1.01 bar
0	1.0000	.997047	4.1932	-
.0500	.9984	1.0034	4.1600	- 73.
.1092	.9970	1.0109	4.1233	- 54.
.2832	.9944	1.0320	4.0285	- 9.4
.4995	.9927	1.0573	3.9254	21.4
.7487	.9920	1.0854	3.8211	45.8
1.0089	.9929	1.1135	3.7280	68.4
1.4430	.9974	1.1581	3.6006	100.8
2.0394	.9947	1.2152	3.4222	108.0

T = 413.90 K (140.75°C)

molality	$\left(\frac{c_{p_s}}{c_{p_w}}\right)_T \left(\frac{\rho_s}{\rho_w}\right)_{25°C}$	$\rho_s(25°C)(g/cm^3)$	$c_{p_s}(Jg^{-1}K^{-1})$	$\phi C_p(Jmol^{-1}K^{-1})$
	P = 5 bar	P = 3.69 bar	P = 3.69 bar	P = 3.69 bar
0	1.0000	.997047	4.2901	-
.0528	.9976	1.0038	4.2510	-137.
.0995	.9961	1.0097	4.2200	-105.
.2491	.9922	1.0279	4.1288	- 61.1
.4986	.9874	1.0572	3.9950	- 24.4
.7486	.9850	1.0853	3.8820	6.3
.9995	.9834	1.1125	3.7810	27.7
1.9407	.9841	1.2060	3.4903	83.6
2.6294	.9936	1.2673	3.3537	120.2

Table 2 (continued)

T = 450.41 K (177.26°C)

molality	$\left(\frac{c_{p_s}}{c_{p_w}}\right)_T$	$\left(\frac{\rho_s}{\rho_w}\right)_{25°C}$	ρ_s(25°C)(gm/cm^3)	c_{p_s} (Jg^{-1}K^{-1})	ϕ_{C_p}(Jmol^{-1}K^{-1})
	P = 10 bar		P = 9.40 bar	P = 9.40 bar	P = 9.40 bar
0	1.0000		.997047	4.3934	-
.0528	.9967		1.0038	4.3494	-215.
.0995	.9940		1.0097	4.3123	-203.
.2491	.9883		1.0279	4.2117	-131.
.4986	.9814		1.0572	4.0664	- 78.2
.7486	.9766		1.0853	3.9417	- 43.5
.9995	.9731		1.1125	3.8315	- 17.9
1.9407	.9677		1.2060	3.5149	46.6

T = 474.68 K (201.53°C)

molality	$\left(\frac{c_{p_s}}{c_{p_w}}\right)_T$	$\left(\frac{\rho_s}{\rho_w}\right)_{25°C}$	ρ_s(25°C)(gm/cm^3)	c_{p_s} (Jg^{-1}K^{-1})	ϕ_{C_p}(Jmol^{-1}K^{-1})
	P = 17 bar		P = 16.04 bar	P = 16.04 bar	P = 16.04 bar
0	1.0000		.997047	4.4966	-
.0528	.9952		1.0038	4.4449	-348.
.0995	.9922		1.0097	4.4056	-289.
.2491	.9848		1.0279	4.2953	-198.

Table 2 (continued)

T = 323.81 K (50.66°C)

molality	$\left(\frac{c_{p_s}}{c_{p_w}}\right)_T$	$\left(\frac{\rho_s}{\rho_w}\right)_{25°C}$	$\rho_s(25°C)(g/cm^3)$	$c_{p_s}(Jg^{-1}K^{-1})$	$\phi C_p(Jmol^{-1}K^{-1})$
	P = 207.2 bar	P = 200 bar	P = 200 bar	P = 200 bar	P = 200 bar
0	1.0000	1.0059	4.1379	-	
.0528	.9985	1.0126	4.1044	- 51.	
.0528	.9985	1.0126	4.1044	- 51.	
.0995	.9975	1.0184	4.0769	- 34.	
.0995	.9973	1.0184	4.0761	- 42.	
.2491	.9948	1.0362	3.9960	- 2.0	
.2491	.9946	1.0362	3.9952	- 5.4	
.4986	.9929	1.0650	3.8805	34.9	
.7486	.9931	1.0928	3.7826	62.7	
.9995	.9946	1.1196	3.6976	84.7	
1.9407	.9907	1.2121	3.4020	104.0	
2.6294	.9756	-	-	-	

T = 414.20 K (131.05°C)

molality	$\left(\frac{c_{p_s}}{c_{p_w}}\right)_T$	$\left(\frac{\rho_s}{\rho_w}\right)_{25°C}$	$\rho_s(25°C)(g/cm^3)$	$c_{p_s}(Jg^{-1}K^{-1})$	$\phi C_p(Jmol^{-1}K^{-1})$
	P = 199.2 bar	P = 200 bar	P = 200 bar	P = 200 bar	P = 200 bar
0	1.0000	1.0059	4.2363	-	
.0528	.9978	1.0126	4.1991	-108.	
.0995	.9963	1.0184	4.1689	- 85.	
.2491	.9927	1.0362	4.0824	- 38.0	
.4986	.9889	1.0650	3.9568	1.5	
.7486	.9866	1.0928	3.8472	26.7	
.9995	.9855	1.1196	3.7509	47.1	
1.9407	.9869	1.2121	3.4696	97.8	
2.6294	.9913	-	-	-	

apparent molal volume is related to the density of the solution, ρ_s, by

$$\phi V = 1/m \left(\frac{1000 + mM}{\rho_s} - \frac{1000}{\rho_w} \right) \tag{7}$$

where M is the molecular weight of sodium sulfate. Values of the fit parameters, $\bar{V}_2^\circ$, $\beta_v^{(0)}$, $\beta_v^{(1)}$, and C_v^ϕ, as well as values of the various constants in Equation (6) are listed in Table 3. The standard deviation of fit for the density data was 5×10^{-5} g/cm^3. The density values at 1.01 bar, listed in Table 2, were calculated from this fit.

The data obtained above 100°C and near the saturated vapor pressure were treated assuming that the ratio $\frac{c_{p_s}}{c_{p_w}}$ does not change over the small interval between the experimental pressure and the saturation pressure of pure water. In addition, the error in using $\left(\frac{\rho_s}{\rho_w}\right)$ at 1.01 bar rather than at the saturation pressure is less than 2×10^{-4} and results in an error in the specific heat capacity of less than 6×10^{-4} $Jg^{-1}\ K^{-1}$.

Table 3

Fit Parameters for Na_2SO_4 Density Data

$\bar{V}_2^\circ = 10.8589\ cm^3\ mol^{-1}$

$\beta_v^{(0)} = 6.25266 \times 10^{-5}\ g\ mol^{-1}\ bar^{-1}$

$\beta_v^{(1)} = -1.10496 \times 10^{-5}\ g\ mol^{-1}\ bar^{-1}$

$C_v^\phi = 2.98866 \times 10^{-5}\ g^2\ mol^{-2}\ bar^{-1}$

$T = 298.15\ K$

$R = 83.1440\ cm^3\ bar\ mol^{-1}\ K^{-1}$

$A_v = 2.8017\ cm^3\ mol^{-1}$

Calculation of heat capacities from the high pressure data was more complicated. Chen, Emmet, and Millero[9] have reported density data for sodium sulfate solutions at high pressures, but the concentration range extends only to .33 molal. The only high concentration data available are values of the bulk compressibility from 1 to 1000 bar reported by Gibson.[10] An estimation of the bulk compressibility to 200 bar, as a percentage of the bulk compressibility to 1000 bar, is shown in Figure 5, where the data of Millero have been used to determine the points below .33 molal. The values of ρ_s listed in Table 2 have been calculated using the estimate of bulk compressibility to 200 bar and the known values of ρ_s at 1.01 bar, and they are thought to be in error by less than $\pm 2 \times 10^{-4}$ g/cm^3.

2. Comparison with Literature Data

Likke and Bromley[2] have published the only comprehensive study of the heat capacities of sodium sulfate solutions at high temperatures. Their data are compared with that of the present study in Figure 6, where the error bars shown for the 180°C data were calculated using the uncertainty of $\pm$ .01 Jg^{-1} K^{-1} (in the specific heat capacity) given by Likke and Bromley. The two sets of data are in agreement well within the stated uncertainty. However, the greater precision of the present measurements is evident at the lower concentrations.

No literature data on sodium sulfate heat capacities are available at pressures greater than the saturated vapor pressure. However, the behavior of the high pressure data obtained in this study seems entirely reasonable. The 200 bar data at 50°C and 140°C are compared with low pressure data in Figures 7 and 8. The pressure dependence of the apparent molal heat capacity of Na_2SO_4 at 50°C is twice as large as that reported by Smith-Magowan and Wood[11] for NaCl.

Figure 5. Estimation of bulk compressibility of Na_2SO_4 solutions. Low concentration points were calculated from the data of Chen, Emmet, and Millero.[9]

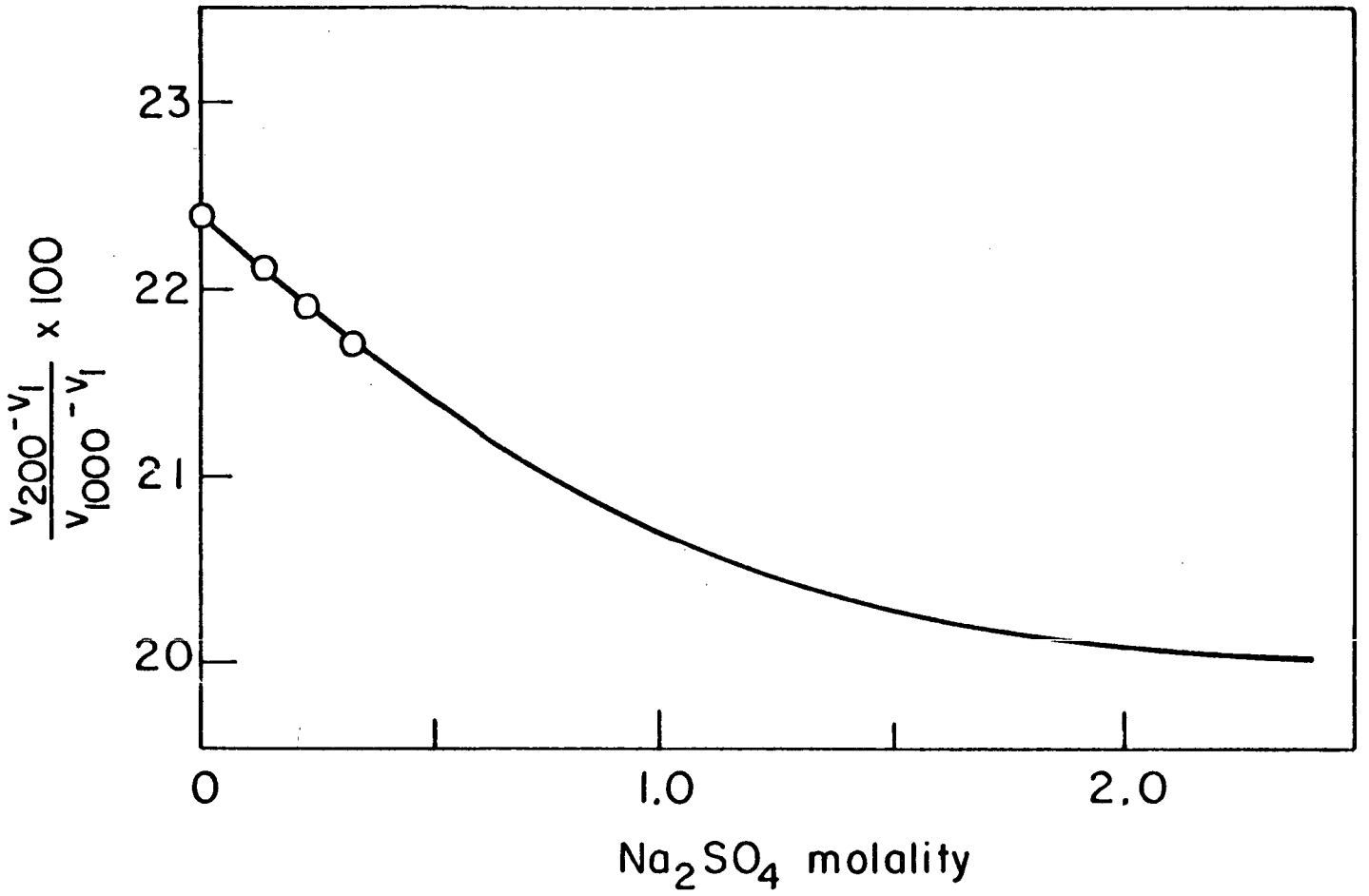
23
22
21
20
$\frac{v_{200}-v_1}{v_{1000}-v_1} \times 100$
0
1.0
2.0
Na_2SO_4 molality

XBL812-5171

Figure 6. Comparison of apparent molal heat capacity values obtained in this study with those published by Likke and Bromley.[2]

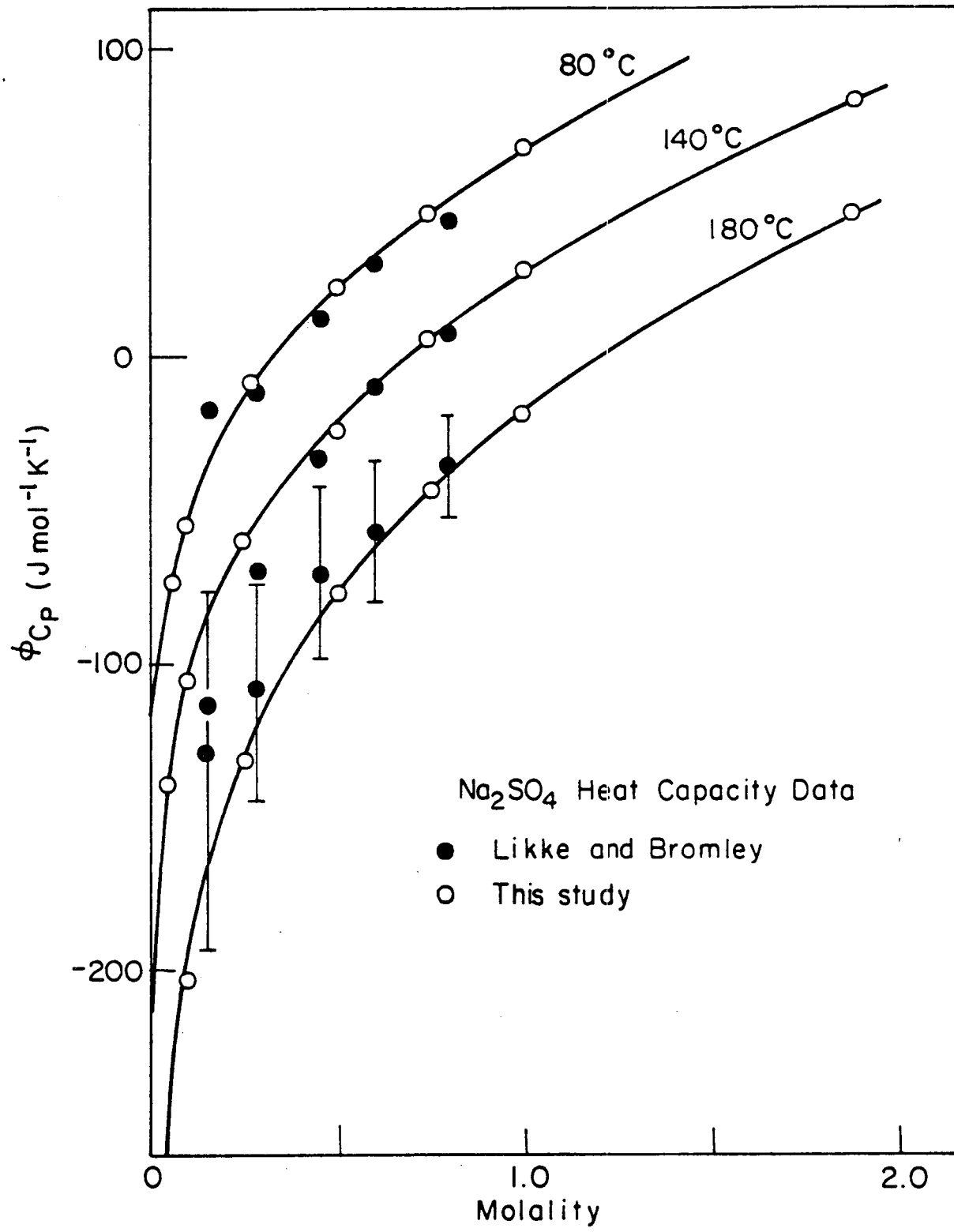
100
0
-100
-200
ϕ_{C_p} (J mol^{-1} K^{-1})
80 °C
140 °C
180 °C
Na_2SO_4 Heat Capacity Data
Likke and Bromley
This study
0
1.0
2.0
Molality

XBL 812-5215

Figure 7. Comparison of apparent molal heat capacities at 1 bar and 200 bar, at 50°C.

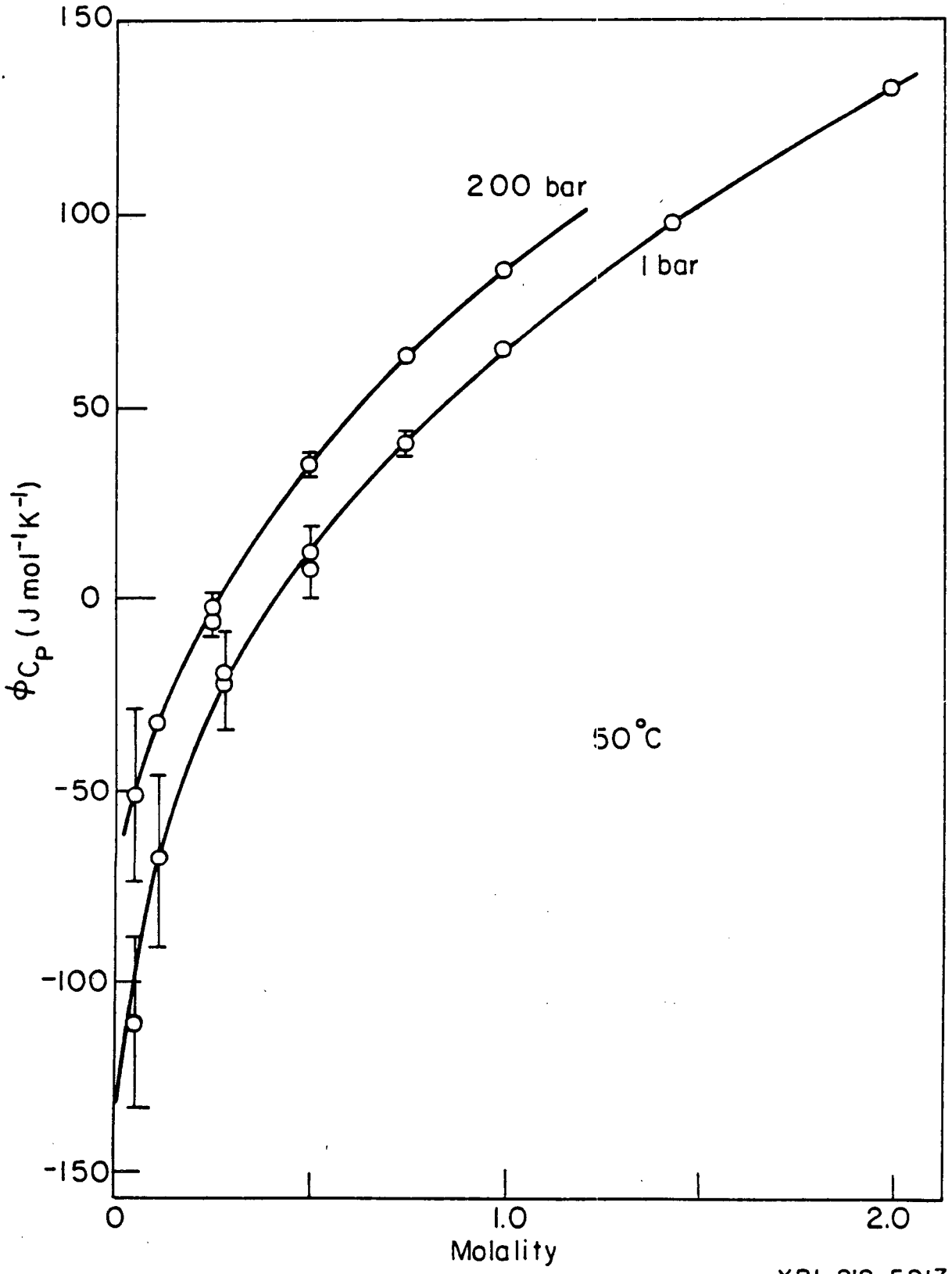
150
100
50
0
-50
-100
-150
ϕC_p (J mol^{-1}K^{-1})
200 bar
1 bar
50 °C
0
1.0
2.0
Molality

XBL 812-5217

Figure 8. Comparison of apparent molal heat capacities at 4 bar and 200 bar, at 140°C.

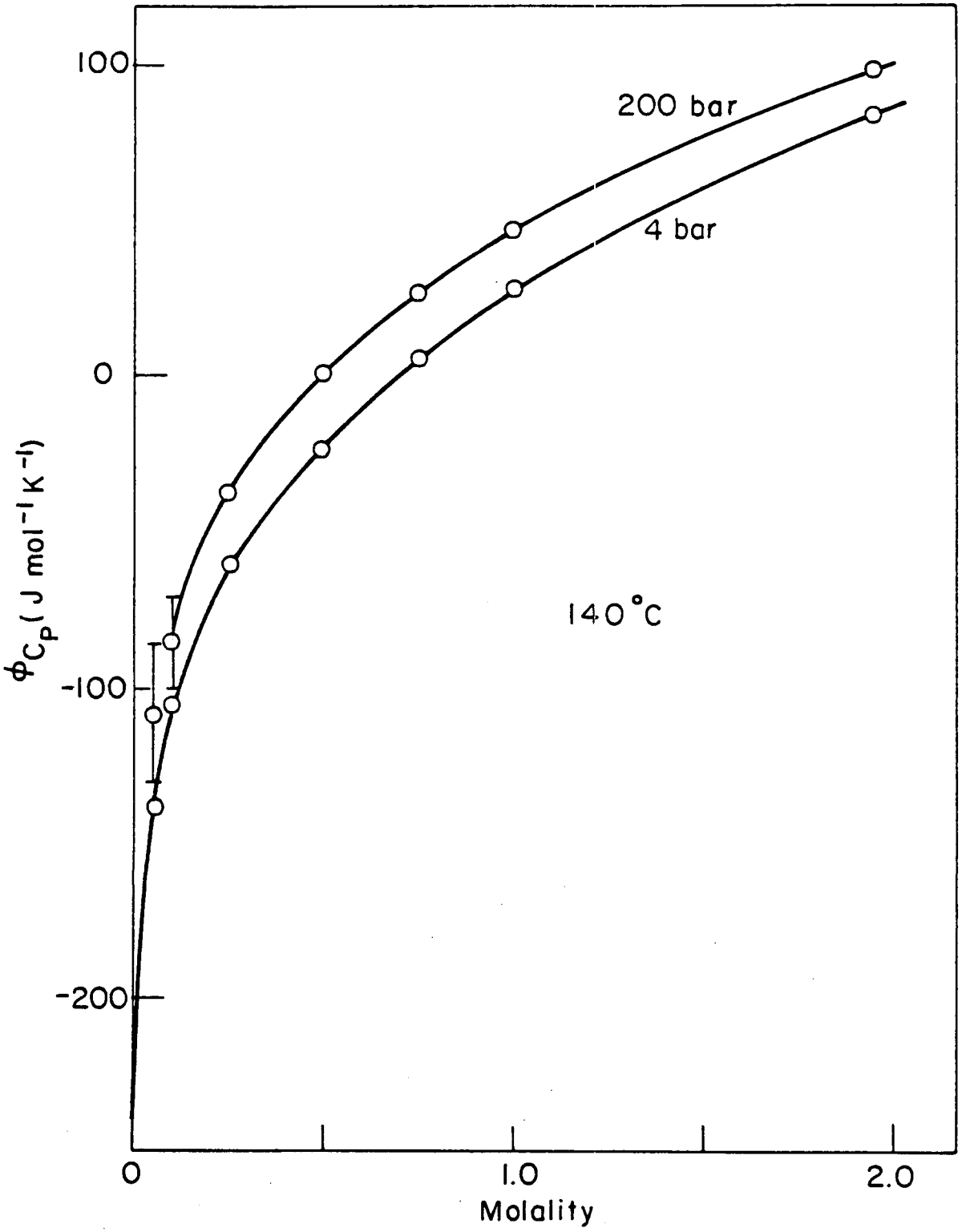

XBL 812-5218

Calculations

1. Review of Equations

Heat capacity data are of major importance because they can be integrated to obtain activity properties. To calculate high temperature activity properties, the heat capacity data must be fit to a temperature dependent equation, and the fitting equation must be integrated twice using enthalpy and activity data to evaluate the integration constants. The system of equations chosen to complete this calculation for sodium sulfate solutions was developed by Pitzer and co-workers[12-15] and was found to describe successfully the properties of sodium chloride solutions at high temperatures.[16,17] The basic equations for the apparent molal heat capacity, ${}^{\phi}C_p$, the apparent molal enthalpy, ${}^{\phi}L$, and the activity and osmotic coefficients, ϕ and $\gamma_{\pm}$, have been derived in Chapter 1 of this thesis. The specific equations for the 2-1 charge type of sodium sulfate are summarized below.

$$
\begin{aligned}
{}^{\phi}C_p = \overline{C}^{\circ}_{p_2} &+ \frac{3A_J}{1.2}\ln(1+1.2I^{\frac{1}{2}}) - 4RT^2m\,\beta^{(0)}_{T^2} \\
&- \frac{2RT^2m}{I}\left(1-(1+2I^{\frac{1}{2}})\,e^{-2I^{\frac{1}{2}}}\right)\beta^{(1)}_{T^2} - \sqrt{2}\,RT^2m^2\,C^{\phi}_{T^2}
\end{aligned}
\tag{8}
$$

with

$$\beta^{(0)}_{T^2} = \left(\frac{\partial^2\beta^{(0)}}{\partial T^2}\right)_{P,m} + \frac{2}{T}\left(\frac{\partial\beta^{(0)}}{\partial T}\right)_{P,m}$$

$$\beta^{(1)}_{T^2} = \left(\frac{\partial^2\beta^{(1)}}{\partial T^2}\right)_{P,m} + \frac{2}{T}\left(\frac{\partial\beta^{(1)}}{\partial T}\right)_{P,m}$$

$$C^{\phi}_{T^2} = \left(\frac{\partial^2 C^{\phi}}{\partial T^2}\right)_{P,m} + \frac{2}{T}\left(\frac{\partial C^{\phi}}{\partial T}\right)_{P,m}$$

$$\phi_L = \frac{3A_H}{1.2} \ln(1+1.2I^{\frac{1}{2}}) - 4RT^2m\ \beta_T^{(0)}$$

$$- \frac{2RT^2m}{I} (1-(1+2I^{\frac{1}{2}})\ e^{-2I^{\frac{1}{2}}})\ \beta_T^{(1)} - \sqrt{2}\ RT^2m^2\ C_T^{\phi} \tag{9}$$

with

$$\beta_T^{(0)} = \left(\frac{\partial\beta^{(0)}}{\partial T}\right)_{P,m}$$

$$\beta_T^{(1)} = \left(\frac{\partial\beta^{(1)}}{\partial T}\right)_{P,m}$$

$$C_T^{\phi} = \left(\frac{\partial C^{\phi}}{\partial T}\right)_{P,m}$$

$$\phi = 1 - 2A_{\phi} \frac{I^{\frac{1}{2}}}{1+1.2I^{\frac{1}{2}}} + \frac{4}{3} m\beta^{(0)} + \frac{4}{3} m\beta^{(1)}\ e^{-2I^{\frac{1}{2}}} + \frac{4\sqrt{2}}{3} C^{\phi} \tag{10}$$

$$\ln \gamma_{\pm} = -2A_{\phi}\left(\frac{I^{\frac{1}{2}}}{1+1.2I^{\frac{1}{2}}} + \frac{2}{1.2} \ln(1+1.2I^{\frac{1}{2}})\right) + \frac{8}{3} m\beta^{(0)} \tag{11}$$

$$+ \frac{2}{3}\frac{m}{I} (1-(1+2I^{\frac{1}{2}} - 2I)\ e^{-2I^{\frac{1}{2}}})\ \beta^{(1)} + 2\sqrt{2}\ m^2\ C^{\phi}$$

Here, $\beta^{(0)}$, $\beta^{(1)}$, and C^{ϕ} are the fitting parameters whose temperature dependence will be determined from the heat capacity data. A_J, A_H, and A_{ϕ} are the Debye-Hückel slopes for the heat capacity, enthalpy, and activity reported by Bradley and Pitzer.[18] $\overline{C}_{p_2}^{\circ}$ is the apparent molal heat capacity at infinite dilution.

Use of Equation (8) to describe the sodium sulfate heat capacities as a function of temperature requires one approximation. The definitions of $\beta_{T^2}^{(0)}$ and the other parameters require temperature derivatives at constant pressure. However, the heat capacity data have been taken along the saturated vapor pressure curve, so that above 100°C the required first derivative of $\beta^{(0)}$ is

$$\left(\frac{\partial\beta^{(0)}}{\partial T}\right)_{sat} = \left(\frac{\partial\beta^{(0)}}{\partial T}\right)_P + \left(\frac{\partial\beta^{(0)}}{\partial P}\right)_T \left(\frac{\partial P}{\partial T}\right)_{sat} . \tag{12}$$

Extensive volumetric data at high temperatures and pressures are required to evaluate the second term in Equation 12. In this study, the second term has been assumed to be negligibly small. This assumption is probably reasonable below 200°C, but it could lead to significant error at higher temperatures.

2. Temperature Dependence of the Heat Capacity

The experimental heat capacity data were first fit to Equation (8) at constant temperature to evaluate $\overline{C}_{p_2}^{\circ}$. These values of $\overline{C}_{p_2}^{\circ}$ were combined with those reported by Gardner, Jekel, and Cobble[19] in a least squares fitting routine to determine their temperature dependence. The two sets of $\overline{C}_{p_2}^{\circ}$ values and the smooth curve given by the fitting equation,

$$\overline{C}_{p_2}^{\circ} = U_1 + U_2T + U_3T^2 + \frac{U_4}{(T-263)} , \tag{13}$$

are shown in Figure 9. The coefficients of Equation (13) are given in Table 4. The values of $\overline{C}_{p_2}^{\circ}$ were fixed by this equation for the rest of the calculations.

Values of ${}^{\phi}C_p - \overline{C}_{p_2}^{\circ}$ at all temperatures, including literature data at 25°C,[19-20] were then fit simultaneously in a linear least squares routine to determine the optimum temperature dependent equations for $\beta_{T^2}^{(0)}$, $\beta_{T^2}^{(1)}$, and $C_{T^2}^{\phi}$. The equations are listed below, while the parameters, U, are given in Table 4:

$$\beta_{T^2}^{(0)}(T) = 6U_5 + \frac{2U_6}{T} + \frac{U_7}{T^2} + \frac{526U_8}{T(T-263)^3} \tag{14}$$

$$\beta_{T^2}^{(1)}(T) = 6U_9 + \frac{2U_{10}}{T} + \frac{U_{11}}{T^2} + \frac{526U_{12}}{T(T-263)^3} + \frac{1360U_{13}}{T(680-T)^3} \tag{15}$$

Figure 9. Comparison of values of the apparent molal heat capacity at infinite dilution. The solid line represents values obtained from the parameters listed in Table 4. Squares represent the data of Gardner, Jekel, and Cobble,[19] and dots represent values obtained in this study.

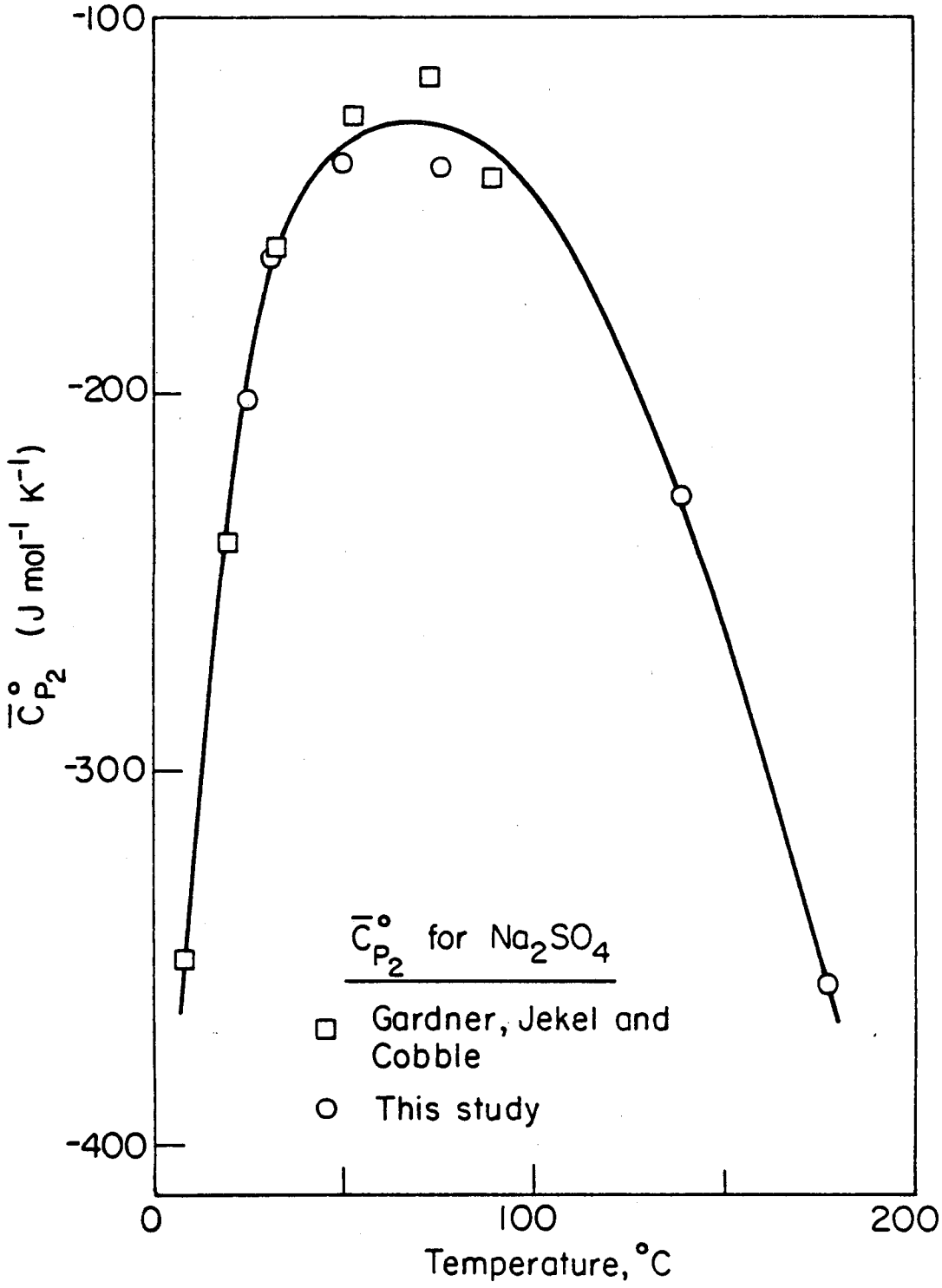
-100
-200
-300
-400
$\bar{C}^{\circ}_{P_2}$ (J mol^{-1} K^{-1})
0
100
200
Temperature, °C
$\bar{C}^{\circ}_{P_2}$ for Na_2SO_4
Gardner, Jekel and Cobble
This study

XBL 812-5174

$$C^{\phi}_{T^2}(T) = \frac{2U_{14}}{T} + \frac{526U_{15}}{T(T-263)^3} . \tag{16}$$

The factors $(T-263)^{-3}$ and $(680-T)^{-3}$ were chosen for convenience as factors which vary rapidly at low and high temperatures, respectively. The values of 263 and 680 have no theoretical significance.

The temperature dependent equations reproduce the heat capacity data below 1 molal to $\pm$ 2 x 10^{-3} Jg^{-1} K^{-1} which is in good agreement with the estimated precision of the data. Between 1 and 1.5 molal, the fit reproduces the data to $\pm$ 3 x 10^{-3} Jg^{-1} K^{-1}. Only data below 1.5 molal were included in the least squares fitting routine, so calculation of heat capacity values from Equations (8) and (14)-(16) should be limited to concentrations below that value.

3. Prediction of the Enthalpy, Activity, and Osmotic Coefficient

To obtain predicted values of the apparent molal enthalpy, osmotic coefficient, and mean activity coefficient, Equations (14)-(16) must be integrated as a function of temperature. The temperature dependent equations for the apparent molal enthalpy are given below:

$$\begin{aligned} \beta_T^{(0)}(T) &= \left(\frac{T_r}{T}\right)^2 \beta_T^{(0)}(T_r) + 1/T^2 \int_{T_r}^{T} T^2 \, \beta_{T^2}^{(0)}(T)\, dT \\ &= \frac{T_r}{T}^{\,2} \beta_T^{(0)}(T_t) + 2U_5\left(T - \frac{T_r^{\,3}}{T^2}\right) + U_6\left(1 - \frac{T_r^{\,2}}{T^2}\right) + U_7\left(\frac{1}{T} - \frac{T_r}{T^2}\right) \\ &\quad - U_8\left(\frac{1}{(T-263)^2} - \frac{T_r^{\,2}}{T^2(T_r-263)^2}\right) \end{aligned} \tag{17}$$

$$\beta_T^{(1)}(T) = \left(\frac{T_r}{T}\right)^2 \beta_T^{(1)}(T_r) + 2U_9\left(T - \frac{T_r^3}{T^2}\right) + U_{10}\left(1 - \frac{T_r^2}{T^2}\right) + U_{11}\left(\frac{1}{T} - \frac{T_r}{T^2}\right)$$
$$- U_{12}\left(\frac{1}{(T-263)^2} - \frac{T_r^2}{T^2(Tr-263)^2}\right) + U_{13}\left(\frac{1}{(680-T)^2} - \frac{T_r^2}{T^2(680-T_r)^2}\right) \quad (18)$$

$$C_T^{\phi}(T) = \left(\frac{T_r}{T}\right)^2 C_T^{\phi}(T_r) + U_{14}\left(1 - \frac{T_r^2}{T^2}\right) - U_{15}\left(\frac{1}{(T-263)^2} - \frac{T_r^2}{T^2(T_r-263)^2}\right) \quad (19)$$

For convenience, the reference temperature, T_r, has been set at 298.15 K. The three integration constants $\beta_T^{(0)}(T_r)$, $\beta_T^{(1)}(T_r)$, and $C_T^{\phi}(T_r)$, can be evaluated by fitting literature data, available at 25°C,[21-23] with Equation (9). The values of the integration constants are listed in Table 4. They differ slightly from the values determined previously by Silvester and Pitzer[24] only because the value of the Debye-Hückel slope, A_H, has been improved.[18]

Prediction of the temperature dependence of the osmotic and activity coefficients requires one more integration, and the resulting equations are listed below:

$$\beta^{(0)}(T) = \beta^{(0)}(T_r) + \int_{T_r}^{T} \beta_T^{(0)}(T)\, dT$$
$$= \beta^{(0)}(T_r) + \beta_T^{(0)}(T_r)\left(T_r - \frac{T_r^2}{T}\right) + U_5\left(T^2 + \frac{2T_r^3}{T} - 3T_r^2\right)$$
$$+ U_6\left(T + \frac{T_r^2}{T} - 2T_r\right) + U_7\left(\ln(T/T_r) + \frac{T_r}{T} - 1\right) \quad (20)$$
$$+ U_8\left(\frac{1}{(T-263)} + \frac{263T-T_r^2}{T(T_r-263)^2}\right)$$

Table 4

Values of the Fitting Parameters for the Heat Capacity of Na_2SO_4 as a Function of Temperature

Integration Constants at T_r = 298.15 K:

$\beta^{(0)}(T_r) = .01958$	$\beta_T^{(0)}(T_r) = .002349$
$\beta^{(1)}(T_r) = 1.113$	$\beta_T^{(1)}(T_r) = .005958$
$C^{\phi}(T_r) = .0057$	$C^{\phi}{}_T(T_r) = -.000479$

Parameters for $\overline{C}_{p_2}{}^{\circ}$

$U_1 = -990.405$

$U_2 = 6.79636$

$U_3 = -.0117779$

$U_4 = -6518.67$

Parameters for Equations (14)-(16):

Fit of Heat Capacity Data Alone	Fit of Heat Capacity and Osmotic Coefficient Data
$U_5 = -6.50891 \times 10^{-6}$	$U_5 = -1.47668 \times 10^{-5}$
$U_6 = 2.26427 \times 10^{-2}$	$U_6 = 4.06323 \times 10^{-2}$
$U_7 = -1.12595 \times 10^{1}$	$U_7 = -1.86055 \times 10^{1}$
$U_8 = -8.80379 \times 10^{-1}$	$U_8 = -5.50520 \times 10^{-1}$
$U_9 = -3.62922 \times 10^{-4}$	$U_9 = -2.86519 \times 10^{-4}$
$U_{10} = 6.57403 \times 10^{-1}$	$U_{10} = 4.88447 \times 10^{-1}$
$U_{11} = -2.19053 \times 10^{2}$	$U_{11} = -1.53799 \times 10^{2}$
$U_{12} = 6.29678 \times 10^{-1}$	$U_{12} = -9.26819 \times 10^{-1}$
$U_{13} = 1.4908 \times 10^{3}$	$U_{13} = 1.46060 \times 10^{3}$
$U_{14} = -6.91609 \times 10^{-4}$	$U_{14} = 8.95033 \times 10^{-5}$
$U_{15} = 4.74519 \times 10^{-1}$	$U_{15} = 3.16960 \times 10^{-1}$

$$\beta^{(1)}(T) = \beta^{(1)}(T_r) + \beta_T^{(1)}(T_r)\left(T_r - \frac{T_r^2}{T}\right) + U_9\left(T^2 + \frac{2T_r^3}{T} - 3T_r^2\right)$$

$$+ U_{10}\left(T + \frac{T_r^2}{T} - 2T_r\right) + U_{11}\left(\ln(T/T_r) + \frac{T_r}{T} - 1\right) \tag{21}$$

$$+ U_{12}\left(\frac{1}{(T-263)} + \frac{263T - T_r^2}{T(T_r-263)^2}\right) + U_{13}\left(\frac{1}{(680-T)} + \frac{T_r^2 - 680T}{T(680-T_r)^2}\right)$$

$$C^{\phi}(T) = C^{\phi}(T_r) + C_T^{\phi}(T_r)\left(T_r - \frac{T_r^2}{T}\right) + U_{14}\left(T + \frac{T_r^2}{T} - 2T_r\right)$$

$$+ U_{15}\left(\frac{1}{(T-263)} + \frac{263T - T_r^2}{T(T_r-263)^2}\right). \tag{22}$$

The values of the integration constants $\beta^{(0)}(T_r)$, $\beta^{(1)}(T_r)$, and $C^{\phi}(T_r)$ at 25°C have been evaluated previously from isopiestic data.[13,15]

4. Comparison with Literature Data

Osmotic coefficients over a range of concentrations and temperatures have been calculated using Equations (10) and (20)-(22). The values obtained from this fit of the heat capacity data alone are compared with literature data[26-31] from 45°C to 120°C in Figure 10, where the osmotic coefficients predicted from this fit are shown by the solid line at low concentrations progressing to the dashed line at high concentrations. Below 100°C, the agreement of data and prediction is excellent, even to concentrations above the 1.5 molal range of the fitting equation. Since the parameters chosen as the integration constants reproduce the osmotic coefficient to high concentrations, this agreement above 1.5 m, at low temperatures, is not too surprising.

Above 100°C, the predicted values trail off at 1.5 m. The reason for this behavior is straightforward. The three fitting parameters of

Figure 10. Comparison of predicted values of the osmotic coefficient with Literature Data. Osmotic coefficients have been calculated from published isopiestic ratios[26-30] referenced to NaCl solutions using the tabulated values of ϕ_{NaCl} given by Pitzer, et al.[17]

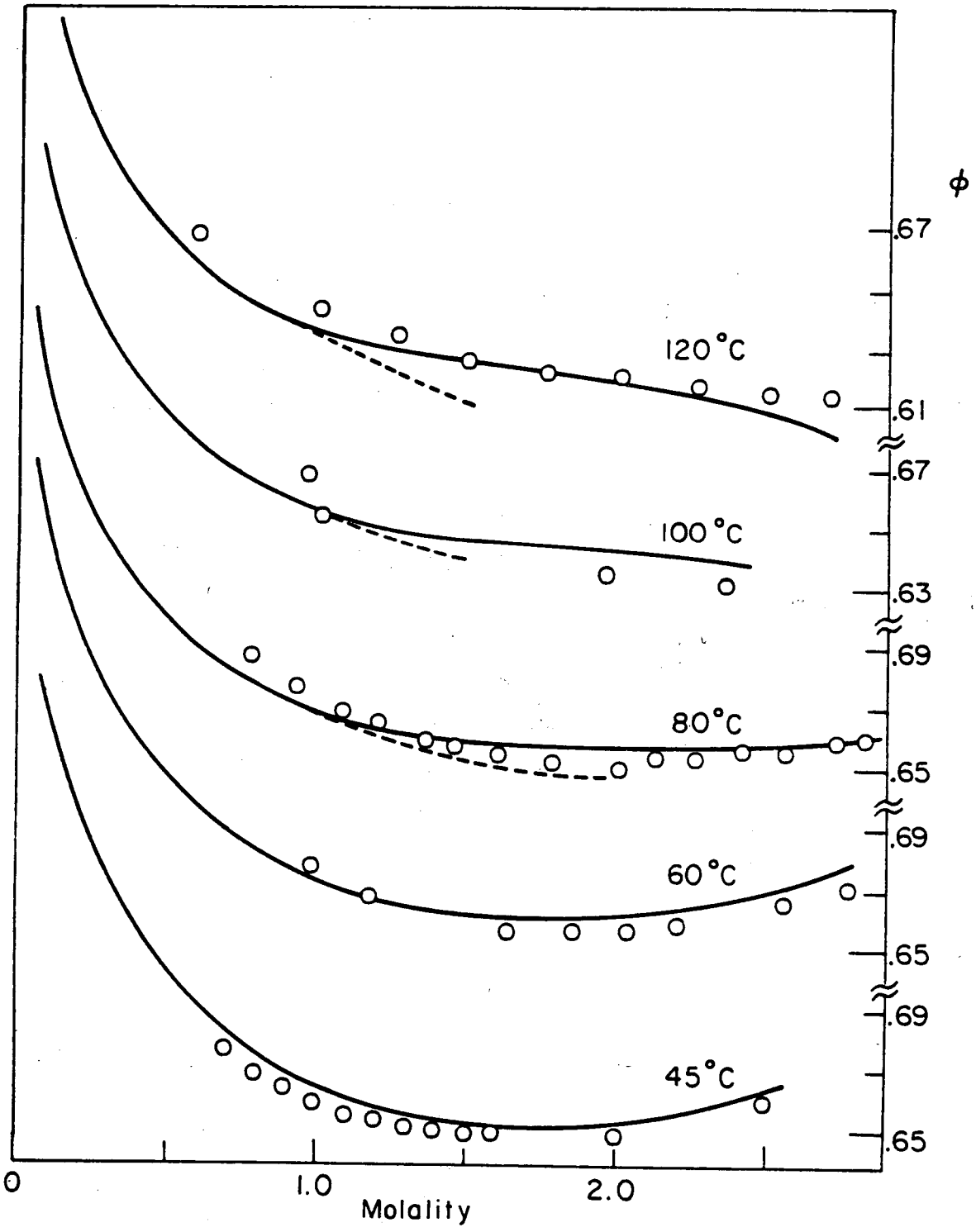
φ
.67
.61
.67
.63
.69
.65
.69
.65
.69
.65
120 °C
100 °C
80 °C
60 °C
45 °C
0
1.0
2.0
Molality

XBL 812-5175

Equation (10) are each important at different concentration ranges. $\beta^{(0)}_{T^2}$ and $\beta^{(1)}_{T^2}$ both account for the effects of short range forces between ions two at a time as well as for longer range forces due to various electrostatic effects. $\beta^{(1)}_{T^2}$ is most important at low concentrations because of its exponentially decaying dependence on the ionic strength, while $\beta^{(0)}_{T^2}$ is important over a wide range of concentration. $C^{\phi}_{T^2}$ describes interactions of ions three at a time, and is most important at high concentrations because of its m^2 concentration dependence. $C^{\phi}_{T^2}$ can not be determined well from the heat capacity measurements, because of the limited concentration range of the data. For this reason, the temperature dependence of C^{ϕ} is not quite correct, and the differences between predicted values of the osmotic coefficient and literature data become larger the higher the temperature.

This situation could be improved by using heat capacity data at higher concentrations in the fitting routine. However, it is very difficult to obtain higher concentration data with the present technique because of the limited solubility of sodium sulfate at room temperature. Another way to improve the fitting equation is to include the osmotic coefficient data in the least squares fitting routine, and redetermine the fit parameters U_5 through U_{15}. This second method has been adopted, and the solid lines in Figure 10 show the osmotic coefficient values calculated from the combined fit of heat capacity and osmotic coefficient data. The temperature parameters determined from the combined fit are listed in the second column of Table 4.

Below 120°C, the combined fit reproduces the osmotic coefficient data to $\pm$ 2%, up to concentrations of 2.5 molal. The uncertainty in calculated values of the apparent molal enthalpy is also estimated to be less than 2% at concentrations up to 2.0 m. However, above 120°C

use of Equations (8)-(22) to calculate the various thermodynamic properties should still be limited to concentrations below 1.5 m, because only the heat capacity data have been used to determine the fit parameters in this region. In addition, some difficulty was encountered in reproducing the heat capacity data near 1.5 m, and this difficulty was not resolved by adding the osmotic coefficient data to the fitting routine. For this reason, the equations presented here should be used to calculate heat capacities only below 1.5 m.

Additional comparisons of thermodynamic properties calculated with the fitting equations and literature data are shown in Figures 11-13. High temperature values of the osmotic coefficient are in substantial agreement with the data of Liu and Lindsay,[32] as illustrated in Figure 11. Figure 12 shows that the predicted values of the apparent molal enthalpy are in general agreement with the data of Snipes, Manly, and Ensor[33] between 40°C and 80°C, although the difference between calculated and experimental values is in some cases as large as 8% of the calculated value. At high temperatures, predictions of the apparent molal enthalpy are in good agreement with values reported by Mayrath[34] at low concentrations. At concentrations between .5 m and 1.0 m, the values of Mayrath[34] are substantially smaller than those obtained in the present study, as shown in Figure 13.

Some literature sources contained data that were not totally consistent with the heat capacity and osmotic coefficient data chosen for this study. High temperature osmotic coefficients obtained from the isopiestic data of Soldano and co-workers[35-36] are substantially larger than those predicted from the fit of the heat capacity data. Heat of dilution data at 50°C reported by Gritsus, Akhumov, and Zhilina[37] also

Figure 11. Comparison of osmotic coefficients for Na_2SO_4 solutions. Solid lines represent osmotic coefficients predicted from the combined fit of heat capacity and osmotic coefficient data. Points are the data of Liu and Lindsay,[32] which were not included in the combined fit.

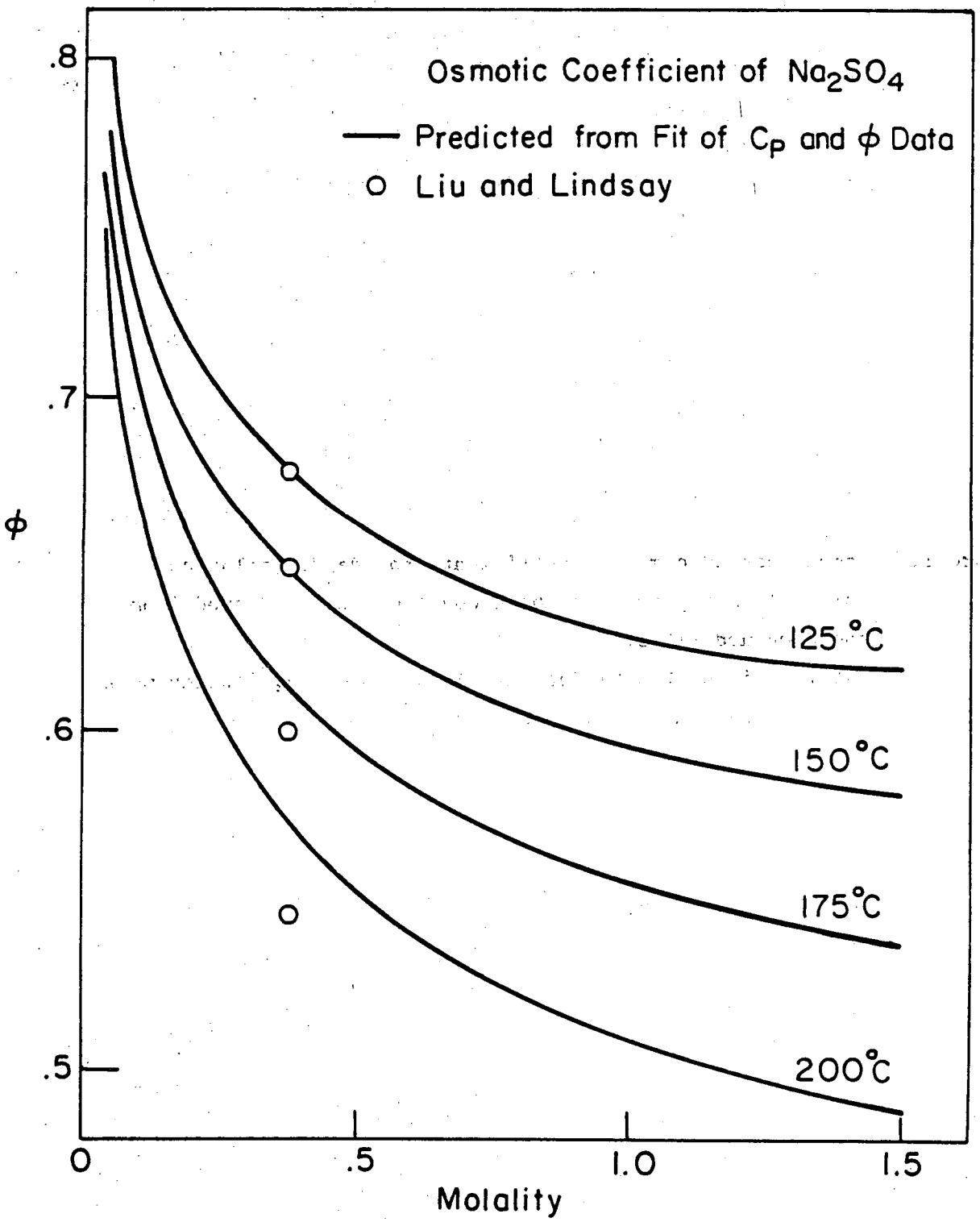
Osmotic Coefficient of Na_2SO_4
Predicted from Fit of C_p and ϕ Data
Liu and Lindsay
.8
.7
.6
.5
ϕ
125 °C
150 °C
175 °C
200 °C
0
.5
1.0
1.5
Molality

XBL 812-5216

Figure 12. Comparison of values of the apparent molal enthalpy. Solid lines represent values predicted from the combined fit of heat capacity and osmotic coefficient data. Points are the data of Snipes, Manly, and Ensor.[33]

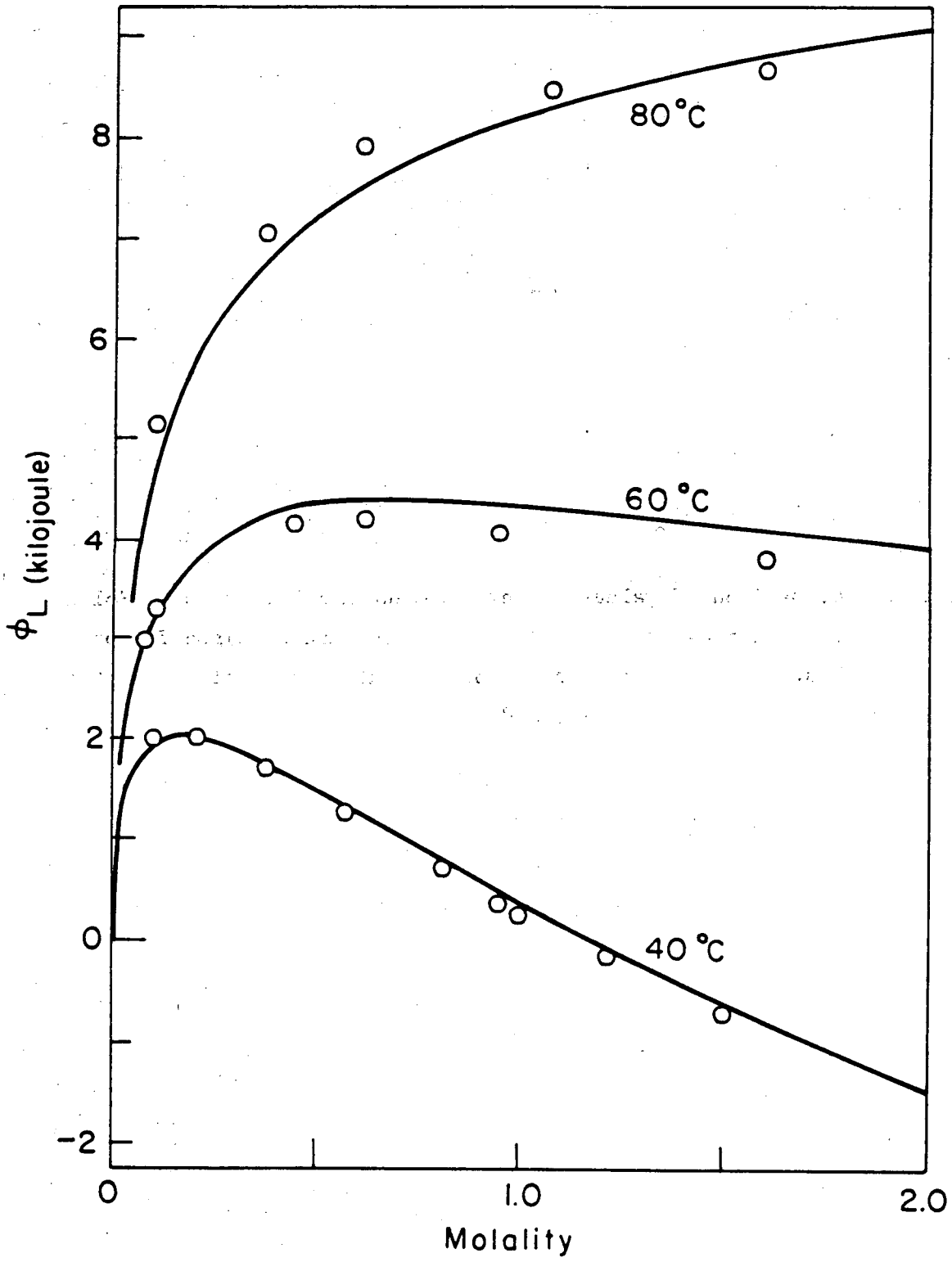

XBL 812-5190

Figure 13. Comparison of apparent molal enthalpies at high temperatures. Solid lines represent values predicted from the combined fit of heat capacity and osmotic coefficient data. Points are the values reported by Mayrath.[34]

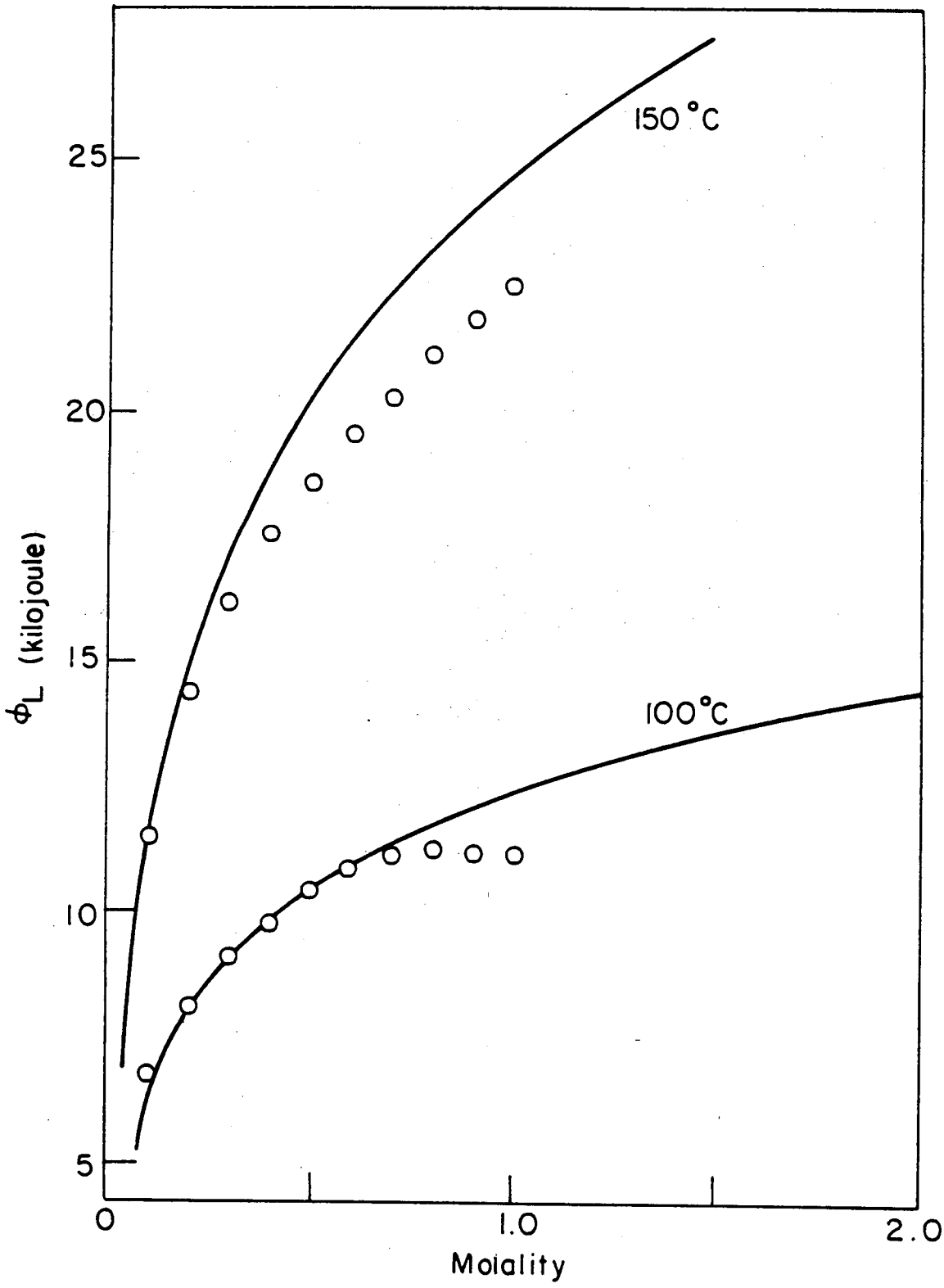

XBL 812-5191

are not in agreement with the predicted values. Harned and Hecker[38] have reported values for the activity coefficient of sodium chloride from 0°C to 40°C, based on emf measurements. The temperature dependence of the activity coefficient from 25°C to 40°C is in reasonable agreement with that obtained in this study, although the Harned and Hecker values for the activity coefficient at 25°C differ from those used in this study. Osmotic coefficients calculated from the vapor pressure difference measurements of Fabuss and Korosi[39] behave erratically at low concentrations, indicating that the precision of the measurements is not sufficient to provide a test of the osmotic coefficient predictions.

Calculated values of the activity and osmotic coefficients, the apparent molal enthalpy, the apparent molal heat capacity, and the specific heat capacity are given in Tables 5-9. The concentration dependence of the mean activity coefficient, at various temperatures, is shown in Figure 14.

The temperature dependences of the parameters, as determined from the combined fit, are shown in Figures 15-17. While the magnitudes of $\beta^{(0)}$, $\beta^{(1)}$, and C^{ϕ} for Na_2SO_4 are smaller than those for NaCl,[16,17] the temperature dependences of the parameters for the two salts are similar. If substantial ion-pairing were occurring at high temperatures, one would expect $\beta^{(1)}$, and to a lesser extent $\beta^{(0)}$, to become smaller with increasing temperature. For Na_2SO_4, only C^{ϕ} shows this behavior, indicating that triple ion interactions are increasing with increasing temperature. Apparently, the electrostatic effects of the decrease in the dielectric constant of water with increasing temperature are well accounted for in the Debye-Hückel term. The remaining short range

Table 5

MEAN ACTIVITY COEFFICIENT OF AQUEOUS SODIUM SULFATE SOLUTIONS

T (°C)	P (BAR)	D-H SLOPE	MOLALITY .050	.100	.250	.500	.750	1.00	1.25	1.50	1.75	2.00	2.25	2.50
25.	1.0	3.91E-01	.536	.454	.348	.273	.232	.206	.188	.175	.165	.158	.152	.148
30.	1.0	3.95E-01	.535	.453	.349	.274	.234	.209	.191	.178	.168	.161	.155	.151
40.	1.0	4.02E-01	.531	.450	.347	.275	.236	.212	.194	.182	.172	.165	.159	.155
50.	1.0	4.10E-01	.526	.446	.344	.273	.236	.212	.195	.183	.174	.166	.160	.156
60.	1.0	4.19E-01	.520	.440	.339	.269	.233	.210	.194	.182	.172	.165	.159	.154
70.	1.0	4.28E-01	.513	.433	.333	.264	.229	.206	.190	.178	.169	.162	.156	.151
80.	1.0	4.38E-01	.505	.424	.325	.258	.223	.200	.185	.173	.164	.157	.151	.146
90.	1.0	4.49E-01	.496	.416	.316	.250	.215	.194	.179	.167	.158	.151	.145	.139
100.	1.0	4.61E-01	.487	.406	.307	.241	.207	.186	.171	.160	.151	.144	.138	.132
110.	1.4	4.73E-01	.477	.396	.297	.232	.198	.178	.163	.152	.143	.136	.130	.124
120.	2.0	4.86E-01	.467	.385	.286	.221	.189	.169	.154	.144	.135	.128	.122	.116
130.	2.7	4.99E-01	.456	.373	.275	.211	.179	.159	.145	.135				
140.	3.6	5.14E-01	.445	.361	.263	.200	.169	.149	.136	.126				
150.	4.8	5.30E-01	.433	.349	.251	.189	.159	.140	.127	.117				
160.	6.2	5.46E-01	.421	.336	.239	.178	.148	.130	.117	.108				
170.	7.9	5.63E-01	.408	.323	.226	.167	.138	.120	.108	.099				
180.	10.0	5.82E-01	.395	.310	.214	.156	.128	.111	.099	.090				
190.	12.5	6.02E-01	.382	.297	.202	.145	.118	.102	.091	.082				
200.	15.5	6.23E-01	.369	.284	.190	.134	.108	.093	.082	.074				

Table 6

OSMOTIC COEFFICIENT OF AQUEOUS SODIUM SULFATE SOLUTIONS

T (°C)	P (BAR)	D-H SLOPE	MOLALITY .050	.100	.250	.500	.750	1.00	1.25	1.50	1.75	2.00	2.25	2.50
25.	1.0	3.91E-01	.829	.794	.740	.692	.662	.643	.632	.627	.627	.631	.638	.648
30.	1.0	3.95E-01	.828	.794	.743	.696	.668	.651	.641	.636	.636	.639	.646	.654
40.	1.0	4.02E-01	.827	.794	.745	.702	.677	.662	.654	.650	.650	.653	.658	.664
50.	1.0	4.10E-01	.825	.792	.745	.705	.682	.669	.662	.659	.659	.661	.665	.669
60.	1.0	4.19E-01	.822	.789	.743	.705	.684	.672	.665	.663	.663	.664	.667	.670
70.	1.0	4.28E-01	.819	.786	.740	.703	.683	.671	.666	.663	.663	.663	.665	.666
80.	1.0	4.38E-01	.815	.781	.735	.699	.679	.668	.663	.660	.659	.659	.659	.659
90.	1.0	4.49E-01	.810	.776	.730	.693	.674	.663	.657	.654	.653	.652	.651	.649
100.	1.0	4.61E-01	.805	.770	.723	.686	.667	.656	.650	.647	.644	.643	.640	.636
110.	1.4	4.73E-01	.799	.763	.715	.677	.658	.647	.641	.637	.634	.631	.627	.622
120.	2.0	4.86E-01	.793	.756	.706	.667	.648	.637	.630	.626	.622	.618	.613	.607
130.	2.7	4.99E-01	.786	.747	.696	.656	.636	.625	.618	.613				
140.	3.6	5.14E-01	.779	.739	.685	.644	.623	.612	.604	.599				
150.	4.8	5.30E-01	.771	.729	.673	.631	.610	.597	.589	.583				
160.	6.2	5.46E-01	.763	.719	.660	.617	.595	.582	.573	.567				
170.	7.9	5.63E-01	.754	.708	.647	.602	.579	.565	.556	.549				
180.	10.0	5.82E-01	.745	.697	.633	.586	.561	.547	.538	.530				
190.	12.5	6.02E-01	.735	.685	.618	.569	.543	.528	.518	.510				
200.	15.5	6.23E-01	.725	.673	.602	.551	.524	.508	.497	.489				

Table 7

APPARENT MOLAL ENTHALPY OF AQUEOUS SODIUM SULFATE SOLUTIONS (KJOULE/MOL)

T (°C)	P (BAR)	D-H SLOPE	MOLALITY .001	.005	.010	.050	.100	.250	.500	.750	1.000	1.250	1.500
25.	1.0	1.98E+03	.29	.57	.73	1.01	.94	.35	-.80	-1.89	-2.89	-3.79	-4.60
30.	1.0	2.15E+03	.32	.64	.82	1.24	1.28	.90	.01	-.88	-1.72	-2.50	-3.19
40.	1.0	2.51E+03	.38	.77	1.02	1.69	1.93	1.94	1.51	.96	.40	-.13	-.61
50.	1.0	2.90E+03	.45	.92	1.22	2.15	2.57	2.96	2.93	2.69	2.39	2.09	1.81
60.	1.0	3.33E+03	.52	1.07	1.44	2.63	3.24	3.98	4.34	4.39	4.33	4.24	4.14
70.	1.0	3.80E+03	.59	1.24	1.68	3.14	3.94	5.04	5.77	6.10	6.26	6.37	6.44
80.	1.0	4.31E+03	.67	1.42	1.93	3.68	4.68	6.14	7.25	7.84	8.23	8.51	8.75
90.	1.0	4.86E+03	.76	1.62	2.20	4.26	5.47	7.31	8.79	9.65	10.25	10.71	11.10
100.	1.0	5.47E+03	.86	1.83	2.50	4.88	6.31	8.55	10.42	11.54	12.34	12.98	13.53
110.	1.4	6.14E+03	.97	2.07	2.83	5.56	7.23	9.87	12.14	13.53	14.54	15.35	16.04
120.	2.0	6.87E+03	1.09	2.32	3.18	6.29	8.21	11.29	13.97	15.64	16.86	17.84	18.67
130.	2.7	7.68E+03	1.22	2.60	3.57	7.09	9.27	12.81	15.92	17.87	19.31	20.47	21.45
140.	3.6	8.56E+03	1.36	2.91	3.99	7.95	10.42	14.44	18.00	20.25	21.92	23.25	24.38
150.	4.8	9.54E+03	1.51	3.24	4.45	8.88	11.66	16.19	20.22	22.78	24.68	26.20	27.48
160.	6.2	1.06E+04	1.68	3.61	4.96	9.90	12.99	18.05	22.58	25.47	27.62	29.34	30.78
170.	7.9	1.18E+04	1.88	4.02	5.51	10.99	14.42	20.05	25.09	28.33	30.73	32.66	34.28
180.	10.0	1.32E+04	2.09	4.47	6.13	12.18	15.96	22.16	27.75	31.34	34.02	36.18	37.99
190.	12.5	1.47E+04	2.32	4.97	6.80	13.46	17.60	24.40	30.54	34.51	37.49	39.89	41.90
200.	15.5	1.64E+04	2.59	5.52	7.54	14.85	19.37	26.75	33.46	37.83	41.12	43.78	46.03

Table 8

APPARENT MOLAL HEAT CAPACITY OF AQUEOUS SODIUM SULFATE SOLUTIONS (JOULE/ MOL DEG)

T (°C)	P (BAR)	D-H SLOPE	$\bar{C}^{\circ}_{p_2}$	MOLALITY .050	.100	.250	.500	.750	1.000	1.250	1.500
25.	1.0	3.28E+01	-196.5	-150.1	-127.9	-81.5	-27.5	13.7	47.0	74.4	96.8
30.	1.0	3.43E+01	-174.8	-129.6	-109.1	-66.9	-18.5	18.6	49.2	75.0	96.9
40.	1.0	3.75E+01	-147.1	-101.9	-82.9	-45.1	-2.6	29.8	56.8	80.2	100.7
50.	1.0	4.09E+01	-132.5	-85.8	-67.1	-31.0	8.5	38.2	63.0	84.6	103.7
60.	1.0	4.46E+01	-126.3	-77.2	-58.3	-22.7	15.3	43.4	66.6	86.7	104.6
70.	1.0	4.87E+01	-126.4	-74.2	-54.7	-18.7	18.7	45.8	67.9	86.9	103.6
80.	1.0	5.32E+01	-131.5	-75.5	-55.1	-18.2	19.2	45.8	67.2	85.3	101.2
90.	1.0	5.82E+01	-140.6	-80.4	-58.9	-20.5	17.5	43.9	64.9	82.4	97.6
100.	1.0	6.37E+01	-153.5	-88.4	-65.5	-25.4	13.6	40.3	61.1	78.3	93.0
110.	1.4	6.99E+01	-169.7	-99.2	-74.9	-32.6	7.9	35.1	56.0	73.1	87.6
120.	2.0	7.68E+01	-189.0	-112.6	-86.6	-42.0	.2	28.3	49.6	66.9	81.3
130.	2.7	8.46E+01	-211.2	-128.3	-100.7	-53.5	-9.3	19.9	41.9	59.6	74.3
140.	3.6	9.34E+01	-236.3	-146.4	-116.9	-67.0	-20.6	9.8	32.8	51.1	66.3
150.	4.8	1.03E+02	-264.1	-166.5	-135.3	-82.7	-34.0	-2.0	22.1	41.4	57.3
160.	6.2	1.15E+02	-294.6	-188.7	-155.7	-100.6	-49.5	-15.8	9.7	30.1	47.1
170.	7.9	1.29E+02	-327.7	-212.8	-178.1	-120.8	-67.4	-31.8	-4.7	17.2	35.5
180.	10.0	1.44E+02	-363.4	-238.6	-202.5	-143.3	-87.9	-50.3	-21.4	2.3	22.2
190.	12.5	1.63E+02	-401.7	-266.1	-228.7	-168.4	-111.3	-71.8	-40.7	-15.0	6.9
200.	15.5	1.86E+02	-442.5	-294.9	-256.8	-196.2	-138.0	-96.5	-63.1	-35.0	-10.7

Table 9

SPECIFIC HEAT CAPACITY OF AQUEOUS SODIUM SULFATE SOLUTIONS (JOULE/G DEG)

T (°C)	P (BAR)	D-H SLOPE	CP WATER	MOLALITY .050	.100	.250	.500	.750	1.000	1.250	1.500
25.	1.0	3.28E+01	4.179	4.142	4.108	4.016	3.889	3.786	3.701	3.628	3.565
30.	1.0	3.43E+01	4.178	4.142	4.109	4.019	3.893	3.789	3.702	3.628	3.564
40.	1.0	3.75E+01	4.178	4.144	4.112	4.024	3.900	3.796	3.708	3.633	3.569
50.	1.0	4.09E+01	4.180	4.147	4.115	4.030	3.907	3.804	3.716	3.640	3.574
60.	1.0	4.46E+01	4.184	4.151	4.120	4.035	3.914	3.811	3.722	3.645	3.579
70.	1.0	4.87E+01	4.189	4.156	4.125	4.041	3.920	3.817	3.728	3.650	3.582
80.	1.0	5.32E+01	4.196	4.163	4.132	4.048	3.927	3.823	3.733	3.654	3.584
90.	1.0	5.82E+01	4.205	4.171	4.140	4.056	3.934	3.830	3.739	3.658	3.587
100.	1.0	6.37E+01	4.217	4.183	4.152	4.066	3.944	3.838	3.746	3.664	3.591
110.	1.4	6.99E+01	4.232	4.197	4.165	4.079	3.955	3.848	3.755	3.671	3.597
120.	2.0	7.68E+01	4.249	4.213	4.181	4.093	3.967	3.859	3.764	3.679	3.603
130.	2.7	8.46E+01	4.268	4.231	4.198	4.108	3.980	3.870	3.773	3.687	3.610
140.	3.6	9.34E+01	4.288	4.251	4.217	4.125	3.994	3.882	3.784	3.696	3.617
150.	4.8	1.03E+02	4.312	4.273	4.238	4.144	4.010	3.895	3.795	3.706	3.625
160.	6.2	1.15E+02	4.339	4.299	4.262	4.165	4.028	3.910	3.807	3.716	3.635
170.	7.9	1.29E+02	4.369	4.327	4.290	4.190	4.048	3.927	3.821	3.728	3.645
180.	10.0	1.44E+02	4.403	4.360	4.322	4.218	4.070	3.945	3.837	3.742	3.657
190.	12.5	1.63E+02	4.443	4.399	4.358	4.250	4.097	3.967	3.855	3.757	3.671
200.	15.5	1.86E+02	4.489	4.443	4.401	4.288	4.127	3.991	3.875	3.775	3.687

Figure 14. Concentration dependence of the mean activity coefficient of Na_2SO_4.

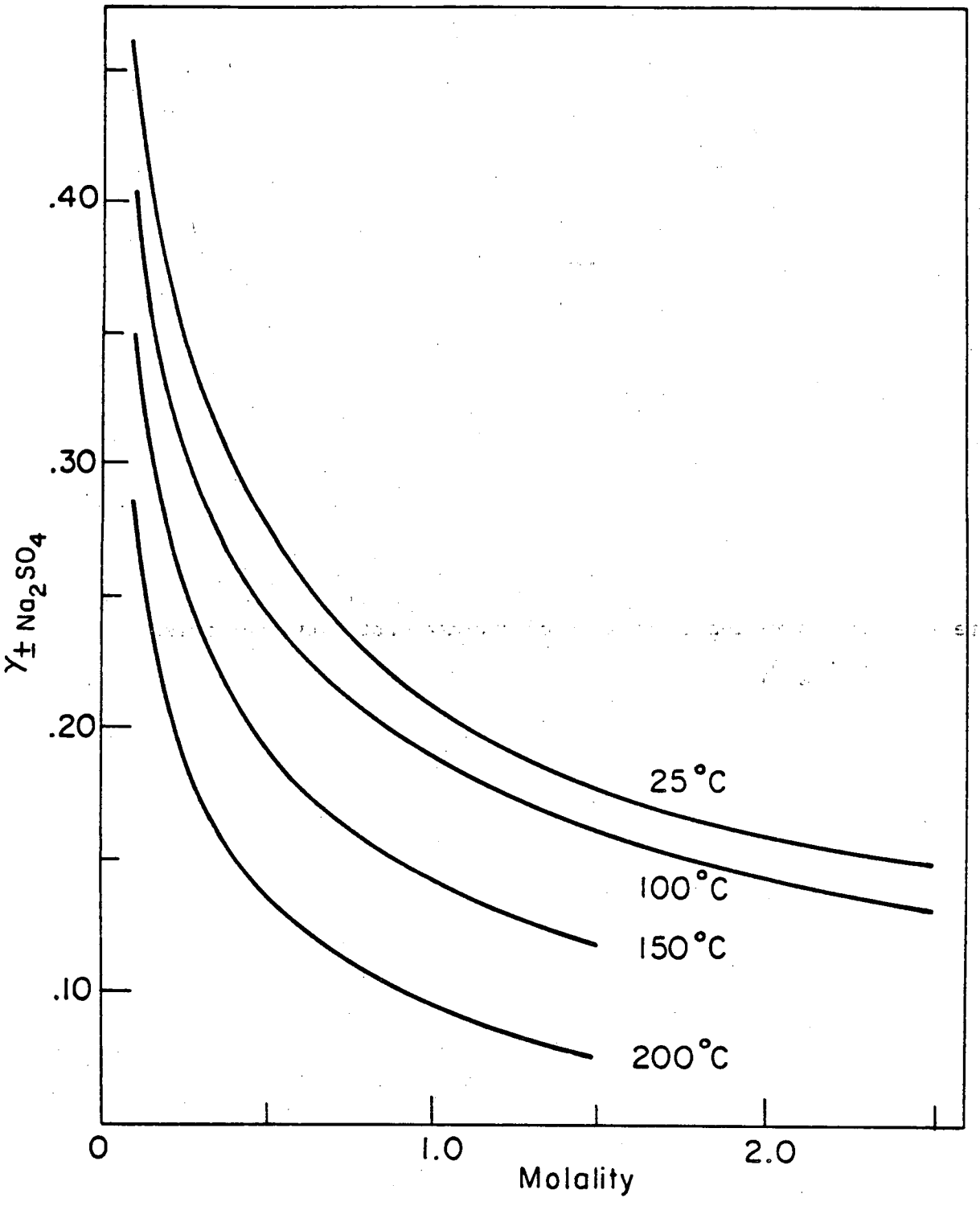

XBL 812-5176

Figure 15. Temperature dependence of the fitting parameters $\beta^{(0)}$, $\beta_T^{(0)}$, and $\beta_{T^2}^{(0)}$.

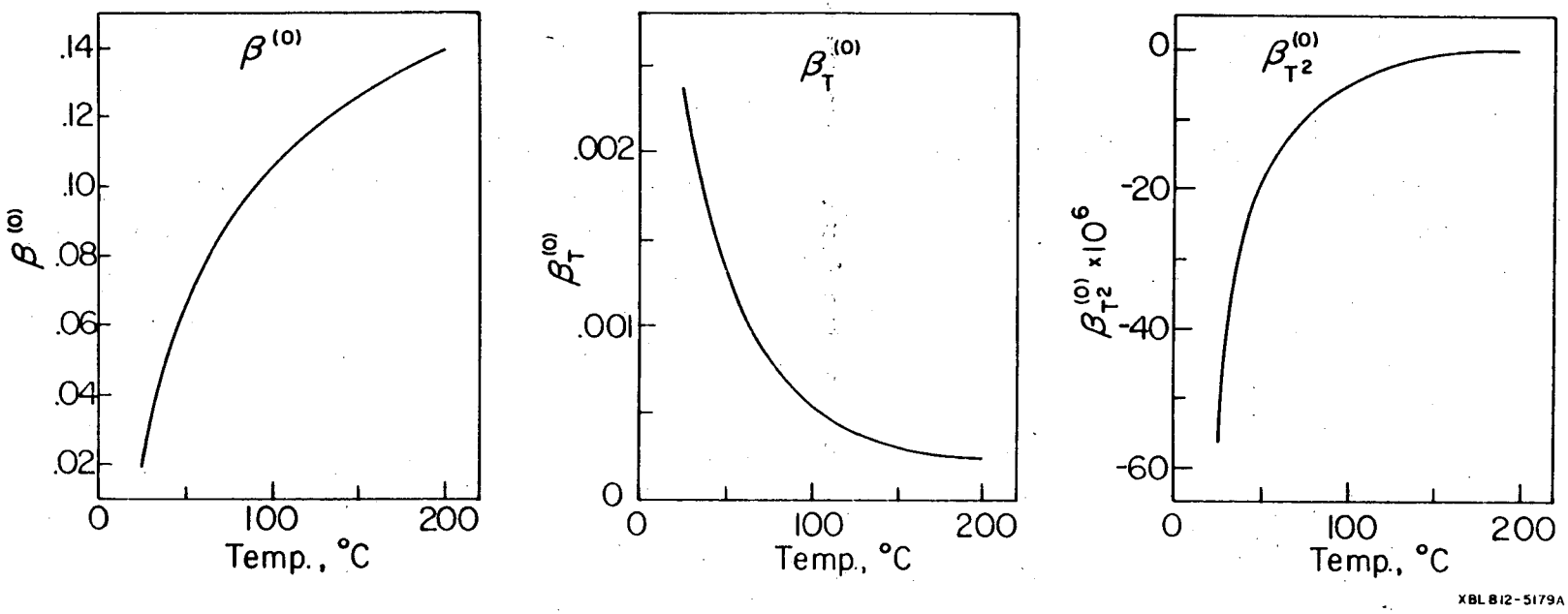
$\beta^{(0)}$
.14
.12
.10
.08
.06
.04
.02
0
100
200
Temp., °C
$\beta_T^{(0)}$
.002
.001
0
0
100
200
Temp., °C
$\beta_{T^2}^{(0)}$
0
-20
-40
-60
$\beta_{T^2}^{(0)} \times 10^6$
0
100
200
Temp., °C
XBL 812-5179A

Figure 16. Temperature dependence of the fitting parameters $\beta^{(1)}$, $\beta_T^{(1)}$, and $\beta_{T^2}^{(1)}$.

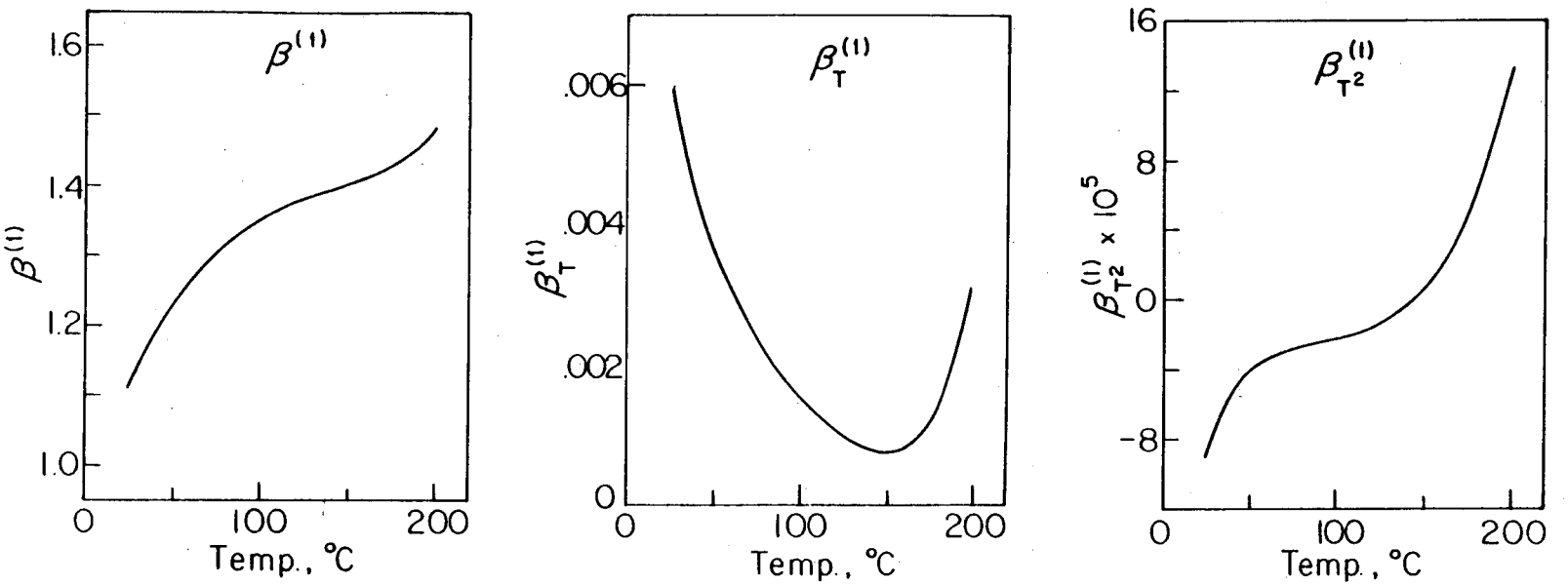

XBL 812-5182A

Figure 17. Temperature dependence of the fitting parameters C^{ϕ}, C^{ϕ}_{T}, and $C^{\phi}_{T^2}$.

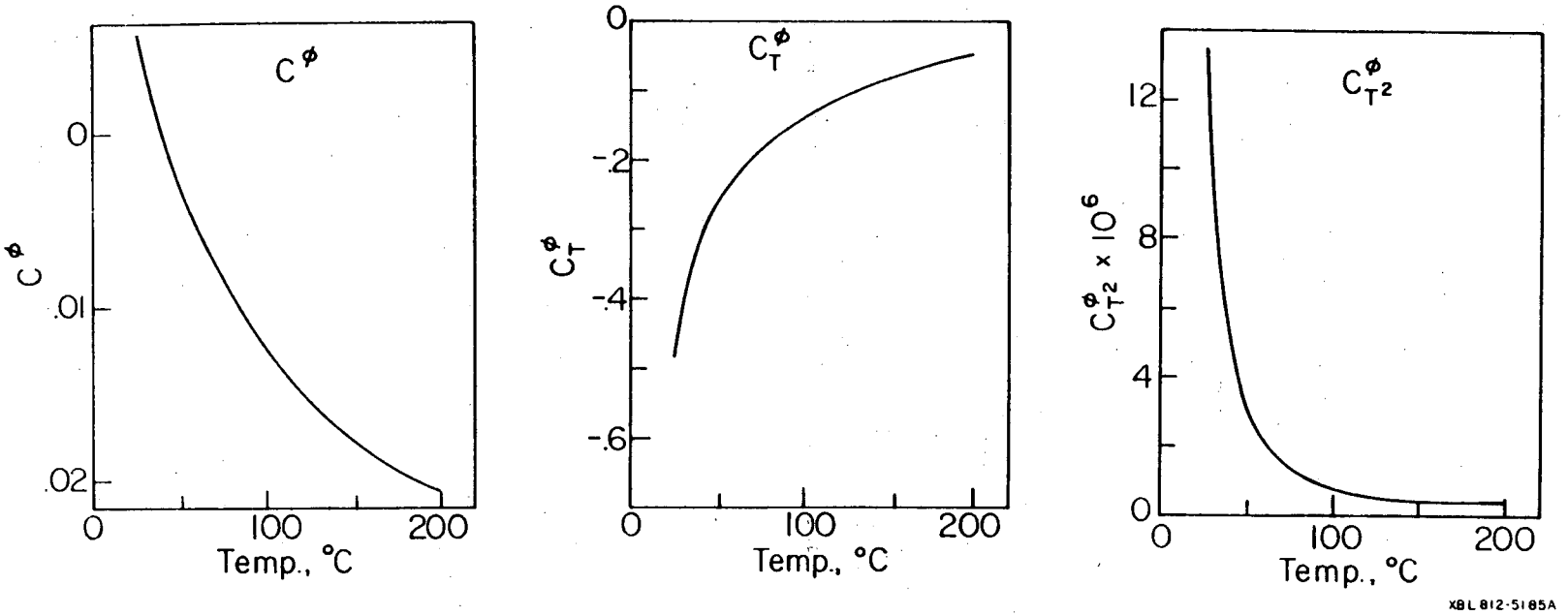
C^{ϕ}
0
.01
.02
0
100
200
Temp., °C
C_T^{ϕ}
0
-.2
-.4
-.6
0
100
200
Temp., °C
$C_{T^2}^{\phi}$
$C_{T^2}^{\phi} \times 10^6$
12
8
4
0
0
100
200
Temp., °C
XBL 812-5185A

interactions between Na^+ and $SO_4^=$ ions, described by $\beta^{(0)}$ and $\beta^{(1)}$, decrease with increasing temperature.

Conclusions

The quality of the heat capacity data obtained in this study and their agreement with literature data indicate that flow calorimetry is a valuable technique for high temperature studies. Indeed, the precision of the present data is five times better than that quoted for the high temperature data in the literature.[2] The successful prediction of osmotic coefficients from a temperature dependent fit of the heat capacity data shows that heat capacity measurements can be used to obtain activity properties of electrolyte solutions at high temperatures.

One drawback to the use of flow calorimetry at high pressures should be mentioned. Reduction of the flow measurements to obtain specific heat capacities requires density data at room temperature and the system pressure. High pressure volumetric data, even at room temperature, are available for only a few electrolyte solutions over a very limited concentration range. In addition, integration of high pressure heat capacity data to obtain activity properties requires enthalpy and activity data at the same pressure to evaluate the integration constants. These are most easily obtained using density and expansivity data, as a function of pressure, to adjust activity and enthalpy data at one bar to the higher pressure. Thus a full treatment of flow calorimetry data requires volumetric properties, as a function of pressure, over a small temperature range. It is hoped that current interest in high pressure flow calorimetry will encourage further work in the determination of these important volumetric properties.

References

1. P. Picker, P.-A. Leduc, P. R. Philip, J. E. Desnoyers, J. Chem. Thermo. 3, 631 (1971).

2. S. Likke and L. A. Bromley, J. Chem. Eng. Data, 18, 189 (1973).

3. H. F. Stimson, Am. J. Phys. 23, 622 (1955).

4. L. Haar, J. Gallagher, and G. S. Kell, Proceedings of the International Association for the Properties of Steam, September (1979).

5. I. V. Olofosson, E. C. Jekel, and J. W. Cobble, J. Phys. Chem. 73, 2017 (1969).

6. G. Perron, J. E. Desnoyers, F. J. Millero, Can. J. Chem. 53, 1134 (1975).

7. R. E. Gibson, J. Phys. Chem. 31, 496 (1927).

8. C.-T. A. Chen, J. H. Chen, and F. J. Millero, J. Chem. Eng. Data, 25, 307 (1980).

9. C.-T. Chen, R. T. Emmet, and F. J. Millero, J. Chem. Eng. Data, 22, 201 (1977).

10. R. E. Gibson, J. Am. Chem. Soc. 56, 4 (1933).

11. D. Smith-Magowan and R. H. Wood, submitted to J. Chem. Thermo.

12. K. S. Pitzer, J. Phys. Chem. 77, 268 (1973).

13. K. S. Pitzer and G. Mayorga, J. Phys. Chem. 77, 2300 (1973).

14. K. S. Pitzer and G. Mayorga, J. Soln. Chem. 3, 539 (1974).

15. K. S. Pitzer and J. J. Kim, J. Am. Chem. Soc. 96, 5701 (1974).

16. L. F. Silvester and K. S. Pitzer, J. Phys. Chem. 8, 1882 (1977).

17. K. S. Pitzer, D. J. Bradley, P. S. Z. Rogers, and J. C. Peiper, Lawrence Berkeley Laboratory Report No. 8973 (1979).

18. D. J. Bradley and K. S. Pitzer, J. Phys. Chem. 83, 1599 (1979).

19. W. L. Gardner, E. C. Jekel, and J. W. Cobble, J. Phys. Chem. 73, 2017 (1969).

20. M. Randall and F. D. Rossini, J. Am. Chem. Soc. 51, 323 (1929).

21. W. E. Wallace and A. L. Robinson, J. Am. Chem. Soc. 63, 958 (1941).

22. E. Lange and H. Streeck, Z. Phys. Chem. Abt. 157, 1 (1931).

23. P. T. Thompson, D. E. Smith, R. H. Wood, J. Chem. Eng. Data, 19, 386 (1974).

24. L. F. Silvester and K. S. Pitzer, J. Soln. Chem. 7, 327 (1978).

25. C. J. Downes and K. S. Pitzer, J. Soln. Chem. 5, 389 (1976).

26. K. L. Hellams, C. S. Patterson, B. H. Prentice, III, and M. J. Taylor, J. Chem. Eng. Data, 4, 323 (1965).

27. W. T. Humphries, C. F. Kohrt, and C. S. Patterson, J. Chem. Eng. Data, 13, 327 (1968).

28. J. T. Moore, W. T. Humphries, and C. S. Patterson, J. Chem. Eng. Data, 17, 180 (1972).

29. C. S. Patterson, L. O. Gilpatrick, and B. A. Soldano, J. Chem. Soc. 2730 (1960).

30. B. A. Soldano and C. S. Patterson, J. Chem. Soc. 937 (1962).

31. Gy. Jakli, T. C. Chan, and W. A. Van Hook, J. Soln. Chem. 4, 71 (1975).

32. C-T Liu and W. T. Lindsay, Office of Saline Water Research and Development Progress Report No. 722, Int-OSW-RDPR-71-722 (1971).

33. H. P. Snipes, C. Manly, and D. D. Ensor, J. Chem. Eng. Data, 20, 287 (1975).

34. J. E. Mayrath, Ph.D. Thesis, University of Delaware, Newark, DE (1980).

35. B. A. Soldano and M. Meek, J. Chem. Soc. 4424 (1963).

36. B. A. Soldano and P. B. Bien, J. Chem. Soc.(A), 1825 (1966).

37. B. V. Gritsus, E. I. Akhumov, and L. P. Zhilina, Zh. Prikl. Khim., 44, 186 (1971).

38. H. S. Harned and J. C. Hecker, J. Chem. Soc. 56, 650 (1934).

39. B. M. Fabuss and A. Korosi, Desalination, 1, 139 (1966).

Chapter 4

SOLUBILITY OF CALCIUM, STRONTIUM, AND BARIUM SULFATES IN SALINE WATERS

Introduction

Many problems in geochemistry and oceanography involve the prediction of mineral solubility in natural brines and seawater. Successful solubility predictions depend on accurate calculation of the activities of ions in these solutions. At least one component of a sparingly soluble salt will necessarily be a minor constituent of a mixed solution. Therefore any model of solution properties used for solubility prediction must describe the activities of minor as well as major constituents.

A number of different models[1-4] have been proposed to calculate activity coefficients, and they are generally successful in predicting the activities of the major components of a mixed electrolyte solution. However, many models fail to predict the activities of minor constituents. The model for electrolyte solution properties developed by Pitzer[5-9] has been used successfully to predict the osmotic coefficient of mixed solutions.[8] In addition, Whitfield[10] has shown that the activity coefficients of the major components in seawater, predicted using Pitzer's equations, are in reasonable agreement with experimental values. However, recent attempts to use this model to predict mineral solubility in seawater have had mixed results. In this chapter, recent data on the solubility of gypsum in common and noncommon ion solutions and in natural seawater have been used to further test the effectiveness of Pitzer's model for solubility prediction.

Literature Review

Two separate studies have concluded that the system of equations developed by Pitzer and Kim[8] to describe mixed electrolyte solutions is not successful in predicting the solubility of $CaSO_4 \cdot 2H_2O$ (gypsum) in seawater. Whitfield[10] found that gypsum solubility in seawater, calculated using the equations of Pitzer and Kim, was 15% lower than the experimental solubility of Marshall and Slusher.[11] Assuming that the discrepancy was due to $CaSO_4^{\circ}$ ion pair formation, he proposed a hybrid approach in which the mean activity coefficient of $CaSO_4$ was calculated through an ion-association equilibrium. His ion-association approach provided a moderate improvement in the solubility calculation at the ionic strength of natural seawater (~.7 m). Culberson, Latham, and Bates[12] measured the solubility of gypsum and celestite ($SrSO_4$) in synthetic seawater. They found that the solubility predicted using the equations of Pitzer and Kim was 25% lower than their experimental results for $CaSO_4 \cdot 2H_2O$, and 18% lower for $SrSO_4$.

Recently, however, Harvie and Weare[13] have successfully reproduced mineral solubility, including gypsum solubility, in a system of the major components of natural waters. They used the mixture equations of Pitzer and Kim, with the addition of terms derived by Pitzer[9] which account for the effects of unsymmetrical mixing. These additional terms are obtained from a purely theoretical treatment of the electrostatic effects of mixing ions of different charge but of the same sign, and they require no empirical adjustment. Harvie and Weare's results indicate that the effects of the terms for unsymmetrical mixing are very important in predicting activity behavior in complex mixtures.

To complete their prediction of gypsum solubility in mixed electrolyte solutions, Harvie and Weare used parameters for pure $CaSO_4$ which are strictly valid only to an ionic strength of .06 m, since the osmotic coefficient data used to determine the parameters extend only to the solubility limit of gypsum at .015 m. However, because they evaluated mixture parameters for $CaSO_4$ using high concentration data, use of the approximate parameters for pure $CaSO_4$ should be adequate. Unfortunately, Harvie and Weare used an incorrect parameter for pure Na_2SO_4, resulting in an inconsistency within their equations. They also used a solubility product for gypsum which is not in agreement with their value for the mean activity coefficient of $CaSO_4$ at saturation in pure water.[1] While the effects of these inconsistencies are probably small in comparison to the accuracy of Harvie and Weare's treatment, they can be important for more precise applications.

Since Harvie and Weare completed their solubility prediction work, extensive new data on the solubility of gypsum in mixed solutions of Na_2SO_4, $CaCl_2$, and NaCl have become available.[14] These data can be used to refine the parameters for pure $CaSO_4$ and it's mixtures. In view of the high precision of the new data and of the inconsistencies in the previous treatments, it seems profitable to re-examine the solubility prediction of gypsum in mixed electrolyte solutions. In addition, new

---

[1] The solubility product given by Harvie and Weare[13] is 2.35×10^{-5}. The known solubility of gypsum in pure water is .01518 ± .00005 m,[14] and the activity coefficient at that concentration calculated from the parameters they used for $CaSO_4$ is .332. At that concentration the activity of water is greater than .999, so that the solubility product can be calculated as

$$K_{sp} = m^2 \gamma_{\pm}^2 a_w^2 = 2.53 \times 10^{-5}.$$

Thus the two values of the solubility product differ by 7%.

data on gypsum solubility in natural seawater, seawater with added $MgCl_2$, agricultural drainage water, and their concentrates also is available.[15] These data provide an excellent test of gypsum solubility in complex, natural systems. Finally the data of Culberson et al.,[12] Templeton,[16] and Davis and Collins[17] can be used to test solubility prediction for $SrSO_4$ and $BaSO_4$, based on parameter estimation using $CaSO_4$ as a model.

Equations

The equations developed by Pitzer and Kim[8] to describe mixed solutions require information on the properties of the pure salts making up the mixture and on the behavior of common ion mixtures. Complete derivations of the mixture equations have been given by Pitzer and Kim and Pitzer.[9,18] Therefore only the final equations for the osmotic coefficient and for the mean activity coefficient of a salt in a mixture are listed below:

$$\phi-1 = (\sum_i m_i)^{-1} \; 2If^{\phi} + 2\sum_c \sum_a m_c m_a \; B_{ca}{}^{\phi} + \frac{(\Sigma mz)}{(z_c z_a)} C_{ca}{}^{\phi} +$$

$$\sum_c \sum_{c'} m_c m_{c'} [\theta_{cc'} + I\theta_{cc'} + \sum_a m_a \psi_{cc'a}] +$$

$$\sum_a \sum_{a'} m_a m_{a'} [\theta_{aa'} + I\theta_{aa'} + \sum_c m_c \psi_{caa'}] \qquad (1)$$

$$\ln\gamma_{MX} = |z_M z_X| f^{\gamma} + (2\nu_M/\nu) \sum_a m_a [B_{Ma} + (\Sigma mz) C_{Ma} + (\nu_X/\nu_M)\theta_{Xa}] + (2\nu_X/\nu)$$

$$\sum_c m_c [B_{cX} + (\Sigma mz) C_{cX} + (\nu_M/\nu_X)\theta_{Mc}] + \sum_c \sum_a m_c m_a \{|z_M z_X| B_{ca}' +$$

$$\nu^{-1}[2\nu_M z_M C_{ca} + \nu_M \psi_{Mca} + \nu_X \psi_{caX}]\} + 1/2 \sum_c \sum_{c'} m_c m_{c'} [(\nu_X/\nu)\psi_{cc'X} +$$

$$|z_M z_X|\theta_{cc'}{}'] + 1/2 \sum_a \sum_{a'} m_a m_{a'}[(\nu_M/\nu)\psi_{Maa'} + |z_M z_X|\theta_{aa'}{}'] \quad (2)$$

The activity of water, a_w, can be calculated from the usual relationship

$$\ln a_w = - \sum_i \nu_i m_i \frac{M_1}{1000} \phi \quad (3)$$

where M_1 is the molecular weight of pure water.

Here ν_M and ν_X are the numbers of ions M and X in the neutral salt and $\nu = \nu_M + \nu_X$. The charges on the ions, in electronic units, are z_M and z_X. The summations are over all cations, c and c', and all anions, a and a'. The ionic strength is

$$I = 1/2 \sum_i m_i z_i^2$$

and

$$(\Sigma\, mz) = \sum_c m_c z_c = \sum_a m_a |z_a| .$$

The Debye-Hückel terms for the osmotic and activity coefficient are given by

$$f^\phi = -A_\phi \frac{I^{\frac{1}{2}}}{1 + 1.2 I^{\frac{1}{2}}} \quad (4)$$

$$f^\gamma = -A_\phi \frac{I^{\frac{1}{2}}}{1 + 1.2 I^{\frac{1}{2}}} + \frac{2}{1.2} \ln(1 + 1.2 I^{\frac{1}{2}}) \quad (5)$$

where the Debye-Hückel slope at 25°C is $A_\phi = .392$.

The terms B^ϕ_{MX}, B_{MX}, B'_{MX}, and C_{MX} are combinations of the parameters for the neutral salt, MX.

$$B_{MX}{}^\phi = \beta^{(0)}_{MX} + \beta^{(1)}_{MX} \exp(-\alpha_1 I^{\frac{1}{2}}) + \beta^{(2)}_{MX} \exp(-\alpha_2 I^{\frac{1}{2}}) \quad (6)$$

$$B_{MX} = \beta_{MX}^{(0)} + \frac{2\beta_{MX}^{(1)}}{\alpha_1^2 I}\,[1-(1+\alpha_1 I^{\frac{1}{2}})\,\exp(-\alpha_1 I^{\frac{1}{2}})] \tag{7}$$

$$+ \frac{2\beta_{MX}^{(2)}}{\alpha_2^2 I}\,[1-(1+\alpha_2 I^{\frac{1}{2}})\,\exp(-\alpha_2 I^{\frac{1}{2}})]$$

$$B'_{MX} = \frac{2\beta_{MX}^{(1)}}{\alpha_1^2 I^2}\,[-1+(1+\alpha_1 I^{\frac{1}{2}}+\tfrac{1}{2}\alpha_1^2 I)\,\exp(-\alpha_1 I^{\frac{1}{2}})] \tag{8}$$

$$+ \frac{2\beta_{MX}^{(2)}}{\alpha_2^2 I^2}\,[-1+(1+\alpha_2 I^{\frac{1}{2}}+\tfrac{1}{2}\alpha_2^2 I)\,\exp(-\alpha_2 I^{\frac{1}{2}})]$$

$$C_{MX} = \frac{C_{MX}^{\phi}}{2|z_M z_X|^{\frac{1}{2}}}\,. \tag{9}$$

For most electrolytes the parameter $\beta_{MX}^{(2)}$ is not needed, and α_1 is assigned the value 2.0. For high valence type electrolytes, including 2-2 electrolytes, the parameter $\beta_{MX}^{(2)}$ is required. For 2-2 electrolytes, $\alpha_1 = 1.4$ and $\alpha_2 = 12.0$.

The additional terms θ_{ij}, θ'_{ij}, and ψ_{ijk} occur only in mixtures of electrolytes. They account for binary interactions of unlike ions, i and j, of the same sign and for ternary interactions of two unlike ions of the same sign with an ion, k, of opposite sign. The binary mixture parameter, θ_{ij}, is composed of two terms,

$$\theta_{ij} = {}^{S}\theta_{ij} + {}^{E}\theta_{ij}(I). \tag{10}$$

The first term, ${}^{S}\theta_{ij}$, is a constant which accounts for the effects of short range interactions. It is the only adjustable parameter in

Equation (10). The second term, ${}^{E}\theta_{ij}(I)$, accounts for the purely electrostatic effects of unsymmetrical mixing. When the ions i and j are of the same charge, ${}^{E}\theta_{ij}(I)$ is zero. When the charges of ions i and j are different, ${}^{E}\theta_{ij}(I)$ depends on the total ionic strength and the charges z_i and z_j. The term $\theta'_{ij} = \frac{\partial\theta_{ij}}{\partial I}$ contains contributions only from ${}^{E}\theta_{ij}(I)$, because ${}^{S}\theta_{ij}$ is assumed to be independent of ionic strength. Values of ${}^{E}\theta_{ij}(I)$ and $\theta'_{ij}(I)$ can be calculated from equations or tables given by Pitzer.[9] The ternary term, ψ_{ijk}, is an adjustable parameter and is considered to be independent of concentration.

Equations (1) and (2) contain a large number of parameters. However, all of the parameters except the ${}^{S}\theta_{ij}$ and ψ_{ijk} are usually evaluated from data on single electrolytes. These parameters are then fixed for the calculation of the properties of a mixture. The mixture parameters ${}^{S}\theta_{ij}$ and ψ_{ijk} are most easily evaluated from data on ternary, common ion mixtures. They are then fixed for the calculation of the properties of a more complex mixture.

Calculations

The example of a sparingly soluble salt presents a special case for the determination of fitting parameters. If one is interested in the activity properties of a fairly insoluble salt in a mixture of moderate ionic strength, the contributions of the parameters for the pure, insoluble electrolyte will be very small. Thus the pure electrolyte terms can be estimated from knowledge of the parameters of similar electrolytes. The mixture parameters θ and ψ can then be evaluated from solubility data, preferably in common ion solutions. Of course, the effect of a sparingly soluble salt on the osmotic coefficient of the solution or on

the activity coefficient of a major component of the mixture will generally be small.

However, the solubility of $CaSO_4 \cdot 2H_2O$ at 25°C is large enough that accurate parameters for pure $CaSO_4$ are desirable. Recently Briggs[14] has obtained extensive data on the solubility of gypsum in common ion solutions of $CaCl_2$ and Na_2SO_4, as well as in more complex solutions of NaCl, $CaCl_2$ + NaCl, and Na_2SO_4 + NaCl. These data can be used to evaluate both the parameters for pure $CaSO_4$ and the mixture parameters, ψ_{Ca,Na,SO_4} and ψ_{Ca,Cl,SO_4}. The binary mixture parameters ${}^S\theta_{Ca,Na}$ and ${}^S\theta_{Cl,SO_4}$ are already known from analysis of other data.[9,20]

The form of the equation used to obtain $CaSO_4$ parameters from the solubility data can be derived as follows. The expression for the solubility product of $CaSO_4 \cdot 2H_2O$ is

$$K_{sp} = \gamma_{\pm}^{2}\, m_{Ca} m_{SO_4}\, a_w^{2} \tag{11}$$

where $\gamma_{\pm}$ is the mean activity coefficient of $CaSO_4$, m_{Ca} and m_{SO_4} are the molalities of calcium and sodium ions, and a_w is the activity of water in the solution. The experimentally determined quantity is $m_{Ca} m_{SO_4} a_w^{2}$, where a_w is included because it can be well determined using estimates of the $CaSO_4$ parameters. The activity coefficient is

$$\begin{aligned} \ln\gamma_{\pm} = \ln\gamma_{\pm}^{*} &+ R_1(m_{Ca},m_{SO_4},I)\, \beta^{(1)}_{CaSO_4} + R_2(m_{Ca},m_{SO_4},I)\, \beta^{(2)}_{CaSO_4} \\ &+ \frac{1}{2} m_{Na}(m_{Ca}+m_{SO_4})\, \psi_{Ca,Na,SO_4} + \frac{1}{2} m_{Cl}(m_{Ca}+m_{SO_4})\, \psi_{Ca,Cl,SO_4} \end{aligned} \tag{12}$$

where $\ln\gamma_{\pm}^{*}$ is the contribution to the activity coefficient calculated from Equation (2) with the unknown parameters $\beta^{(1)}_{CaSO_4}$, $\beta^{(2)}_{CaSO_4}$, ψ_{Ca,Na,SO_4}, and ψ_{Ca,Cl,SO_4} set to zero. In this case, since four parameters and the

solubility product have to be determined, the value of the parameter $\beta^{(0)}_{CaSO_4}$ was fixed at .2. Because the concentration of $CaSO_4$ is never very high, the $C^{\phi}_{CaSO_4}$ parameter is not needed and has been set to zero. The two terms R_1 and R_2 are the ionic strength dependent coefficients of $\beta^{(1)}_{CaSO_4}$ and $\beta^{(2)}_{CaSO_4}$,

$$R_n = \frac{2\beta^{(n)}}{\alpha_n^2 I} \{(m_{Ca}+m_{SO_4})[1-(1+\alpha_n I^{\frac{1}{2}}) \exp(-\alpha_n I^{\frac{1}{2}})] + \frac{4m_{Ca}m_{SO_4}}{I} [-1+(1+\alpha_n I^{\frac{1}{2}} + \tfrac{1}{2}\alpha_n^2 I) \exp(-\alpha_n I^{\frac{1}{2}})]\} \quad (13)$$

where n = 1 or 2. The final form of the fitting equation is obtained by taking the natural logarithm of Equation (11) and substituting Equation (12),

$$\ln(m_{Ca}m_{SO_4}a_w^2) + 2\ln\gamma_{\pm}^{*} = \ln K_{sp} - 2R_1\,\beta^{(1)}_{CaSO_4} - 2R_2\,\beta^{(2)}_{CaSO_4} - m_{Na}(m_{Ca}+m_{SO_4})\,\psi_{Ca,Na,SO_4} - m_{Cl}(m_{Ca}+m_{SO_4})\,\psi_{Ca,Cl,SO_4} \quad (14)$$

All of the terms on the left side of the equation are known, and the right side is linear in all of the unknown parameters. Thus this equation can be used with any standard, linear least squares routine to determine the five unknown parameters simultaneously from solubility data. One final iteration, using the new values of the parameters to calculate a_w, insures that the equations are internally consistent. It is important to determine simultaneously the values of the solubility product and the $CaSO_4$ parameters, in order to maintain internal consistency between the solubility product, the known solubility of gypsum in pure water, and the activity coefficient calculated with the $CaSO_4$ parameters.

Results

The results of a least squares fit of Briggs' solubility data, using Equation (14), are given in Table 1. The low concentration, electromotive force data of Lilley and Briggs[19] also were included in the fit, since these data describe the activity properties of $CaSO_4$ at concentrations below gypsum solubility. The experimental activity coefficients listed in Table 1 are calculated from the solubility data and the value of the solubility product obtained with the least squares fit. The agreement between calculated and experimental values is very good, showing that Pitzer's specific interaction equations are successful in describing the activity properties of a minor component in mixed solutions.

The values of the parameters obtained with the least squares fit, as well as the parameters for the other salts in the mixtures, are given in Tables 2 and 3. The parameters $\beta^{(1)}_{CaSO_4}$ and $\beta^{(2)}_{CaSO_4}$ are similar to the parameters for other 2-2 electrolytes. The mixture parameters ψ_{Ca,Na,SO_4} and ψ_{Ca,Cl,SO_4} are very different from those obtained by Harvie and Weare[13] (-.067 vs -.023 for ψ_{Ca,Na,SO_4} and -.027 vs 0 for ψ_{Ca,Cl,SO_4}). The two sets are not strictly comparable however, because Harvie and Weare used the old value of .020 for θ_{Cl,SO_4}, while the improved value of .030 determined by Downes and Pitzer[20] was used in this study. The value of $^{-}$.027 for ψ_{Ca,Cl,SO_4} is similar to that of $^{-}$.020 for ψ_{Mg,Cl,SO_4}. The parameter ψ_{Ca,Na,SO_4} is more negative than most ternary mixture parameters, indicating large, triplet interactions between Ca^{++}, Na^{+}, and $SO_4^{=}$ ions. The value of the gypsum solubility product determined in the least squares fit is 2.615×10^{-5}, in good agreement with the value of 2.63×10^{-5} obtained by Lilley and Briggs[19] from an analysis of their

Table 1

Least Squares Fit of Gypsum Solubility Data[a]

Ionic Strength	molality Ca^{++}	molality $SO_4^{=}$	molality Na^{+}	molality Cl^{-}	Water Activity	Exp. $\gamma_{\pm CaSO_4}$	Δ[b]
.06272	.01603	.01463		.00280	1.000	.334	-0[c]
.06568	.01721	.01406		.00630	1.000	.329	0
.06977	.01880	.01338		.01083	.999	.323	-0
.07611	.02116	.01264		.01702	.999	.313	-0
.09194	.02679	.01156		.03045	.999	.291	-0
.11614	.03517	.01062		.04910	.999	.265	-1
.16284	.05104	.00973		.08263	.998	.230	-2
.24837	.07978	.00904		.14147	.997	.191	-2
.35070	.11403	.00861		.21084	.995	.164	-2
.52314	.17165	.00819		.32693	.992	.137	-3
.95359	.31528	.00777		.61501	.985	.105	-2
1.39953	.46402	.00745		.91314	.978	.089	-1
2.76801	.92066	.00604		1.82924	.951	.072	0
4.19427	1.39658	.00455		2.78406	.915	.070	1
6.22156	2.07297	.00267		4.14060	.854	.081	-1
.06560	.01428	.01711	.00565		1.000	.327	1[d]
.06554	.01427	.01709	.00565		1.000	.328	0
.07057	.01353	.01901	.01096		.999	.319	0
.07058	.01353	.01901	.01096		.999	.319	0
.07746	.01292	.02151	.01718		.999	.307	1
.07737	.01290	.02149	.01718		.999	.307	0
.09183	.01200	.02661	.02922		.999	.286	0
.09184	.01200	.02661	.02922		.999	.286	0
.12040	.01109	.03644	.05069		.999	.255	-1
.12055	.01113	.03648	.05069		.999	.254	-1
.15303	.01078	.04742	.07327		.998	.227	0
.15242	.01063	.04726	.07327		.998	.229	-1
.21027	.01022	.06668	.11292		.997	.196	-2
.21025	.01022	.06668	.11292		.997	.196	-2
.33475	.01003	.10824	.19642		.996	.156	-3
.33477	.01004	.10825	.19642		.996	.156	-3
.50569	.01024	.16515	.30982		.993	.125	-2
.50564	.01023	.16514	.30982		.993	.125	-2
.79588	.01083	.26168	.50171		.990	.097	-2
.79582	.01081	.26167	.50171		.990	.097	-2
1.30661	.01201	.43153	.83904		.984	.072	-1
1.30658	.01201	.43153	.83904		.984	.072	-1
2.16298	.01385	.71638	1.40506		.975	.053	-0
2.16292	.01383	.71636	1.40506		.975	.053	-0
3.48199	.01616	1.15528	2.27825		.961	.039	-0
3.48200	.01616	1.15528	2.27825		.961	.039	-0
5.14737	.01793	1.70981	3.38376		.944	.031	-1
5.14746	.01796	1.70984	3.38376		.944	.031	-1

Table 1 (continued)

Ionic Strength	molality Ca^{++}	$SO_4^{=}$	Na^+	Cl^-	Water Activity	Exp. $\gamma_{\pm CaSO_4}$	Δ^b
.06869	.01576	.01576	.00565	.00565	.999	.325	-0[e]
.06871	.01576	.01576	.00565	.00565	.999	.325	-0
.07322	.01609	.01609	.00887	.00887	.999	.318	0
.07310	.01606	.01606	.00887	.00887	.999	.319	-0
.08855	.01708	.01708	.02022	.02022	.999	.300	0
.08856	.01708	.01708	.02022	.02022	.999	.300	0
.09879	.01768	.01768	.02809	.02809	.999	.290	0
.09870	.01765	.01765	.02809	.02809	.999	.290	0
.12583	.01913	.01913	.04929	.04929	.998	.268	0
.12593	.01916	.01916	.04929	.04929	.998	.267	0
.15106	.02042	.02042	.06940	.06940	.997	.251	1
.15100	.02040	.02040	.06940	.06940	.997	.251	1
.18463	.02165	.02165	.09803	.09803	.996	.237	-2
.18583	.02195	.02195	.09803	.09803	.996	.234	1
.18581	.02194	.02194	.09803	.09803	.996	.234	1
.25489	.02473	.02473	.15598	.15598	.994	.208	1
.25492	.02474	.02474	.15598	.15598	.994	.208	1
.30596	.02649	.02649	.20000	.20000	.993	.194	1
.30604	.02651	.02651	.20000	.20000	.993	.194	1
.39905	.02944	.02944	.28129	.28129	.990	.175	2
.39905	.02944	.02944	.28129	.28129	.990	.175	2
.45939	.03111	.03111	.33494	.33494	.988	.166	1
.45968	.03119	.03119	.33494	.33494	.988	.166	2
.52746	.03293	.03293	.39575	.39575	.986	.157	2
.52738	.03291	.03291	.39575	.39575	.986	.158	2
.64623	.03566	.03566	.50359	.50359	.983	.146	1
.64641	.03570	.03570	.50359	.50359	.983	.146	2
.76337	.03812	.03812	.61088	.61088	.979	.137	1
.76344	.03814	.03814	.61088	.61088	.979	.137	2
.97493	.04196	.04196	.80710	.80710	.972	.125	1
.97496	.04196	.04196	.80710	.80710	.972	.125	1
1.20695	.04534	.04534	1.02560	1.02560	.965	.117	1
1.20690	.04533	.04533	1.02560	1.02560	.965	.117	1
1.72444	.05096	.05096	1.52060	1.52060	.948	.106	1
1.72412	.05088	.05088	1.52060	1.52060	.948	.106	1
2.23744	.05431	.05431	2.02020	2.02020	.929	.101	1
2.23751	.05433	.05433	2.02020	2.02020	.929	.101	1
2.76027	.05602	.05602	2.53620	2.53620	.910	.100	1
2.76017	.05599	.05599	2.53620	2.53620	.910	.100	1
3.24317	.05614	.05614	3.01860	3.01860	.890	.102	1
3.24316	.05614	.05614	3.01860	3.01860	.890	.102	1
4.21813	.05168	.05168	4.01140	4.01140	.849	.117	-3
4.21810	.05168	.05168	4.01140	4.01140	.849	.117	-3
5.67902	.04783	.04783	5.48770	5.48770	.781	.137	4
5.67876	.04776	.04776	5.48770	5.48770	.781	.137	4

Table 1 (continued)

Ionic Strength	molality Ca^{++}	$SO_4^{=}$	Na^{+}	Cl^{-}	Water Activity	Exp. $\gamma_{\pm CaSO_4}$	Δ[b]
.07617	.01851	.01426	.00637	.01487	.999	.315	-0[f]
.08936	.02138	.01374	.01147	.02676	.999	.299	-0
.11146	.02623	.01310	.01968	.04592	.998	.276	-0
.14644	.03393	.01246	.03219	.07512	.998	.249	-0
.19764	.04524	.01183	.05010	.11691	.997	.222	-1
.31295	.07079	.01118	.08939	.20861	.994	.183	-0
.43749	.09843	.01082	.13139	.30661	.991	.158	0
.65766	.14731	.01038	.20536	.47922	.987	.133	0
.90096	.20134	.01007	.28686	.66942	.981	.116	1
1.59233	.35489	.00912	.51856	1.21009	.965	.093	1
2.72107	.60555	.00752	.89689	2.09297	.935	.081	1
4.18414	.93046	.00539	1.38736	3.23752	.890	.081	0
6.14444	1.36586	.00308	2.04379	4.76933	.819	.096	-4
.09442	.02063	.01469	.01783	.02972	.999	.294	-0[g]
.11521	.02402	.01444	.02872	.04786	.998	.275	-0
.16575	.03232	.01407	.05474	.09124	.997	.241	1
.23349	.04347	.01366	.08941	.14904	.995	.211	1
.33807	.06078	.01327	.14248	.23748	.993	.181	1
.52691	.09209	.01280	.23783	.39643	.988	.151	1
.74709	.12866	.01239	.34873	.58127	.983	.130	1
.89183	.15272	.01219	.42150	.70256	.979	.121	1
1.45762	.24672	.01126	.70622	1.17714	.964	.101	1
2.52698	.42431	.00930	1.24474	2.07476	.933	.087	1
3.93600	.65832	.00672	1.95433	3.25752	.887	.087	1
6.10765	1.01925	.00356	3.04635	5.07772	.803	.106	-3
.09096	.01831	.01609	.01993	.02437	.999	.298	-0[h]
.11822	.02100	.01671	.03852	.04710	.998	.274	0
.15591	.02458	.01736	.06481	.07925	.997	.248	1
.21976	.03035	.01803	.11068	.13533	.995	.220	1
.32167	.03932	.01872	.18499	.22619	.993	.190	1
.51639	.05595	.01928	.32927	.40261	.987	.158	1
.67484	.06926	.01941	.44766	.54736	.982	.142	2
.94668	.09187	.01929	.65179	.79696	.975	.125	2
1.51944	.13901	.01829	1.08412	1.32557	.957	.106	2
2.50520	.21937	.01539	1.83171	2.23966	.924	.095	2
3.95729	.33749	.01076	2.93407	3.58752	.870	.098	2
6.05864	.50949	.00565	4.52452	5.53219	.781	.122	3

Table 1 (continued)

Ionic Strength	molality Ca^{++}	$SO_4^{=}$	Na^+	Cl^-	Water Activity	Exp. $\gamma_{\pm}$ $CaSO_4$	Δ [b]
.34749	.01220	.07858	.23232	.09957	.994	.166	0[i]
.34751	.01220	.07858	.23232	.09957	.994	.166	0
.51827	.01220	.11653	.36516	.15650	.990	.137	0
.51818	.01217	.11650	.36516	.15650	.990	.137	0
.99351	.01259	.22218	.73356	.31439	.981	.099	1
.99356	.01260	.22219	.73356	.31439	.981	.098	1
1.48346	.01302	.33110	1.11330	.47713	.972	.080	1
1.48344	.01302	.33110	1.11330	.47713	.972	.080	1
1.94651	.01331	.43403	1.47255	.63110	.964	.070	1
1.94645	.01329	.43402	1.47255	.63110	.964	.070	1
3.01098	.01341	.67059	2.30015	.98579	.943	.057	1
3.01100	.01342	.67060	2.30015	.98579	.943	.057	1
5.04641	.01212	1.12276	3.88727	1.66599	.901	.049	0
5.04627	.01209	1.12273	3.88727	1.66599	.901	.049	0
.35603	.01418	.06406	.24944	.14966	.993	.171	1[j]
.35597	.01416	.06405	.24944	.14966	.993	.171	1
.52300	.01416	.09188	.38865	.23319	.989	.143	1
.52297	.01415	.09188	.38865	.23319	.989	.143	1
1.01908	.01432	.17462	.80151	.48091	.978	.105	1
1.01903	.01431	.17461	.80151	.48091	.978	.105	1
1.48217	.01435	.25181	1.18730	.71238	.967	.088	2
1.48225	.01437	.25183	1.18730	.71238	.967	.088	2
1.96506	.01425	.33226	1.59006	.95404	.956	.078	2
1.96501	.01423	.33224	1.59006	.95404	.956	.078	2
2.97909	.01348	.50100	2.43766	1.46260	.932	.067	2
2.97916	.01350	.50102	2.43766	1.46260	.932	.067	2
5.04057	.01064	.84364	4.16503	2.49903	.878	.061	1
5.04053	.01063	.84363	4.16503	2.49903	.878	.062	1
.35465	.01727	.04900	.25382	.19036	.992	.177	1[k]
.35461	.01726	.04899	.25382	.19036	.992	.177	1
.53435	.01757	.06914	.41251	.30937	.987	.149	2
.53436	.01757	.06914	.41251	.30937	.987	.149	2
1.01296	.01773	.12241	.83738	.62802	.975	.113	2
1.01305	.01775	.12243	.83738	.62801	.975	.113	2
1.47752	.01746	.17388	1.25125	.93841	.963	.096	2
1.47753	.01747	.17389	1.25125	.93841	.963	.096	2
1.97426	.01688	.22876	1.69486	1.27111	.949	.087	2
1.97427	.01689	.22876	1.69486	1.27111	.949	.087	2
2.96791	.01506	.33816	2.58459	1.93839	.921	.078	2
2.96794	.01506	.33817	2.58459	1.93838	.921	.078	2
5.03934	.01025	.56566	4.44292	3.33210	.854	.079	2
5.03952	.01030	.56571	4.44292	3.33209	.854	.078	2
.06072	.01518	.01518				.338	-1[l]
.03992	.00998	.00998				.388	3
.02399	.00600	.00600				.454	9
.01334	.00334	.00334				.535	14
.00801	.00200	.00200				.609	14
.00444	.00111	.00111				.681	21
.00263	.00066	.00066				.751	11

[a] Gypsum solubility product is 2.615×10^{-5} at 25°C.

[b] $\Delta = [\gamma_{\pm}\ (\text{calc}) - \gamma_{\pm}\ (\text{exp})] \times 10^{3}$.

[c] $CaCl_2$ solutions.

[d] Na_2SO_4 solutions.

[e] NaCl solutions.

[f] $CaCl_2$ + NaCl, $m_{CaCl_2}/m_{NaCl} = .66$.

[g] $CaCl_2$ + NaCl, $m_{CaCl_2}/m_{NaCl} = .33$.

[h] $CaCl_2$ + NaCl, $m_{CaCl_2}/m_{NaCl} = .11$.

[i] Na_2SO_4 + NaCl, $m_{Na_2SO_4}/m_{NaCl} = .66$.

[j] Na_2SO_4 + NaCl, $m_{Na_2SO_4}/m_{NaCl} = .33$.

[k] Na_2SO_4 + NaCl, $m_{Na_2SO_4}/m_{NaCl} = .17$.

[ℓ] Electromotive force data.

Table 2

Parameters for Pure Electrolytes at 25°C

Salt	$\beta^{(0)}$	$\beta^{(1)}$	$\beta^{(2)}$	C^{ϕ}
Na_2SO_4	.019575	1.1130		.00570
NaCl	.07650	.2664		.00127
NaBr	.09730	.2791		.00116
$NaNO_3$	.00680	.1783		-.00072
K_2SO_4	.04995	.7792		0.
KCl	.04835	.2122		-.00084
KBr	.05690	.2212		-.00180
KNO_3	-.08160	.0494		.00660
$MgSO_4$	.22100	3.3430	-37.23	.02500
$MgCl_2$	.35235	1.6815		.00519
$MgBr_2$	.43270	1.7530		.00312
$Mg(NO_3)_2$	.36710	1.5850		-.02062
$CaSO_4$[c]	.20000	3.1973	-54.24	0.
$CaCl_2$	.31590	1.6140		-.00034
$CaBr_2$	.38160	1.6130		-.00257
$Ca(NO_3)_2$	.21080	1.4090		-.02014
$SrSO_4$[d]	.20000	3.1973	-54.24	0.
$SrCl_2$[b]	.29180	1.5603		-.00446
$SrBr_2$	.33110	1.7120		.00123
$Sr(NO_3)_2$	.13460	1.3800		-.01992
$BaSO_4$[d]	.20000	3.1973	-54.24	0.
$BaCl_2$	.26280	1.4963		-.01938
$BaBr_2$	.31455	1.5698		-.01596
$Ba(NO_3)_2$	-.03230	.8025		0.

[a] Values of the parameters are taken from Reference 8 unless otherwise noted.

[b] Parameters from Reference 12.

[c] Parameters evaluated in this study.

[d] Parameters estimated from $CaSO_4$.

Table 3

Mixed Electrolyte Parameters at 25°C

(For Use With the Higher Order Electrostatic Terms)[a]

i	j	K	$S_{\theta_{ij}}$	ψ_{ijk}
Na	K	SO_4	-.012	-.010[b]
		Cl		-.0018
		Br		-.0022
		NO_3		-.0012
Na	Mg	SO_4	.07[b]	-.023[b]
		Cl		-.010[b]
		NO_3		-
Na	Ca (Sr,Ba)	SO_4	.07[b]	-.067[e]
		Cl		-.007[b]
		Br		(-.007)
		NO_3		-
K	Mg	SO_4	0.0[d]	-.048[d]
		Cl		-.022[d]
		Br		(-.022)
		NO_3		-
K	Ca (Sr,Ba)	SO_4	.032[b]	-
		Cl		-.025[b]
		Br		(-.025)
		NO_3		-
Mg	Ca (Sr,Ba)	SO_4	.010	.02[e]
		Cl		0.0
		Br		(0.0)
		NO_3		-

[a] Values of the parameters are taken from Reference 8 unless otherwise noted.

[b] Parameters from Reference 9.

Table 3 (continued)

i	j	K	$S_{\theta_{ij}}$	ψ_{ijk}
SO_4	Cl	Na	.03[c]	0.0[c]
		K		-.005[c]
		Mg		-.020[c]
		Ca(Sr,Ba)		-.027[e]
SO_4	Br	Na	(.03)	(0.0)
		K		(-.005)
		Mg		(-.020)
		Ca(Sr,Ba)		(-.029)
SO_4	NO_3	Na	.062[e]	-
		K		-
		Mg		-
		Ca(Sr,Ba)		0.0[e]
Cl	Br	Na	0.0	0.0
		K		0.0
		Mg		-
		Ca(Sr,Ba)		-
Cl	NO_3	Na	.016	-.006
		K		-.006
		Mg		0.0
		Ca(Sr,Ba)		-.017
Br	NO_3	Na	(.016)	(-.006)
		K		(-.006)
		Mg		(0.0)
		Ca(Sr,Ba)		(-.017)

[c] Parameters from Reference 20.

[d] Parameters from Reference 13.

[e] Parameters evaluated in this study.

electromotive force data. This value is over 10% larger than that used by Harvie and Weare.[13]

Two previous studies by Whitfield[10] and by Culberson, Latham, and Bates[12] have concluded that Pitzer's equations are not successful in predicting gypsum solubility. However, neither study used the term $^{E}\theta_{ij}$, which accounts for the purely electrostatic effects of unsymmetrical mixing.

Using the treatment presented in Paper IV,[8] which does not include $^{E}\theta_{ij}$, it is not possible to fit simultaneously all of Brigg's solubility data. It is possible to determine parameters $\beta^{(1)}_{CaSO_4}$, $\beta^{(2)}_{CaSO_4}$, ψ^{*}_{Ca,Na,SO_4}, and ψ^{*}_{Ca,Cl,SO_4} from only the common-ion solubility data. (Here the symbol ψ^{*} is used to differentiate the mixture parameters determined without $^{E}\theta_{ij}$, since they will not be the same as those evaluated when $^{E}\theta_{ij}$ is included.) When these parameters are used to predict gypsum solubility in NaCl solutions, the predicted solubilities are systematically low. The calculated activity coefficients are compared to those derived from knowledge of the gypsum solubility constant and the experimental solubilities in Figure 1. The predicted activity coefficients are about 20% high at NaCl concentrations above .5 molal. This is the same type of behavior found in the two previous studies. The problem can be completely overcome by using the full, unsymmetrical mixing equations derived in Paper V.[9]

Prediction of Gypsum Solubility in Seawater

The prediction of gypsum solubility in seawater and natural brines of widely varying composition provides a final test of the effectiveness of Pitzer's equations. To complete these calculations, the unknown

Figure 1. Mean activity coefficient of $CaSO_4$ in solutions of NaCl saturated with gypsum. The solid line represents values calculated without $^{E}\theta$. Points are from the solubility data of Briggs.[14]

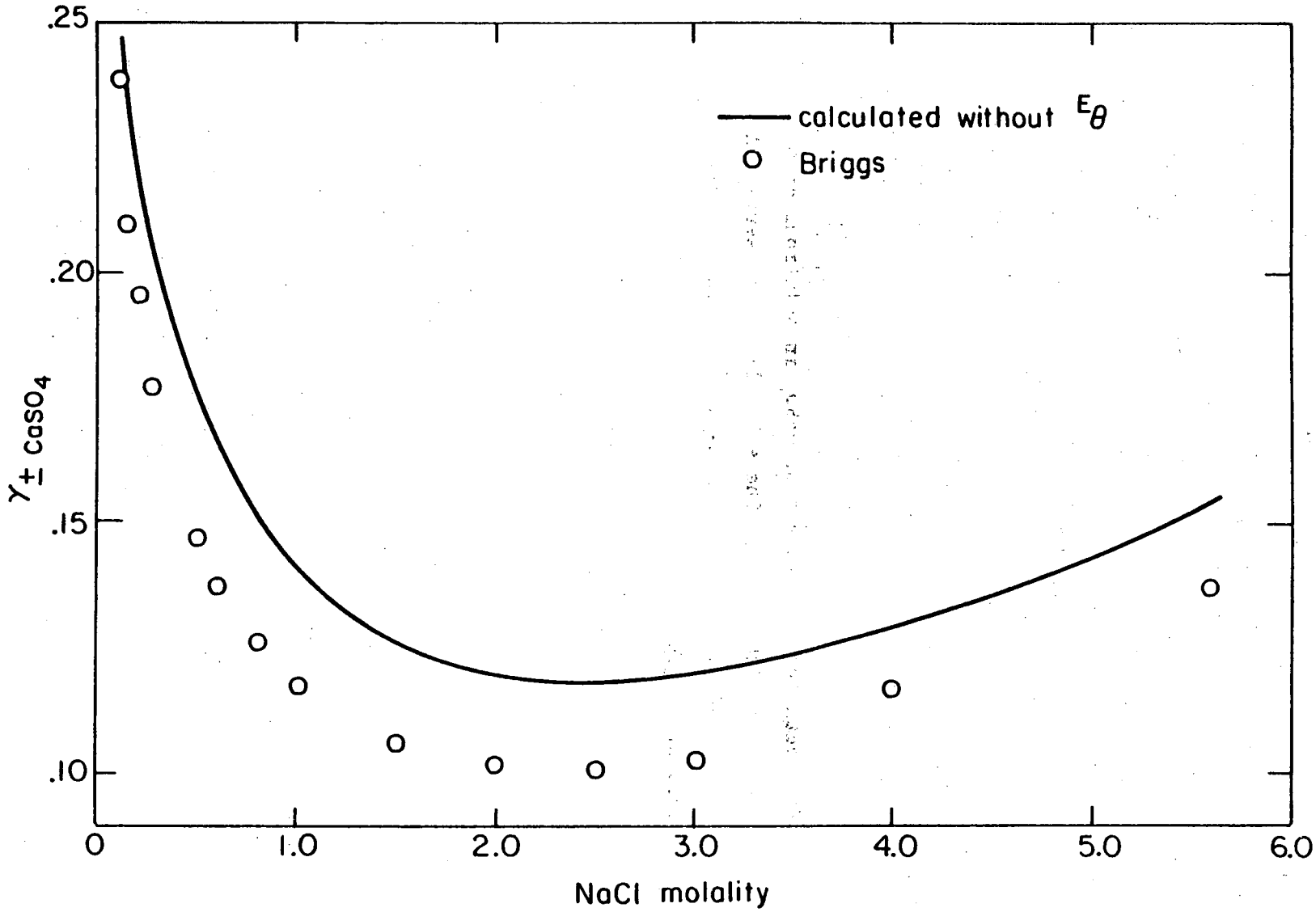
.25
.20
.15
.10
$\gamma_{\pm}$ CaSO$_4$
0
1.0
2.0
3.0
4.0
5.0
6.0
NaCl molality
calculated without E_θ
Briggs

XBL 812-5166

parameters ψ_{Mg,Ca,SO_4} and ψ_{Ca,SO_4,NO_3} have been determined from an analysis of gypsum solubility in the appropriate common ion solutions. Although Harvie and Weare[13] have previously given a value for ψ_{Mg,Ca,SO_4}, they used a gypsum solubility product and $CaSO_4$ parameters which differ from those determined in this study. Thus, to retain internal consistency, the values of these parameters have been redetermined.

The equation used to determine the mixture parameters is

$$\frac{1}{m_k}\left(\ln\gamma_{\pm_{CaSO_4}} - \ln\gamma_{\pm}^{*}\right) = \frac{1}{2}\left(m_{Ca}+m_{SO_4}\right)\psi_{k,Ca,SO_4} + {}^{S}\theta_{jk} \qquad (15)$$

where k represents Mg^{++} or NO_3^-. For mixtures of $CaSO_4$ and $MgSO_4$, ${}^{S}\theta_{jk}$ represents ${}^{S}\theta_{Mg,Ca}$. In mixtures of $CaSO_4$ and $Ca(NO_3)_2$, ${}^{S}\theta_{jk}$ is ${}^{S}\theta_{NO_3,SO_4}$. Again, $\gamma_{\pm}^{*}$ is the activity coefficient calculated from Equation (2) with only the unknown mixture parameters set to zero. The experimental value $\ln\gamma_{\pm_{CaSO_4}}$ is determined from the solubility data and the known value of the solubility product.

The values of ${}^{S}\theta_{SO_4,NO_3}$ and ψ_{Ca,SO_4,NO_3} were determined as the intercept and slope of a graph of

$$\frac{1}{m_{NO_3}}\left(\ln\gamma_{\pm_{CaSO_4}} - \ln\gamma_{\pm}^{*}\right)$$

versus $\frac{1}{2}\left(m_{Ca} + m_{SO_4}\right)$. The value of ${}^{S}\theta_{Mg,Ca}$ has already been determined from osmotic coefficient data for the system $MgCl_2 - CaCl_2$. Therefore only ψ_{Ca,Mg,SO_4} was determined from data on the solubility of $CaSO_4 \cdot 2H_2O$ in $MgSO_4$. Included in Table 3 are the values of the three parameters determined in this manner.

Extensive data on gypsum solubility in natural seawater, agricultural drainage water, and their concentrates have recently been published

by Adler, Glater, and McCutchan.[15] The concentrations of the various ions, which they give in terms of weight and concentration factors, have been converted to molalities using density data tabulated in the same publication. In some cases the solutions did not satisfy electroneutrality conditions, and the concentration of Na^+ or Cl^- was increased arbitrarily to achieve charge balance. Parameters for single electrolytes and the mixture parameters used in the calculations are listed in Tables 2 and 3. In many cases the mixture parameters are unknown. Those enclosed in parentheses have been estimated from knowledge of the parameters of similar salts, and others have been set to zero. Parameters for mixtures containing K^+ and Mg^{++} have been taken from Harvie and Weare.[13]

The predicted values of calcium and sulfate concentrations and the mean activity coefficient of $CaSO_4$ are compared with the experimental values in Tables 4 and 5. The predicted activity coefficient is in very good agreement with the experimental value even at very high concentrations and high levels of magnesium augmentation.

Culberson, Latham, and Bates[12] have measured the solubility of gypsum in synthetic seawater, and their data also have been used to test gypsum solubility predictions. The composition of their synthetic seawater at 35% salinity is listed in Table 6. Their measured gypsum solubilities in normal, slightly concentrated, and slightly diluted seawater of varying magnesium concentrations are compared with predicted values in Table 7. Again, the agreement of the predicted and measured solubilities is excellent.

Other measurements of gypsum solubility in seawater dilutents and concentrates up to an ionic strength of 4 m have been compiled by

Table 4

Gypsum Solubility in Natural Seawater at 25°C[a]

Ionic Strength	Water Activity	Na^+	K^+	Mg^{++}	Cl^-	Experimental Ca^{++}	Experimental $SO_4^=$	Calculated Ca^{++}	Calculated $SO_4^=$	Exp. $\gamma_{\pm}$ $CaSO_4$	Calc. $\gamma_{\pm}$ $CaSO_4$
		molality									
.8057	.981	.4852	.0100	.0553	.5674	.0319	.0510	.0314	.0505	.129	.131
1.5152	.961	.9808	.0202	.1118	1.1470	.0359	.0745	.0351	.0737	.103	.105
2.2267	.940	1.4887	.0307	.1697	1.7410	.0362	.0948	.0350	.0936	.093	.095
2.5829	.928	1.7455	.0360	.1989	2.0412	.0353	.1044	.0339	.1030	.091	.093
2.9435	.916	2.0068	.0414	.2287	2.3468	.0343	.1137	.0324	.1118	.089	.093
.8980	.979	.4859	.0103	.0830	.6240	.0333	.0524	.0334	.0525	.125	.125
1.6986	.958	.9849	.0209	.1682	1.2648	.0369	.0756	.0374	.0761	.101	.100
2.4999	.934	1.4959	.0317	.2555	1.9211	.0378	.0966	.0367	.0955	.091	.092
2.9068	.920	1.7582	.0373	.3003	2.2579	.0373	.1064	.0353	.1044	.088	.091
3.3145	.907	2.0222	.0429	.3454	2.5969	.0343	.1138	.0334	.1129	.090	.092
.9887	.978	.4857	.0103	.1107	.6791	.0368	.0560	.0353	.0545	.115	.119
1.8758	.954	.9851	.0209	.2245	1.3774	.0411	.0800	.0393	.0782	.093	.097
2.7696	.927	1.5003	.0318	.3420	2.0977	.0410	.1003	.0380	.0973	.086	.091
3.2219	.913	1.7639	.0374	.4020	2.4663	.0401	.1098	.0362	.1059	.084	.091
3.6793	.897	2.0316	.0431	.4630	2.8406	.0376	.1179	.0338	.1141	.086	.092
1.0791	.977	.4860	.0103	.1384	.7347	.0377	.0569	.0371	.0563	.113	.115
2.0531	.951	.9863	.0209	.2809	1.4911	.0417	.0807	.0410	.0800	.093	.094
3.0348	.921	1.5031	.0319	.4281	2.2724	.0407	.1000	.0391	.0984	.087	.090
3.5322	.905	1.7679	.0375	.5034	2.6725	.0392	.1090	.0367	.1065	.086	.090
4.0357	.887	2.0368	.0432	.5800	3.0791	.0370	.1174	.0338	.1142	.087	.093
1.1696	.975	.4863	.0103	.1662	.7906	.0394	.0586	.0388	.0580	.109	.111
2.2284	.947	.9866	.0209	.3372	1.6039	.0430	.0820	.0426	.0816	.091	.092
3.2941	.915	1.5029	.0318	.5136	2.4433	.0414	.1008	.0398	.0992	.087	.089
3.8397	.896	1.7699	.0375	.6049	2.8775	.0396	.1094	.0370	.1068	.087	.091
4.3897	.877	2.0399	.0432	.6972	3.3164	.0367	.1173	.0336	.1142	.089	.094

[a] Data of Adler, Glater, and McCutchan.[15]

Table 5

Gypsum Solubility in Agricultural Drainage Water at 25°C[a]

Ionic Strength	Water Activity	molality									Exp. $\gamma_{\pm}$	Calc. $\gamma_{\pm}$
							Experimental		Calculated			
		Na^+	K^+	Mg^{++}	Cl^-	NO_3^-	Ca^{++}	$SO_4^=$	Ca^{++}	$SO_4^=$	$CaSO_4$	$CaSO_4$
.1617	.998	.0601	.0002	.0082	.0187	.0013	.0120	.0403	.0121	.0405	.233	.231
.2167	.997	.0902	.0002	.0123	.0281	.0020	.0115	.0540	.0117	.0542	.205	.203
.2729	.996	.1205	.0003	.0164	.0375	.0026	.0114	.0682	.0115	.0683	.184	.183
.3298	.996	.1509	.0004	.0206	.0470	.0033	.0114	.0825	.0114	.0825	.167	.167
.3866	.995	.1813	.0005	.0247	.0564	.0039	.0113	.0967	.0113	.0967	.156	.155
.4451	.994	.2124	.0005	.0290	.0661	.0046	.0115	.1115	.0113	.1113	.144	.145
.1883	.998	.0639	.0002	.0165	.0270	.0013	.0127	.0410	.0131	.0414	.225	.220
.3228	.996	.1280	.0003	.0331	.0541	.0026	.0121	.0688	.0127	.0694	.178	.173
.4586	.994	.1922	.0005	.0496	.0812	.0039	.0121	.0972	.0126	.0977	.150	.147
.5274	.993	.2246	.0005	.0580	.0949	.0046	.0121	.1115	.0126	.1120	.140	.137
.5967	.992	.2572	.0006	.0664	.1087	.0052	.0122	.1261	.0126	.1265	.131	.129
.6656	.991	.2895	.0007	.0748	.1223	.0059	.0122	.1404	.0126	.1408	.125	.123

[a] Data of Adler, Glater, and McCutchan.[15]

Table 6

Composition of Synthetic Seawater

Species	Molality	Comments
Na^+	.48523	
K^+	.01058	
Mg^{++}	.05518	
Ca^{++}	.01068	
Sr^{++}	.00009	
Cl^-	.56824	Cl^- replaced HCO_3^-
Br^-	.00094	Br^- + F^- concentration
$CO_3^=$	.02927	

Table 7

Gypsum Solubility in Seawater at 25°C

Ionic Strength	Mg^{++}	Ca^{++}	$SO_4^{=}$	$\gamma_{\pm CaSO_4}$	Ca^{++}	$SO_4^{=}$	$\gamma_{\pm CaSO_4}$
		molal concentration					
		experimental[a]			calculated		
.5562	.00	.05075	.02253	.153	.05028	.02206	.156
.7228	.01742	.04854	.02928	.138	.04806	.02880	.140
.9397	.03930	.04646	.03809	.125	.04595	.03758	.126

[a] Data of Culberson, Latham, and Bates.[12]

Marshall and Slusher.[11] Although the values are tabulated at 30°C, they can be used for comparison because the solubility of gypsum changes very little over the 25-30°C range. The solubilities also were not all measured in seawaters of exactly the same composition. However, the compositions are similar enough to make a rough quantitative comparison. Water has been removed or added to the seawater composition given in Table 6 in order to calculate the predicted gypsum solubilities over a large ionic strength range. The predicted solubility values are compared with the various measurements in Figure 2. Again, agreement of predicted and measured gypsum solubilities is very good even at ionic strengths above 4 molal. These results indicate that the system of mixture equations developed by Pitzer can be used to predict the activity properties of even minor components in a complex mixture.

Prediction of Strontium and Barium Sulfate Solubility

The parameters obtained for calcium sulfate can be used to predict the solubility of celestite and barite in mixed solutions. Although the solubilities of strontium and barium sulfates are much lower than that of gypsum, the activity coefficients of these 2-2 electrolytes should be similar to those of $CaSO_4$. Comparison of the predicted solubilities with experimental results provides a test of the use of approximate parameters in mineral solubility predictions. Accurate prediction of the solubility of celestite and barite in seawater is of interest because of the importance of these sulfates in mineral formation. Mixed strontium and barium sulfate scales deposited from oil well field waters also are a common problem in petroleum production.

Figure 2. Gypsum solubility in seawater. The solid line represents solubilities predicted using Pitzer's equations and the $CaSO_4$ parameters determined in this study. Points are from data reported by Marshall and Slusher;[11] Culberson, Latham, and Bates;[12] and Adler, Glater, and McCutchan.[15]

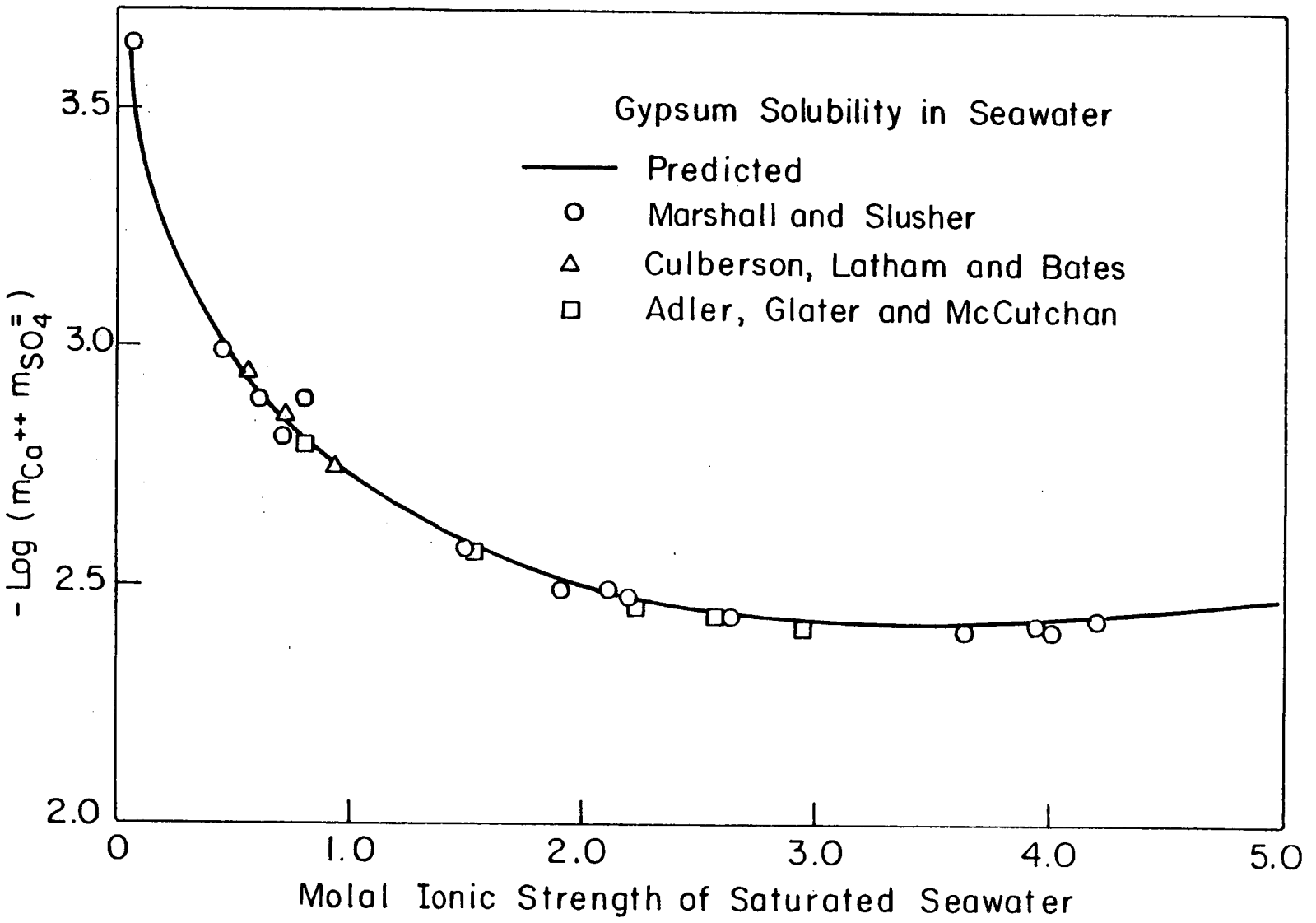
Gypsum Solubility in Seawater
Predicted
Marshall and Slusher
Culberson, Latham and Bates
Adler, Glater and McCutchan
- Log ($m_{Ca^{++}}$ $m_{SO_4^{=}}$)
3.5
3.0
2.5
2.0
0
1.0
2.0
3.0
4.0
5.0
Molal Ionic Strength of Saturated Seawater

XBL 812-5188

Solubility products for $SrSO_4$ and $BaSO_4$, which are consistent with the approximate values of the activity coefficients, can be calculated as follows. For $SrSO_4$, the solubility in pure water determined by Culberson, et al.[12] is $6.44 \pm .01 \times 10^{-4}$ molal. At that concentration, the activity coefficient of $SrSO_4$, calculated using the $CaSO_4$ parameters, is .765. The solubility product is

$$K^{\circ}_{SrSO_4} = \gamma^2_{\pm SrSO_4} m_{Sr} m_{SO_4} = 2.43 \times 10^{-7}.$$

For $BaSO_4$, the solubility in pure water given by Templeton[16] is 1.08×10^{-5} m. The activity coefficient of $BaSO_4$ at that concentration, approximated using the $CaSO_4$ parameters, is .970. The solubility product is

$$K^{\circ}_{BaSO_4} = \gamma^2_{\pm BaSO_4} m_{Ba} m_{SO_4} = 1.10 \times 10^{-10}.$$

To maintain internal consistency, it is important to use solubility products determined in this manner. Use of a different solubility product will result in an inconsistency between the assumed values of the activity coefficient and the known solubility in pure water.

The solubility of $SrSO_4$ in NaCl solutions has been measured by Lucchesi and Whitney,[21] Davis and Collins,[17] Strübel,[22] and Culberson, Latham, and Bates.[12] Their experimental values are compared with the predicted solubilities in Figure 3. The predicted value is in good agreement with the recent determination of Culberson, et al. at .7 m NaCl. The measurements of Davis and Collins are high compared to this value. Overall, the predicted solubilities in NaCl solutions are in reasonable agreement with the experimental determinations to an ionic strength of at least 1.5 m. The predicted solubilities of $SrSO_4$ in

Figure 3. $SrSO_4$ solubility in solutions of NaCl and $MgCl_2$. Solid lines represent solubilities predicted using $CaSO_4$ parameters to approximate $SrSO_4$ behavior. Points represent data of Davis and Collins;[17] Culberson, Latham, and Bates;[12] Lucchesi and Whitney;[21] and Strübel.[22]

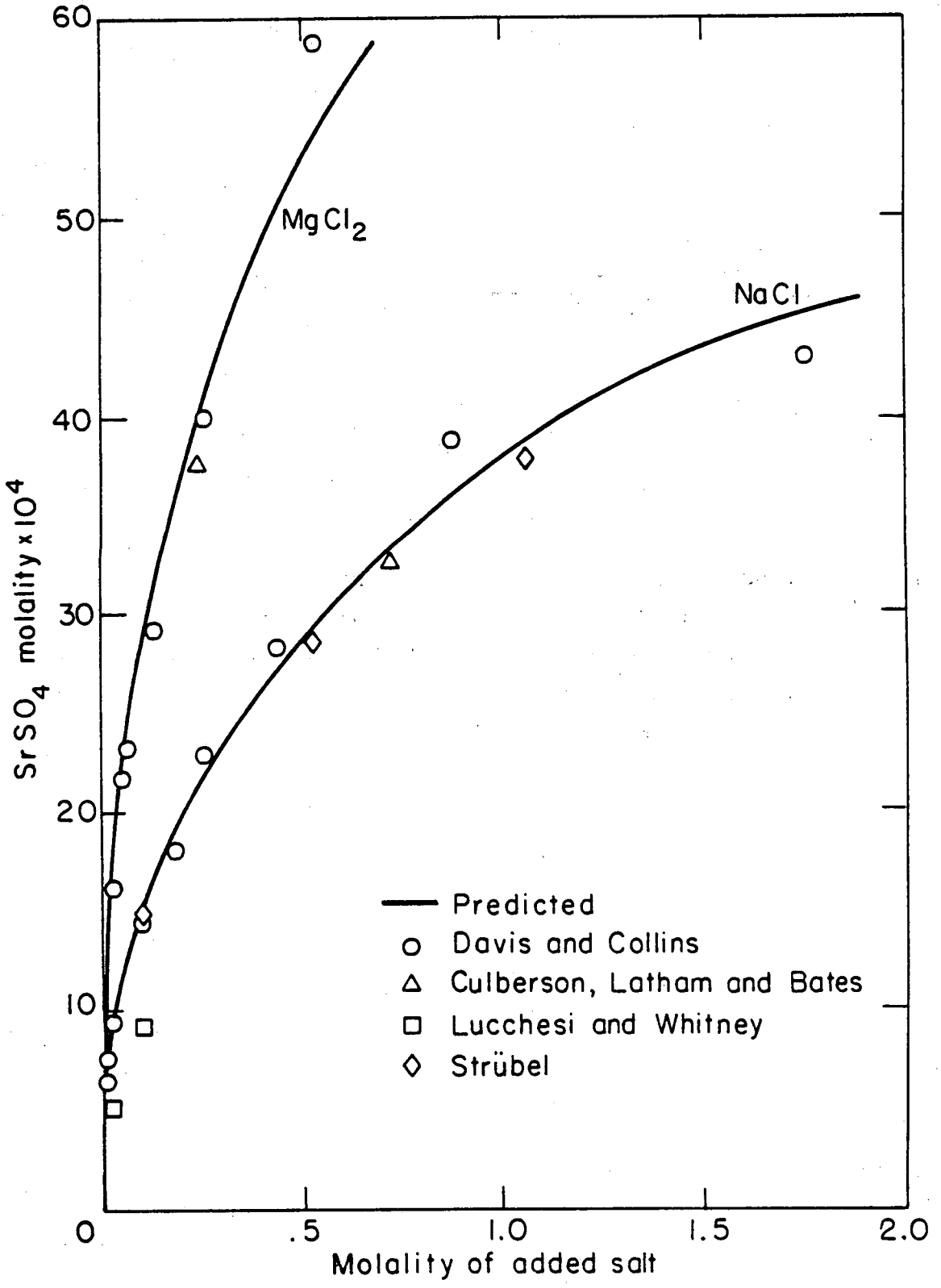
60
50
40
30
20
10
0
.5
1.0
1.5
2.0
$SrSO_4$ molality x 10^4
Molality of added salt
$MgCl_2$
NaCl
Predicted
Davis and Collins
Culberson, Latham and Bates
Lucchesi and Whitney
Strübel

XBL 812-5167

solutions of $MgCl_2$ also are in good agreement with the data. Celestite solubility in seawaters of varying magnesium and calcium concentrations are compared with the measurements of Culberson et al.[12] in Table 8. The predicted values are slightly higher than the measured solubilities in all cases. However, the maximum difference in predicted and experimental values is less than 3.5%. These results indicate that prediction of $SrSO_4$ solubility in high NaCl content brines and seawaters will be reasonably accurate to ionic strengths of 1 molal.

The solubility of $BaSO_4$ in NaCl solutions has been measured by Neuman,[23] Templeton,[16] Strübel,[24] and Davis and Collins.[17] Predicted and measured values of barite solubility are compared in Figure 4. Again, the predicted solubilities are in good agreement with the data of Davis and Collins up to .5 m NaCl, but are below the measured values at higher NaCl concentrations. The calculated solubilities of $BaSO_4$ in solutions of $MgCl_2$ are close to the experimental values up to an ionic strength of 1.5 molal. Since this behavior is analogous to that of $SrSO_4$, one would expect the predicted barite solubility in 35% salinity seawater to be within 5% of the true value. However, the predicted concentration of Ba^{++} at saturation is 2.09×10^{-7} m, while the solubility measured at 20°C by Burton, Marshall, and Phillips[25] is 3.5×10^{-7} m barium. One possible reason for this discrepancy is the large dependence of barite solubility on particle size. Lemarchands[26] has found that the apparent solubility of barite can increase by a factor of three as the particle size is reduced. The predicted activity coefficient of $BaSO_4$, .134, is 16% higher than the value calculated by Hanor,[27] and 14% lower than that given by Whitfield.[10]

Table 8

Celestite Solubility in Seawater at 25°C

Seawater	molal concentration							
	Mg^{++}	Ca^{++}	$Sr^{++} \times 10^3$	$SO_4^{=}$	$\gamma_{\pm CaSO_4}$	$Sr^{++} \times 10^3$	$SO_4^{=}$	$\gamma_{\pm CaSO_4}$
			experimental[a]			calculated		
1	.06598	0.0	.414	.029679	.141	.426	.029691	.139
2	.05519	.01076	.416	.029682	.140	.429	.029695	.138
3	.03801	.02795	.423	.029689	.139	.434	.029700	.137
4	.02099	.04497	.422	.029689	.139	.434	.029706	.136

[a] Data of Culberson, Latham, and Bates.[12]

Figure 4. $BaSO_4$ solubility in solutions of NaCl and $MgCl_2$. Solid lines represent solubilities predicted using $CaSO_4$ parameters to approximate $BaSO_4$ behavior. Points represent data of Davis and Collins,[17] Templeton,[16] and Strübel.[24]

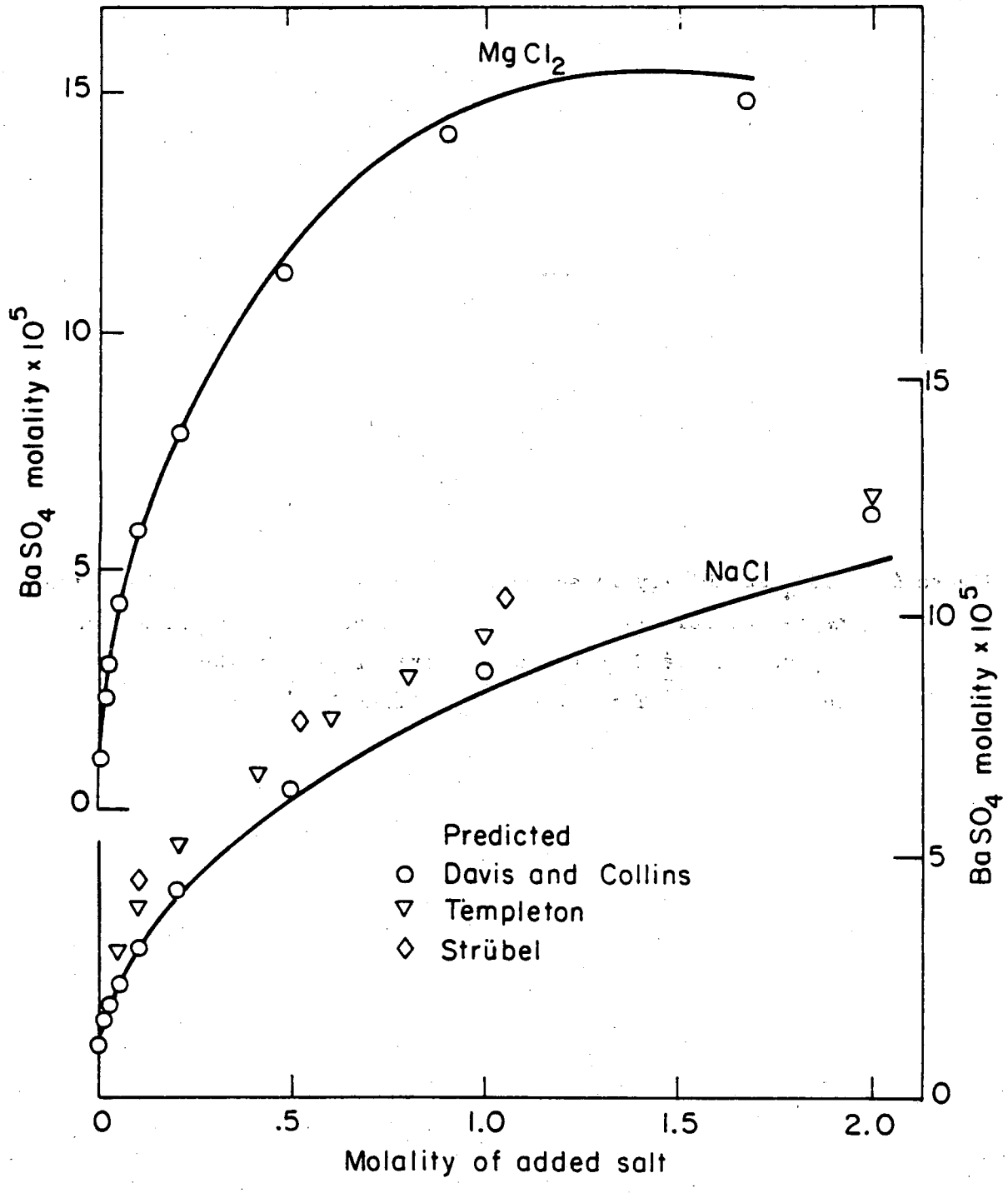
MgCl2
NaCl
Predicted
Davis and Collins
Templeton
Strübel
BaSO4 molality x 10^5
Molality of added salt
0
.5
1.0
1.5
2.0
5
10
15

XBL 812-5168

Another interesting aspect of barite solubility prediction is the formation of a mixed $BaSO_4$-$SrSO_4$ solid solution. Precipitation of a barite containing strontium would be expected to lower the solubility of barium sulfate because of the lower activity of $BaSO_4$ in the solid solution. Hanor[27] has discussed in detail the estimation of $BaSO_4$ and $SrSO_4$ activities in a non-ideal solid solution, so that in principle one could calculate the effect of a solid solution on solubility. Unfortunately, the situation is further complicated by an experimental determination[28] of $BaSO_4$ and $SrSO_4$, in 1 m NaCl, in equilibrium with a natural barite containing 8.5% $SrSO_4$. The activities of $SrSO_4$ and $BaSO_4$ in this solid solution can be calculated from the solubility products and the predicted solution activities. The activity of solid $SrSO_4$, .024, is in good agreement with the value of .017 obtained from Harnor's treatment. However, the activity of solid $BaSO_4$ is close to 1, not .87 as predicted by Hanor. Either the predicted activity coefficient of $BaSO_4$ in solution is 10% too high, or the solid activity predicted by Hanor is too low. Certainly further experimental studies of $BaSO_4$ and $SrSO_4$ solutions in equilibrium with well characterized, mixed solids are needed before barite solubility in natural systems can be accurately predicted.

Conclusion

The system of equations developed by Pitzer has previously been shown to reproduce the activity of water and the activity properties of major components in mixed solutions.[8,10] This study has shown that Pitzer's specific interaction model also can reproduce the properties of minor components in a complex mixture. In addition, a method of

determining electrolyte parameters from solubility data has been described. Parameter estimation using information on similar electrolytes also was shown to be successful for sparingly soluble salts.

The agreement between experimentally determined activity coefficients and those calculated in this chapter indicates that Pitzer's model can be used to predict accurately the properties of electrolytes in natural brines and seawater. The importance of a predictive model lies in its ability to calculate activity properties in solutions over a wide range of composition and concentration not studied experimentally. As an example of this use of Pitzer's model, the calculated activity coefficients of eighteen salts in seawater are listed as a function of ionic strength in Table 9.

The effectiveness of this model in describing solubility behavior at 25°C is encouraging. Future work will involve extension of the model to high temperatures, since many hydrothermal, geochemical, and industrial problems require solubility prediction in this regime. A large body of data is available on the solubilities of minerals in various solutions at high temperatures. However, new data on the high temperature, solution activities of the major components of natural brines ($NaCl$, $NaSO_4$, KCl, K_2SO_4, $MgCl_2$) and on the properties of their common ion mixtures will be required.

Table 9

Predicted Activity Coefficients in Seawater

Ionic Strength	.05	.10	.30	.50	.72	1.00	1.50	2.00
ϕ	.928	.914	.900	.899	.904	.913	.935	.961
Na_2SO_4	.641	.563	.441	.388	.352	.323	.290	.270
NaCl	.820	.777	.708	.680	.663	.654	.651	.659
NaBr	.822	.780	.714	.689	.676	.670	.675	.691
K_2SO_4	.637	.557	.430	.373	.333	.300	.262	.237
KCl	.817	.772	.695	.660	.637	.620	.603	.597
KBr	.819	.774	.700	.669	.649	.635	.625	.626
$MgSO_4$	.417	.327	.212	.172	.148	.131	.115	.108
$MgCl_2$	.669	.602	.509	.477	.461	.454	.461	.481
$MgBr_2$	.670	.605	.515	.485	.473	.470	.484	.513
$CaSO_4$	.412	.322	.206	.166	.142	.124	.107	.098
$CaCl_2$	.664	.596	.500	.465	.447	.437	.438	.451
$CaBr_2$	.665	.599	.505	.474	.458	.452	.460	.481
$SrSO_4$	.411	.320	.204	.163	.138	.120	.102	.092
$SrCl_2$	.663	.594	.496	.460	.440	.428	.425	.434
$SrBr_2$	.664	.597	.501	.468	.451	.443	.446	.463
$BaSO_4$	.410	.318	.201	.159	.134	.115	.096	.085
$BaCl_2$	.661	.592	.491	.453	.431	.416	.408	.412
$BaBr_2$	.663	.594	.496	.461	.442	.431	.428	.439

[a] Seawater composition given in Table 6 with $[Sr^{++}] = 8.95 \times 10^{-5}$ m and $[Ba^{++}] = 1.37 \times 10^{-7}$ m. Other concentrations were obtained by adding or removing water.

References

1. P. J. Reilly, R. H. Wood, and R. A. Robinson, J. Phys. Chem. 75, 1305 (1971).

2. M. Whitfield, Mar. Chem. 1, 251 (1973).

3. R. M. Garrels and M. E. Thompson, Am. J. Sci. 260, 57 (1962).

4. G. Scatchard, R. M. Rush, and J. S. Johnson, J. Phys. Chem. 74, 3786 (1970).

5. K. S. Pitzer, J. Phys. Chem. 77, 268 (1973).

6. K. S. Pitzer and G. Mayorga, J. Phys. Chem. 77, 2300 (1973).

7. K. S. Pitzer and G. Mayorga, J. Soln. Chem. 3, 539 (1974).

8. K. S. Pitzer and J. J. Kim, J. Am. Chem. Soc. 96, 5701 (1974).

9. K. S. Pitzer, J. Soln. Chem. 4, 249 (1975).

10. M. Whitfield, Mar. Chem. 3, 197 (1975).

11. W. L. Marshall and R. Slusher, J. Chem. Eng. Data, 13, 83 (1968).

12. C. H. Culberson, G. Latham, and R. G. Bates, J. Phys. Chem. 82, 2693 (1978).

13. C. E. Harvie and J. H. Weare, Geochim. Cosmochim. Acta, 44, 981 (1980).

14. C. C. Briggs, Ph.D. Thesis, University of Sheffield, Sheffield, England (1978).

15. M. S. Adler, J. Glater, and J. W. McCutchan, J. Chem. Eng. Data, 24, 187 (1979).

16. C. C. Templeton, J. Chem. Eng. Data, 5, 514 (1960).

17. J. W. Davis and A. G. Collins, Environmental Sci. and Tech. 5, 1039 (1971).

18. K. S. Pitzer, "Theory: Ion Interaction Approach", in "Activity Coefficients in Electrolyte Solutions", R. M. Pytkowicz, Ed., CRC Press, Boca Raton, Florida (1979).

19. T. H. Lilley and C. C. Briggs, Proc. Roy. Soc. Lond., A 349, 355 (1976).

20. C. J. Downes and K. S. Pitzer, J. Soln. Chem. 5, 389 (1976).

21. P. J. Lucchesi and E. D. Whitney, J. Appl. Chem. 12, 277 (1962).

22. G. Strübel, Neues. Jahrb. Mineral. Monatsh. 99 (1966).

23. E. W. Neuman, J. Am. Chem. Soc. 55, 879 (1933).

24. G. Strübel, Neues. Jahrb. Mineral. Monatsh. 223 (1967).

25. J. D. Burton, N. J. Marshall, and A. J. Phillips, Nature, 217, 834 (1968).

26. M. Lemarchands, C. R. Acad. Sci. Paris, 187, 601 (1928).

27. J. S. Hanor, Geochim. Cosmochim. Acta, 33, 894 (1969).

28. H. Gundlach, D. Stoppel, and G. Strübel, Neues. Jahrb. Mineral. Ahb. 116, 321 (1972).